

NEW MEXICO DEPARTMENT OF TRANSPORTATION

## RESEARCH BUREAU

Innovation in Transportation

# Development of a Flexible Pavement Database for Local Calibration of MEPDG

**Prepared by:**

University of New Mexico  
Albuquerque, NM 87131

**Prepared for:**

New Mexico Department of Transportation  
Research Bureau  
7500B Pan American Freeway NE  
Albuquerque, NM 87109

**In Cooperation with:**

The US Department of Transportation  
Federal Highway Administration

**Report NM08MSC-02**

JUNE 4, 2012

## SUMMARY PAGE

1. Report No. NM08MSC-02		2. Recipient's Catalog No.	
3. Title and Subtitle Development of a Flexible Pavement Database for Local Calibration of MEPDG		4. Report Date June 2012	
5. Author(s): Rafiqul A. Tarefder, Nasrin Sumee, Jose I. Rodriguez, Sriram Abbina, and Karl Benedict		6. Performing Organization Report No. 456-17	
7. Performing Organization Name and Address University of New Mexico Department of Civil Engineering MSC01 1070, 1 University of New Mexico Albuquerque, NM 87131		8. Performing Organization Code 456A	
10. Sponsoring Agency Name and Address Research Bureau 7500B Pan American Freeway PO Box 94690 Albuquerque, NM 87199-4690		9. Contract/Grant No. 456-304	
11. Type of Report and Period Covered Final Report June 2008 –June 2012		12. Sponsoring Agency Code	
13. Supplementary Notes None			
14. Abstract <p>A comprehensive and reliable database capable of storing variables of flexible pavements is required for local calibration and effective statewide implementation of the Mechanistic Empirical Pavement Design Guide (MEPDG) in New Mexico. In this study, such a database (called MEPDG database) has been designed and populated with data including material properties, pavement structural characteristics, traffic, climatic conditions, and performance data from existing NMDOT databases and other formats. Using the database, MEPDG was calibrated to represent the local materials and pavement conditions of New Mexico. A set of calibration coefficients have been recommended for designing NMDOT pavements and allow for level 2 MEPDG analysis. In addition, advanced statistical analyses such as parametric and nonparametric regressions were performed to rank New Mexico pavement design inputs as high-to-moderate-to-low sensitive to pavement performance.</p>			
15. Key Words Mechanistic Empirical Pavement Design Guide, Database, Calibration, Distress, flexible pavement		16. Distribution Statement Available from NMDOT Research Bureau	
17. Security Classification of this Report None	18. Security Classification of this page None	19. Number of Pages 301	20. Price N/A

# **Development of a Flexible Pavement Database for Local Calibration of MEPDG**

## **Final Report**

By

Rafiqul A. Tarefder, Ph.D., P.E.  
Nasrin Sumee, Graduate Research Assistant  
Jose I. Rodriguez, Graduate Research Assistant  
Sriram Abbina, Graduate Research Assistant  
Karl Benedict, Director, EDAC

Department of Civil Engineering  
MSC01 1070, Albuquerque, N.M. 87131  
University of New Mexico

## **Report NM08MSC-02**

A Report on Research Sponsored by  
New Mexico Department of Transportation  
Research Bureau

in Cooperation with  
The U.S. Department of Transportation  
Federal Highway Administration

June 2012

NMDOT Research Bureau  
7500B Pan American Freeway NE  
PO Box 94690  
Albuquerque, NM 87199-4690  
(505) 841-9145

© New Mexico Department of Transportation

## PREFACE

The research reported herein describes the development of a MEPDG database for local calibration of the MEPDG in the State of New Mexico. The MEPDG database was designed in an Oracle platform and populated with data of NMDOT's LTPP and other pavement sections. Using the developed database, local calibration of MEPDG and sensitivity study were performed. It is hoped that the developed MEPDG database is populated as new pavement data become available, and calibration coefficients are updated periodically.

## NOTICE

The United States government and the State of New Mexico do not endorse products or manufacturers. Trade or manufacturers' names appear herein solely because they are considered essential to the object of this report. This information is available in alternative accessible formats. To obtain an alternative format, contact the NMDOT Research Bureau, 7500B Pan American Freeway NE, PO Box 94690, Albuquerque, NM 87199-4690, (505)-841-9145

## DISCLAIMER

This report presents the results of research conducted by the authors and does not necessarily reflect the views of the New Mexico Department of Transportation. This report does not constitute a standard or specification.

## EXECUTIVE SUMMARY

One of the objectives of this project was the development of the New Mexico flexible pavement database comprising of design, construction, materials, traffic, climate, and performance data required for local calibration of Mechanistic Empirical Pavement Design Guide (MEPDG). The other objectives were to perform the local calibration of MEPDG using the developed MEPDG database, and to conduct sensitivity study of the MEPDG for New Mexico Department of Transportation (NMDOT) pavements.

To achieve the first objective, data fields that were required for local calibration of MEPDG were identified as well as NMDOT's existing database structures were evaluated. The architecture of the MEPDG database was designed to run in an Oracle platform with Geographical Information System (GIS) and Web interface capabilities. The MEPDG database tables and data attributes were designed based on relational database concept. To that end, NMDOT's existing databases were collected, analyzed, and relevant data from these databases were identified and extracted to populate the MEPDG database. Most of the NMDOT's existing databases lack from proper documentation, and only dump copy of the NMDOT's existing databases were available. Therefore, several procedures were developed to extract data from the existing database (dump file), to analyze the database tables and data, and to populate the MEPDG database with few relevant data. It was found that among 30 existing databases only 3 to 4 databases contain data that are useful to the MEPDG database. As per data collection, paper and soft copies such as excel, text, LIMS, website format of design, construction, asphalt mix design, pavement structural design, soils and aggregate properties, and subgrade strength data were collected, analyzed, and used for population of the MEPDG database. In addition, raw traffic data from several Weigh-In-Motion (WIM) stations were collected and analyzed for axle load spectra and used to populate the MEPDG database. Over the year, pavement performance data have been collected by NMDOT in qualitative formats, which were then converted to quantitative formats for the MEPDG use. NMDOT's existing database lack from the climatic and water table depth data, which were therefore, collected from the State Office of Engineers. These data exist in GIS format, and do not match with the pavement location. These data were modeled to generate pavement location specific climatic and water table data, and populated into the MEPDG database using Open Geospatial Consortium Mapping Services available in Oracle. Attempts were made to develop web interface (frontend) to display some of the data and tables the MEPDG database (backend). These web enhancement or interfaces provides access to various data of a particular location of the pavement. Specifically, web pages for accessing traffic data, distress data, mix data, soils data, pavement location, layers, and axle load spectra were developed and stored in the MEPDG server. Finally, the procedure for the MEPDG database maintenance, data integrity, and growth were prescribed.

To achieve the second objective, the developed MEPDG database was analyzed further near the end of this project to determine the complete set of data that are suitable for local calibration of the MEPDG. For the purpose of calibration, it was necessary to find NMDOT pavement sections with performance data spanning for a number of years. For this reason, initial local calibration was performed using only Long Term Pavement Performance (LTPP) data. A total of 11 pavement sections from the LTPP sections located in New Mexico were used for initial local calibration. The permanent deformation, alligator cracking, and longitudinal cracking models

were calibrated. In calibration methodology, the target was fixed to reduce the residual sum of squared errors, defined by the square of the difference between predicted and measured distress, so that any bias is eliminated and precision is increased. Initial calibration results suggest that there is significant bias in the permanent deformation prediction by default MEPDG coefficients. This suggests that regional conditions significantly affect the MEPDG's performance models, which were calibrated using LTPP sections spread throughout the U.S.

In this study, MEPDG sensitivity analysis was performed to understand the impacts and relationships of the hundreds of input variables contained in the MEPDG with national calibration coefficients. The MEPDG includes a large set of input variables, which makes traditional Monte-Carlo based sensitivity analysis impractical to use. Therefore, the sensitivity analyses were pursued using more advanced statistical techniques namely parametric and nonparametric regressions. Based on the sensitivity study results, New Mexico inputs were classified as groups of highly, moderately, and slightly sensitive to pavement performances such as rutting, alligator cracking, longitudinal cracking, and roughness. From further analysis and population of the MEPDG database towards the end of this project, it became evident that a total of 24 data sets or pavement sections were complete in the NMDOT's MEPDG database. To that end, a refined local calibration of MEPDG was carried out using 11 LTPP and 13 NMDOT pavement sections (total 24). Local calibration coefficients of the rutting, fatigue cracking, and IRI models were determined and recommended for future design of pavements in the State of New Mexico using the MEPDG.

## **ACKNOWLEDGEMENTS**

The authors would like to express their sincere gratitude and appreciation to Jeff Mann, Pavement Design Section Head of NMDOT, for being the advocate of this project and his regular support, sponsorship, and suggestions. The authors would like to thank Bob Meyers, previously Materials Bureau Chief and currently, Geotechnical Section Manager, NMDOT Materials Bureau, for his sponsorship and support for this project. The UNM research team appreciates the valuable service and time of the Project Manager Mr. Virgil Valdez for this project.

The UNM research team would like to thank the Project Technical panel for their valuable suggestions during the quarterly meeting. Special thanks go to several Project Panel members namely, Robert McCoy, Pavement Exploration Section Head, NMDOT Materials Bureau, and Parveez Anwar, State Asphalt Engineer, and Chuck Slocter, Database Developer, for their assistance and suggestions for this project.

This project is funded by the New Mexico Department of Transportation (NMDOT)'s Research Bureau. The authors would like to thank the research Bureau Chief, Scott McClure for his support, and Administrator, Dee Billingsley for her fine accounting and reimbursements. The authors would like to thank several members and personnel at UNM for their support. Special thanks go Rebekah Lucero, UNM Civil Engineering accountant.

## TABLE OF CONTENT

<b>Chapter 1: INTRODUCTION</b>	12
PURPOSE	12
MEPDG BACKGROUND	13
Models in MEPDG	14
Analysis Sequence in the MEPDG	14
Levels of MEPDG Analysis	15
Basics of Local Calibration	16
Need for the MEPDG Database	20
METHODOLOGY	20
REPORT ORGANIZATION	21
 <b>Chapter 2: REVIEW OF EXISTING DATABASES</b>	20
INTRODUCTION	22
NMDOT's EXISTING DATABASES	22
Transportation Information Management System (TIMS)	23
Highway Maintenance Management System (HMMS)	23
Decision Support System (DSS)	23
Pontis	24
Site Manager	24
Laboratory Information Management System (LIMS)	24
GIS Database	24
Orify	24
Pavement Management System (PMS) Data	25
ANALYSIS OF EXISTING DATABASES	25
REVIEW OF LTPP DATABASE	26
Monitoring and Data Collection Procedure	31
Principles of Traffic Data Collection	32
Traffic Data Storage	32
Traffic Data Reporting	33
Historical Traffic Data at GPS Locations	33
Traffic Database	33
REVIEW OF CLIMATIC DATA	33
Ground Water Depth Processing and Extraction Service	38
Climate Data Acquisition and Processing	41
Open Geospatial Consortium Mapping Services	44
FWD DATA	47
 <b>Chapter 3: DESIGN OF MEPDG DATABASE</b>	47
INTRODUCTION	49
IDENTIFY MEPDG DATA FIELDS	49
General Input	49
General Information	49



Site/Project Identifications	51
Analysis Parameters	52
Traffic Input	53
Design/Analysis Levels	53
Traffic Module Data Analyses	53
Climatic Input	56
Structural Input	57
DESIGN OF DATABASE ARCHITECTURE	58
Creation of Tables in MEPDG Database	59
<b>Chapter 4: POPULATION OF MEPDG DATABASE</b>	73
Traffic Tables	74
Distress Tables	76
FWD Data	81
Mix Data	83
<b>Chapter 5: WEB APPLICATIONS OF MEPDG DATABASE</b>	106
Pavement Structure Design Data	109
Mix Design Data	113
Soil data	119
Subgrade Design Data	120
Climate Details	124
<b>Chapter 6: DATABASE MAINTENANCE AND INTEGRITY</b>	124
Database Maintenance	127
Data Integrity	127
Database Backup	127
Database Security	127
Data Exchange Protocol	128
Data Reduction	130
Restoring Database from Backup	130
Database Query Examples	131
<b>Chapter 7: INITIAL LOCAL CALIBRATION</b>	130
INTRODUCTION	133
PAVEMENT SECTIONS FOR INITIAL CALIBRATION	133
DATA FOR INITIAL CALIBRATION	135
Traffic Data	135
Climatic Data	135
Structural Data	136
Materials Data	137
Performance Data	139
INITIAL CALIBRATION	141
Permanent Deformation Model	142
Prediction of Permanent Deformation in the MEPDG	142
Calibration of the Permanent Deformation Model	143

Validation of the Permanent Deformation Model	146
Alligator (Bottom-Up) Cracking Model	147
Prediction of Alligator Cracking in the MEPDG	147
Calibration of the Alligator Cracking Model	148
Validation of the Alligator Cracking Model	151
Longitudinal (Top-Down) Cracking Model	152
Prediction of Longitudinal Cracking in the MEPDG	152
Calibration of the Longitudinal Cracking Model	152
Validation of the Longitudinal Cracking Model	154
Remarks	155
<b>Chapter 8: SENSITIVITY STUDY BY PARAMETRIC TECHNIQUES</b>	153
INTRODUCTION	156
OBJECTIVES	157
DEFINING INPUTS-OUTPUTS	157
Inputs	157
Latin Hypercube Sampling (LHS)	159
MEPDG Outputs	161
PARAMETRIC STATISTICAL TECHNIQUES	162
Tests Based On Gridding	162
Common Means (CMN)	162
Common Locations (CL)	165
Statistical Independence (SI)	168
FLEXIBLE GRID FREE TESTS	169
Simple Linear Regression (LREG)	169
Quadratic Regression (QREG)	172
Rank Correlation Coefficient (RCC)	172
Squared Rank Differences (SRD)	175
SUMMARY OF INPUT IDENTIFICATION	176
RANKING OF INPUTS BY RANK REGRESSION	178
Results of Ranking	179
Output Y <sub>1</sub> (Terminal IRI)	179
Output Y <sub>2</sub> (Longitudinal Cracking)	181
Output Y <sub>3</sub> (Alligator Cracking)	183
Output Y <sub>4</sub> (Transverse Cracking)	184
Output Y <sub>5</sub> (AC Rut)	185
Output Y <sub>6</sub> (Total Rut)	186
SUMMARY OF RANKING	188
CONCLUSIONS	189
<b>Chapter 9: SENSITIVITY STUDY BY NONPARAMETRIC TECHNIQUES</b>	188
INTRODUCTION	191
RECENT SENSITIVITY STUDIES	191
DATA	193
NONPARAMETRIC REGRESSION PROCEDURE	195
Multivariate Adaptive Regression Splines (MARS)	195

Gradient Boosting Machine (GBM)	196
Sensitivity Measure	196
Total Variance Index (T)	197
Confidence Intervals (CI)	197
RESULTS AND DISCUSSION	197
Output Y1 (Terminal IRI)	197
Output Y2 (Longitudinal Cracking)	200
Output Y3 (Alligator Cracking)	203
Output Y4 (Transverse Cracking)	205
Output Y5 (AC Rutting)	207
Output Y6 (Total Rutting)	210
CONCLUSIONS	213
 <b>Chapter 10: LOCAL CALIBRATION</b>	 214
INTRODUCTION	217
OBJECTIVES	218
PAST STUDIES	218
Calibration Practice Performed in NCHRP Projects	222
The Local Calibration by State Agencies	224
PAVEMENT SECTIONS FOR CALIBRATION	226
CALIBRATION-VALIDATION METHODOLOGY	227
PERMANENT DEFORMATION MODEL	228
Prediction of Permanent Deformation in the MEPDG	228
Calibration of the Permanent Deformation Model	229
Validation of the Permanent Deformation Model	232
ALLIGATOR (BOTTOM-UP) CRACKING MODEL	232
Prediction of Alligator Cracking in the MEPDG	232
Calibration of the Alligator Cracking Model	233
Validation of the Alligator Cracking Model	234
LONGITUDINAL (TOP-DOWN) CRACKING MODEL	236
Prediction of Longitudinal Cracking in the MEPDG	236
Calibration of the Longitudinal Cracking Model	236
Validation of the Longitudinal Cracking Model	238
INTERNATIONAL ROUGHNESS INDEX (IRI) MODEL	239
Prediction of IRI in the MEPDG	239
Calibration of the IRI Model	239
Validation of the IRI Model	241
SUMMARY OF LOCAL CALIBRATION COEFFICIENTS	242
CONCLUSIONS	242
 <b>Chapter 11: CONCLUSIONS AND IMPLEMENTATION PLAN</b>	 241
CONCLUSIONS	244
IMPLEMENTATION PLAN	254
 <b>REFERENCES</b>	 255

<b>Appendix 2.1</b>	259
Python Program for the Retrieval and Processing of Daily Climate Normal Data from NOAA's Servers	
<b>Appendix 2.2</b>	263
Sample "Complete" Climate Normal File from New Mexico Coop Station NM290041	
<b>Appendix 2.3</b>	267
Sample "Partial" Climate Normal File from New Mexico Coop Station NM290022	
<b>Appendix 2.4</b>	268
Partial Sample ASCII Text File Containing Daily Climate Normal Values for Import into Oracle Database	
<b>Appendix 3.1</b>	269
Definition of Data Elements	269
<b>Appendix 3.2</b>	286
SQL Script	
<b>Appendix 4.1</b>	299
Python Script to Populate All Distress Data	
<b>Appendix 4.2</b>	304
Test.Map File Code	

## Chapter 1

# INTRODUCTION

### PURPOSE

NMDOT has made a recent movement from the AASHTO's 1993 empirical pavement design method to the Mechanistic Empirical Pavement Design Guide (MEPDG). The empirically based AASHTO 1993 design procedure cannot predict pavement performance accurately because it was developed based on limited AASHTO road tests in the 1960s. On the other hand, MEPDG (currently known as DARWin-ME) is a product of more than 20 years of pavement research and experience. It better predicts pavement performance through better utilization of local materials, factors such as present-day traffic conditions and regional climate, as opposed to the traditional empirical design methods. Nationally as well as in New Mexico, the use of MEPDG has resulted in significant improvements in pavement design, including savings from the selection of more economical combinations of materials. However, the input parameters and calibration coefficients addressing the conditions prevalent in New Mexico are unknown for ensuring an accurate design using the MEPDG. To that end, the goal of this research was set to develop design input parameters required by NMDOT designers, and to determine the calibration coefficients for New Mexico conditions.

The MEPDG uses stresses and strains in a pavement system calculated from the pavement response model (mechanistic part) to predict the performance (empirical part) of the pavement. The empirical nature of the MEPDG stems from the fact that the pavement performance predicted from laboratory-developed performance models is adjusted based on the observed performance from the field to reflect the differences between predicted and actual field performance. The performance models used in the MEPDG have been calibrated using limited national databases and thus, it is necessary to calibrate these models for implementation by taking into account local materials, traffic information, and environmental conditions. Thus, the coefficients incorporated in the performance models can be regarded as national averages (default coefficients). Although the NMDOT can use those models with "default" coefficients (Level 3 design), a higher level of reliability (accurate and economic) can be achieved by adjusting these model coefficients to represent the local conditions prevalent in New Mexico (Level 2 design).

The term local calibration here means to determine the performance model coefficients by reducing or minimizing the difference between the measured and predicted distresses of NMDOT pavements. In order to calibrate the MEPDG distress functions for New Mexico conditions, data from local pavements were collected. Some of these data reside in NMDOT's various databases, which have been designed and maintained with specific objectives, but not considering their potential use for pavement design at the time. Specifically some of these databases have been designed for network level applications, not to calibrate data intensive performance models such as those typical of mechanistic-empirical design models. In this study, NMDOT's various existing databases were collected, analyzed, and explored for data. A central MEPDG database was developed and populated with data from the various databases already in

existence, and a calibration of MEPDG was performed for New Mexico conditions using the developed database.

The primary goal of the research project is the successful implementation of MEPDG for the design and analysis of new and rehabilitated flexible pavements in New Mexico. The research project has two main objectives, which are to:

- Develop a flexible pavement database to be populated with data required for calibration of the MEPDG for New Mexico conditions.
- Perform local calibration of the MEPDG that is the process of making adjustments to the distress model coefficients to account for model limitations in predicting NMDOT's pavement behavior.

## **MEPDG BACKGROUND**

Since the adoption of the 1993 AASHTO Guide for Design of Pavement Structures, which was an improvement to the AASHTO 1986 Guide or AASHTO 1972, it was realized that there is a dire need to move towards a mechanistically based pavement design procedure. It was challenging to take the 1993 Guide (empirical-based) to the next level of analysis (mechanistic-empirical). In order to meet this challenge, the AASHTO Joint Task Force on Pavements, the National Cooperative Highway Research Program (NCHRP), and the Federal Highway Administration (FHWA) sponsored the development of a Mechanistic- Empirical pavement design procedure under NCHRP 1-37A in 1996. The specific goal was to develop an AASHTO mechanistic-empirical pavement design procedure by the year 2002. The final report of the NCHRP 1-37a was completed in March 2004 and was released to the public for review and evaluation. An Independent Review of the NCHRP 1-37A was conducted by NCHRP under project 1-40A and it was completed in 2006. The Independent review has resulted in a number of improvements, many of which were incorporated into the MEPDG under NCHRP Project 1-40D. Two products of project 1-40D are namely, a version 1.0 of the MEPDG software, and an updated MEPDG document. The AASHTO format of the current MEPDG document was completed in 2007. The MEPDG became an AASHTO Standard in 2008, and NMDOT has adopted the MEPDG or DARWin-ME in 2011.

The major benefits of adopting the MEPDG are long-term. While it is possible that immediate benefits may be seen in terms of thinner pavement or pavement with different controlled behavior, it is more likely that the benefits will be identified in the long term. Some of the benefits of MEPDG are listed below:

- The effects of differences in climatic conditions on pavement performance can be included in the design.
- Better utilization of the available construction materials can be made.
- Effects of different vehicle types, axle configurations, and tire types can be incorporated in the design process.
- Estimates of the consequences of new loading conditions (e.g., the damaging effects of increased loads) can be evaluated.

- Better pavement diagnostic techniques, such as improved procedures to evaluate premature distress, can be developed.
- Consideration can be given to seasonal and aging effects on materials and designs.

## Models in MEPDG

Figure 1 shows the mechanistic and empirical part of the MEPDG. The mechanistic models generate responses including stresses, strains, and deflections at critical locations of a pavement structure. Inputs to such models consist of the fundamental mechanical properties of the materials, applied wheel and axle loads, climatic conditions, and pavement structures including the number and thickness of layers. Pavement responses are then used as inputs to the empirical models to estimate pavement performance. The empirical models are regression equations, which are used to obtain a best fit between actual field performance and predicted distresses. Pavement performance, which is obtained from these empirical models, is measured in terms of distresses such as rutting, fatigue cracking, roughness. The disadvantage of the regression approach is that the models are limited to the conditions under which they are developed because they cannot include all the variables that affect the predicted distress. When the values of the variables are similar to those in the original data set, the regression models work well. However, when the models are applied to a different situation with different factors, the predictions are not accurate and hence the model requires local calibration.

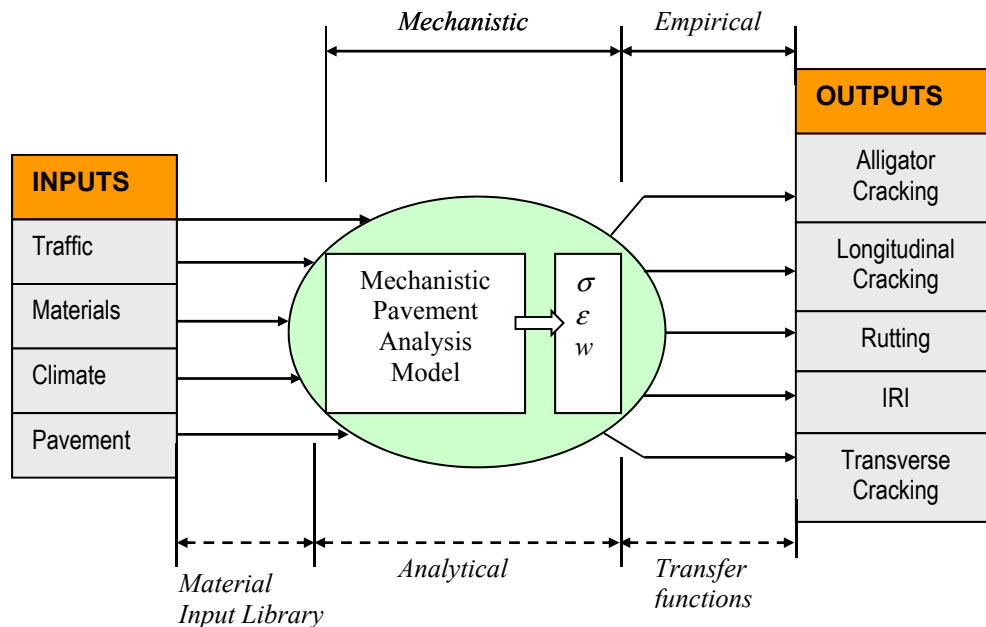


**FIGURE 1 Components of MEPDG**

## Analysis Sequence in the MEPDG

The MEPDG is based on mechanistic-empirical principles, where it assumes that pavement can be modeled as a multilayered elastic structure (i.e., software YULEA, WESLEA, LEAP,

MNLAYER). The MEPDG performs a time-stepping process, where the following sequence of operations is undertaken. At time =  $t$ :

1. The temperature and moisture profiles through the pavement are generated for the conditions at time =  $t$  (*Environment*).
2. The spectrum of traffic loadings, at time =  $t$ , is defined (*Traffic*).
3. The elastic properties and thickness of each layer ( $E$ ,  $\mu$ ,  $h$ ) are defined from the initial input, the age since construction, the temperature and moisture profiles, and the speed (duration or frequency) of each load (*Materials*).
4. The structural analysis is performed to estimate critical stresses and strains within the structure. Also, the structural analysis is performed to determine the non-load-related stresses and strains (i.e., due to thermal and moisture gradients) (*Mechanistic*).
5. The incremental distresses are computed based on the critical stresses and strains (or their increments). These distresses include rutting, cracking, and roughness (IRI). They are computed based on empirical models (*Empirical*).
6. Changes in initial material parameters ( $E$ ,  $\mu$ ) resulting from the computed incremental damage are estimated. For example, if a HMA layer (e.g.,  $E = 400$  ksi) is found to have been over-stressed and damaged during this time interval, its effective modulus may be reduced (say to 375 ksi psi) for the ensuing time interval (*State-Update*).
7. The time scale is incremented to  $t = t_0 + \Delta t$ , and the cycle repeated.

### Levels of MEPDG Analysis

In the MEPDG, three levels of input (Level 1, Level 2, and Level 3) can be used. The issue concerning when and where to use the individual design levels has not yet been objectively established because of the difficulty in determining the design level to practice. Theoretically, the determination of one specific design level is dependent on the importance of the project. For instance, the design of a project with significant importance, such as an interstate highway, will be assigned Level 1 input, whereas the design of a local low volume road can be categorized as Level 3 design. On the other hand, each design level requires specific input, especially for the higher levels; but the resources may not exist. For instance, a new highway design project with Level 1 input requirements usually does not have site-specific traffic information, because there is no WIM or AVC deployed at that site. In this situation, Level 2 may be adopted as an alternative, although its importance requires Level 1 data input. The recommendations for selecting a design level are as follows:

- Level 1 represents the highest accuracy level. It is recommended for most high volume highways, where early failures may cause important safety or economic consequences. The highway facilities using Level 1 design may include interstate highways, high volume U.S. highways, and state highways.



- Level 2 represents an intermediate level of accuracy. This level should be applied when the resources necessary for Level 1 are not available. This level can be used for most high-grade highway facilities, which may include interstate, U.S., and state highways. In addition, under certain conditions, such as the design of a new highway (Level 1) when not all site-specific information may be available, Level 2 may also be used in combination with Level 1. Level 2 is the most widely and practically used level for new and rehabilitated pavement designs.
- Level 3 represents the lowest accuracy level. This level can be used to design low volume highways such as Farm to Market (FM) and other local roadways where the potential implication of an early failure will not be associated with significant economic impacts. In addition, if there is insufficient data to support a highway design with Level 2 input, Level 3 can be used instead.

It can be pointed out that for pavement design practices, the input levels can be mixed in order to match a given situation. For example, Level 2 traffic, Level 1 material, and Level 3 climatic data can be used as inputs.

### Basics of Local Calibration

The local calibration process can be defined as minimizing the difference between the MEPDG predicted output values and the field observed distresses of New Mexico's flexible pavements. Local calibration is done through adjusting the distress model coefficients in MEPDG. There have been two NCHRP research projects that are closely related to the calibration of MEPDG. These are the NCHRP 9-30(001) and NCHRP 1-40B. Under the NCHRP 9-30(001) project, pre-implementation studies involving verification and recalibration were conducted in order to quantify the bias and residual error of the flexible pavement distress models included in the MEPDG. Based on the findings from the NCHRP 9-30(001) study, the NCHRP 1-40B project focuses on the calibration refinement study of the load-related distress prediction models for flexible pavements and HMA overlays. The NCHRP Project 1-40B produced a MEPDG User Manual and Local Calibration Guide, which was published as an Interim Guide in 2008. Distress model coefficients in MEPDG are discussed in detail below:

#### *Calibration Coefficients of the Rutting Models*

An incremental damage approach is used in the MEPDG to calculate the damage or rutting in each layer. As a first step, the accumulated plastic strains are calculated at the mid-depth of each layer during each season. The total permanent deformation is then calculated as the sum of permanent deformation in all layers and is mathematically expressed as:

$$RD = \sum_{i=1}^{nLayer} h_i \epsilon_i^p \quad (1)$$

where  $RD$  = Rut Depth,  $nLayer$  = number of layers,  $\epsilon_p$  = total plastic strain in layer  $i$ , and  $h$  = layer thickness.

**Asphalt Concrete Rutting:** The empirical models used in MEPDG to predict asphalt layer rutting are:

$$\frac{\varepsilon_p}{\varepsilon_r} = k_z \beta_{r1} 10^{k_1} T^{k_2 \beta_{r2}} N^{k_3 \beta_{r3}} \quad (2)$$

$$k_z = (C_1 + C_2 \times \text{depth}) \times 0.328196^{\text{depth}} \quad (3)$$

$$C_1 = -0.1039 \times h_{ac}^2 + 2.4868 \times h_{ac} - 17.342 \quad (4)$$

$$C_2 = 0.0172 \times h_{ac}^2 - 1.7331 \times h_{ac} + 27.428 \quad (5)$$

where  $\varepsilon_p$  = plastic strain,  $\varepsilon_r$  = resilient strain,  $T$  = layer temperature,  $N$  = number of load repetition,  $h_{ac}$  = thickness of AC layer, and  $k_z$  = function of total asphalt layers thickness and depth to computational point, to correct for the confining pressure at different depths. For national calibration, the value of coefficients:  $k_1 = -3.35412$ ,  $k_2 = 1.5606$ , and  $k_3 = 0.4791$ . The regression parameters:  $\beta_{r1}$ ,  $\beta_{r2}$ ,  $\beta_{r3}$  are the local calibration coefficients, which will be determined to represent the New Mexico conditions in the proposed study.

**Unbound Materials Rutting:** Equation 6 represents the rutting model of MEPDG for unbound granular base and subgrade materials:

$$\delta_a(N) = \beta_{s1} k_l \left( \frac{\varepsilon_o}{\varepsilon_r} \right) e^{-\left(\frac{\rho}{N}\right)^\beta} \varepsilon_v h \quad (6)$$

where  $\delta_a$  = permanent deformation for the layer,  $N$  = number of load repetition,  $\varepsilon_v$  = average vertical strain,  $h$  = thickness of the layer,  $\varepsilon_o$ ,  $\beta$ ,  $\rho$  = material properties,  $\varepsilon_r$  = resilient strain. For national calibration, the value of  $k_l = 2.03$  for (granular) and  $k_l = 1.35$  (fine-grained). The regression parameter:  $\beta_{s1}$  is the local calibration coefficient, which needs to be determined separately for granular base, sub-base and subgrade materials representing the New Mexico conditions.

### *Calibration Coefficients of the Fatigue Cracking Models*

The MEPDG utilizes an approach that models both top-down and bottom-up cracking scenarios. As a first step, the *fatigue damages* are determined at the surface for top-down cracking, and at the bottom of each asphalt layer for bottom up cracking. The fatigue damage is then correlated to the fatigue cracking using empirical models. Estimation of fatigue damage is based upon Miner's Law, which states that damage is given by the following relationship:

$$D = \sum_{i=1}^T \frac{n_i}{N_i} \quad (7)$$

where  $D$  = damage, that is the ratio of predicted number of traffic load repetitions to the allowable number of load repetitions,  $T$  = total number of periods,  $n_i$  = actual traffic for period  $i$ ,  $N_i$  = allowable load repetitions in period  $i$ . In the following paragraphs, the model for determining  $N_i = N_f$  from materials strength is discussed.

**Asphalt Concrete Fatigue:** The allowable number of load repetitions is given by:

$$N_f = 0.00432 \times 10^M \times \beta_{f1} k_1 \left( \frac{1}{\epsilon_t} \right)^{k_2 \beta_{f2}} \left( \frac{1}{E} \right)^{k_3 \beta_{f3}} \quad (8)$$

$$M = 4.84 \left( \frac{V_b}{V_a + V_b} - 0.69 \right) \quad (9)$$

where  $N_f$  = allowable number of repetitions in fatigue cracking,  $\epsilon_t$  = tensile strain at critical location,  $E$  = stiffness of the material,  $k_1$ ,  $k_2$ ,  $k_3$  = model coefficients,  $C$  = laboratory to field adjustment factor,  $V_b$  = percent effective binder content,  $V_a$  = percent air voids. For national calibration, the specified values for  $k_1$ ,  $k_2$  and  $k_3$  are 0.007566, 3.9492, and 1.281 respectively. The regression parameters:  $\beta_{f1}$ ,  $\beta_{f2}$ , and  $\beta_{f3}$  are the local calibration coefficients, which will be determined to represent the New Mexico conditions.

AC Top-down Cracking: The AC top down cracking model of MEPDG is presented below:

$$FC_{top} = \left( \frac{C_4}{1 + e^{C_1 - C_2 \times \log_{10} D}} \right) \times 10.56 \quad (10)$$

where  $FC_{top}$  = top-down fatigue cracking,  $D$  = percent damage,  $C_1$ ,  $C_2$ ,  $C_4$  = regression coefficients. Currently, specified values of  $C_1$ ,  $C_2$  and  $C_4$  are 7, 3.5 and 1000 respectively. These regression coefficients:  $C_1$ ,  $C_2$ ,  $C_4$  will be determined to represent the New Mexico conditions in the proposed study.

AC Bottom-up Cracking: The AC bottom up cracking model of MEPDG can be presented as follows.

$$FC_{bottom} = \left( \frac{C_4}{1 + e^{C_1 \times C'_1 - C_2 \times C'_2 \times \log_{10} (100 D)}} \right) \times 10.56 \quad (11)$$

$$C'_2 = -2.40874 - 39.748 \times (1 + h_{ac})^{-2.856} \quad (12)$$

$$C'_1 = -2 \times C'_2 \quad (13)$$

where  $FC_{bottom}$  = bottom up fatigue cracking (ft /mile),  $h_{ac}$  = thickness of the AC layer and  $C_1$ ,  $C_2$ ,  $C_4$  = regression coefficients. Currently, specified values of  $C_1$ ,  $C_2$  and  $C_4$  are 1.0, 1.0, and 6000, respectively. These regression coefficients:  $C_1$ ,  $C_2$ ,  $C_4$  will be determined to represent the New Mexico conditions in the proposed study.

**Chemically Stabilized Material (CSM) Fatigue:** The allowable number of load repetitions (to be used in Equation 7) is given by:

$$N_f = 10^{\left\{ \frac{k_1 \beta_{c1} - \left( \frac{\sigma_s}{M_r} \right)}{k_2 \beta_{c2}} \right\}} \quad (14)$$

where  $N_f$  = number of repetitions to fatigue cracking,  $\sigma_s$  = tensile stress (psi),  $M_r$  = modulus of rupture (psi),  $k_1$ ,  $k_2$  = . For national calibration, the specified values of regression coefficients:  $k_1$

and  $k_2$  are 1.0 and 1.0. The parameters:  $\beta_{c1}$  and  $\beta_{c2}$  are the local calibration coefficients, which will be determined to represent the New Mexico conditions in the proposed study.

CSM Cracking: The following model has been incorporated in MEPDG to calculate fatigue cracking of chemically stabilized base material:

$$FC_{ctb} = C_1 + \frac{C_2}{1 - e^{C_3 - C_4(\text{damage})}} \quad (15)$$

where  $FC_{ctb}$  = fatigue cracking in chemically stabilized base, and  $C_1$ ,  $C_2$ ,  $C_3$  and  $C_4$  = regression coefficients. Currently, specified values for  $C_1$ ,  $C_2$ ,  $C_3$  and  $C_4$  are 1.0, 1.0, 0.0 and 1000, respectively. These regression coefficients:  $C_1$ ,  $C_2$ ,  $C_3$  will be determined to represent the New Mexico conditions in the proposed study.

### *Calibration Coefficients of Thermal Fracture Model*

The thermal fracture model incorporated in the MEPDG is given below:

$$C_f = 400 \times N \left( \frac{\log C / h_{ac}}{\sigma} \right) \quad (16)$$

$$\Delta C = (k \times \beta_t)^{n+1} \times A \times \Delta K^n \quad (17)$$

$$A = 10^{4.389 - 2.52 \times \log(E \times \sigma_m \times n)} \quad (18)$$

where  $C_f$  = observed amount of thermal cracking,  $k$  = regression coefficient determined through field calibration,  $N$  = standard normal distribution,  $\sigma$  = standard deviation of the log of the depth of cracks in the pavements,  $C$  = crack depth,  $h_{ac}$  = thickness of the asphalt layer,  $\Delta C$  = change in the crack depth due to a cooling cycle,  $\Delta K$  = change in the stress intensity factor due to a cooling cycle,  $A$ ,  $n$  = fracture parameters for the asphalt mixture,  $E$  = mixture stiffness,  $\sigma_m$  = undamaged mixture tensile strength,  $\beta_t$  = calibration parameter. For national calibration, the specified values of  $k$  for level 1, level 2 and level 3 are 1.5, 0.5 and 1.5 respectively. The parameter  $\beta_t$  is the local calibration coefficient, which will be determined to represent the New Mexico conditions in the proposed study.

### *Calibration Coefficients of IRI Model*

International Roughness Index (IRI) is used to predict changes in pavement smoothness over time as a function of pavement properties at a given time. The functional relation of IRI with rutting, fatigue, cracking, and site factors is given below:

$$IRI = IRI_0 + \langle C_1, C_2, C_3 \rangle \times IRI_D + C_4 \times IRI_S$$

where  $IRI_0$  = Initial IRI,  $IRI_D$  = Increase due to surface distresses (rutting, fatigue cracking, transverse cracking),  $IRI_S$  = Increase from site specific factors such as swelling soils, frost susceptible soils. The parameters:  $C_1$ ,  $C_2$ ,  $C_3$  are the local calibration coefficients, which will be determined to represent the New Mexico conditions in the proposed study.

## Need for the MEPDG Database

Local calibration of MEPDG requires a flexible pavement database, which will contain data of material properties, pavement structural characteristics, highway traffic information, environmental conditions, and pavement performance such as cracking, rutting, and roughness. NMDOT's existing databases contain few of such information. Many of these existing databases have been designed and maintained with specific objectives, and have not been optimized for pavement design needs. For example, Consolidated Highway Database System (CHDB) have been designed for network level applications rather than calibration of project level data intensive performance models such as those typical of the MEPDG. Therefore, a central MEPDG database is required.

## METHODOLOGY

The research approach has two phases shown in Figure 2.

In Phase 1, a comprehensive MEPDG database was developed and populated with data mined from NMDOT's existing databases. Phase 1 includes the following tasks: review of MEPDG status including advances/barriers of successful implementation of MEPDG, review of NMDOT existing databases, review of Term Pavement Performance (LTPP) database and FWD data, design of MEPDG database architecture, population of the MEPDG database with existing data, adaptation of the architecture to handle evolving data and purposes, data integration and database maintenance. The focus of the UNM research team was to develop a relatively simple database, with a normalized structure, that runs under modern personal computer operating systems, and which can be operated by engineering and technician personnel not trained in advanced database theory.

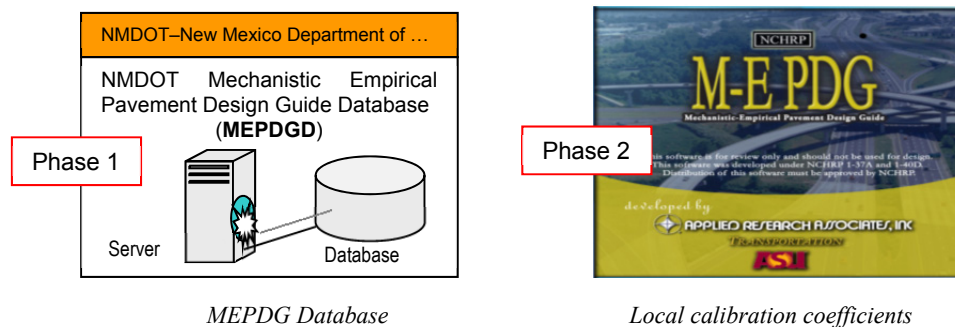


**FIGURE 2 Research Methodologies (Phases)**

In Phase 2, local calibration of MEPDG for New Mexico's condition was performed with the available data in the developed MEPDG database. Phase 2 includes several tasks such as: an in-depth analysis of the database to identify and rank the available inputs for MEPDG calibration; conducting initial calibration with the best available data; analyzing input sensitivity on the predicted distress levels; and refinement of calibration with more data and model execution experience.

## **REPORT ORGANIZATION**

Chapter 1 describes the purpose of this project, background, research methodology and research phases. Chapter 2 describes the NMDOT's existing databases and data related to the MEPDG inputs and outputs. Chapter 3 describes the architecture of the MEPDG database and database design methodology. Chapter 4 describes data, data source, and how they were populated into the MEPDG database. Chapter 5 shows the screenshots of the Web interfaces and related python and PHP programs. Chapter 6 prescribes the maintenance and management protocol of the developed MEPDG database. Chapter 7 describes complete datasets from NMDOT's LTPP sections and initial calibration of MEPDG using those data. Chapters 8 and 9 are related to sensitivity study using advanced statistical analyses namely parametric and nonparametric regressions, respectively. Chapter 10 is about the refined local calibration of the MEPDG using 23 complete data sets or pavement sections in New Mexico. Finally, Chapter 11 describes the conclusions and recommendations of this study.

## Chapter 2

### REVIEW OF EXISTING DATABASES

#### INTRODUCTION

This chapter includes the collection, review and analysis of NMDOT's existing databases and data useful to the MEPDG.

#### NMDOT's EXISTING DATABASES

The UNM research team organized a meeting on November 25, 2008 with NMDOT database owners. Based on the meeting discussion, it was found that there were about 30 existing databases of which 22 databases might have data related to MEPDG data. It was also noted that these databases had assigned to 22 personnel. These databases are listed in Table 2.1.

**TABLE 2.1 Databases from NMDOT**

No	Data Programs	Name	Data Availability	Comments
1	NMDOT Logo Fund	LOGOT	No	Access not required
2	Trades	TRADASPLAY	No	Access not required
3	Police Accidents Report	ARCS	No	Access not required
4	Training Wizard	TRAIT	No	Access not required
5	Human Resources Logos	HRLOG	No	Access not required
6	Ignition Interlock	DRAEGER, IIDAP IGNITIONSTAGE	No	Access not required
7	Items for Auction	AUCTION	No	Access not required
8	IT Budget	ITBUDGET	No	Access not required
9	Oracle Data integrator	ODI	No	Access not required
10	Transportation Information Management System	TIMS	Yes	Access required
11	Highway Maintenance Management System	HMMS	Yes	Access required
12	Decision Support System	DSS	Yes	Access required
13	Bridge Management System	Pontis (PONT)	Yes	Access required
14	Bridge Design and Rating System	Virtis/Opis	No	Access not required
15	Site Manager	HOSBT, HOSMT, HOSMU	Yes	Access required
16	Fleet Anywhere	FAT	No	Access not required
17	Material Testing	LIMS	Yes	Access required
18	Statewide Transportation Improvement Program	STIP, STIPDRP	No	Access not required
19	Bridge	CHDB	Yes	Included in TIMS
20	AASHTO Pes/Las	TPLCT	No	Access not required
21	GIS database	SDE	Yes	Access required
22	Orify	Orify	Yes	Access required

Finally, 13 databases/programs were not considered because they do not contain any important data related to MEPDG Database. The remaining 9 databases were considered for the MEPDG data source and they are listed in Table 2.2. A short description of these databases is given below:

**TABLE 2.2 Selected databases from NMDOT**

Serial No	Data Programs	Name
1	Transportation Information Management System	TIMS
2	Highway Maintenance Management System	HMMS
3	AASHTO Decision Support System	DSS
4	Bridge Management System	Pontis (PONT)
5	Site Manager	HOSBT, HOSMT, HOSMU
6	Material Testing	LIMS
7	GIS database	SDE
8	Orify	
9	Pavement Management System	PMS <sup>1</sup>

<sup>1</sup>Not included in central database. Operated in NMDOT it section

### **Transportation Information Management System (TIMS)**

TIMS database mainly contains data related to managing transportation infrastructure, inventory, attributes and assets. This database is still under development. In its current form, TIMS mainly contains data of traffic, traffic safety and control information. It has replaced the old Consolidated Highway Database (CHDB), developed in 1980's. The data that were available in the CHDB database are mostly related to project design, pavement conditions and traffic volume. In addition to CHDB data, data such as WIM data, LTPP data, MPO/RPO traffic database, district maintenance office data and field sensors will be available in TIMS in future.

### **Highway Maintenance Management System (HMMS)**

HMMS database contains data related to maintenance activities including date, location, type of activity, labor, equipment, materials used. HMMS stores information required to support subsystem such as pavement and bridge. HMMS is in place for more than 30 years to support management and maintenance activities successfully. HMMS exchanges information with the other systems such as the FMIS, Fleet Anywhere System, etc.

### **Decision Support System (DSS)**

DSS is designed to manage data to support production and timely distribution of short-term, site-specific now casts/forecasts. The DSS enables evaluation for bid monitoring and evaluation, vendor and market analysis, and as-bid to as-built analysis, item price estimation and the



planning and budgeting process. It does not include any construction data. However, it can provide the information about type of project, location (latitude and longitude) of project and other general information.

### **Pontis**

Pontis is a comprehensive bridge management system developed as a tool to assist in the task of bridge management. Pontis stores bridge inventories and records inspection data. It is used for maintenance tracking and federal reporting. Additionally, it provides a full scenario of location of bridges, milepost and as built drawings.

### **Site Manager**

Site Manager is a contract management system, designed as an easy-to-use tool for state highway agencies for large and small projects. Site Manager is an integrated series of computerized forms for entering and viewing all information needed for a contract from the planning stage to the archival stage in a central database. It reflects the most up-to-date information available. It can take information about contractor payroll forms and other documents, contract administration, daily work reports, change orders, civil rights and materials management.

### **Laboratory Information Management System (LIMS)**

LIMS is used for the management of samples, laboratory users, instruments, standards and other laboratory functions such as invoicing, management, and workflow automation. It is one of the most important databases, which contains some data for MEPDG. All test results, conducted in NMDOT laboratories for cement, aggregate, soils, asphalt, and other materials are available in this database. Example of data extracted and used to populate MEDPG data base are binder properties, R-value, etc.

### **GIS Database**

Geographic Information System (GIS) data are useful for programs involving spatial analysis and mapping. NMDOT has gathered many data over the years to support the GIS program. Current GIS applications in right-of-way involve: property/asset management including airspace leasing; excess land inventory; excess land disposition; land and water rights acquisition; and miscellaneous applications for road exchanges. NMDOT maps such as New Mexico Traffic Flow Maps (2006), Milepost Maps are available.

### **Orify**

This database includes thirty-three types of road features for each road segment. This database is also useful for calculating total road cost. It also delivers data related to physical attributes of pavements.

## Pavement Management System (PMS) Data

PMS data were collected with the assistance of Mr. Robert Young of NMDOT. Both qualitative and quantitative forms of pavement distress data were collected. The UNM research team has converted the distress data to quantitative values.

## ANALYSIS OF EXISTING DATABASES

The UNM research team reviewed NMDOT connection procedure to determine the accessibility of the above databases. It was revealed that these databases are not accessible outside DOT's hub. Consequently, only a data bump copy was available to the UNM researchers. Review of databases from the bump copy was a daunting task due to the complexity of database structures, lack of documentation and variable platforms. Some of these databases are being run on mainframe, and most databases have been upgraded to the oracle platform. For example, DSS database has about 349 tables, among which 162 tables have no data at all.

**TABLE 2.3 Selected tables from DSS**

Table Name	Description
T_AGG_MSTR_CNTNT	Records test result data for the detail level information for the Total Moisture Content of Aggregate by Drying tests.
T_AGG_SPC_GR	Record test result data for the detail level information for the specific gravity of soils tests.
T_BIT_CONC_MIXBLND	Contains the composition of materials for a mix design.
T_CLA_LMP_FRIBLPRT	Record test result data for the detail level information for the Clay Lumps and Friable Particles in Aggregate tests.
T_LOS_ANGELES_ABR	Record test result data for the detail level information for the Los Angeles Abrasion tests.
T_M226_BNDR_SPC	Record test result data for the detail level information for the AASHTO M226 Binder Specification tests.
T_MARSHALL	Records all header information associated with a Marshall Mix Design. This information allows the department to verify performance and production of materials based on test results in comparison to the mix design values.
T_MATL_GRDN_DTL	Allows the department to define a list of the gradation specification values for a specific material. These values are used in various test screens to compare test results to specification limits.
T_MATL_GRDN_HDR	Allows the department to identify all gradations that may be used for a specific material. This list is used after a sample has been entered to allow the user to identify the gradations
T_NUC_DNSTY_HDR	Record test result data for the Header level information for the Nuclear Density tests.
T_NAMGSO4_SNDNSHDR	Record test result data for the header level information for the Sodium or Magnesium Sulfate Soundness tests.
T_MIX_DSN_GRDN	Records blended gradations for a mix design.
T_NAMGSO4_SDNSTDITL	Record test result data for the detail level information for the Sodium or Magnesium Sulfate Soundness tests.
T_NUC_DNSTY_DTL	Record test result data for the detail level information for the Nuclear Density tests.
T_NAMGSO4_SNDNSHDR	Record test result data for the header level information for the Sodium or Magnesium Sulfate Soundness tests.

About 295 tables have their corresponding description (entity) in the table. Data were extracted and analyzed from these tables. Data from only 14 tables were found to be related to the MEPDG database. These data are listed in the Tables 2.3 and 2.4. Among these 14 tables, 2 of them contain data of soil properties. The rest of the tables are related to data of asphalt properties (Table 2.5).

**TABLE 2.4 Summary of DSS tables**

Category	Table Name
SOIL	T_AGG_MSTR_CNTNT
	T_AGG_SPC_GR
ASPHALT CONCRETE	T_BIT_CONC_MIXBLND
	T_CLA_LMP_FRIBLPRT
	T_LOS_ANGELES_ABR
	T_M226_BNDR_SPC
	T_MARSHALL
	T_MATL_GRDN_DTL
	T_MATL_GRDN_HDR
	T_MIX_DSN_GRDN
	T_NAMGSO4_SNDNSHDR
	T_NAMGSO4_SNDNSHDR
BINDER	T_NUC_DNSTY_DTL
	T_NUC_DNSTY_HDR

**TABLE 2.5 Useful information of DSS to MEPDG database**

<ul style="list-style-type: none"> <li>• T_AGG_MSTR_CNTNT <ul style="list-style-type: none"> <li>◦ Percentage of moisture in Aggregate</li> </ul> </li> <li>• T_AGG_SPC_GR <ul style="list-style-type: none"> <li>◦ Bulk specific gravity</li> </ul> </li> <li>• T_BIT_CONC_MIXBLND <ul style="list-style-type: none"> <li>◦ Bulk specific gravity</li> </ul> </li> <li>• T_CLA_LMP_FRIBLPRT <ul style="list-style-type: none"> <li>◦ Clay Content in Aggregate</li> </ul> </li> <li>• T_LOS_ANGELES_ABR <ul style="list-style-type: none"> <li>◦ Properties of Aggregates</li> </ul> </li> <li>• T_M226_BNDR_SPC <ul style="list-style-type: none"> <li>◦ Specific Gravity</li> <li>◦ Penetration</li> </ul> </li> <li>• T_MARSHALL <ul style="list-style-type: none"> <li>◦ Bulk Specific Gravity</li> </ul> </li> </ul>	<ul style="list-style-type: none"> <li>• T_MATL_GRDN_DTL <ul style="list-style-type: none"> <li>◦ Gradation</li> </ul> </li> <li>• T_MATL_GRDN_HDR <ul style="list-style-type: none"> <li>◦ Gradation</li> </ul> </li> <li>• T_MIX_DSN_GRDN <ul style="list-style-type: none"> <li>◦ Gradation</li> </ul> </li> <li>• T_NAMGSO4_SNDNSDTL <ul style="list-style-type: none"> <li>◦ Gradation</li> </ul> </li> <li>• T_NAMGSO4_SNDNSHDR <ul style="list-style-type: none"> <li>◦ Gradation</li> </ul> </li> <li>• T_NUC_DNSTY_DTL <ul style="list-style-type: none"> <li>◦ Density</li> <li>◦ Moisture content</li> </ul> </li> <li>• T_NUC_DNSTY_HDR <ul style="list-style-type: none"> <li>◦ Max Density</li> </ul> </li> </ul>
--	---

## REVIEW OF LTPP DATABASE

LTPP stands for Long Term Pavement Performance Program. It is an information management system and world's largest pavement performance database. UNM research team has identified all significant sections of LTPP in New Mexico and gathered data.

LTPP deals with various experiments in General Pavement Studies (GPS) and Specific Pavement Studies (SPS) that began in 1989 and early 1990s, respectively. LTPP has data of climatic

conditions, material properties, traffic volumes and loads, pavement layer thicknesses, and pavement performance. Total 8.5 gigabytes of LTPP data are online and 45 gigabytes are offline. The database is divided into modules containing similar sets of tables. There are 16 general data module. Each of the modules contains some tables that describe the structure and content of the database, and general comments tables. These tables contain different types of data collected by LTPP program for different issues. The data types are codes, region, deflection, etc. There are 430 tables in the entire LTPP database. Each table contains some data elements consist of date, number, temperature, time, etc. There are about 8000 unique data elements in the LTPP database.

The first step to extract data from the database is to select the LTPP test sections of region or state (New Mexico, state code is 35). LTPP experiments are subdivided into different modules such as climate, general, inventory, monitoring, maintenance, test sections, SPS sections, and traffic. Data from the tables can be extracted and exported to MS Excel format.

**TABLE 2.6 List of LTPP studies in New Mexico**

Experiment No	Description	Section ID Number	County	Route Number	Latitude (deg)	Longitude (deg)
GPS-1	Asphalt Concrete (AC) Pavement on Granular Base	35-1003-1	CHAVES	70	33.38	104.73
		35-1005-1	SANTA FE	25	35.51	106.24
		35-1022-1	SAN JUAN	44	36.37	107.83
		35-1112-1	LEA	62	32.63	103.52
GPS-2	AC Pavement on Bound Base	35-2006-1	SANDOVAL	44	36.17	107.33
		35-2118-1	QUAY	40	35.17	103.47
GPS-3	Jointed Plain Concrete Pavement	35-3010-1	LEA	62	32.64	103.52
GPS-6A	Existing AC Overlay of AC Pavement (existing at the start of the program)	35-1002-1	LINCOLN	70	33.37	104.92
		35-1002-2	LINCOLN	70	33.37	104.92
		35-2007-1	RIO ARRIBA	44	36.25	107.6
		35-6033-1	SOCORRO	25	34.2	106.93
		35-6035-1	CIBOLA	40	35.08	107.65
		35-6035-2	CIBOLA	40	35.08	107.65
		35-6401-1	CIBOLA	40	35.04	107.48
GPS-6D	AC Overlay on Previously Overlaid AC Pavement Using Conventional Asphalt	35-6033-2	SOCORRO	25	34.2	106.93
GPS-6S	AC Overlay of Milled AC Pavement Using Conventional or Modified Asphalt	35-2007-2	RIO ARRIBA	44	36.25	107.6
		35-2118-2	QUAY	40	35.17	103.47

The volume of the LTPP database is huge. The data are stored using a relational database design to store massive amounts of data in a very organized fashion. The UNM research team has extracted reviewed and evaluated all the useful LTPP data of New Mexico. The GPS and SPS

sections in New Mexico are listed Tables 2.6 and 2.7. The locations of GPS and SPS sections are shown in Google map (Figure 2.1 and 2.2)

**TABLE 2.7 List of LTPP studies in New Mexico**

Experiment Number	Description	Section ID Number	County	Route Number	Latitude (deg)	Longitude (deg)
SPS-1	Strategic Study of Structural Factors for Flexible Pavements	35-0101-1	DONA ANA	25	32.68	107.07
		35-0102-1	DONA ANA	25	32.68	107.07
		35-0103-1	DONA ANA	25	32.68	107.07
		35-0104-1	DONA ANA	25	32.68	107.07
		35-0105-1	DONA ANA	25	32.68	107.07
		35-0106-1	DONA ANA	25	32.68	107.07
		35-0107-1	DONA ANA	25	32.68	107.07
		35-0108-1	DONA ANA	25	32.68	107.07
		35-0109-1	DONA ANA	25	32.68	107.07
		35-0110-1	DONA ANA	25	32.68	107.07
		35-0111-1	DONA ANA	25	32.68	107.07
		35-0112-1	DONA ANA	25	32.68	107.07
SPS-5	Rehabilitation of AC Pavements	35-0501-3	GRANT	10	32.2	108.28
		35-0502-2	GRANT	10	32.2	108.28
		35-0503-2	GRANT	10	32.2	108.28
		35-0504-2	GRANT	10	32.2	108.28
		35-0505-2	GRANT	10	32.2	108.28
		35-0506-3	GRANT	10	32.2	108.28
		35-0507-3	GRANT	10	32.2	108.28
		35-0508-3	GRANT	10	32.2	108.28
		35-0509-3	GRANT	10	32.2	108.28
SPS-8	Strategic Study of Structural Factors for Flexible Pavements	35-0801-2	GRANT	1014	32.19	108.3
SPS-9	Superpave Asphalt Binder Study	35-901-3	GRANT	10	32.2	108.25
		35-902-3	GRANT	10	32.2	108.25
		35-903-3	GRANT	10	32.2	108.25
		35-959-3	GRANT	10	32.2	108.25

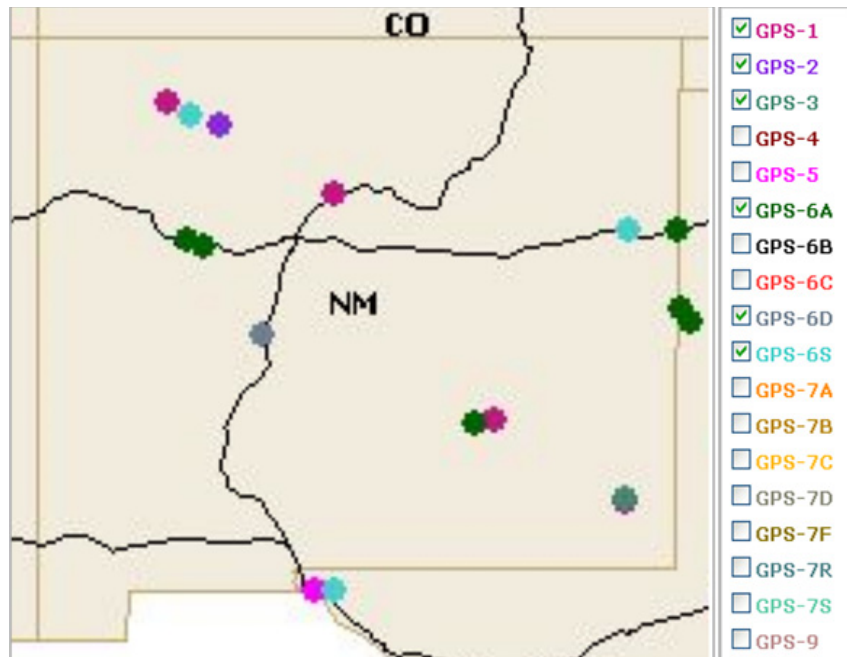


**FIGURE 2.1 GPS Sections of New Mexico**

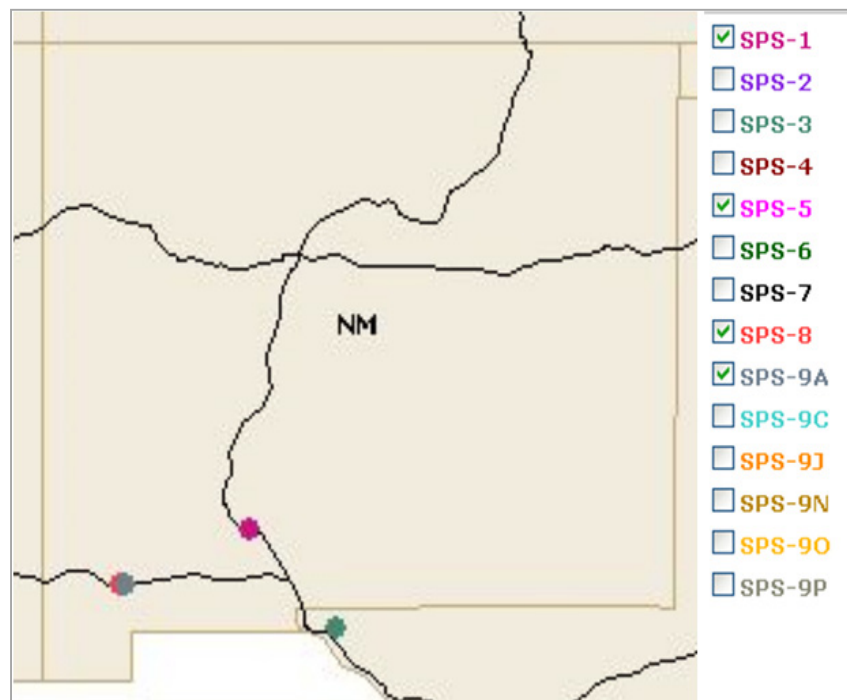


**FIGURE 2.2 SPS Sections of New Mexico**

A question was raised about the laboratory testing data of the LTPP sections of NM. Another question was about traffic data collection. Answers to some of the questions regarding LTPP data are described below:

Q1. Who did the lab tests for E\*, and M<sub>r</sub> data of LTPP's GPS sections?

ROAD NAME	LTPP SECTION	SHRP ID	LAYER NO	LAB
US-70	GPS	1002	1/2	Law Engineering, Atlanta, GA
		1003	1/2	
US-62		1112	3	Braun Intertec, Edina, MN
		1112	1/2	Law Engineering, Atlanta, GA
		3010	1/2	
US-44		2007	7	Braun Intertec, Edina, MN
		2007	2	Law Engineering, Atlanta, GA
		2006	1/2	
		1022	1/2	
US-40		2118	1/2/3	Law Engineering, Atlanta, GA
		6035	1/3	
		6401	1/3	

Q2: Who did the lab tests for E\*, and M<sub>r</sub> data of LTPP's SPS sections?

ROAD NAME	LTPP SECTION	SHRP ID	LAYER NO	LAB
I-25	SPS-1	0101	4	Braun Intertec, Edina, MN
		0105	4	
		0105	5	
		0106	4	
		0106	5	
		0107	5	
		0108	5	
		0112	5	
		0112	6	
		0101	1	Law Engineering, Atlanta, GA
		0102		
		0103		
		0105		
		0106		
		0107		
		0108		
		0109		
		0110		
		0111		
		0112		
I-10	SPS-5	0503	7	Braun Intertec, Edina, MN
		0504	3/4/5/7	
		0505	3/4/5	
		0507	7	
		0508	3/4/7	
		0801	3	
		0802	3	

Q3: What do you know about traffic data collection of LTPP Sections?

LTPP traffic data consists of traffic volume, vehicle classification, monthly and hourly distribution, and axle loading information for each General Pavement Studies (GPS) test location. Historical traffic has also been retrieved for the GPS sites. The traffic data include distribution of traffic by vehicle classes; days of data collected; and distribution of axle loads for single, tandem, and tridem axles by vehicle class. For locations where traffic data have been collected for all lanes, the data include average annual daily traffic (AADT) and percent trucks.

The properties of LTPP traffic data for the GPS sections are discussed further below:

### **Monitoring and Data Collection Procedure**

Traffic data were collected separately for the lanes (or lane) being monitored. Because each lane experiences different traffic, each should be considered as a separate test section. For LTPP, data collection is planned only for the outside lane in one direction. Data forms have been developed to capture information on sections in-service before the start of monitoring in 1990. Data collected from 1990 forward has been submitted in one of the electronic record formats documented in FHWA's *Traffic Monitoring Guide* (TMG), second through fourth editions. Data are submitted between twice a month and annually. Except for special cases, monthly submittal is preferred, and quarterly is typical. In the absence of electronic data on a section, a set of data forms has been provided for recording estimates of traffic during that timeframe.

Three alternatives are employed for collecting traffic data at the GPS test locations (Rada 1994):

- Preferred traffic data collection - permanent, year-round weigh-in-motion (WIM) equipment installed at each site and operated continuously. Figure 2.3 shows the site monitoring layout for a preferred data collection system.
- Desirable traffic data collection - a permanent, year round automatic, site specific, vehicle classifier, supplemented by and one week of weigh-in-motion measurements for each season at each study site.
- Minimum traffic data collection - a year-round vehicle classifier, counting a minimum of one full year during each five-year period, supplemented by one 48-hour weekend and one 48 hour weekday weigh-in-motion session conducted during each season of the year.



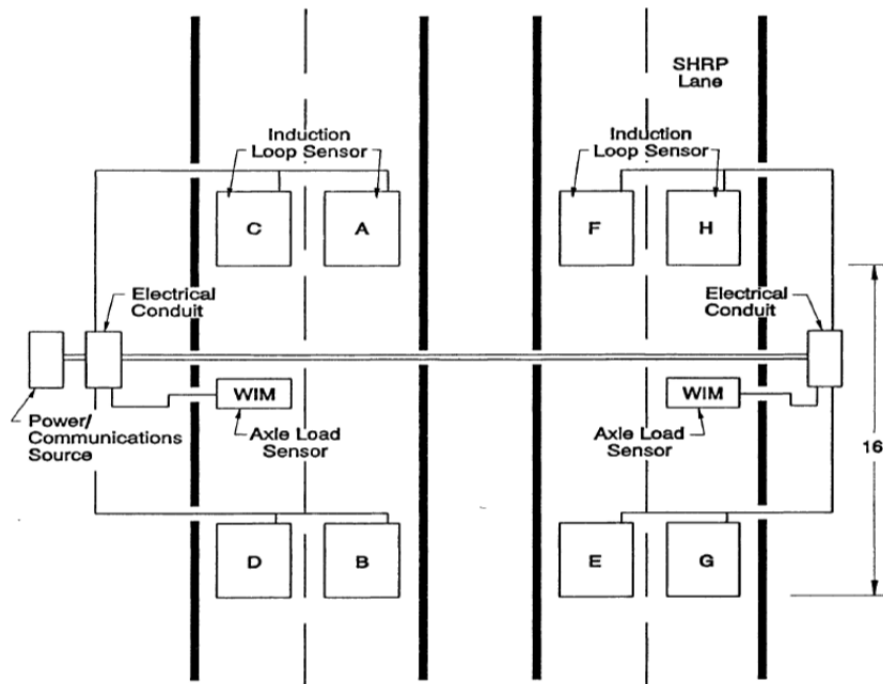


**FIGURE 2.3 LTPP site monitoring Layout (Rada, G. R. 1994)**

## Principles of Traffic Data Collection

The traffic data collection plan recognized the following major principles:

- Traffic loading estimates should be the result of onsite measurements wherever possible.
- Data from all LTPP locations should be treated consistently in collection, submission, review, and aggregation, without modification to reflect “expected” values.
- Data included in the database should follow the principle of “truth in data”. The term “truth in data” has been defined to include the following:
  - Practices and conditions under which the data have been collected must be reported.
  - Editing of traffic data must be documented and a record of the original (unedited) data must be retained.
  - Data variance estimates should be reported when possible.

## Traffic Data Storage

Data for individual vehicles require considerable computer storage, so these are expected to be stored offline rather than directly in the LTPP Information management System (IMS). Appropriate summary data such as numbers of axles in certain weight categories, vehicles in

certain classes, equivalent axle loads, etc., are to be calculated from the raw data and stored in the LTPP IMS.

Data have been submitted using the TMG classification schemes (Truck Weight Study 6-digit and 13-bin) as well as agency-defined schemes. All offline data and daily summaries are provided in the classification scheme used for submission. All data provided from online sources summarized at the monthly or annual level are in the TMG 13-bin classification scheme.

## **Traffic Data Reporting**

Traffic data reporting for LTPP is separated into two categories: historical and monitoring. Historical traffic data are defined to cover the period from the dates the pavement sections were initially opened to traffic (or from the date of the most recent overlay or rehabilitation project) through 1989. The overall purpose of historical traffic data collection is to obtain the best estimate of annual traffic levels on each test section before the time monitoring began on that section. The monitored traffic data cover traffic data collection activities initiated for monitoring the LTPP test section. Traffic data are reported in hourly and per-vehicle formats for traffic volume, vehicle classification, and truck axle weight.

## **Historical Traffic Data at GPS Locations**

Historical traffic data provides background information, an explanation of the historical and monitoring traffic data requirements, historical data forms, monitoring data formats, and baseline information about collecting and processing of traffic data. Historical data was initially retrieved from the files for two sites in each SHA. Historical traffic data was received for over 95% of GPS test locations which is an important element in a number of early data analysis studies (Rada, G. R. 1994).

## **Traffic Database**

LTPP database does not contain “raw” traffic monitoring measurements. The raw traffic data are stored in a separate traffic database. The Central Traffic Database (CTDB) contains the raw traffic data submitted to the LTPP program that were used to compute the annual estimates contained in the pavement performance. Raw traffic monitoring data provided to the LTPP program are subjected to a quality control and assurance process involving review by the submitting agency. These data are then used to produce the variety of annual estimates stored in the pavement performance database. LTPP adopted Federal traffic data monitoring submission standard formats.

## **REVIEW OF CLIMATIC DATA**

Currently, climatic data from 13 weather stations are available in MEPDG for New Mexico. The weather stations included in the Integration Climatic Model (ICM) are listed in Table 2.8.

**TABLE 2.8 Weather stations located in New Mexico which are in MEPDG**

Weather Station	Latitude (degrees. Minutes)	Longitude (degrees. Minutes)	Elevation (ft)	Location
Albuquerque	35.02	-106.37	5308	Albuquerque Intl Sunpt Apt
Carlsbad	32.2	-104.16	3234	Cavern City Air Trml Arpt
Clayton	36.27	-103.09	4971	Calyton Muni Airpark Arpt
Clines Corners	35	-105.4	7092	Clines Corners
Deming	32.16	-107.43	4304	Deming Municipal Airport
Farmington	36.44	-108.14	5531	Four Corners Regional Arpt
Gallup	35.31	-108.47	6469	Gallup municipal Airport
Las Vegas	35.39	-105.08	6862	Las Vegas municipal Arpt
Raton	36.44	-104.3	6362	Raton Muni/Crews Field Apt
Roswell	33.19	-104.32	3652	Roswell Indus Air Cntr Apt
Santa Fe	35.37	-106.05	6335	Santa Fe Municipal Airport
Truth or Consequences	33.14	-107.16	4823	Trh or Conseqces Muni Arpt
Tucumcari	35.11	-103.36	4056	Tucumcari Municipal Arpt

The UNM research team decided to include more weather stations for MEPDG implementation in New Mexico. As for the requirements of MEPDG, UNM research team sorted the data into categories listed in Table 2.9, which are especially useful to MEPDG. GIS map of weather stations selected for New Mexico in MEPDG are presented in the Figure 2.4. In this map, the green dots represent the weather stations that are available in the MEPDG. It is evident from the figure that the green dots are not evenly distributed. There are several grids or regions that do not have any weather station in MEPDG. It may be beneficial to the NM MEPDG if more weather station data are available. Therefore, the UNM research team has gathered information (location) of the points that are at the center of the grid box shown in Figure 3. Table 10 shows the additional weather stations' latitude and longitudes. About 22 weather stations locations, additional to existing 13 stations, were considered for MEPDG implementation in New Mexico. The locations were selected based on their proximity to the road network. These stations were incorporated into the MEPDG database. Data from the weather stations at or near these grid box/points are collected and stored in MEPDG database.

**TABLE 2.9 Climatic Data for New Mexico from the Climate Atlas**

The climatic-related inputs required for MEPDG	Corresponding Data in Climate Atlas	
Hourly air temperature (The Design Guide needs climatic data at each time step.)	Filename	Description
	TEMP02A	Mean Daily Maximum Temperature
	TEMP12A	Record Extreme Maximum Temperature
	TEMP02B	Mean Daily Minimum Temperature
	TEMP13B	Mean Extreme Minimum Temperature
	TEMP12B	Record Extreme Minimum Temperature
	TEMP03	Mean Daily Average Temperature
	TEMP04	Mean Daily Temperature Range
	TEMP07	Median/Mean Length of Freeze-Free Period
	HDD08	Mean Total Heating Degree Days
	TEMP20	Record Maximum Heating Degree Days
	CDD09	Mean Total Cooling Degree Days
	TEMP18	Record Maximum Cooling Degree Days
Precipitation	PREC01	Mean Total Precipitation
	PREC15B	Mean Maximum Daily Precipitation
	PREC16	Record Total Precipitation
	PREC26	Mean Number of Days with Measurable Precipitation
	SNOW14	Mean Total Snowfall
	SNOW27	Mean Maximum Daily Snowfall
	SNOW28	Record Total Snowfall
	SNOW31	Mean Number of Days with Measurable Snowfall (Thresholds)
Hourly Wind Speed (As the computational method illustrated in the Design Guide, daily wind speeds are required for the design)	SNOW33	Dates of First/Last Snowfall
	WIND60B	Mean Wind Speed
	WIND60A	Mean Wind Speed and Prevailing Direction
Hourly percentage Sunshine (used to define cloud cover)	WIND60C	Fastest Mile of Wind
	SKYC51A	Mean Number of Clear Days (Sunrise to Sunset)
	SKYC51B	Mean Number of Partly Cloudy Days (Sunrise to Sunset)
	SKYC51C	Mean Number of Cloudy Days (Sunrise to Sunset)
	FOG44	Mean Number of Days with Heavy Fog
	SUN52	Mean Sunshine Percentage
	SUN53	Mean Sunshine Total Hours
Hourly relative humidity	SKYC50	Mean Sky Cover (Sunrise to Sunset)
	RH23	Mean Relative Humidity

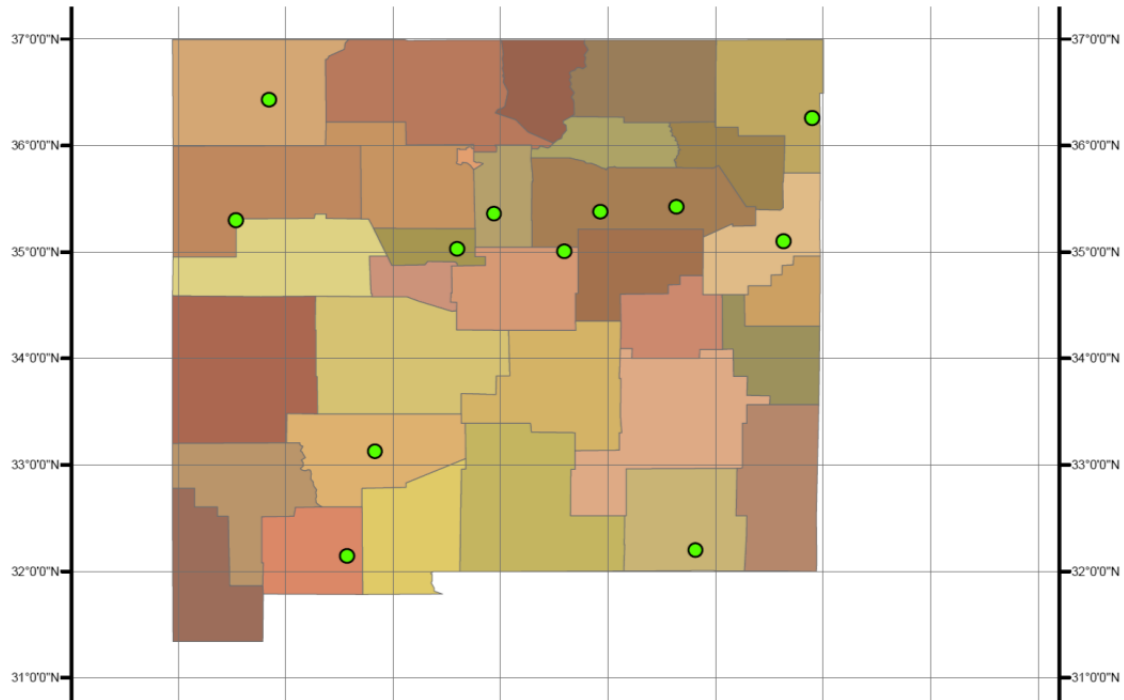


**FIGURE 2.4 Weather Stations Located in New Mexico whose Data are in MEPDG**

**TABLE 10 Proposed weather stations located in New Mexico**

Location ID	Longitude (degrees in Minutes)	Latitude (degrees in Minutes)
1	-108.22	36.74
2	-107.61	36.77
3	-106.56	36.73
4	-107.87	35.2
5	-104.47	35.46
6	-103.39	35.39
7	-108.51	34.32
8	-107.6	34.09
9	-106.74	34.78
10	-105.27	34.6
11	-104.27	34.47
12	-103.19	34.42
13	-108.76	33.72
14	-106.86	33.94
15	-105.26	33.39
16	-104.5	33.42
17	-103.75	33.41
18	108.31	32.75
19	-107.48	32.6
20	-106.76	32.32
21	-105.41	32.6
22	-103.39	32.71

Weather stations located near to the boarder of New Mexico in surrounding states are also considered. Their latitude and longitudes are listed in Tables 2.11 to 2.14.

**TABLE 2.11 Proposed weather stations located in Colorado**

Location ID	Longitude (degrees in Minutes)	Latitude (degrees in Minutes)
1	-108.29	37.14
2	-107.50	37.17
3	-106.8	37.41
4	-102.32	37.1
5	-107.19	38.26
6	-105.13	38.28
7	-102.22	38.49

**TABLE 2.12 Proposed weather stations located in Arizona**

Location ID	Longitude (degrees in Minutes)	Latitude (degrees in Minutes)
1	-111.4	35.08
2	-110.51	31.25
3	-111.27	36.56
4	-111.59	33.26
5	-109.38	32.51
6	-111.55	33.37
7	-109.23	34.31
8	-110.58	32.08

**TABLE 2.13 Proposed weather stations located in Texas**

Location ID	Longitude (degrees in Minutes)	Latitude (degrees in Minutes)
1	-101.43	35.13
2	-101.23	35.42
3	-100.17	34.26
4	-102.33	36.01
5	-100.55	29.22
6	-106.23	31.49
7	-102.55	30.55
8	-104.49	31.5
9	-101.49	33.4

**TABLE 2.14 Proposed weather stations located in Oklahoma**

Location ID	Longitude (degrees in Minutes)	Latitude (degrees in Minutes)
1	-99.46	36.18
2	-101.31	36.41

## **Ground Water Depth Processing and Extraction Service**

In preparation for the determination of ground water depth for road segments selected for modeling in MEPDG, source data for depth to ground water were obtained from the New Mexico Office of the State Engineer. These data were processed into derived products from which ground water depth could be extracted for arbitrary points within the state, including points that correspond with MEPDG road segments. Finally, an Open Geospatial Consortium (OGC) Web Map Service (WMS) and associated Python CGI (Web) script were created that allow for both online mapping and data value extraction from the derived ground water depth products. This capability allows for the retrieval of ground water values for any X-Y location within the state of NM as an XML file that can be programmatically processed for ingest into a database or used to initialize a model run. The remainder of this section outlines the process used to generate the derived data products and the access model available through the WMS service.

The source data for the estimation of ground water depth on statewide bases is the OSE Well Data set available for download from the Office of the State Engineer's (OSE) geospatial data Web page ([http://www.ose.state.nm.us/water\\_info\\_data.html](http://www.ose.state.nm.us/water_info_data.html)). The specific ESRI shape file downloaded from the OSE site is ose\_Wells\_nov08.shp. This shape file contains Well data as of November 2008, including data for each Well on depth to ground water. These data are represented as points with associated attributes. In order to generalize these points to a format that streamlines extraction of attribute values for nearby locations, two geospatial data products were derived from this point coverage.

The derived geospatial data products are of two types - a vector data file that consists of voronoi polygons surrounding each Well location. Each polygon is assigned the attributes of the Well point encompassed by the polygon. Each polygon encompasses the region for which the associated Well location is the closest Well. An illustration of the generated voronoi polygons and associated Well locations is provided in Figure 2.5. These polygons provide the ability to select any coordinate within New Mexico, and one polygon will be returned that corresponds with that coordinate. The attributes for the selected polygon represents the values associated with the OSE Well location closest to the selected coordinate.

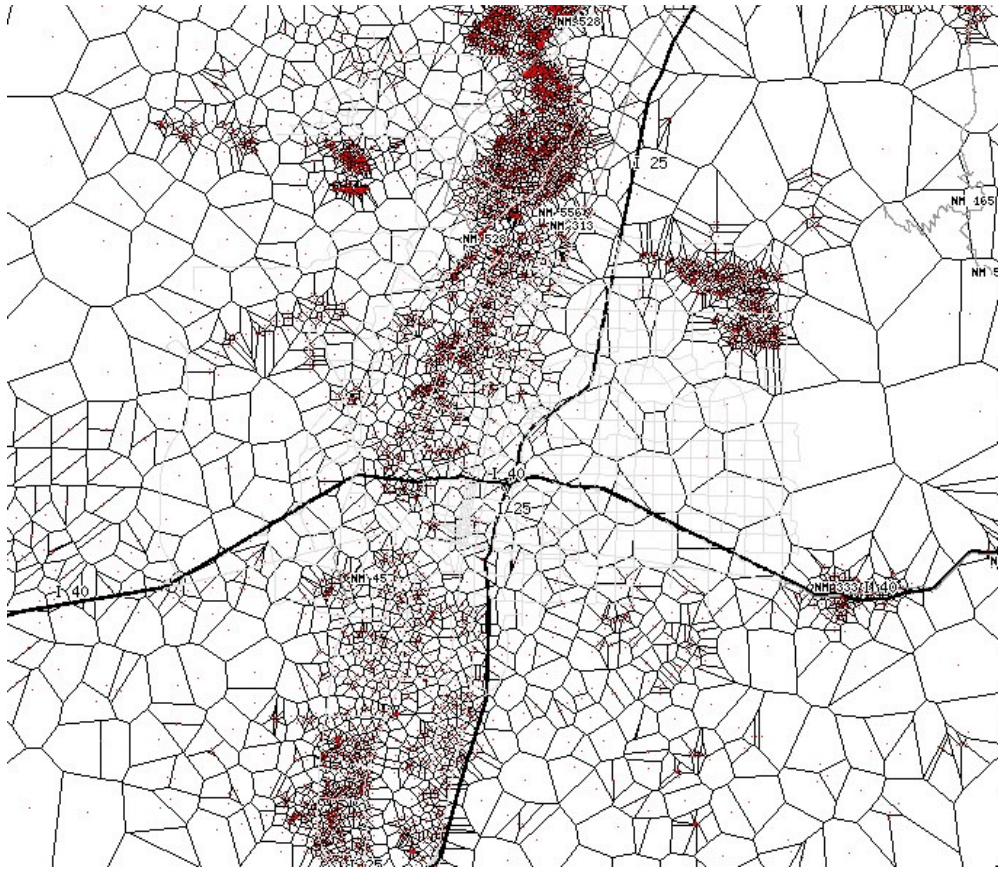


**FIGURE 2.5 Region Around Albuquerque Showing Well Locations (Red Dots) and Related Voronoi Polygons**

The second derived data product involves statistical manipulation of the point data to generate a continuous surface of interpolated ground water depth values for the entire state of New Mexico. This continuous surface is represented by a geospatial raster data model, in which there are derived values (for each pixel in the raster) calculated at a 1 km interval over the entire state. The statistical approach used to calculate the values for each of the pixels in the raster is an inverse distance weighting method in which the six well locations closest to each pixel are averaged to create the value for the pixel. Furthermore, well locations that are closer to the pixel are given a greater weight in the calculation of the ground water depth for each pixel than more distant well locations. The resulting raster for the same region shown in Figure 2.6.



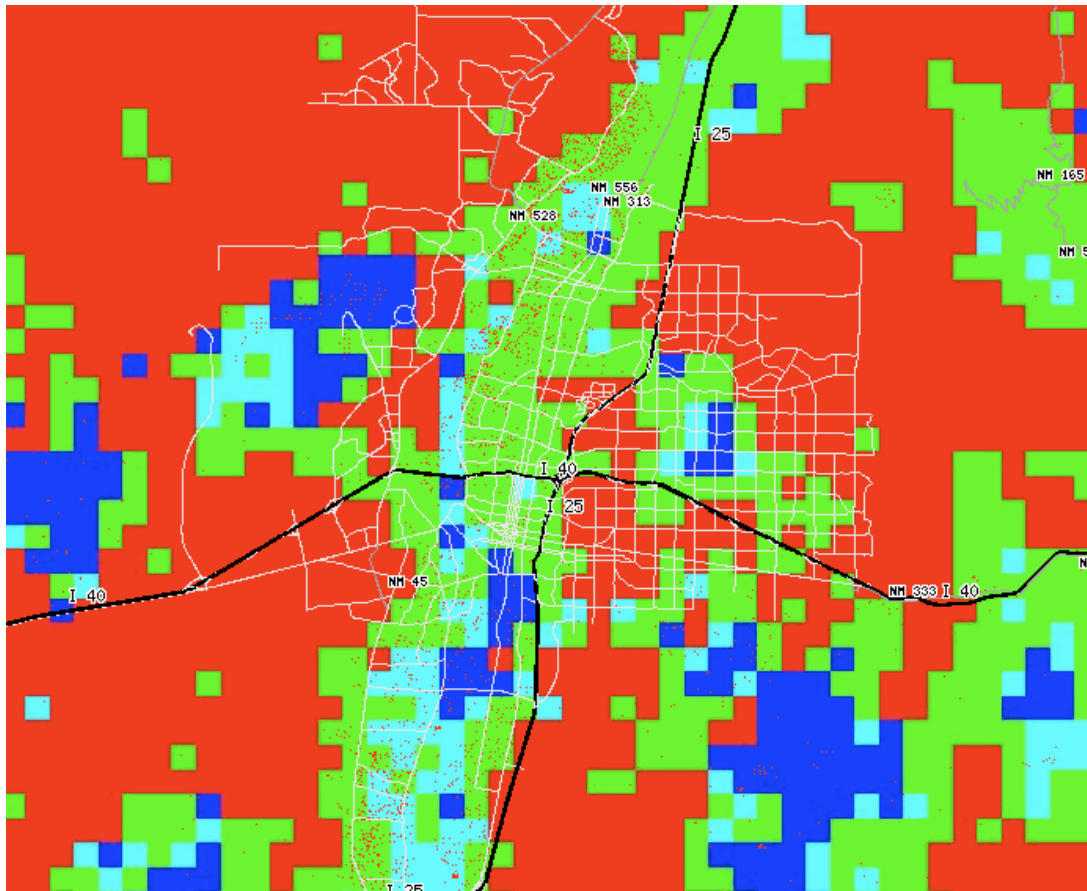


**FIGURE 2.6 Region around Albuquerque Showing Well Locations (Red Dots) and Related Inverse Distance Weighted Raster Model of Ground Water Depth**

These derived data products were then used to create an OGC WMS that supports the WMS GetFeatureInfo request that returns attributes associated with a specified map request and pixel location within that request. The map images shown in both Figures 2.4 and 2.5 are the product of WMS GetMap requests against the service. GetMap requests return a map image (a picture of mapable data) for a specified area of interest (bounding box) and combination of map layers (well locations and interpolated data layers in the case of Figures 2.5 and 2.6). A GetFeatureInfo request to the same service includes the information required of a GetMap request, but also specifies which pixel within the returned map image should be used to retrieve the data values for a specific location. For example, the following WMS request returns the following XML data:

#### Request

```
http://edacwms.unm.edu/cgi-bin/mapfiles/ce_data?service=wms&version=1.1.1&request=getfeatureinfo&CRS=EPSG:4326&BBOX=-105.00001,34.99999,-104.99999,35.00001&width=3&height=3&layers=osewells_vor&query_layers=osewells_idw&info_format=application/vnd.ogc.gml&x=1&y=1
```

#### Response

```
<?xml version="1.0" encoding="ISO-8859-1"?>
<msGMLOutput
```

```

xmlns:gml="http://www.opengis.net/gml"
xmlns:xlink="http://www.w3.org/1999/xlink"
xmlns:xsi="http://www.w3.org/2001/XMLSchema-instance">
<osewells_idw_layer>
  <osewells_idw_feature>
    <gml:boundedBy>
      <gml:Box srsName="EPSG:4326">
        <gml:coordinates>-109.489685,0.000316 -
109.489685,0.000316</gml:coordinates>
      </gml:Box>
    </gml:boundedBy>
    <x>-105.00234</x>
    <y>34.998166</y>
    <value_0>175</value_0>
    <value_list>175</value_list>
    <class>3</class>
    <red>255</red>
    <green>0</green>
    <blue>0</blue>
  </osewells_idw_feature>
</osewells_idw_layer>
</msGMLOutput>

```

The provides XML data package can then be processed by other computer programs or even read by a human to extract the information requested for the specific location. To further streamline the data extraction process, a simple python scripts was developed that allows for a web request to be submitted that specifies only layer (or layers) of interest and the coordinate of the point for which data should be obtained. This allows for the use of a vastly simplified request model which hides some of the complexity of the GetFeatureInfo request shown above. For example, the same result presented above may be generated using the following request.

[http://edacwms.unm.edu/cgi-bin/mapfiles/gfi?layers=osewells\\_idw&x=-105.00234&y=34.998166](http://edacwms.unm.edu/cgi-bin/mapfiles/gfi?layers=osewells_idw&x=-105.00234&y=34.998166)

This simplification provides a much more straightforward request model for any location within the State of New Mexico, for either the voronoi polygon-based ground water depth data, or the inverse distance weighted ground water estimates.

## Climate Data Acquisition and Processing

An alternative source for climate normal data from NOAA was obtained in support of the project. An online version of NOAA's National Climate Atlas was accessed, and the entire collection of shapefiles for the Atlas was downloaded. Many of these files appeared to be corrupt, so an alternative resource for climate normal data was sought. The NOAA Climate Atlas of the United States (2002) was obtained, and the climate average shapefiles extracted from the disk. This process resulted in 1644 individual shapefiles being copied first to a local hard drive, and then to one of EDAC's data servers for further processing.

Two outstanding issues relate to these data. First, the shapefiles consist of polygons representing categorized climate value ranges and not discrete values. Figure 2.7 illustrates one of these data sets. These data need to have the ranges extracted from the defined categories, and derived single values determined for use in initialization of the MEPDG model. Second, while the extracted shapefiles are internally consistent in terms of their spatial reference system (i.e. map projection), they do not include the required .prj (a text file that defines the spatial reference system for a shape file) that allows the automatic integration of these data with other geospatial data.

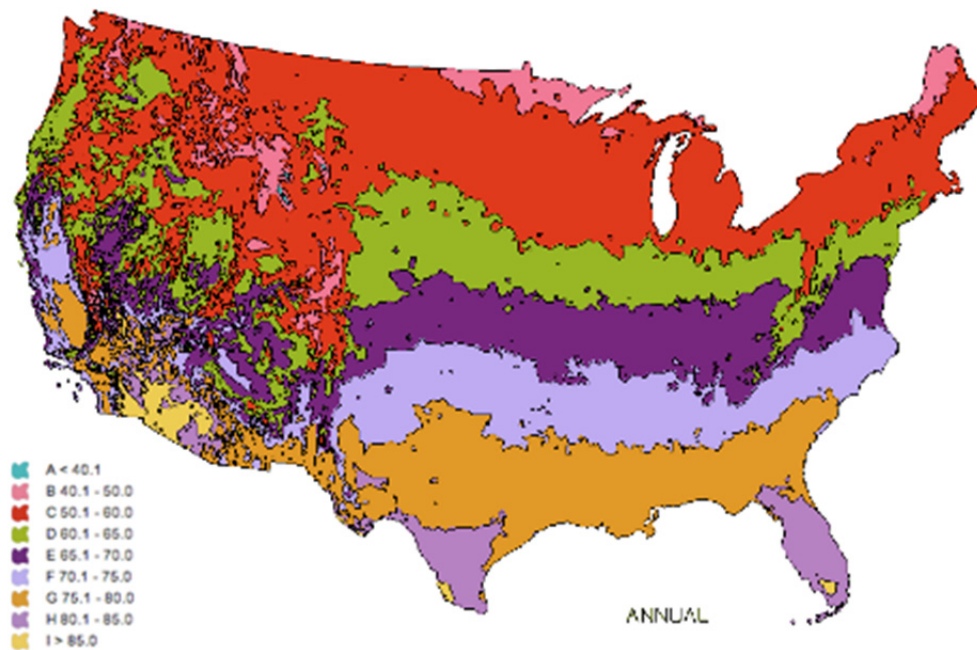


**FIGURE 2.7 Annual average temperature shape file from the NOAA Climate Atlas of the United States**

These issues were resolved by following steps. First, a .prj file was generated for each of the 1644 shapefiles, allowing for the streamlined integration of these data into geographic information and data management systems. Second, the obtained climate data was imported into a geodatabase for further processing and management. Once the data have been imported into the geodatabase, derived climate values were calculated based upon the ranges provided by the imported shapefiles. Finally, Open Geospatial Consortium Web Map Services were enabled for each of the shapefiles so that a value extraction system, like that already developed for the ground water depth data, was used to obtain the climate data values for any arbitrary X-Y coordinate pair within the MEPDG project area.

To streamline the data acquisition process, lists of meteorological stations were extracted from the NCDC web site that provides a search and listing capability for weather stations within each state, formatted as an HTML table. These HTML tabular data were extracted from the web pages for NM, AZ, UT, CO, OK, and TX, and saved locally as ASCII text files that could be used to drive an automated data retrieval process that attempted to request the daily climate summary from NOAA's web site for summary data by individual station. This extraction process resulted

in combined collection of 5,900 individual entries that were used in the generation and processing of data from NOAA's servers. A sample of the format and content of these extracted data is provided in the following text block:

Abbott - Abbott, NM, United States - Colfax County	01 Jul 1946	31 Jul 1950	290022
COOP			
Abbott 1 SE - Abbott, NM, United States - Colfax County	01 Jul 1950	Present	290022
B COOP			
Abiquiu - Abiquiu, NM, United States - Rio Arriba County	01 Jul 1947	30 Nov 1949	290039
COOP			
Abiquiu Dam - Abiquiu, NM, United States - Rio Arriba County	01 Jun 1957	Present	290041
COOP COOP-A AB			
Acomita Airport - Acomita, NM, United States - Valencia County	01 Nov 1933	30 Apr 1953	
290074 23057 COOP CAA			
Adams Diggings - NM, United States	01 Jul 1947	31 Aug 1951	290079
COOP			
Adobe Rch - NM, United States - Catron County	01 Jul 1946	01 Apr 1994	290119
AB COOP			
Afton - Afton, NM, United States - Dona Ana County	01 Jul 1946	31 May 1949	290125
COOP			
Afton 5 ESE - Afton, NM, United States - Dona Ana County	01 May 1949	30 Nov 1986	
290125 COOP			
Afton 6 NE - Afton, NM, United States - Dona Ana County	21 Aug 1987	16 Dec 1999	290125
B COOP			

As can be seen in the above sample, some stations have multiple entries - with each entry representing a different period of operation, or other changed parameters relating to the station. The key variable used out of these station lists is the "coop-ID" column, which, in the sample is represented by the numeric values starting with 29, and ranges from 290022 through 290125 in the listing.

The automated data acquisition script (see Appendix 2.1) extracts the coop-ID value from the station list for each state, and uses it to formulate a data request for the daily climate summary for that specific station. This script was run separately for each state, and produced a variety of outputs, including the files returned by NOAA's servers as a result of the data request (consisting of either an error message indicating that the requested file does not exist, or a data file containing either a full climate summary (temperature, heating- and cooling-degree days, precipitation) or a partial climate summary (precipitation only), and a compilation of the data files in a format suitable for import into the project's Oracle database. The number of files retrieved for each state is summarized in Table 2.15. Samples of a full climate normal file and a partial climate normal file are included in Appendices 2.2 and 2.3, respectively.

The other product of the data acquisition program was an ASCII text file that contains a line of data for each day of the year, for each coop station, for each measurement (only including

temperature and precipitation - cooling- and heating-degree-days were excluded from the data import process). These ASCII text files have been partially imported into the Oracle database - into a table named climate\_normals. A partial sample of one of the generated ASCII text files is included in Appendix 2.4.

The integration of these data into the project database enabled processing and visualization of the climate normal data for New Mexico and the surrounding region. With these data in hand it is possible to apply statistical models to the interpolation of the climate normal data to determine climate conditions for any location within the state of New Mexico, enabling the refined execution of MEPDG model runs that take into account a variety of climate-based scenarios, depending upon the statistical models employed in defining the daily meteorological conditions to which specific road segments are likely to be subjected.

**TABLE 2.15 Proposed weather stations located in Oklahoma**

State	Number of Full Climate Normal Files	Number of Partial Climate Normal Files	Number of Error Files	Total Number of Stations Attempted
New Mexico	123	19	567	709
Arizona	148	27	375	550
Utah	159	23	395	577
Colorado	162	33	489	684
Oklahoma	117	82	403	602
Texas	215	134	651	1000
	924	318	2880	4122

### **Open Geospatial Consortium Mapping Services**

In order to enable efficient and flexible visualization of project spatial data, an Open Geospatial Consortium (OGC) Web Map Service (de la Beaujardiere 2006) was developed on the project server for the delivery of map images based upon data stored in the spatial component (Oracle Spatial) of the project database. This section outlines the process of developing the service.

After the development of the WMS service, the mepdg.unm.edu server had OGC (Open Geospatial Consortium) compliant mapping capabilities. This was accomplished through the installation of ms4w (MapServer 4 Windows) on the server.

The installation and configuration was based upon instructions provided on the ms4w web site<sup>1</sup> with particular attention to the instructions relating to the integration of Oracle Spatial (SDO) with ms4w<sup>2</sup>, which worked well for the Oracle 11 installation in use for the project.

As part of the server configuration, a free-standing Apache service was replaced by the Apache MS4W Server which consists of Apache with Mapserver integration.

The OGC WMS standard can be used by any mapping client like ArcGIS, QuantumGIS or a web client in a webpage that includes an online mapping framework such as OpenLayers<sup>3</sup> to implement image tiling.

In the development of the WMS service it was tested using connections to the local server through requests that include reference to the MapServer executable CGI that was installed on the server. The base request URL includes the hostname, the executable, and a pointer to the mapfile (the configuration file for the service being deployed). The complete base URL looks like this:

<http://localhost/cgi-bin/mapserv.exe?map=mapfiles/test.map>

In order to obtain the service metadata (an XML document that provides information about the service, including the data layers that are available from the service), a WMS GetCapabilities request may be submitted to the server:

<http://localhost/cgi-bin/mapserv.exe?map=mapfiles/test.map&service=WMS&request=GetCapabilities&version=1.1.1>

Client applications (such as ArcGIS) may use this request to automatically configure themselves to access the map layers available from the service.

Map images from the service are requested through the use of a WMS GetMap request. This request includes information about the area of interest for the request, the layer(s) that should be included in the generated map image, the format of the image to be returned, the pixel dimensions of the image to be returned, and the coordinate system of the request bounding box and returned image. A sample GetMap request for a map image generated by the service is as follows:

<http://localhost/cgi-bin/mapserv.exe?map=mapfiles/test.map&service=WMS&request=getmap&version=1.1.1&layers=test&width=200&height=200&bbox=-109,33,-107,35&style=&SRS=EPSG:4326&format=image/jpeg>

For this to work it is necessary to create a map file<sup>4</sup> in the file system. In the configuration of the MEPDG service, the map file is located at:

C:\ms4w\Apache\cgi-bin\mapfiles\test.map

---

<sup>1</sup> [http://maptools.org/ms4w/index.phtml?page=README\\_INSTALL.html](http://maptools.org/ms4w/index.phtml?page=README_INSTALL.html)

<sup>2</sup> [http://maptools.org/ms4w/index.phtml?page=README\\_INSTALL.html#oracle-10g](http://maptools.org/ms4w/index.phtml?page=README_INSTALL.html#oracle-10g)

<sup>3</sup> <http://www.openlayers.org/>

<sup>4</sup> <http://mapserver.org/mapfile/index.html#mapfile>

This file is used by MapServer as the configuration file for the service and processes the request received through a web CGI environment to produce the map image. Once the map file was generate, a number of configuration issues were identified and dealt with to complete the configuration. A summary of the troubleshooting steps is presented below.

#### Error 1:

##### **Connection error**

```
<?xml version='1.0' encoding="ISO-8859-1" standalone="no" ?>
<!DOCTYPE                                     ServiceExceptionReport                SYSTEM
"http://schemas.opengis.net/wms/1.1.1/exception_1_1_1.dtd">
<ServiceExceptionReport version="1.1.1">
<ServiceException>
msDrawMap(): Image handling error. Failed to draw layer named &#39;test&#39;,.
msOracleSpatialLayerOpen(): OracleSpatial error. Cannot create OCI Handlers. Connection
failure. Check the connection string. Error: ORA-12154: TNS:could not resolve the connect
identifier specified
.
</ServiceException>
</ServiceExceptionReport>
```

##### **Solution for Connection error:**

Add a full TNS service connection string in the map file: For example:

From: CONNECTION "dbuser/Rafi1234@gismepdg"

To: CONNECTION  
 "dbuser/\*\*\*\*\*@(DESCRIPTION=(ADDRESS\_LIST=(ADDRESS=(PROTOCOL=TCP)(HOST=localhost)(PORT=1521)))(CONNECT\_DATA=(SID=gismepdg)))"

#### Error 2:

##### **Index Error**

```
<?xml version='1.0' encoding="ISO-8859-1" standalone="no" ?>
<!DOCTYPE                                     ServiceExceptionReport                SYSTEM
"http://schemas.opengis.net/wms/1.1.1/exception_1_1_1.dtd">
<ServiceExceptionReport version="1.1.1">
<ServiceException>
msDrawMap(): Image handling error. Failed to draw layer named &#39;test&#39;,.
msOracleSpatialLayerWhichShapes(): OracleSpatial error. Error: ORA-13226: interface not
supported without a spatial index
ORA-06512: at &quot;MDSYS.MD&quot;, line 1723
ORA-06512: at &quot;MDSYS.MDERR&quot;, line 8
ORA-06512: at &quot;MDSYS.SDO_3GL&quot;, line 1195
. Query statement: SELECT rownum, GEOM FROM COUNTY2008 WHERE SDO_FILTER(
GEOM,                                     MDSYS.SDO_GEOMETRY(2003,                                     NULL,
NULL,MDSYS.SDO_ELEM_INFO_ARRAY(1,1003,3),MDSYS.SDO_ORDINATE_ARRAY(
-108.995,33.005,-107.005,34.995) ),&#39;querytype=window&#39;) = &#39;TRUE&#39;.
Check your data statement.
</ServiceException>
```

</ServiceExceptionReport>

**Solution for Index error:**

```
CREATE INDEX county2008_idx ON COUNTY2008 (GEOM) INDEXTYPE IS
MDSYS.SPATIAL_INDEX;
```

Error 3:

**Error**

```
<?xml version='1.0' encoding="ISO-8859-1" standalone="no" ?>
<!DOCTYPE ServiceExceptionReport SYSTEM
"http://schemas.opengis.net/wms/1.1.1/exception_1_1_1.dtd">
<ServiceExceptionReport version="1.1.1">
<ServiceException>
msDrawMap(): Image handling error. Failed to draw layer named &#39;test&#39;.
msOracleSpatialLayerWhichShapes(): OracleSpatial error. Error: ORA-29902: error in executing
ODCIIndexStart() routine
ORA-13208: internal error while evaluating [window SRID does not match layer SRID]
operator
ORA-06512: at &quot;MDSYS.SDO_INDEX_METHOD_10I&quot;, line 333
. Query statement: SELECT rownum, GEOM FROM COUNTY2008 WHERE SDO_FILTER(
GEOM, MDSYS.SDO_GEOMETRY(2003, NULL,
NULL,MDSYS.SDO_ELEM_INFO_ARRAY(1,1003,3),MDSYS.SDO_ORDINATE_ARRAY(
-108.995,33.005,-107.005,34.995) ),&#39;querytype=window&#39;) = &#39;TRUE&#39;.
Check your data statement.
</ServiceException>
</ServiceExceptionReport>
```

**Solution change for error:**

DATA "GEOM FROM COUNTY2008"

to:

DATA "GEOM FROM COUNTY2008 USING SRID 4326"

## FWD DATA

FWD Data has been collected from NMDOT. Data are available from 2001 to 2009. The sample datasets from FWD database is shown in Tables 2.16 and 2.17. Data from 2006 to 2009 has been populated into the database. MEPDG database not only includes the raw data from FWD test, but also data of calculated Resilient Modulus ( $M_r$ ) and R-value. For the unbound granular materials and subgrade materials group, the pavement response model needs material inputs such as resilient modulus. Therefore, resilient modulus is gathered from FWD test for rehabilitation and reconstruction of the existing pavement layer. Also, general correlations between soil index and strength properties such as R-value can be used for estimating  $M_r$ .



**TABLE 2.16(a) Sample datasets of FWD database in MEDPG database**

DYNAMIC_LOAD	FWD_ID	MAT_TEMP	MILEPOST	RESILIENT_MODULUS	SPACING_0	SPACING_12
8970	122	45	177.5	"15,399"	3.53	2.86
8980	123	44.7	177.5	"14,967"	3.52	2.83
8950	124	44.7	177.5	"14,855"	3.49	2.82
9220	125	49.4	177.624	"16,538"	3.32	2.7
9200	126	49.4	177.624	"17,692"	3.29	2.67
9230	127	47.2	177.674	"16,409"	3.55	2.92
9140	128	47.2	177.722	"18,558"	3.1	2.53
9160	129	47.2	177.722	"18,599"	3.1	2.43
9130	130	48.3	177.816	"17,474"	3.33	2.65

**TABLE 2.16(b) Sample datasets of FWD database in MEDPG database**

DYNAMIC_LOAD	SPACING_18	SPACING_24	SPACING_36	SPACING_60	SPACING_8	SUBGRADE_R_VALUE
8970	2.72	2.49	2.33	1.8	3.06	56
8980	2.7	2.47	2.4	1.68	3.07	55
8950	2.7	2.48	2.41	1.96	3.05	55
9220	2.52	2.3	2.23	1.14	3.03	58
9200	2.47	2.26	2.08	1.12	2.95	60
9230	2.74	2.46	2.25	0.56	3.19	57
9140	2.26	2.06	1.97	0.51	2.76	61
9160	2.26	2.05	1.97	0.43	2.75	61
9130	2.44	2.22	2.09	0.58	2.88	59

**TABLE 2.17 Documentation of FWD data**

Column Name	Description
DYNAMIC_LOAD	Impulse load generated in the test
FWD_ID	FWD ID
MAT_TEMP	Material temperature
MILEPOST	Milepost for the section
SPACING_0	The deflection at spacing load plate
SPACING_8	The deflection at spacing 8 inches from load plate
SPACING_12	The deflection at spacing 12 inches from load plate
SPACING_18	The deflection at spacing 18 inches from load plate
SPACING_24	The deflection at spacing 24 inches from load plate
SPACING_36	The deflection at spacing 36 inches from load plate
SPACING_60	The deflection at spacing 60 inches from load plate
SUBGRADE_R_VALUE	Calculated Subgrade R-value
RESILIENT_MODULUS	Calculated Resilient Modulus

## Chapter 3

### DESIGN OF MEPDG DATABASE

#### INTRODUCTION

This chapter describes the tasks of identifying required MEPDG input and output variables, determining the optimal database structure, and designing a database capable of manipulating, storing and processing the data as required by the MEPDG design software.

#### IDENTIFY MEPDG DATA FIELDS

In this study, most of the essential data elements required for successful calibration of MEPDG were identified. The MEPDG is organized into four fundamental types of inputs:

- General input
- Traffic input
- Climate input
- Structural input

Figure 3.1 is a brief overview of data fields used in the MEPDG software for conventional flexible pavement.

#### General Input

The general information consists of inputs required by the software program that describe the nature of the project, the timeline, the design criteria that the agency specifies, and miscellaneous information that can serve to identify the project files. The General project information can be entered into the MEPDG program from three individual screens, which are shown in Tables 3.1, 3.2 and 3.3.

#### General Information

**Design Life:** The design life is the expected service life of the pavement in years. Pavement performance is predicted over the design life beginning from the month the pavement is open to traffic. The conventional asphalt concrete (AC) pavement has a 10-year design life.

**Base/Subbase Construction Month:** This is the month and year when the subgrade is prepared for the pavement construction. This input is required only for new flexible pavement construction.

**Pavement Construction Month:** This input is required only for new flexible pavement construction. This is the month when the surface (asphalt or concrete) layer is placed. Changes to the surface layer material properties due to time and environmental conditions are considered beginning from the pavement construction month.

**Traffic Open Month:** This is the month and year when traffic is expected to move on the pavement being designed. The *Design Guide* software predicts pavement performance beginning from this month. However, changes to the material properties are considered from the construction months.

**Pavement Restoration Month:** This input parameter appears only for restoration design and is essentially the month and year when the restoration is performed.

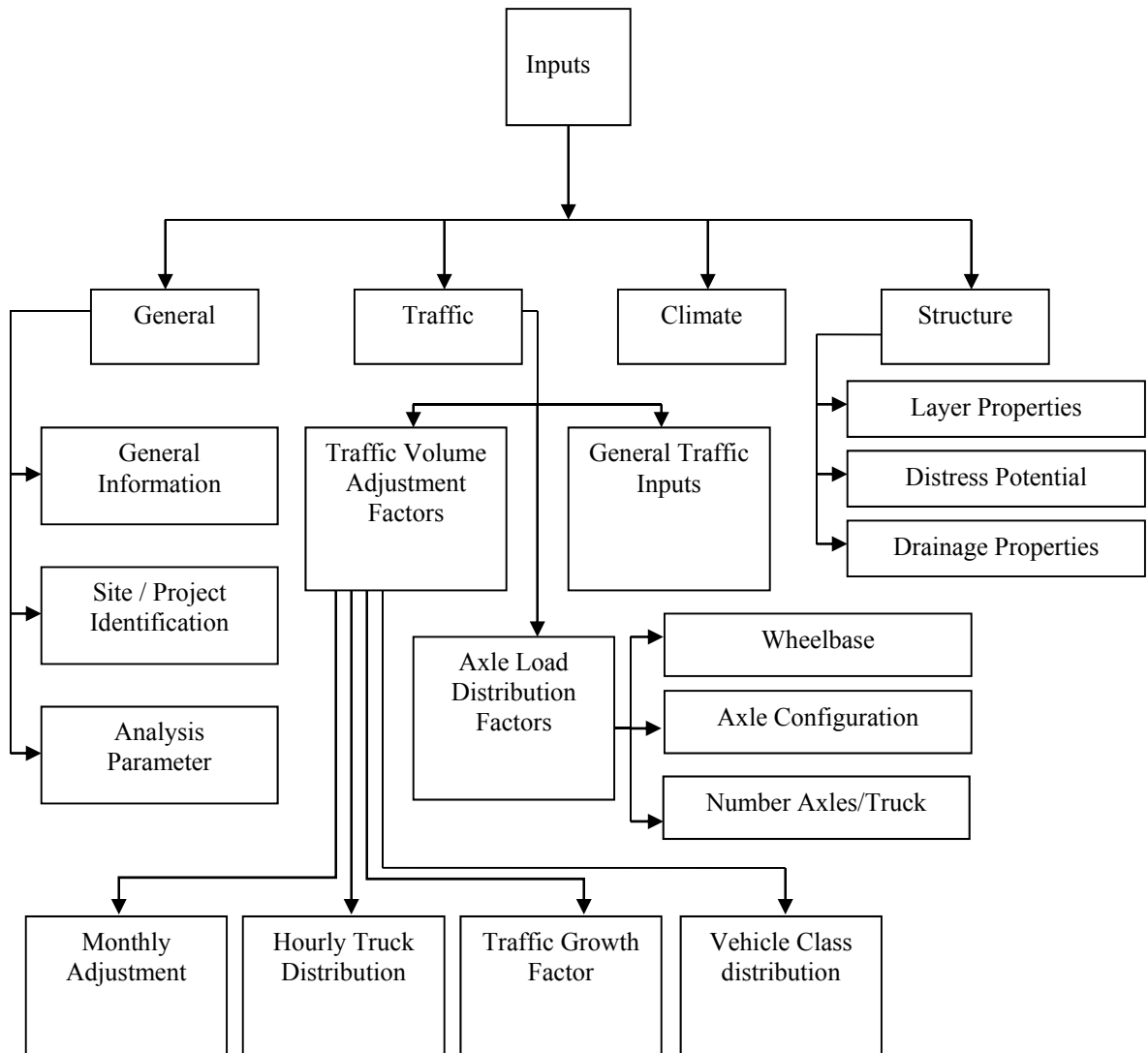


**FIGURE 3.1 The MEPDG Inputs**

**TABLE 3.1 General information**

Design Life (years):				
Type of Design:	Type	Criteria	Year	Month
New Pavement	Flexible Pavement	Base/ Subgrade Construction:		
		Pavement Construction:		
		Traffic Open		
	Jointed Plain Concrete Pavement	Pavement Construction:		
		Traffic Open		
	Continuously Reinforced Concrete Pavement	Pavement Restoration Construction:		
		Traffic Open		
Restoration	Jointed Plain Concrete Pavement	Existing Pavement Construction:		
		Pavement Restoration Construction:		
		Traffic Open		
Overlay	Asphalt Concrete Overlay	Existing Pavement Construction:		
		Pavement Overlay Construction:		
		Traffic Open		
	PCC Overlay	Existing Pavement Construction:		
		Pavement Overlay Construction:		
		Traffic Open		

**Existing Pavement Construction Month:** This input is required by only restoration and rehabilitation designs. This is the month and year when the existing pavement was built. The information provided here is used to estimate the age and strength properties of the pavement structure that is being restored or rehabilitated.

**Pavement Overlay Construction Month:** This input parameter appears only for rehabilitation design and is essentially the month and year when the overlay is built. Changes to the overlay material properties due to time and environmental conditions are considered beginning from the pavement overlay construction month.

**Flexible Pavement:** This is a pavement with an asphalt concrete surface. Such pavement structure maintains intimate contact with, distributes loads to the subgrade, and depends on aggregate interlock, particle friction, and cohesion for stability.

**Asphalt Concrete Overlay:** This is a rehabilitation option when the existing pavement (rigid or flexible) is overlaid with an asphalt concrete layer.

**PCC Overlay:** This is a rehabilitation option when the existing pavement (rigid or flexible) is overlaid with a Portland cement concrete layer. The new overlay can be either a JPCP or a CRCP layer.

### Site/Project Identifications

The Site Identification Data allows the user to provide information that would typically be useful for identification and documentation purposes only. Information here will in no way affect the analysis or design processes. Inputs on this screen include items that will help identify the location and stationing of the project. Users would typically find this information useful when designing different sections along a large project site.

**TABLE 3.2 Site/Project identification**

Location:		
Project ID:		
Section ID:		
Date:		
Stations/Milepost:	Station/Milepost Input:	
	Station/Milepost Begins:	
	Station/Milepost End:	
Traffic Direction:	East Bound	
	North Bound	
	South Bound	
	West Bound	

**Analysis Parameters**

The analysis type and the basic criteria for performance prediction are specified on this Table below. These Data fields are mainly for the designer to select a trial design and then analyze the design in detail to determine if it meets the applicable performance criteria established by the designer. Several distress types are considered for performance evaluation of flexible and rigid pavements. The designs that meet the applicable performance criteria are then considered feasible from a structural and functional viewpoint and can be further considered for other evaluations.

It is expected that at the end of the 10-year design life, the pavement will have no more than an IRI of 172 in/mile, AC surface down or longitudinal cracking of 1000 ft/mile, bottom up fatigue cracking of 25 percent, AC thermal fracture (transverse cracking) of 1000 ft/mile. The total permanent deformation in the AC layer shall not exceed 0.25 inches and that in the total pavement not exceed 0.75 inches. In addition, if a chemically stabilized layer is used, the fatigue fracture in the layer shall not exceed 25 percent. These criteria are to be satisfied at a reliability of 90 percent.

**TABLE 3.3 Analysis parameters**

Initial IRI (in/mi)			
Performance Criteria:		Limit	Reliability (%)
Flexible Pavement	Terminal IRI (in/mile)		
	AC Surface Down Cracking Long Cracking (ft/mi)		
	AC Bottom up Cracking Alligator Cracking (%)		
	AC Thermal Fracture (ft/mi)		
	Chemically Stabilized Layer Fatigue Fracture (%)		
	Permanent Deformation Total Pavement (in)		
	Permanent Deformational only (in)		

## **Traffic Input**

This is one of the four required categories of inputs. Traffic data (number and weight of trucks) is a key data element for the design and analysis of pavement structures. As with all other inputs, traffic inputs can be provided in three levels depending upon the extent of traffic information available for the given project and the accuracy therein. The full axle-load spectrum data for single, tandem and tridem axles is needed for MEPDG for both new pavement and rehabilitation design procedures it is required for estimating the loads that are applied to a pavement's design life.

### **Design/Analysis Levels**

It is recognized that however, some users may not have the sufficient data over time. To facilitate the use of the Guide by different users, a hierarchical approach is predicted for developing the traffic inputs to the new pavement and rehabilitation design process. This 4 hierarchical approach for traffic is divided into four levels. These four levels are briefly defined below.

**Level 1 Inputs: Site Specific Vehicle Classification and Axle weight Data:** Level 1 requires the gathering and analysis of site-specific traffic data. It is recommended for use in evaluating or designing most high-volume highways. The traffic data measured at the site includes counting and classifying the number of vehicles traveling over the roadway, along with the breakdown by lane and direction, and measuring the axle loads for each vehicle class over a sufficient period of time to reliably determine the design traffic. Level 1 is considered the most accurate because it uses the actual axle weights and vehicle class spectrum measured over or near the project site.

**Level 2 Inputs: Site-Specific Vehicle Classification Data and Regional Axle Weight Data:** Level 2 is identical to Level 1 with the exception that it does not require site-specific axle Weight data. Regional or state axle Weight data for similar highways can be used to develop the axle load spectra for each vehicle class that can be used for a specific project or roadway.

**Level 3 Inputs: Regional Vehicle Classification and Axle Weight Data:** Level 3 is similar to Levels 1 and 2, but does not require site specific data other than AADT and percent trucks information. Regional or State vehicle classification and axle Weight data for similar highway classifications are used to develop axle load spectra or distributions for each vehicle class that can be used for a specific project.

### **Traffic Module Data Analyses**

Eight types of traffic data are required for developing the traffic module in support MEPDG and evaluation procedure for both new pavement designs and pavement rehabilitation designs. These are listed below:

**AVC Data:** AVC data are used to determine the normalized vehicle class or truck distribution over a specified period of time. These vehicle classification data are needed for Levels 1, 2 and 3 inputs. Default values are provided for Level 4 inputs. These default values are truck traffic distribution dependent.

**WIM Data:** WIM data are used to determine the normalized axle load distribution or spectra for each axle type within each vehicle class. These axle Weight data are needed for levels 1, 2 and 3 inputs. The default values (level 4) are vehicle class and axle type specific, which are used to determine the number of axles for each vehicle class and axle type over a specified time.

**Average Annual Daily Truck Traffic (AADTT):** The average annual daily truck traffic is needed for the base year for levels 1, 2 and 3. For level 3 inputs, where traffic measurements are unavailable for the roadway, these values can be estimated from traffic studies of similar highways or represent regional averages.

**Average Annual Daily Traffic (AADT) or Vehicle Counts:** The average annual daily traffic is needed for the base year, but is only required for level 4 inputs.

**Percent Trucks:** Percent trucks represent the percentage of vehicle classes 4- 13 in the traffic stream. The percent truck is required for the base year for the level four inputs.

**Truck Traffic Classification (TTC) for Pavement Structural Design:** This factor classifies those highways into groups with similar truck traffic features or characteristics that are needed for pavement structural designs for selecting the default values for the level four inputs of various traffic parameters.

**Loading Details of the Axle Load and Axle Configuration:** Default values are provided for each of the following elements that describe the details of the tire and axle loads.

- Tire pressure
- Tire and axle load
- Axle and tire spacing
- Average number of axles by axle type per vehicle classification or truck type.

**Traffic Factors:** Following elements are needed for different types of highways:

- Traffic time distribution factors:
  - Seasonal or monthly distribution factors
  - Average hourly distribution of traffic
- Weekday and Weekend truck traffic factors
- Directional distribution factor
- Lane distribution factor
- Lateral distribution factor
- Traffic growth factor or function

Tables 3.4 and 3.5 are schematics of the traffic inputs a user needs to make for different input levels.

**TABLE 3.4 Traffic inputs**

Input Name			Input value
Project Name			
Design Life (years)			
Opening Date			
AADTT	Year		
	Initial two-way AADTT		
Number of Lanes in Design Direction			
Percent of Trucks in Design Direction			
Percent of Trucks in Design Lane			
Operational Speed			
Traffic Volume Adjustment Factors	Monthly Adjustment		
	Vehicle Class Distribution		
	Hourly Distribution		
	Traffic Growth factors		
Axle Load Distribution Factors	Axle Load Distribution		
	Axle Type	Single Axle	
		Tandem Axle	
		Tridem Axle	
Quad Axle			

**TABLE 3.5 Traffic inputs**

Input Name				Input value
Axle Load Distribution Factors	Distribution Type	Normal Distribution		
		Cumulative Distribution		
General Traffic Inputs	Lateral traffic Wander	Mean Wheel Location		
		Traffic wander standard deviation		
		Design lane width		
	Number axles/Truck			
	Axle Configuration	Avg axle width		
		Dual tire spacing		
		Tire pressure		
		Axle spacing	Tandem Axle	
			Tridem Axle	
			Quad Axle	
	Wheelbase	Average axle spacing	Short	
			Medium	
			Long	
		Percent of trucks	Short	
			Medium	
			Long	



## Climatic Input

Environmental conditions have a significant effect on the performance of both flexible and rigid pavements. Some external factors such as precipitation, temperature, freeze-thaw cycles, and depth to water table affect temperature and moisture contents of unbound materials are directly related to the load-carrying capacity of the pavement. Without these, there are some internal factors, which also play a significant role for this issue, such as: drain ability of paving layers, infiltration potential of pavement, and susceptibility of pavement materials to moisture and freeze thaw damage.

The following Weather related information is required to perform flexible pavement design:

- Weather related data
  - Hourly air temperature over the design period
  - Hourly precipitation over the design period
  - Hourly wind speed over the design period
  - Hourly percentage sunshine over the design period
  - Hourly ambient relative humidity values
- Ground water table depth
  - Seasonal or constant water table depth at the project site

Weather related data could be obtained directly from Weather station data for a given site, if available. For locations, within the United States, they can be obtained from the National Climatic Data Center (NCDC) database. The design guide software includes an extensive climatic database for over 800 locations in the US and a capability to interpolate between the available sites. All these necessary climatic information at any given sites within the US can be generated by using the following inputs of Table 3.6.

**TABLE 3.6 Climatic data**

Input Name			Input Data
Project Name			
Depth of water table	Seasonal	Spring (April)	
		Summer (July)	
		Fall (October)	
		Winter (January)	
	Annual average		
Climatic data	Interpolate climatic data for given location	Latitude	
		Longitude	
		Elevation	
	Climatic Data for a specific Weather station		

## Structural Input

This category of inputs are to specify the structural, design, and material aspects for the performance evaluation.

Pavement Structure:

- Number of Layers
- Layer Number
- Layer Type
- Representative Thickness

Aggregate Gradation for Asphalt Mix:

- Layer Number
- Layer Type
- Percentage Retained  $\frac{3}{4}$ " Sieve
- Percentage Retained  $\frac{3}{8}$ " Sieve
- Percentage Retained #4 Sieve
- Percentage Passing #200 Sieve

Effective Binder Content by Volume at Time of Construction

- Layer Number
- Layer Time
- Binder Content by Weight,  $P_b$
- Specific Gravity of the Binder,  $G_b$
- Bulk Specific Gravity of the Mix,  $G_{mb}$
- Maximum Theoretical Specific Gravity of the Mix,  $G_{mm}$
- Bulk Specific Gravity of the Aggregate,  $G_{sb}$
- Effective Specific Gravity of the Aggregate,  $G_{se}$
- Effective Binder Content by Volume at Time of Construction,  $V_{be}$

Original Air Voids (at Time of Construction) and Total Unit Weight

- Layer Number
- Layer Type
- Air Voids at Age = t
- Age = t
- Mean Annual Air Temperature,  $Maat$
- Original Viscosity at 77 °F
- Original Air Voids
- Total Unit Weight

### Asphalt Binder Data

- Layer Number
- Layer Type
- Viscosity Grade
- Penetration Grade
- Penetration at 77F
- Viscosity at 140F
- Viscosity at 275F

### Unbound Materials Data

- Layer Number
- Layer Type
- Dry Thermal Conductivity
- Dry Heat Capacity
- Liquid Limit
- Plastic Limit
- Plasticity Index
- Percent Passing #200 Sieve
- Percent Passing #4 Sieve
- Diameter  $D_{60}$
- Optimum Moisture Content from LTPP Database
- Estimated Optimum Moisture Content for Level 3 Analysis
- Maximum Dry Unit Weight from LTPP Database
- Estimated Maximum Dry Unit Weight for Level 3 Analysis
- Specific Gravity of Solids
- Saturated Hydraulic Conductivity
- AASHTO Soil Classification
- Unified Soil Classification System (USCS) Classification
- Estimated Resilient Modulus based on AASHTO Soil Classification

## DESIGN OF DATABASE ARCHITECTURE

A relational database was designed to run in Oracle platform incorporating GIS capability. The database includes the data tables listed in Table 3.7. The Data elements are provided in Appendix 3.1.

**TABLE 3.7 MEPDG Database Tables**

TABLE NAME	DESCRIPTION
COUNTY	County number
DISTRICT	District number
ENV_CONDITIONS	Environmental condition
ENV_PRECIP_VAR	Precipitation
ENV_WATER_TABLE	Water table depth
PAV_ADMIX	Asphalt additive
PAV_BINDER	Asphalt binder
PAV_CONSTR	Construction information
PAV_FIELD_PERF	Field performance summary
PAV_FIELD_PERF_IRI	IRI information
PAV_FIELD_PERF_CRACK	Crack information
PAV_FIELD_PERF_RUT	Rut information
PAV_LAYER	Layer information
PAV_LAYER_BASE	Base information
PAV_LAYER_HMA	HMA information
PAV_LAYER_HMA_CREEP	HMA creep test results
PAV_LAYER_HMA_MOD	HMA resilient modulus
PAV_LAYER_SOIL	Soil information
PAV_LAYER_SS_US_MOD	Granular material modulus
PAV_LAYER_STSC	Surface treatment information
PAV_MIX	Asphalt mix information
PAV_MIX_JMF	Asphalt mix job mixture formula
PAV_SECTION	Pavement section general information
TST_FATIGUE	Fatigue test results
TST_HWTD	Hamburg wheel test results
TRAFFIC	General traffic information
TRAFFIC_AXLE_LOAD_VAR	Axle load distribution

### Creation of Tables in MEPDG Database

Oracle developer was installed on a server machine. The research team has created a SQL script, which creates tables and their relationships in MEPDG database. The SQL script is given in Appendix 3.2. An example of DSS data creation in MEPDG is described below:

#### *DSS Database Creation*

At first, a new database named DSS is created in MEPDG Oracle Database server. It is created using DBCA (Database Configuration Assistant) tool which is shown in Figure 3.2. Figure 3.3 further explains how to create a DBCA in oracle.

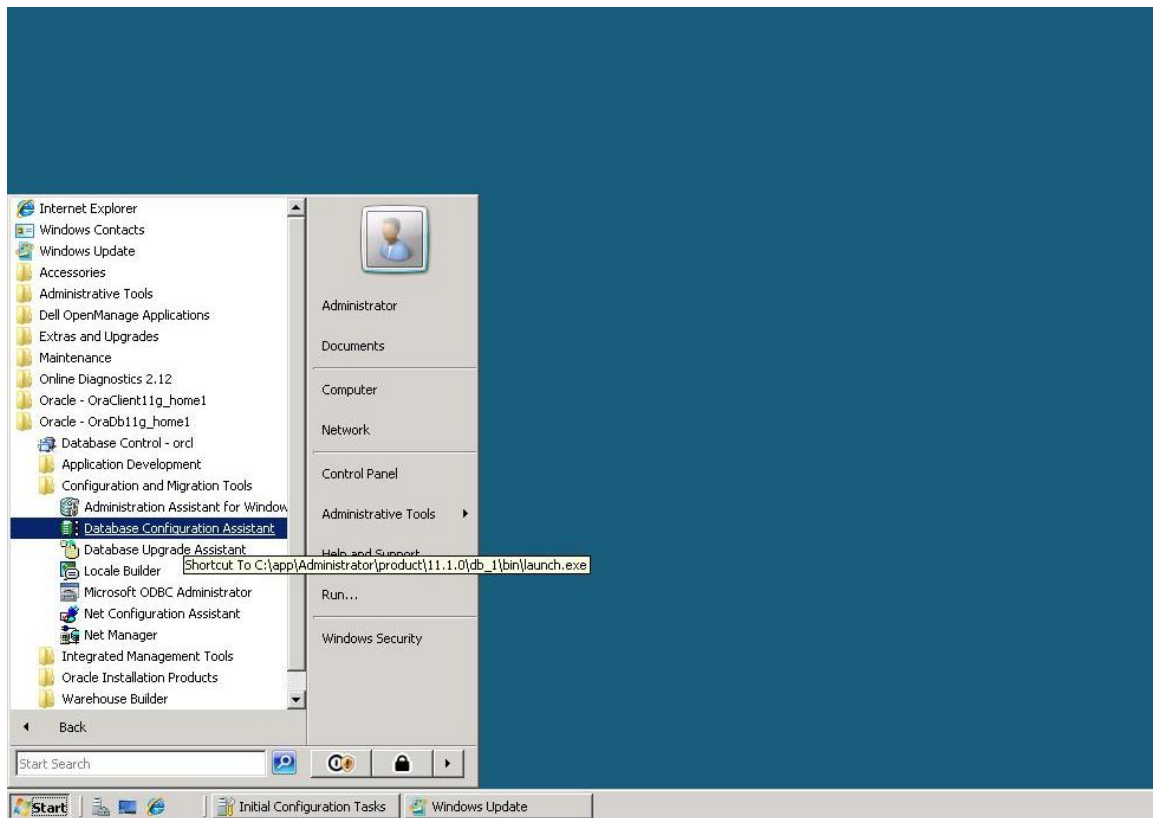


**FIGURE 3.2 Connection to DBCA Tool in windows**

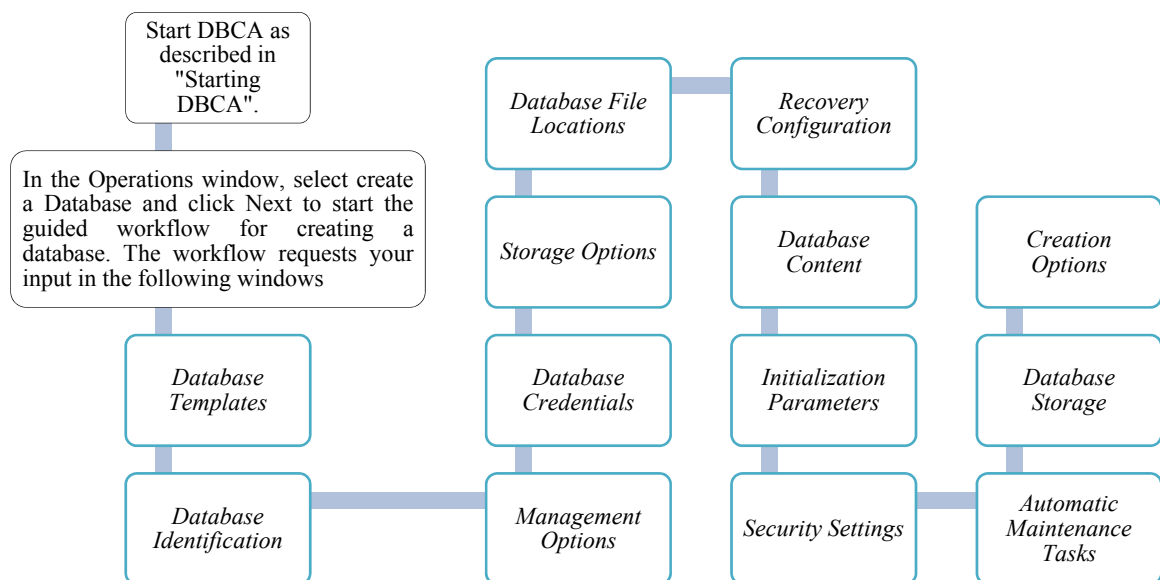


**FIGURE 3.3 Create a Database Using DBCA**

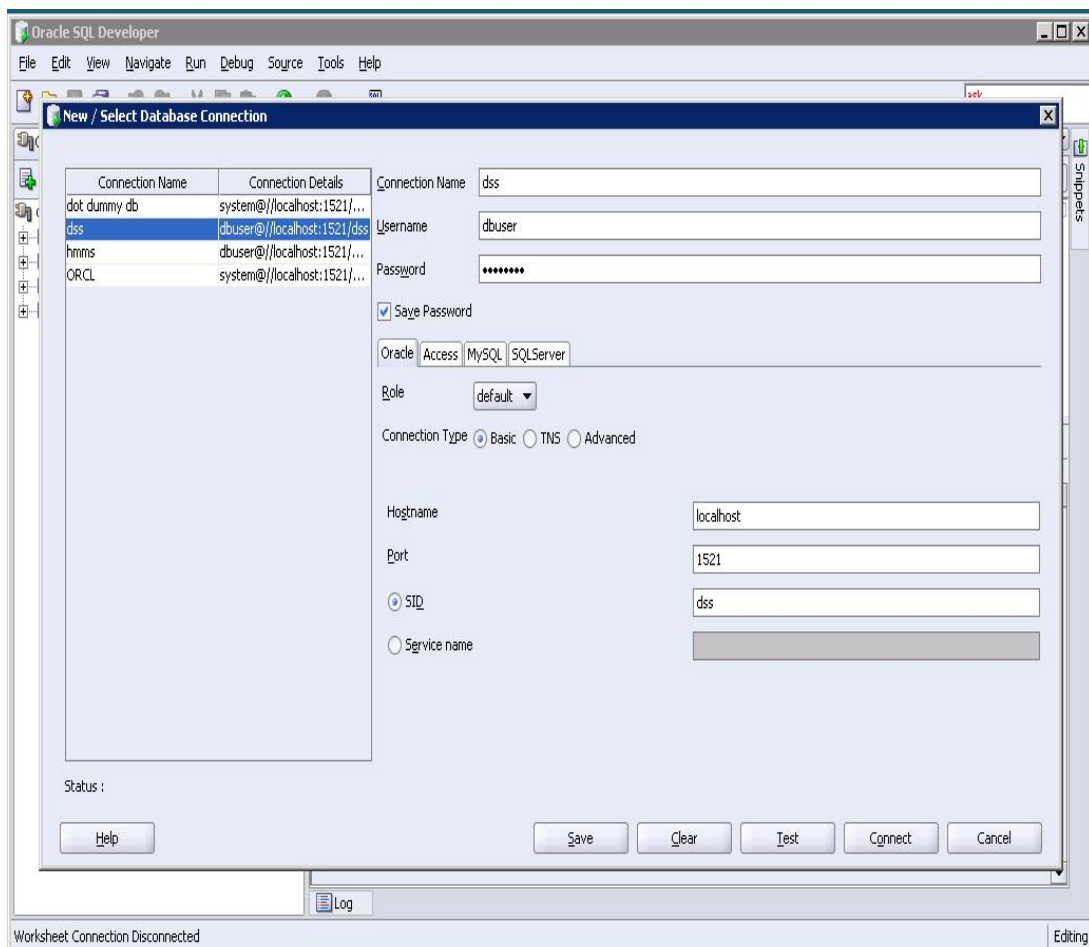
### *BUSER Creation*

Next, User named 'dbuser' is created in DSS database. The research team has created this user because in 'system' user there are many system related tables and to avoid confusion with those system tables. User should log on to server using SQL plus login into system account. The following command is run for creating user.

#### Run Script for DSS

```
CREATE USER dbuser IDENTIFIED BY password
DEFAULT TABLESPACE USERS
TEMPORARY TABLESPACE TEMP
PROFILE DEFAULT;
GRANT CONNECT, RESOURCE TO dbuser;
```

### Database Connection in Oracle Developer

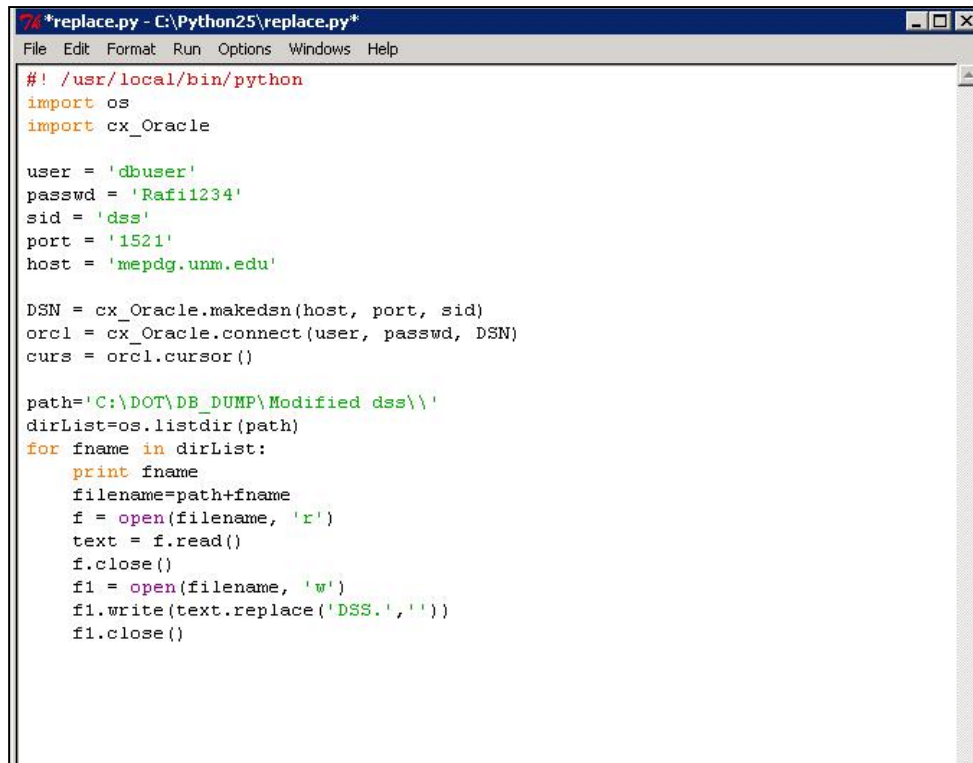


### *Extracting Data from DSS SQL Scripts*

The DSS database table format was not compatible to the format Oracle database table. Therefore, research team has written a python script, which uses regular expression module to

change the table name from database table to a normal table. This is an automated script, which runs on all SQL scripts and changes that particular string wherever it exists. The python script is shown below.

### Python Script for DSS Database



```
#!/usr/local/bin/python
import os
import cx_Oracle

user = 'dbuser'
passwd = 'Rafi1234'
sid = 'dss'
port = '1521'
host = 'mepdg.unm.edu'

DSN = cx_Oracle.makedsn(host, port, sid)
orcl = cx_Oracle.connect(user, passwd, DSN)
curs = orcl.cursor()

path='C:\DOT\DB_DUMP\Modified dss\'
dirList=os.listdir(path)
for fname in dirList:
    print fname
    filename=path+fname
    f = open(filename, 'r')
    text = f.read()
    f.close()
    f1 = open(filename, 'w')
    f1.write(text.replace('DSS.', ''))
    f1.close()
```

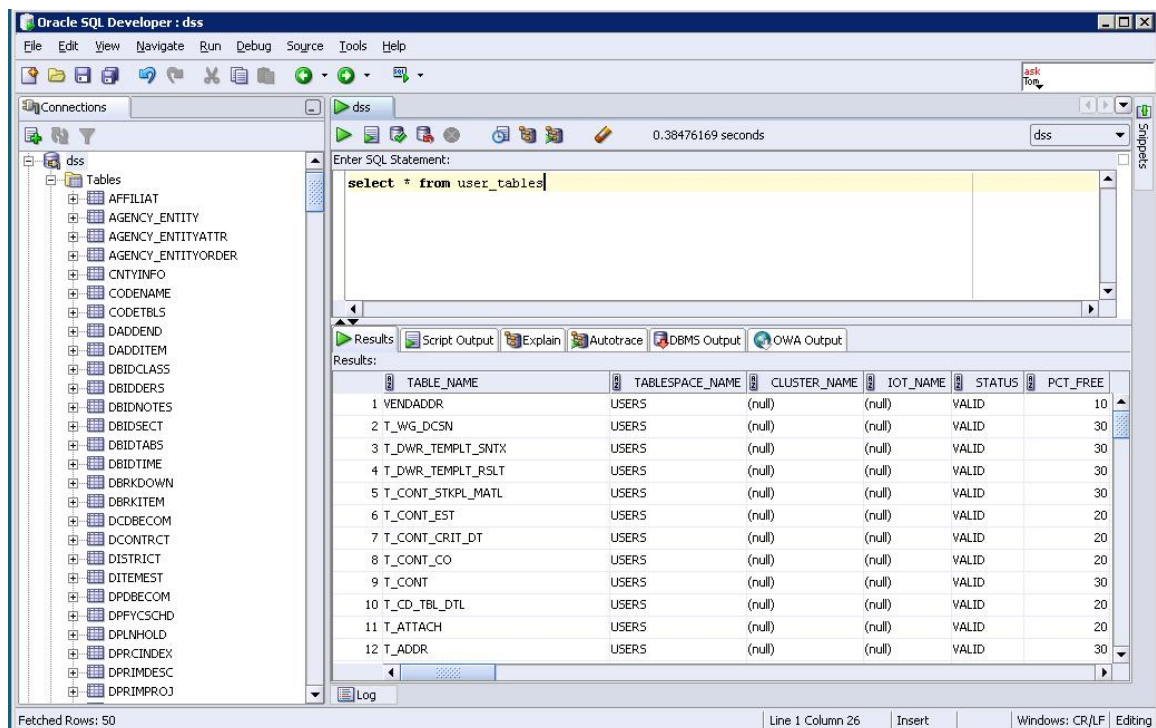
The research team has written an automated script in python language, which reads each SQL file, extracts data, and inserts that data into Oracle database. The automated python script is shown below:

## Extracting Data from DSS SQL Scripts

```
*automatedscript_quotationchange_final.py - C:\Python25\automatedscript_quotationchange_final.py
File Edit Format Run Options Windows Help
#! /usr/local/bin/python
import os
import cx_Oracle
import re
user = 'dbuser'
passwd = 'Raf11234'
sid = 'hame'
port = '1521'
host = 'mepdg.umn.edu'
DSN = cx_Oracle.makedsn(host, port, sid)
octl = cx_Oracle.connect(user, passwd, DSN)
curs = octl.cursor()
path='C:\DOT\DB_DUMP\dsa\'
dirlist=os.listdir(path)
for fname in dirlist:
    filename=path+fname
    f = open(filename, 'r')
    text = str(f.read())
    l=text.split("\n")
    flag = 0
    i = 0
    while i < len(l):
        a = l[i].count('"')
        if a%2 == 0:
            query=l[i]
            if re.search("[a-zA-Z0-9]", query):
                if not re.search("SET DEFINE OFF", query):
                    print 'testing --> ' + query
                    curs.execute(str(query))
            else:
                query=l[i]
                for j in range(i+1, len(l)):
                    query1 = query1 + ";" + l[j]
                    b = query1.count('"')
                    if b%2 == 0:
                        i = j
                        if re.search("[a-zA-Z0-9]", query1):
                            if not re.search("SET DEFINE OFF", query1):
                                print 'testing --> ' + query1
                                curs.execute(str(query1))
                        break
                    i = i + 1
    f.close()
curs.close()
```

After the script was successfully executed, all the tables are created and data is inserted into particular tables. The list of tables created in DSS database is shown below:

### List of Tables Created in DSS Database



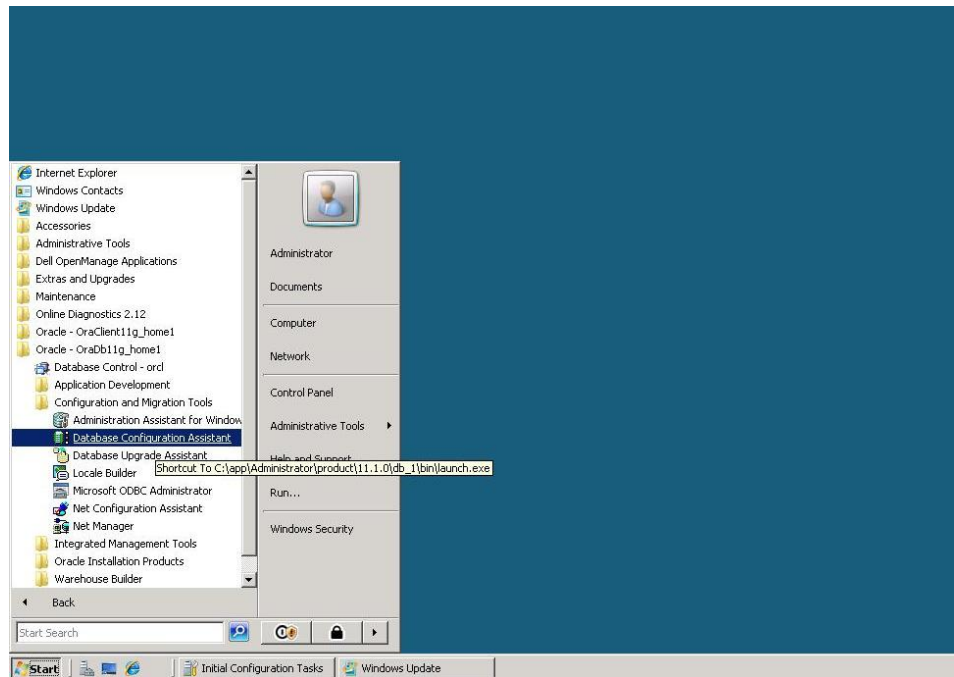
TABLE_NAME	TABLESPACE_NAME	CLUSTER_NAME	IOT_NAME	STATUS	PCT_FREE
1 VENDADDR	USERS	(null)	(null)	VALID	10
2 T_WG_DCSN	USERS	(null)	(null)	VALID	30
3 T_DWR_TEMPLT_SNTX	USERS	(null)	(null)	VALID	30
4 T_DWR_TEMPLT_RSLT	USERS	(null)	(null)	VALID	30
5 T_CONT_STKPL_MATL	USERS	(null)	(null)	VALID	30
6 T_CONT_EST	USERS	(null)	(null)	VALID	20
7 T_CONT_CRIT_DT	USERS	(null)	(null)	VALID	20
8 T_CONT_CO	USERS	(null)	(null)	VALID	20
9 T_CONT	USERS	(null)	(null)	VALID	30
10 T_CD_TBL_DTL	USERS	(null)	(null)	VALID	20
11 T_ATTACH	USERS	(null)	(null)	VALID	20
12 T_ADDR	USERS	(null)	(null)	VALID	30



### *HMMS Database Creation*

As a first step, a new database named Highway Maintenance Management System (HMMS) is created in Oracle Database server. It is created using DBCA (Database Configuration Assistant) tool.

#### Connection to DBCA Tool in Windows



The steps of database creation are given below:

#### Step 1: Create DBUSER:

User named 'dbuser' is created in DSS database. The research team has created this user because in 'system' user there are many system related tables. There is a possibility that database table might be confused with the system tables. User can log on to server using SQL plus login into System account and run the following command for creating user.

#### Run Script for HMMS

---

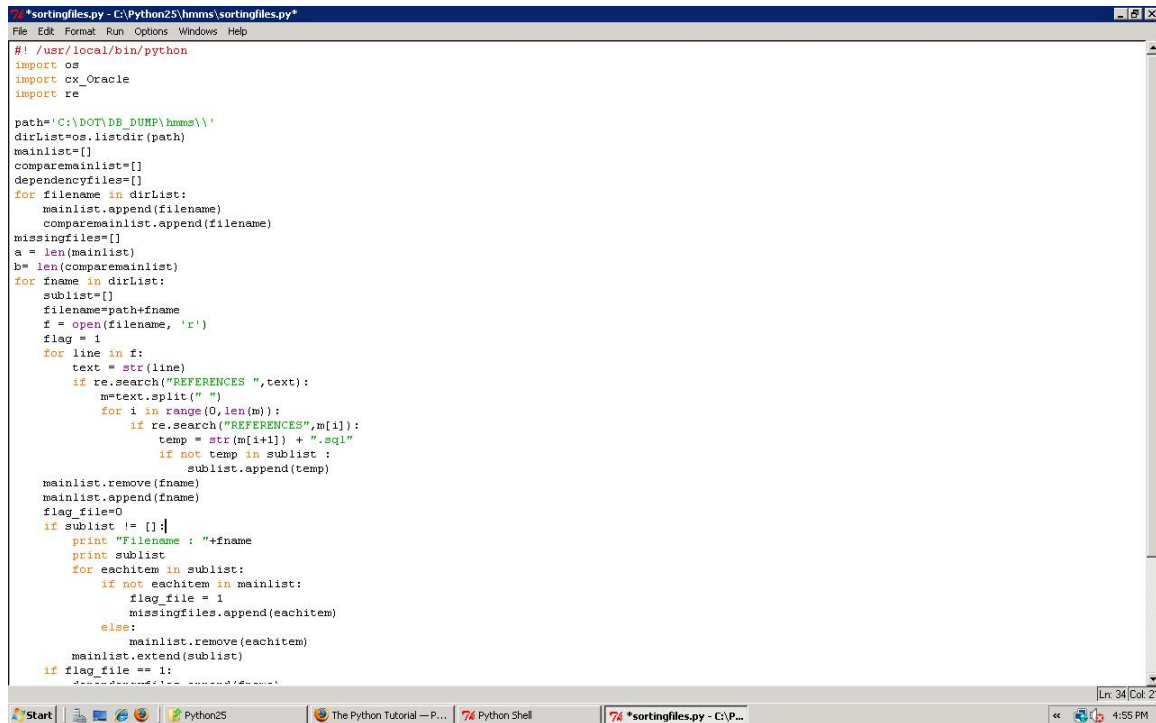
```
CREATE USER dbuser IDENTIFIED BY password
DEFAULT TABLESPACE USERS
TEMPORARY TABLESPACE TEMP
PROFILE DEFAULT;
GRANT CONNECT, RESOURCE TO dbuser;
```

---

## Step 2: Run HMMS SQL Scripts

Research team has written a python script, which outputs the list of files order for execution. After the execution of the above script, the script below will output the list of files in a particular order for execution.

### Dependency of SQL Files in HMSS Database



```
#!/usr/local/bin/python
import os
import cx_Oracle
import re

path='C:\DOT\DB_DUMP\hmms\*'
dirlist=os.listdir(path)
mainlist=[]
comparemainlist=[]
dependencyfiles=[]
missingfiles=[]
a = len(mainlist)
b = len(comparemainlist)
for fname in dirlist:
    sublist=[]
    filename=path+fname
    f = open(filename, 'r')
    flag = 1
    for line in f:
        text = str(line)
        if re.search("REFERENCES ",text):
            m=text.split(" ")
            for i in range(0,len(m)):
                if re.search("REFERENCES",m[i]):
                    temp = str(m[i+1]) + ".sql"
                    if not temp in sublist :
                        sublist.append(temp)
    mainlist.remove(fname)
    mainlist.append(fname)
    flag_file=0
    if sublist != []:
        print "Filename : "+fname
        print sublist
        for eachitem in sublist:
            if not eachitem in mainlist:
                flag_file = 1
                missingfiles.append(eachitem)
            else:
                mainlist.remove(eachitem)
                mainlist.extend(sublist)
    if flag_file == 1:
        dependencyfiles.append(fname)
        continue
    else:
        mainlist.remove(fname)
        mainlist.append(fname)
        flag_file=0
        continue
    if flag_file == 1:
        dependencyfiles.append(fname)
        continue
    else:
        mainlist.remove(fname)
        mainlist.append(fname)
        flag_file=0
        continue
```

Research team has written the following automatic python script, which reads each SQL file according to the order and extracts data and inserts that data into Oracle database.

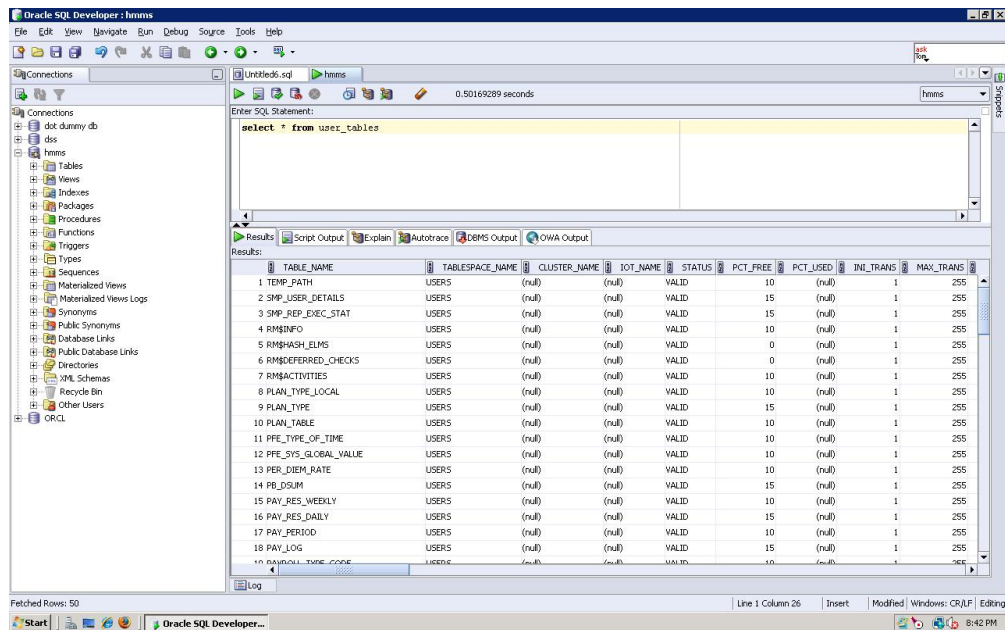
## Automatic Python Script

```
76 *automatedscript_quotationchange_final.py - C:\Python25\automatedscript_quotationchange_final.py*
File Edit Format Run Options Windows Help

#!/usr/local/bin/python
import os
import cx_Oracle
import re
user = 'dbuser'
passwd = 'Rafi1234'
sid = 'hmms'
port = '1521'
host = 'mepdg.unm.edu'
DSN = cx_Oracle.makedsn(host, port, sid)
orcl = cx_Oracle.connect(user, passwd, DSN)
curs = orcl.cursor()
path='C:\DOT\DB_DUMP\hmms\'
dirList=os.listdir(path)
for fname in dirList:
    sql="select table_name from user_tables where table_name='"+fname[:4]+'"'
    curs.execute(sql)
    j=curs.fetchall()
    k=0
    for row in j:
        k=1
        if k == 1:
            continue
        filename=path+fname
        f = open(filename, 'r')
        text = str(f.read())
        l=text.split(";")
        flag = 0
        i = 0
        while i < len(l):
            a= l[i].count("'")
            if a%2 == 0:
                query=l[i]
                if re.search("[a-zA-Z0-9]", query):
                    if not re.search("SET DEFINE OFF", query):
                        curs.execute(str(query))
            else:
                query1=l[i]
                for j in range(i+1, len(l)):
                    query1 = query1 + ";" + l[j]
                    b = query1.count("'")
                    if b%2 == 0:
                        i = j
                        if re.search("[a-zA-Z0-9]", query1):
                            if not re.search("SET DEFINE OFF", query1):
                                curs.execute(str(query1))
                        break
            i = i + 1
```

After the script was executed, all the tables are created and data is inserted into particular tables. The list of tables created in HMSS database is shown below.

## List of Tables Created in HMSS Database



The screenshot shows the Oracle SQL Developer interface with the 'hmms' database selected. The 'Tables' folder in the left pane is expanded, displaying a list of 18 tables. The main window shows the 'Enter SQL Statement' area with the query 'select \* from user\_tables' and the 'Results' pane displaying the table details.

	TABLE_NAME	TABLESPACE_NAME	CLUSTER_NAME	IOT_NAME	STATUS	PCT_FREE	PCT_USED	INI_TRANS	MAX_TRANS
1	TEMP_PATH	USERS	(null)	(null)	VALID	10	(null)	1	255
2	SMP_USER_DETAILS	USERS	(null)	(null)	VALID	15	(null)	1	255
3	SMP_REP_EXEC_STAT	USERS	(null)	(null)	VALID	15	(null)	1	255
4	RM\$INFO	USERS	(null)	(null)	VALID	10	(null)	1	255
5	RM\$HASH_ELMS	USERS	(null)	(null)	VALID	0	(null)	1	255
6	RM\$DEFERRED_CHECKS	USERS	(null)	(null)	VALID	0	(null)	1	255
7	RM\$ACTIVITIES	USERS	(null)	(null)	VALID	10	(null)	1	255
8	PLAN_TYPE_LOCAL	USERS	(null)	(null)	VALID	10	(null)	1	255
9	PLAN_TYPE	USERS	(null)	(null)	VALID	15	(null)	1	255
10	PLAN_TABLE	USERS	(null)	(null)	VALID	10	(null)	1	255
11	PFE_TYPE_OF_TIME	USERS	(null)	(null)	VALID	10	(null)	1	255
12	PFE_SYS_GLOBAL_VALUE	USERS	(null)	(null)	VALID	10	(null)	1	255
13	PER_OIEM_RATE	USERS	(null)	(null)	VALID	10	(null)	1	255
14	PLD_DIM	USERS	(null)	(null)	VALID	15	(null)	1	255
15	PAY_RES_WEEKLY	USERS	(null)	(null)	VALID	10	(null)	1	255
16	PAY_RES_DAILY	USERS	(null)	(null)	VALID	15	(null)	1	255
17	PAY_PERIOD	USERS	(null)	(null)	VALID	10	(null)	1	255
18	PAY_LOG	USERS	(null)	(null)	VALID	15	(null)	1	255
19	PAYROLL_TIME_CODE	USERS	(null)	(null)	VALID	10	(null)	1	255

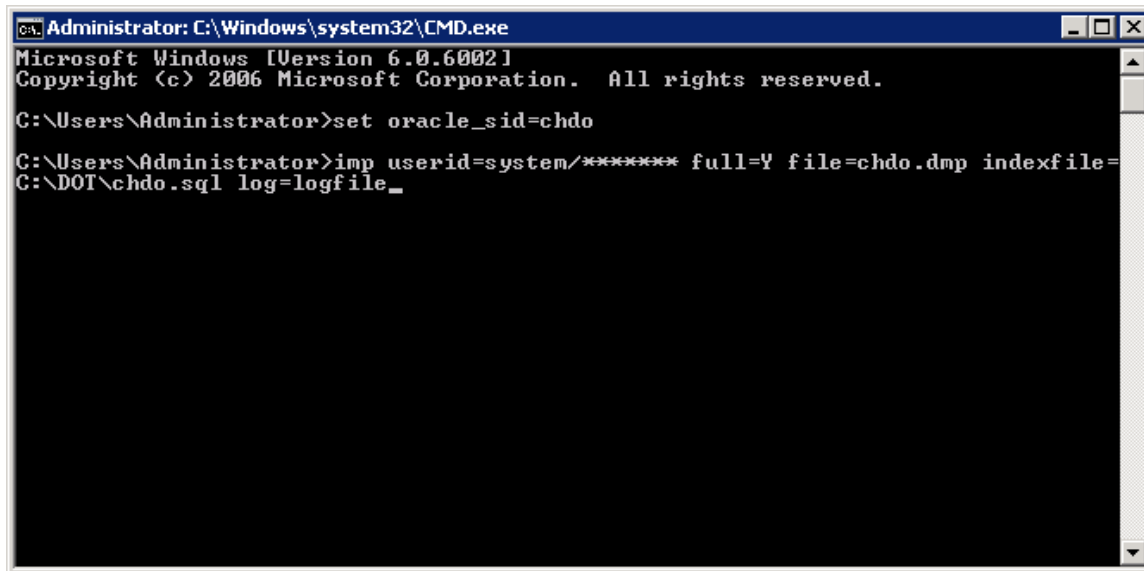
## CHDB Database

UNM research team collected the CHDB dump files. As a first step, UNM research team has created a new database named CHDB in the MEPDG Oracle Database server stationed at UNM. The new database, which is a mirror of the NMDOT's CHDB database, is created using DBCA (Database Configuration Assistant) tool in Oracle.

### *Locate DMP File and Inspect SQL index file*

As a 2nd step, CHDB.sql is extracted from the CHDB.dmp file. Research team has extracted this SQL file for inspecting the username of the database and also the names of table spaces. Using windows command prompt, the following commands were run for extracting the SQL file from the DMP file. Below is a screenshot of how to run the import command in windows command prompt.

Running import command for creating CHDO.SQL script file from DMP file in Windows Command Prompt



```
Administrator: C:\Windows\system32\CMD.exe
Microsoft Windows [Version 6.0.6002]
Copyright (c) 2006 Microsoft Corporation. All rights reserved.

C:\Users\Administrator>set oracle_sid=chdo

C:\Users\Administrator>imp userid=system/***** full=Y file=chdo.dmp indexfile=
C:\DOT\chdo.sql log=logfile_
```

#### *LEV User Creation*

As a third step, a user name 'LEV' is created in CHDB database. Research team has created this user to match username 'LEV' used in DMP file. Then the users login to server and also login to system account using SQL plus. The following command is run for creating user.

##### Run Script for LEV user Creation

```
CREATE USER LEV IDENTIFIED BY PASSWORD DEFAULT
TABLESPACE USERS
TEMPORARY TABLESPACE TEMP
PROFILE DEFAULT;
GRANT CONNECT, RESOURCE TO CHDO;
```

#### *TableSpace Creation*

As a step four, TableSpaces named USER\_DATA, INDEX\_DATA are created in CHDB database under LEV user. The same tablespaces are used in DMP file. Again, users login to server and 'LEV' account using SQL plus. The following commands are run for creating tablespace.

##### Run Script for USER\_DATA tablespace Creation

```
CREATE TABLESPACE USER_DATA DATAFILE '
C:\DOT\DUMP_APRIL_09_DOT\Exports\CHDO\USER_DATA.DBF'
SIZE 1000M
AUTOEXTEND ON MAXSIZE 2000M
EXTENT MANAGEMENT LOCAL UNIFORM SIZE 64K;
```

### Run Script for INDEX\_DATA tablespace Creation

---

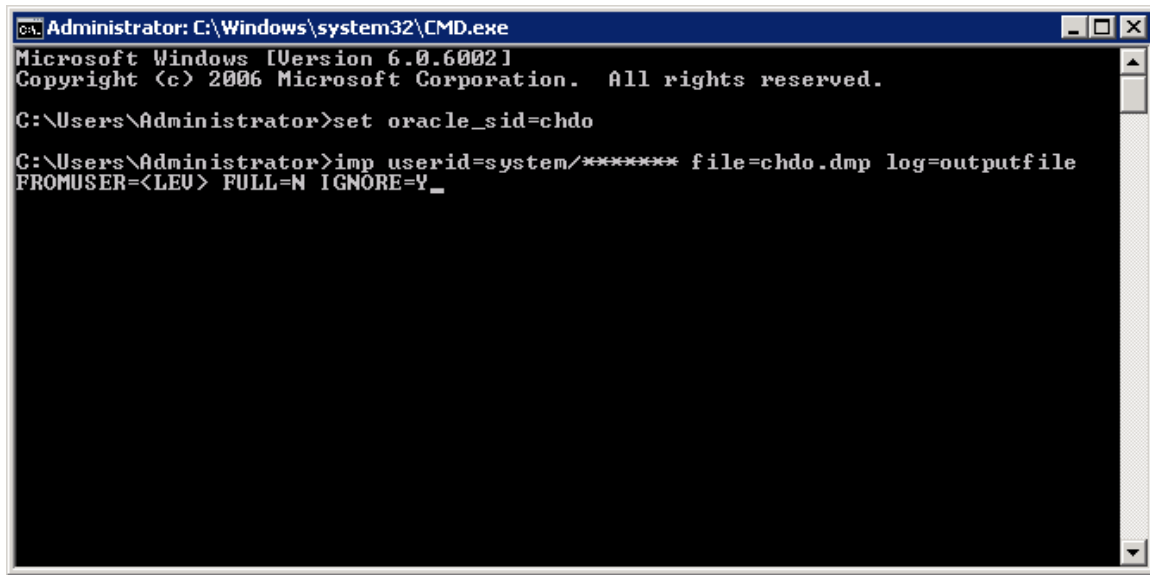
```
CREATE TABLESPACE INDEX_DATA DATAFILE '  
C:\DOT\DUMP_APRIL_09_DOT\Exports\CHDO\INDEX_DATA.DBF'  
SIZE 1000M  
AUTOEXTEND ON MAXSIZE 2000M  
EXTENT MANAGEMENT LOCAL UNIFORM SIZE 64K;
```

---

#### *Extracting Data from DMP File for CHDB*

In this task, the research team has created tables and dumped data into respective tables using CHDB.dmp file. After logging in, the following command is run for creating tables and dumping data into respective tables. Below is a screenshot of how to extract data from DMP File.

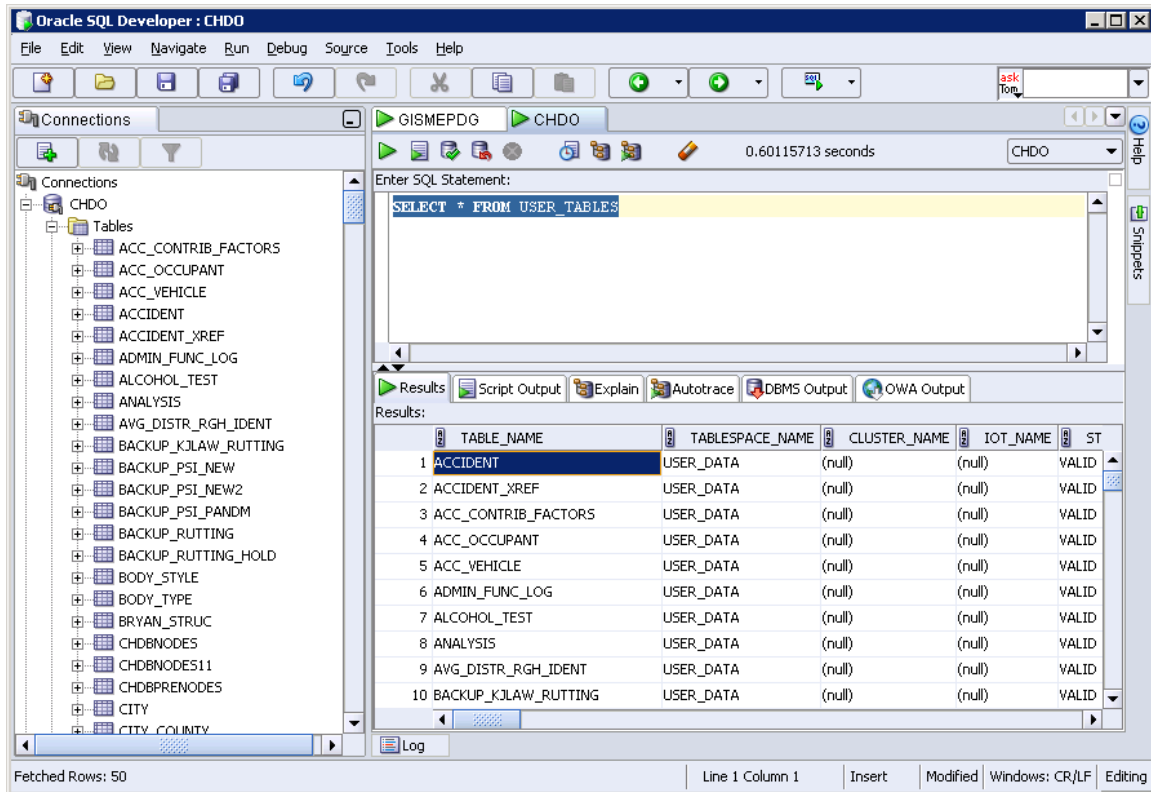
#### *Extract Data for CHDB database using Import command in Windows Command Prompt*



```
Administrator: C:\Windows\system32\CMD.exe  
Microsoft Windows [Version 6.0.6002]  
Copyright (c) 2006 Microsoft Corporation. All rights reserved.  
  
C:\Users\Administrator>set oracle_sid=chdo  
  
C:\Users\Administrator>imp userid=system/***** file=chdo.dmp log=outputfile  
FROMUSER=<LEU> FULL=N IGNORE=Y_
```

After the command is successfully executed, all the tables are created and data are inserted into particular tables. Below is a screenshot of a list of tables created in CHDB database using SQL Developer software.

## Viewing Tables in CHDB Database



### *Annual Traffic*

Research team has analyzed data tables in CHDB and TIMS database. In these two databases, the following tables and views contain the annual traffic information.

#### CHDB

- 1) DSV\_TRAFFIC\_SECTIONS\_VIEW
- 2) TRAF\_MAIN\_VIEW
- 3) EXOR\_VIEW\_TRAF\_ANNUAL

#### TIMS

- 4) NM\_INV\_ITEMS\_ALL
- 5) V\_NM\_TSAN
- 6) V\_NM\_CSIT

## POPULATION OF MEPDG DATABASE

This chapter deals with the population of the MEPDG database using data from appropriate data sources including LTPP, paper copy of data, data from NMDOT Website, laboratory spread sheet, and various databases currently in use by NMDOT.

UNM Research team has collected “dumps” copy of data as well as downloaded data (e.g., traffic data) from the NMDOT Website, and put them in a text file which contains data in a format compatible with the MEPDG database columns data type. Next, data were used to populate respective tables in MEPDG database using Python script shown below.

```
#InsertScript_Traffic_count_2007.py - C:\Python25\Inserting Data into MMDOT\InsertScript_Traffic_co... x
```

```
File Edit Format Run Options Windows Help

#!/usr/local/bin/python
import os
import cx_Oracle
import re

user = 'dbuser'
passwd = '*****'
sid = 'gismepdg'
port = '1521'
host = 'mepdg.unmm.edu'


DSN = cx_Oracle.makedsn(host, port, sid)
orcl = cx_Oracle.connect(user, passwd, DSN)
curs = orcl.cursor()



fname='TRAFFIC_2007.txt'
f = open(fname, 'r')
text = str(f.read())
a=re.split("\t\\n",text)
i = 0
while i < len(a):
    sql='''insert into TRAFFIC_COUNT
(traffic_id,pstd_rte,aadt_year_2007,hisgrfac,hisaxfac,hissefac,aadt_2007,aad
aad_m_2007,aawet_p_2007,aawet_m_2007,aawdt_p_2007,aawdt_m_2007,fuaadme_200
shvycompk_2007,shvycomav_2007,chvycmpk_2007,chvycomav_2007,k_factor_2007,
dir_fac_2007,pkhrrvol_2007,rtsys) values
(%s,%s','%s','%s','%s','%s',
%s,%s,%s,%s,%s,%s,%s,%s,%s,%s,'%s') ''' % (a[i],a[i+1],a[i+2] ,
print sql
curs.execute(sql)
curs.execute("commit")
print "Inserted"
i = i + 22
f.close
```

71



## Data in District Table

The screenshot shows the Oracle SQL Developer interface with the 'DISTRICT' table selected in the 'Tables' pane. The SQL statement 'select district\_id,district\_name from district' is entered in the 'Enter SQL Statement' field. The 'Results' pane displays the following data:

DISTRICT_ID	DISTRICT_NAME
1	6 district6
2	1 district1
3	2 district2
4	3 district3
5	4 district4
6	5 district5

The status bar at the bottom indicates 'All Rows Fetched: 6' and 'Line 1 Column 33'.

## Data in County Table

The screenshot shows the Oracle SQL Developer interface with the 'COUNTY' table selected in the 'Tables' pane. The SQL statement 'select county\_id, county\_name, district\_id from county' is entered in the 'Enter SQL Statement' field. The 'Results' pane displays the following data:

COUNTY_ID	COUNTY_NAME	DISTRICT_ID
1	Bernalillo	3
2	Catron	6
3	Chaves	2
4	Cibola	6
5	Colfax	4
6	Curry	2
7	De Baca	2
8	Dona Ana	1
9	Eddy	2
10	Grant	1
11	Guadalupe	4
12	Harding	4
13	Hidalgo	1
14	Lea	2
15	Lincoln	2
16	Los Alamos	5
17	Luna	1
18	McKinley	6
19	Mora	4
20	Otero	2

The status bar at the bottom indicates 'All Rows Fetched: 33' and 'Line 1 Column 30'.

## Data in PAV\_SECTION Table

The screenshot shows the Oracle SQL Developer interface with the PAV\_SECTION table selected in the schema browser. The table contains 20 rows of data. The status bar indicates 750 rows were fetched.

SECTION_ID	ROUTE_NAME	BEG_MPNT	END_MPNT
1	11766 FL4413	0.89	1.07
2	7954 NM0209	1.41	2.216
3	7672 NM0159	0	30.551
4	8410 NM0292	0	1.01
5	8216 NM0252	39.2	43.106
6	8329 NM0272	0	3.01
7	8966 NM0411	0	3.965
8	8901 NM0395	0	0.48
9	8519 NM0313	0	3.27
10	8590 NM0317	0.189	1.002
11	23788 NM0359	0.417	2.616
12	17172 NM0300	0	1.448
13	8512 NM0311	0	20.869
14	23038 NM0329	0.303	0.852
15	7808 NM0188	0	0.068
16	21046 NM0263	1.754	2
17	25586 NM0344	5.32	17.372
18	19568 NM0126	1.1	1.311
19	7911 NM0206	19.279	37.35
20	23995 NM0333	8.118	10.119

## Data in TRAFFIC Table

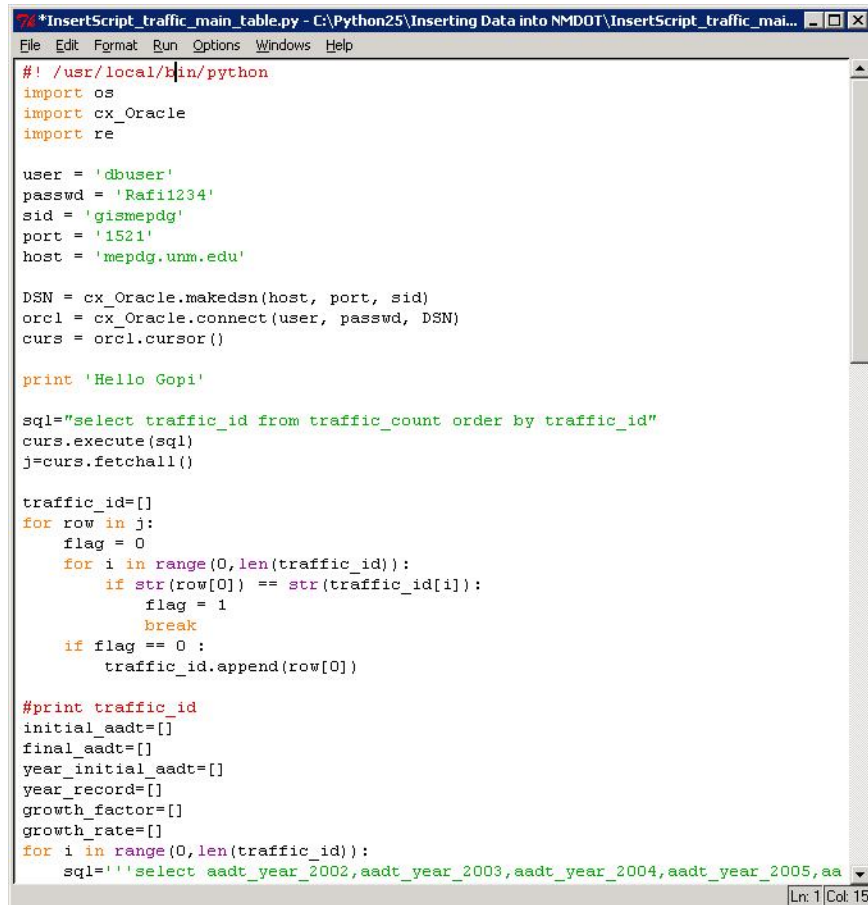
The screenshot shows the Oracle SQL Developer interface with the TRAFFIC table selected in the schema browser. The table contains 19 rows of data. The status bar indicates 50 rows were fetched.

TRAFFIC_ID	PSTD_RTE	HISGRFAC	HISAXFAC	HISSEFAC	AADT_YEAR
1	10373 IG4161	INTSLGURB	INTSLGURB	INTSLGURB	2007
2	17898 IG4154	INTSRUR	INTSRUR	INTSRUR	2007
3	10354 IG4081	INTSSMURB	INTSSMURB	INTSSMURB	2007
4	10341 IG4016	INTSSMURB	INTSSMURB	INTSSMURB	2007
5	10330 IG2414	INTSRUR	INTSRUR	INTSRUR	2007
6	10328 IG2404	INTSRUR	INTSRUR	INTSRUR	2007
7	10316 IG2335	INTSRUR	INTSRUR	INTSRUR	2007
8	22428 IG2276	INTSLGURB	INTSLGURB	INTSLGURB	2007
9	10297 IG2242	INTSRUR	INTSRUR	INTSRUR	2007
10	10525 IN2259	INTSRUR	INTSRUR	INTSRUR	2007
11	10514 IN2229	INTSLGURB	INTSLGURB	INTSLGURB	2007
12	10498 IN2175	INTSRUR	INTSRUR	INTSRUR	2007
13	10896 IV2460	INTSRUR	INTSRUR	INTSRUR	2007
14	10897 IU4158	INTSLGURB	INTSLGURB	INTSLGURB	2007
15	10482 IN2071	INTSRUR	INTSRUR	INTSRUR	2007
16	10475 IN2019	INTSRUR	INTSRUR	INTSRUR	2007
17	10470 IN1162	INTSRUR	INTSRUR	INTSRUR	2007
18	10458 IN1082	INTSSMURB	INTSSMURB	INTSSMURB	2007
19	18728 IR2435	INTSRUR	INTSRUR	INTSRUR	2007

## Traffic Tables

UNM Research Team has extracted the data from TRAFFIC\_COUNT table, converted the traffic data into MEPDG format, and stored it in TRAFFIC\_NMDOT\_GIS table. GIS feature is implemented on the traffic data and stored it in TRAFFIC\_NMDOT\_GIS table. Parameters such as growth factor, growth rate, and initial\_AADT values were calculated based on data available in TRAFFIC\_NMDOT\_GIS table. Next data are inserted into TRAFFIC\_GENERAL\_GROWTH\_RATE table.

### Python Script I for Traffic\_General\_Growth\_Rate Table



```
#!/usr/local/bin/python
import os
import cx_Oracle
import re

user = 'dbuser'
passwd = 'Rafii234'
sid = 'gismepdg'
port = '1521'
host = 'mepdg.unm.edu'

DSN = cx_Oracle.makedsn(host, port, sid)
orcl = cx_Oracle.connect(user, passwd, DSN)
curs = orcl.cursor()

print 'Hello Gopi'

sql="select traffic_id from traffic_count order by traffic_id"
curs.execute(sql)
j=curs.fetchall()

traffic_id=[]
for row in j:
    flag = 0
    for i in range(0,len(traffic_id)):
        if str(row[0]) == str(traffic_id[i]):
            flag = 1
            break
    if flag == 0 :
        traffic_id.append(row[0])

#print traffic_id
initial_aadt=[]
final_aadt=[]
year_initial_aadt=[]
year_record=[]
growth_factor=[]
growth_rate=[]
for i in range(0,len(traffic_id)):
    sql='''select aadt_year_2002,aadt_year_2003,aadt_year_2004,aadt_year_2005,aa
```

## Python Script for Traffic\_General\_Growth\_Rate Table

```

*InsertScript_traffic_main_table.py - C:\Python25\Inserting Data into NMDOT\InsertScript_traffic_mai...
File Edit Format Run Options Windows Help

    j1=curs.fetchall()
    for row1 in j1:
        initial_aadt.append(row1[0])
        final_aadt.append(row1[1])
    elif str(row[3]) != 'None':
        year_initial_aadt.append(row[3])
        sql='''select aadt_2005,aadt_2007 from traffic_count where traffic_i
        curs.execute(sql)
        j1=curs.fetchall()
        for row1 in j1:
            initial_aadt.append(row1[0])
            final_aadt.append(row1[1])
    elif str(row[4]) != 'None':
        year_initial_aadt.append(row[4])
        sql='''select aadt_2006,aadt_2007 from traffic_count where traffic_i
        curs.execute(sql)
        j1=curs.fetchall()
        for row1 in j1:
            initial_aadt.append(row1[0])
            final_aadt.append(row1[1])
    else:
        year_initial_aadt.append(row[5])
        sql='''select aadt_2007,aadt_2007 from traffic_count where traffic_i
        curs.execute(sql)
        j1=curs.fetchall()
        for row1 in j1:
            initial_aadt.append(row1[0])
            final_aadt.append(row1[1])
Y1=float(initial_aadt[i])
Y2=float(final_aadt[i])
growth_factor.append(pow(Y2/Y1,float(1)/float(year_record[i]))-1)
growth_rate.append(growth_factor[i]*100)
print traffic_id[i],"->",year_initial_aadt[i],"->",initial_aadt[i],"->",year
sql='''insert into TRAFFIC_GROWTH_GENERAL_RATE
(traffic_id,growth_factor,growth_rate,initial_aadt,year_initial_aadt,year_re
(%s,%s,%s,%s,%s,%s)'''%(traffic_id[i],growth_factor[i],growth_rate[i],initia
curs.execute(sql)
curs.execute("commit")

curs.close()
Ln: 1 Col: 15

```

## TRAFFIC\_GENERAL\_GROWTH\_RATE TABLE

The screenshot shows the Oracle SQL Developer interface with the 'TRAFFIC\_GENERAL\_GROWTH\_RATE' table selected in the schema browser. The SQL statement 'select \* from TRAFFIC\_GENERAL\_GROWTH\_RATE' is entered in the SQL window, and the results are displayed in the Results pane. The table has 15 rows of data, with columns: TRAFFIC\_ID, YEAR\_INI, GROWTH\_FACTOR, GROWTH\_RATE, and INITIAL\_AADT. The row for TRAFFIC\_ID 1951 is highlighted.

TRAFFIC_ID	YEAR_INI	GROWTH_FACTOR	GROWTH_RATE	INITIAL_AADT
1	1909	-0.0136557765038	-1.36557765038	20243
2	1917	-0.0561027183107	-5.61027183107	33495
3	1951	0.0302074436017	3.02074436017	20870
4	1959	0.0367114727988	3.67114727988	21358
5	1963	-0.0379724716835	-3.79724716835	26645
6	2009	0.0331271998402	3.31271998402	30157
7	2015	0.0398883552907	3.98883552907	43625
8	2035	0.0310940859548	3.10940859548	104243
9	2055	0.0331326350627	3.31326350627	106121
10	2059	0.0398897477881	3.98897477881	106121
11	2061	0.0331331337702	3.31331337702	93282
12	2063	0.0398863975729	3.98863975729	99246
13	2073	0.0398875431759	3.98875431759	119623
14	2087	0.0331305653251	3.31305653251	150736
15	2103	0.0398869596657	3.98869596657	154904

### *Distress Tables*

As mentioned previously, NMDOT collects distress data in a qualitative format. The research team has analyzed the data and using python script populated the data into DISTRESS\_DATA\_MEPDG table. The following screenshots show the python script (Appendix 1) and table of the DISTRESS\_DATA.

## Python Script for DISTRESS\_DATA Table

```
File Edit Format Run Options Windows Help
```

```
#! /usr/local/bin/python
import os
import cx_Oracle
import re

user = 'dbuser'
passwd = 'Rafi1234'
sid = 'gismepdg'
port = '1521'
host = 'mepdg.unm.edu'

DSN = cx_Oracle.makedsn(host, port, sid)
orcl = cx_Oracle.connect(user, passwd, DSN)
curs = orcl.cursor()

fname='DISRESS_DATA.txt'
f = open(fname, 'r')
text = str(f.read())
a=re.split("\t|\n",text)
fl=open('Insert_2007.txt','w')
i = 0
while i < len(a):
    sql=''insert into DISTRESS_DATA values
    (%s,%s','%s','%s','%s','%s',
     %s,%s,%s,%s,%s,%s,%s,%s,%s,%s,%s,%s,'%s')'''%(a[i],a[i+1],a[i+2],
    print sql
#     curs.execute(sql)
    fl.write(sql+"\n")
#     curs.execute("commit")
    print "Inserted"
    i = i + 22
f.close
fl.close
```

Taskbar icons: Oracle SQL D..., 3 python, Microsoft Exc..., 6th Quarterly ..., 2 Windows E..., Microsoft Pow...



## DISTRESS\_DATA Table

The screenshot shows the Oracle SQL Developer interface. The title bar indicates the connection is 'TABLE DBUSER.DISTRESS\_DATA@GISEMPDG'. The left pane shows a tree of tables, with 'DISTRESS\_DATA' selected. The right pane displays the table's structure and data. The table has 5 columns: ID, PATCHING, EDGE\_CRACKS, ALLIGATOR\_CRACKS, TRANSVERSE\_CRACKS, and LONGITUDINAL. The data is displayed in a grid with 19 rows.

ID	PATCHING	EDGE_CRACKS	ALLIGATOR_CRACKS	TRANSVERSE_CRACKS	LONGITUDINAL
1	1	100	56	100	67
2	2	100	34	100	67
3	3	100	34	100	67
4	4	100	56	78	67
5	5	100	78	67	67
6	6	100	34	67	78
7	7	100	78	67	78
8	8	100	100	67	67
9	9	100	100	67	56
10	10	100	100	67	67
11	11	100	100	78	67
12	12	100	100	34	100
13	13	100	100	100	56
14	14	100	100	56	67
15	15	100	100	100	67
16	16	100	78	100	67
17	17	100	78	100	67
18	18	100	100	100	67
19	19	100	100	100	67

Fetches Rows: 55      Editing

## Python Script for DISRESS\_PMS\_DATA Table

79



## DISTRESS\_PMS\_DATA Table

The screenshot shows the Oracle SQL Developer interface. On the left, the 'Tables' list in the 'Connections' pane includes various tables, with 'DISTRESS\_PMS\_DATA' highlighted. The main window displays the 'Data' tab for the 'DISTRESS\_PMS\_DATA' table. The table has 6 columns: MILE\_POST, LANE\_DIRECTION, ROUTE, ROUTE\_NAME, YEAR\_DATA\_TAKEN, and ALLIGATOR\_CRACK. The data is presented in a grid with 19 rows. The status bar at the bottom indicates 'Fetching Rows: 55' and 'Editing'.

MILE_POST	LANE_DIRECTION	ROUTE	ROUTE_NAME	YEAR_DATA_TAKEN	ALLIGATOR_CRACK
1	1.022 M	I00010	I10	1996	0
2	3.012 M	I00010	I10	1996	0
3	5.012 M	I00010	I10	1996	0
4	7.012 M	I00010	I10	1996	0
5	9.012 M	I00010	I10	1996	0
6	10.992 M	I00010	I10	1996	0
7	12.992 M	I00010	I10	1996	0
8	15.012 M	I00010	I10	1996	0
9	17.012 M	I00010	I10	1996	0
10	19.002 M	I00010	I10	1996	0
11	21.022 M	I00010	I10	1996	0
12	23.012 M	I00010	I10	1996	0
13	25.022 M	I00010	I10	1996	0
14	27.032 M	I00010	I10	1996	0
15	29.042 M	I00010	I10	1996	0
16	31.042 M	I00010	I10	1996	0
17	33.042 M	I00010	I10	1996	0
18	35.052 M	I00010	I10	1996	0
19	37.052 M	I00010	I10	1996	0

The python script and the FWD\_DATA\_FILES table are shown below:

### Python Script for FWD\_DATA\_FILES Table

```
dsnread.py - C:\Python25\Test_fwd\dataread.py
File Edit Format Run Options Windows Help

DSN = cx_Oracle.makedsn(host, port, sid)
orcl = cx_Oracle.connect(user, passwd, DSN)
curs = orcl.cursor()

path='C:\Users\Administrator\Desktop\Gopi\RA\Test_FWD Data\\fwd\FWD 2005\'
dirList=os.listdir(path)
for fname in dirList:
    if not re.search(".DAT",fname):
        print fname
        break
filename = path+fname
print filename
f = open(filename, 'r')
text = str(f.read())
a=re.split("\t|\n",text)
time1=re.split("e:| **",a[1])
time=time1[3]
date=time1[2]
temp= re.split(": ",a[4])
location=temp[1]
temp = re.split(": ",a[5])
tempareture=temp[1]
print location,time,date,tempareture
for i in range(8,len(a)-2):
    if not re.search("Note:",a[i]):
        b=re.split(" ",a[i])
        for j in b:
            if j == '':
                b.remove('')
        if '' in b:
            b.remove('')
        print b
        sql='''insert into FWD_DATA_FILES (year,file_name,dateof,timeof,loca
(%s,%s,%s,%s,%s,%s,%s,%s,%s,%s,%s,%s,%s,%s,%s,%s))'''% ("2005"
        print sql
        curs.execute(sql)
        curs.execute("commit")

f.close()
```

## FWD\_DATA\_FILES Table

The screenshot shows the Oracle SQL Developer interface. On the left, the 'Tables' tree under the 'GISEMPDG' schema lists various tables, with 'DISTRESS\_PMS\_DATA' highlighted. The main pane displays the 'Data' tab for the 'DISTRESS\_PMS\_DATA' table. The table has 6 columns: MILE\_POST, LANE\_DIRECTION, ROUTE, ROUTE\_NAME, YEAR\_DATA\_TAKEN, and ALLIGATOR\_CRACK. The data is presented in a grid with 19 rows. The status bar at the bottom indicates 'Fetching Rows: 55' and 'Editing'.

MILE_POST	LANE_DIRECTION	ROUTE	ROUTE_NAME	YEAR_DATA_TAKEN	ALLIGATOR_CRACK
1	1.022 M	I00010	I10	1996	0
2	3.012 M	I00010	I10	1996	0
3	5.012 M	I00010	I10	1996	0
4	7.012 M	I00010	I10	1996	0
5	9.012 M	I00010	I10	1996	0
6	10.992 M	I00010	I10	1996	0
7	12.992 M	I00010	I10	1996	0
8	15.012 M	I00010	I10	1996	0
9	17.012 M	I00010	I10	1996	0
10	19.002 M	I00010	I10	1996	0
11	21.022 M	I00010	I10	1996	0
12	23.012 M	I00010	I10	1996	0
13	25.022 M	I00010	I10	1996	0
14	27.032 M	I00010	I10	1996	0
15	29.042 M	I00010	I10	1996	0
16	31.042 M	I00010	I10	1996	0
17	33.042 M	I00010	I10	1996	0
18	35.052 M	I00010	I10	1996	0
19	37.052 M	I00010	I10	1996	0

### Mix Data

HMA mix data were collected from Materials Bureau for different project locations. Research team has analyzed the data files and populated data (2006-2008) into MIX\_DESIGN table using python script. NMDOT has provided data in Excel sheet. The excel data were converted into text file and then text data was populated in MIX\_DESIGN table using python script. The screenshot of python script and MIX\_DATA\_MEPDG table are shown below.

## Python Script for Insetting Mix Design Data into the MIX\_DESIGN Table

```
MIX_DESIGN.py - C:\Python25\Mix\MIX_DESIGN.py
File Edit Format Run Options Windows Help

user = 'dbuser'
passwd = 'Rafi1234'
sid = 'gismepdg'
port = '1521'
host = 'mepdg.unm.edu'

DSN = cx_Oracle.makedsn(host, port, sid)
orcl = cx_Oracle.connect(user, passwd, DSN)
curs = orcl.cursor()

print 'Hello Gopi'
fname='Mix_2006.txt'
f = open(fname, 'r')
text = str(f.read())
text=text.replace("'",'')
a=re.split("\t|\n",text)
i = 0
for j in range(0,len(a)):
    print j
    print a[j]
    if(j==50):
        break

while i < len(a):
    sql='''insert into MIX_DESIGN values
        (seq_mix_id.nextval,'2006','%s','%s','%s','%s','%s','%s','%s','%s',
        '%s','%s','%s','%s','%s','%s','%s','%s','%s','%s','%s','%s',
        '%s','%s','%s','%s','%s','%s','%s','%s','%s')'''%(a[i],a[i+1],a[i+2],a[i+3],a[i+4],a[i+5],a[i+6],a[i+7],a[i+8],a[i+9],a[i+10],a[i+11],a[i+12],a[i+13],a[i+14],a[i+15],a[i+16],a[i+17],a[i+18],a[i+19],a[i+20],a[i+21],a[i+22],a[i+23],a[i+24],a[i+25],a[i+26],a[i+27],a[i+28],a[i+29],a[i+30],a[i+31],a[i+32],a[i+33],a[i+34],a[i+35])

    print sql
    curs.execute(sql)
    curs.execute("commit")
    print "Inserted"
    i = i + 40
f.close
```

## MIX\_DATA\_MEPDG Table

The screenshot shows the Oracle SQL Developer interface with the 'MIX\_DATA\_MEPDG' table selected in the 'Connections' pane. The 'Enter SQL Statement' area contains the query: `select * from mix_data_mepdg`. The 'Results' pane displays the following data:

	SML_MIX_DES	NMDOT_LAB	PCN	PROJECT_NUMBER	LOCATION	
20	20080D1003087R	2009000117	4063	AC0GRIP0IM001002(122)130	0	I01
21	20090CMD001001	2009000114	Various	Commercial Mix Design	Various	Var
22	20090CMD002002	2009000115	Various	Commercial Mix Design	Various	Var
23	20090CMD003003	2009000116	Various	Commercial Mix Design	Various	Var
24	20090CMD004005	2009000118	Various	Commercial Mix Design	Various	Var
25	20090CMD004005R	2009000123	Various	Commercial Mix Design	Various	Var
26	20090CMD006014	2009000688	Various	Commercial Mix Design	Various	Var
27	20090CMD007015	2009000689	Various	Commercial Mix Design	Various	Var
28	20090CMD008017	2009000691	Various	Commercial Mix Design	Various	Var
29	20090CMD009018	2009000692	Various	Commercial Mix Design	Various	Var
30	20090CMD010019	2009000693	Various	Commercial Mix Design	Various	Var
31	20090CMD011021	2009001077	Various	Commercial Mix Design	Various	0
32	20090D1001006	2009000119	4063	AC0GRIP0IM001002(122)130	0	I01
33	20090D1002008	2009000121	4063	AC0GRIP0IM001002(122)130	0	I01
34	20090D1003020	2009001076	2133	IM001002(106)78	Deming	I01
35	20090D2001012	2009000686	D2410	NH007007(5)412	Portales	US
36	20090D2002016	2009000690	D2410	NH007007(5)412	Portales	US

The status bar at the bottom indicates 'All Rows Fetched: 42' and 'Line 1 Column 29 Insert Windows: CR/LF Editing'.

## AXLE LOAD SPECTRA

Traffic in MEPDG is defined by the magnitude and frequency of the loads applied during the pavement design life. The previous versions of the AASHTO Guide for Pavement Design characterized traffic by defining the equivalent single axle load (ESAL). However, the MEPDG uses a more complex approach and requires a larger number of traffic inputs. The MEPDG adopts a hierarchical approach for the design inputs, defining three levels of traffic data input (Levels 1 through 3) on the basis of available data accuracy and reliability. Level 1 input correspond to site-specific traffic data; Level 2 is used when only regional or statewide traffic data are available; and Level 3 is defined for default national values or estimates based on local experience.

Axle load spectra can be only obtained from weigh-in-motion data. For each truck vehicle passing, this equipment record tabulation formed with the vehicle type (FHWA class 4 through 13) and the number, spacing, and weight of axles. There are different technologies for WIM systems such as load cell, bending plate, and piezo sensor. The dynamic weight measured by these systems is not the same as the actual static weight, because there is an inherent error associated with these technologies. Each one of them has a particular accuracy and reliability.



The axle load spectra can be defined as the percentage of the total axle applications within each load interval for a specific axle type (single, tandem, tridem, and quad) and vehicle class (classes 4 through 13). The following equation can be used to compute the axle load distribution factors:

$$ALDF_{ijk} = \frac{\text{No. of axles for class } i, \text{ month } j, \text{ and load range } k}{\text{Total No. of axles for class } i \text{ and month } j} \times 100$$

Axle load spectra have been proved to have strong influence on pavement performance.

### **Weigh-in-Motion Data in New Mexico**

Currently, fourteen WIM stations are collecting weight and classification data throughout New Mexico. These WIM sites are operated by New Mexico Department of Transportation (NMDOT). Three of them use bending plate systems (IRD 1058), and the remaining use piezoelectric sensors (Mikros Raktel 8000). Table 4.1 shows the name, code, location, and type of technology of each of the WIM sites. Vado site is right now under construction.

The condition of the road surface, the calibration of the system, and the temperature in the case of piezoelectric sensors are factors that affect significantly the weight measurement. Therefore, some inaccuracy in the data collected by these WIM stations is expected. The weigh-in-motion data collected during the year 2010 are used for the following analyses.

### **Development of Axle Load Spectra**

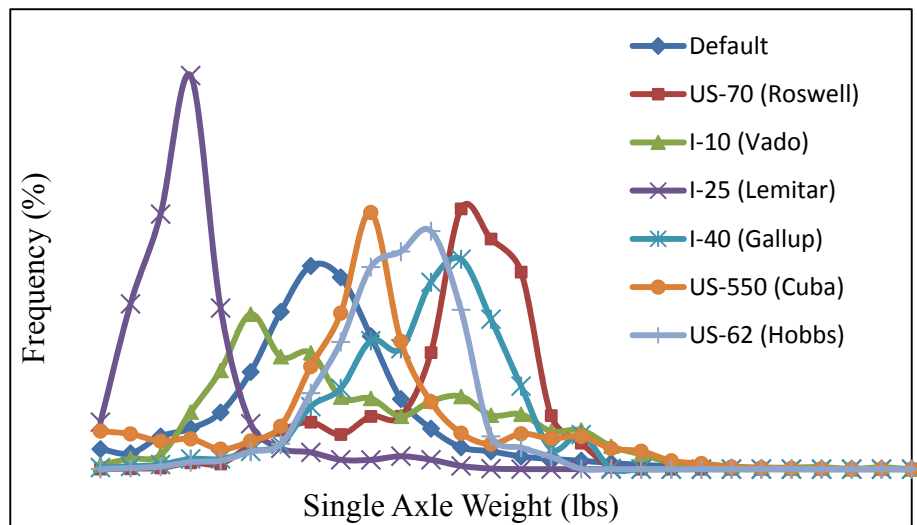
Weigh-in-motion data is required and processed in order to obtain axle load spectra which are one of the most important inputs in the MEPDG. This process is external to MEPDG. TrafLoad v1.0.8 is software for processing and analysis of weigh-in-motion data that was created under NCHRP Project 1-39. In this case TrafLoad is not effective to process and produce axle load spectra as in many other cases reported in the literature.

Therefore, an algorithm has been implemented in Visual Basic to process weigh-in-motion data and to compute the corresponding axle load spectra. This algorithm is based on the spacing between axles and the weight of each axle. A limit spacing value is defined such that when there are two, three or four consecutive axles separated by a distance smaller than the limit spacing value, then these axles are considered as tandem, tridem or quad respectively. A single axle is separated from the surrounding axles by a distance greater than the limit spacing. This algorithm has been proved to reproduce correctly the axle configuration of most of the trucks being used currently in New Mexico roads.

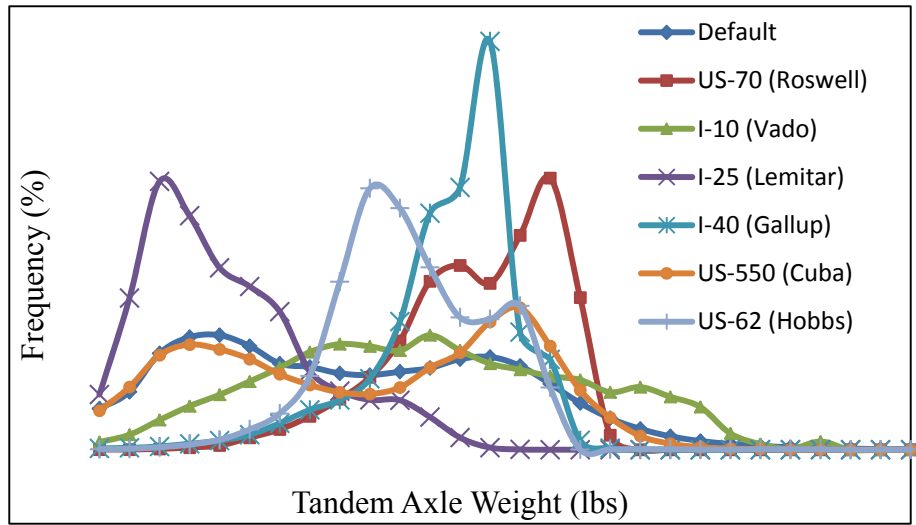
**TABLE 4.1 Location and type of WIM technology**

Site Name	Site Code	County	Road Name	Milepost	Type of Technology
HATCHITA	4	GRANT	I-10	50.05	PIEZO
LOGAN	100	QUAY	US-54	328	PIEZO
GALLUP	111	MCKINLEY	I-40	10.7	PIEZO
HOBBS	202	LEA	US-62/180	84	PIEZO
LEMITAR	252	SOCORRO	I-25	158.8	PIEZO
RINCON	300	DONA ANA	I-25	37.2	PIEZO
TUCUMCARI	B20	QUAY	I-40	340.9	PIEZO
RATON	B28	COLFAX	I-25	445	PIEZO
ROSWELL	916	ROOSEVELT	US-70	354.3	PIEZO
VADO	74	DONA ANA	I-10	155.6	PIEZO
TULAROSA	919	OTERO	US-70	231.65	PIEZO
SAN ANTONIO	915	SOCORRO	US-380	15.7	PIEZO
SAN YSIDRO	103	SANDOVAL	US-550	24.738	BENDING PLATE
CUBA	102	SANDOVAL	US-550	71.051	BENDING PLATE
BLOOMFIELD	155	SAN JUAN	US-550	121.5	BENDING PLATE

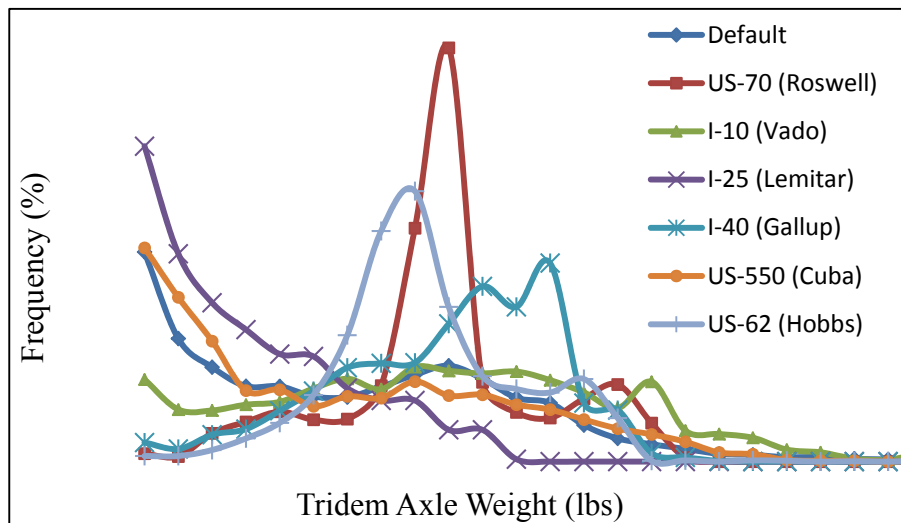
The aforementioned subroutine is used to obtain the axle load spectra at New Mexico WIM sites for single, tandem, tridem and quad axles. The site-specific axle load spectra for New Mexico weigh-in-motion sites versus MEPDG default is plotted in Figure 4.1. It is shown that site-specific axle load spectra can be very different from one location to another and very different from the MEPDG default values as well.



(a) Single Axle Load Spectra



(b) Tandem Axle Load Spectra



(c) Tridem Axle Load Spectra

**FIGURE 4.1 Axle Load Spectra for New Mexico WIM sites**

The monthly axle load spectra and the yearly average axle load spectra are determined at each weigh-in-motion site. Figure 4.2 represents the axle load spectra for several months along the year and the average spectrum. All of them are very similar, and therefore, it seems that the monthly variation of axle load spectra can be neglected without having consequences in the prediction of pavement performance.



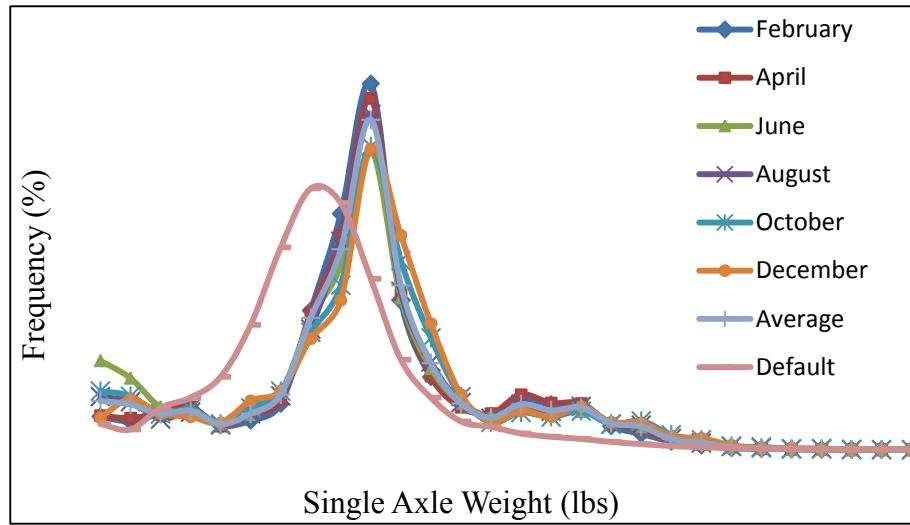


**FIGURE 4.2 Monthly and Average Axle Load Spectra**

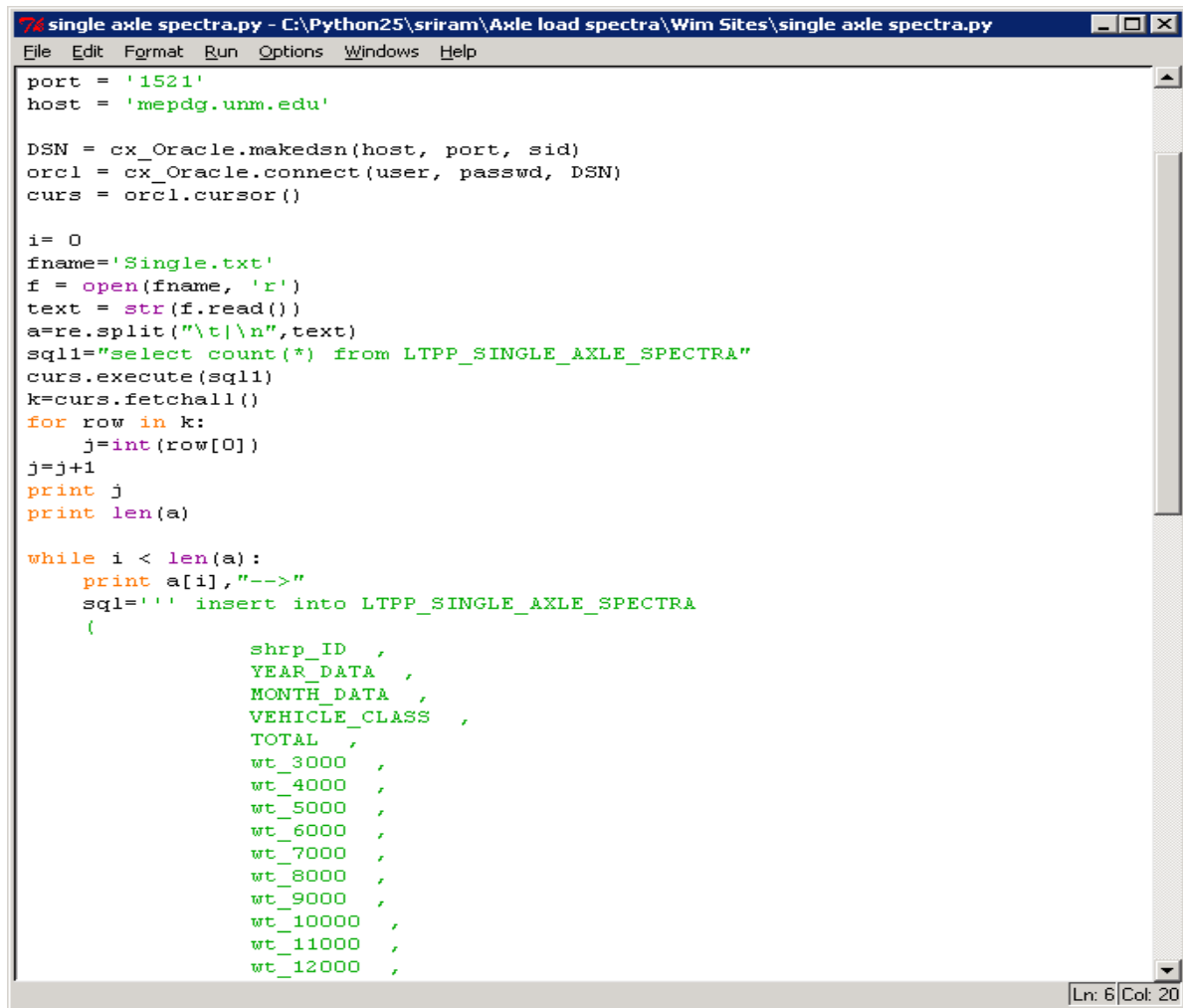
*Remarks*

- An axle load spectrum is a new input required by MEPDG for pavement performance prediction.
- Site-specific axle load spectra are determined by processing weigh-in-motion data with an algorithm.
- Axle load spectra can be very different from one location to another and also different from the default values.
- Monthly variation of axle load spectra is not observed, and thus, the average spectrum can be used for the whole year.

**Population of Axle Load Spectra Data**

The research team collected the raw data and processed the raw data for all WIM sites. The processed data was in the format of excel sheets. The processed data was then populated into the MEPDG data base using Python scripts. The snapshots of the scripts used to insert data and Axle load spectra data in MEPDG database are show below.

## Snapshot of Script for Inserting Axle Load Spectra Data



```
single axle spectra.py - C:\Python25\sriram\Axle load spectra\Wim Sites\single axle spectra.py
File Edit Format Run Options Windows Help

port = '1521'
host = 'mepdg.unm.edu'

DSN = cx_Oracle.makedsn(host, port, sid)
orcl = cx_Oracle.connect(user, passwd, DSN)
curs = orcl.cursor()

i= 0
fname='Single.txt'
f = open(fname, 'r')
text = str(f.read())
a=re.split("\t|\n",text)
sql1="select count(*) from LTPP_SINGLE_AXLE_SPECTRA"
curs.execute(sql1)
k=curs.fetchall()
for row in k:
    j=int(row[0])
j=j+1
print j
print len(a)

while i < len(a):
    print a[i], "-->"
    sql=''' insert into LTPP_SINGLE_AXLE_SPECTRA
    (
        shrp_ID ,
        YEAR_DATA ,
        MONTH_DATA ,
        VEHICLE_CLASS ,
        TOTAL ,
        wt_3000 ,
        wt_4000 ,
        wt_5000 ,
        wt_6000 ,
        wt_7000 ,
        wt_8000 ,
        wt_9000 ,
        wt_10000 ,
        wt_11000 ,
        wt_12000 ,
    )
    values
    (
        %s,
        %s,
        %s,
        %s,
        %s,
        %s,
        %s,
        %s,
        %s,
        %s,
        %s,
        %s,
        %s,
        %s,
        %s
    )
'''
    curs.execute(sql % (a[i], a[i], a[i], a[i], a[i], a[i], a[i], a[i], a[i], a[i], a[i], a[i], a[i], a[i], a[i]))
    i=i+1
```

Ln: 6 Col: 20

## Snapshot of Axle Load Spectra in Database

SHRP_ID	YEAR_DATA	MONTH_DATA	VEHICLE_CLASS	TOTAL	WT_3000	WT_4000	WT_5000	WT_6000	WT_7000	WT_8000
5	350100	2002	November	4	100	11.64	3.88	5.07	11.04	9.85
6	350100	2002	November	5	100	18.38	23.85	22.73	12.85	7.83
7	350100	2002	November	6	100	14.29	0	7.14	0	14.29
8	350100	2002	November	7	100	14.29	0	7.14	0	14.29
9	350100	2002	November	8	100	18.54	18.14	14.74	15.79	9.85
10	350100	2002	November	9	100	1.05	2.48	2.91	5.39	6.82
11	350100	2002	November	11	100	5	10	10	7.5	2.5
12	350100	2002	December	4	100	13.48	2.7	3.68	8.09	16.42
13	350100	2002	December	5	100	21.57	21.4	24.61	17.94	6.27
14	350100	2002	December	6	100	20.45	0	0	10.24	10.24
15	350100	2002	December	7	100	0	0	25	0	0
16	350100	2002	December	8	100	25.64	16.95	22.34	14.08	6.39
17	350100	2002	December	9	100	2.28	2.7	2.1	5.99	14.5
18	350100	2002	December	11	100	7.09	0	3.54	19.64	12.56
19	350500	2008	February	4	100	1.11	0	1.11	0	2.22
20	350500	2008	February	5	100	8.2	13.39	11.22	20.16	10.13
21	350500	2008	February	6	100	0	0	0	10	0
22	350500	2008	February	8	100	0	3.53	8.51	12.24	12.86
23	350500	2008	February	9	100	0.03	0.11	0.54	0.74	0.46
24	350500	2008	February	11	100	0	0	0	0.37	0
25	350500	2008	March	4	100	0.04	0.19	0.55	1.06	1.11
26	350500	2008	March	5	100	8.8	15.01	7.94	16.56	11.5
27	350500	2008	March	6	100	0.53	0.8	1	4.12	2.79
28	350500	2008	March	7	100	0	0	0	0	0
29	350500	2008	March	8	100	0.25	4.38	7.97	11.5	10.77
30	350500	2008	March	9	100	0.02	0.11	0.4	0.71	0.51
31	350500	2008	March	11	100	0.04	0.03	0.01	0.1	0.15
32	350500	2008	April	4	100	0.06	0.29	0.64	1.16	1.21
33	350500	2008	April	5	100	7.72	14.83	8.13	16.49	12.03
34	350500	2008	April	6	100	1.45	1.37	0.68	1.75	2.74
35	350500	2008	April	7	100	0	0	0	0	0
36	350500	2008	April	8	100	0.13	4.26	7.33	11.32	11.29
37	350500	2008	April	9	100	0.02	0.12	0.41	0.79	0.51

## MEPDG Database to GIS Mapping

MEPDG County data were converted to Geo-Spatial data using WMS (Web Map Service) and Python script (Appendix 2). First the Geometry boundary values are gathered and then these values were converted into shapefile format. They were then which are to be inserted into Oracle database. After that we have written a test.map file which is used by WMS to display the data in Geo-Spatial format. The following steps describe about how to map the County table to GIS.

1. Download and unzip official County boundary file from RGIS/NM  
[http://rgisedac.unm.edu/boundaries/2007fe\\_35\\_county00.zip](http://rgisedac.unm.edu/boundaries/2007fe_35_county00.zip)
2. Open a shell window and execute shp2sdo.exe spatial conversion tool (shapefiles to Oracle tables):  
[http://www.oracle.com/technology/software/products/spatial/files/shp2sdo\\_readme.html](http://www.oracle.com/technology/software/products/spatial/files/shp2sdo_readme.html)  
 >set oracle\_sid=gismepdg  
 > shp2sdo.exe -o fe\_2007\_35\_county00 -g geom -d -x \(-109.050173,-103.001964\) -y

\(31.332172, 37.000293\) -s 4326 -t 0.000000005 -v

3. Execute the newly generated sql file fe\_2007\_35\_county00.sql
4. If the DIMINFO field has zeros in it, it means it has to be updated.

```
UPDATE USER_SDO_GEOM_METADATA SET DIMINFO =  
SDO_DIM_ARRAY(SDO_DIM_ELEMENT('X', -109.050173, 31.332172,  
0.000000005),SDO_DIM_ELEMENT('Y', -103.001964, 37.000293, 0.000000005) )  
WHERE TABLE_NAME = 'FE_2007_35_COUNTY00';
```

Do the same with COUNTY2008 table:

```
UPDATE USER_SDO_GEOM_METADATA SET DIMINFO =  
SDO_DIM_ARRAY(SDO_DIM_ELEMENT('X', -109.050173, 31.332172,  
0.000000005),SDO_DIM_ELEMENT('Y', -103.001964, 37.000293, 0.000000005) )  
WHERE TABLE_NAME = 'COUNTY2008';
```

5. Create a spatial index for fe\_2007\_35\_county00 table:

```
CREATE INDEX FE_2007_35_COUNTY00_IDX (GEOM) INDEXTYPE IS  
MDSYS.SPATIAL_INDEX;
```

6. Test with QGIS the WMS service is instantiated from:

<http://localhost/cgi-bin/mapserv.exe?map=mapfiles/counties.map>

The mapfile needed to be modified in the EXTENT definition. It should say:

EXTENT -109.050173 31.332172 -103.001964 37.000293

in both counties.map (belongs to FE\_2007\_35\_COUNTY00) and test.map (COUNTY2008).

Recall the location for mapfiles is in

C:\ms4w\Apache\cgi-bin\mapfiles. Test.map is described in Appenedix 4.2.

7. Update COUNTY2008 geometries by executing:

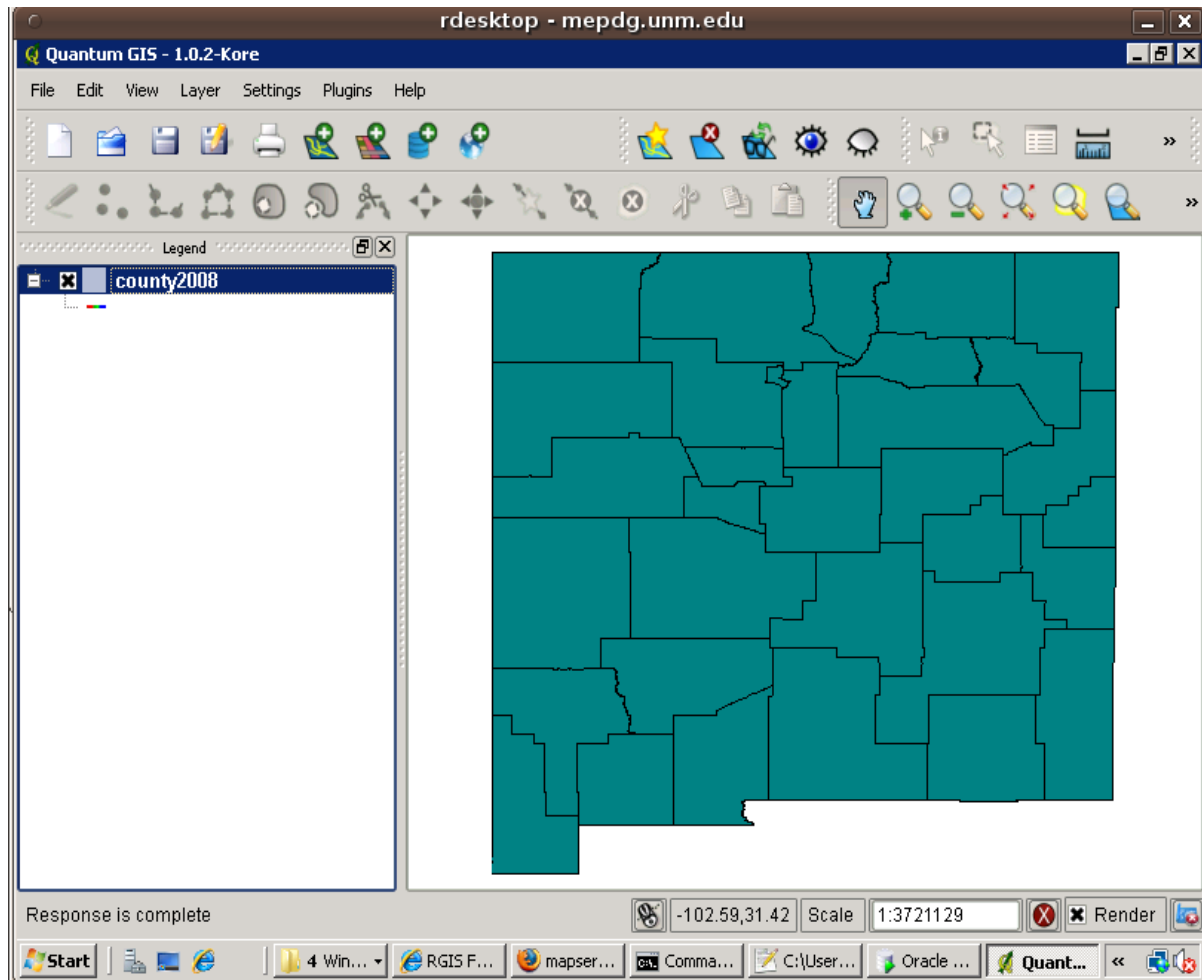
```
UPDATE COUNTY2008 SET geom = (SELECT geom FROM  
FE_2007_35_COUNTY00 WHERE COUNTY2008.NAME =  
FE_2007_35_COUNTY00.NAME00);
```

8. Rebuild the index COUNTY2008\_IDX with SQLDeveloper.

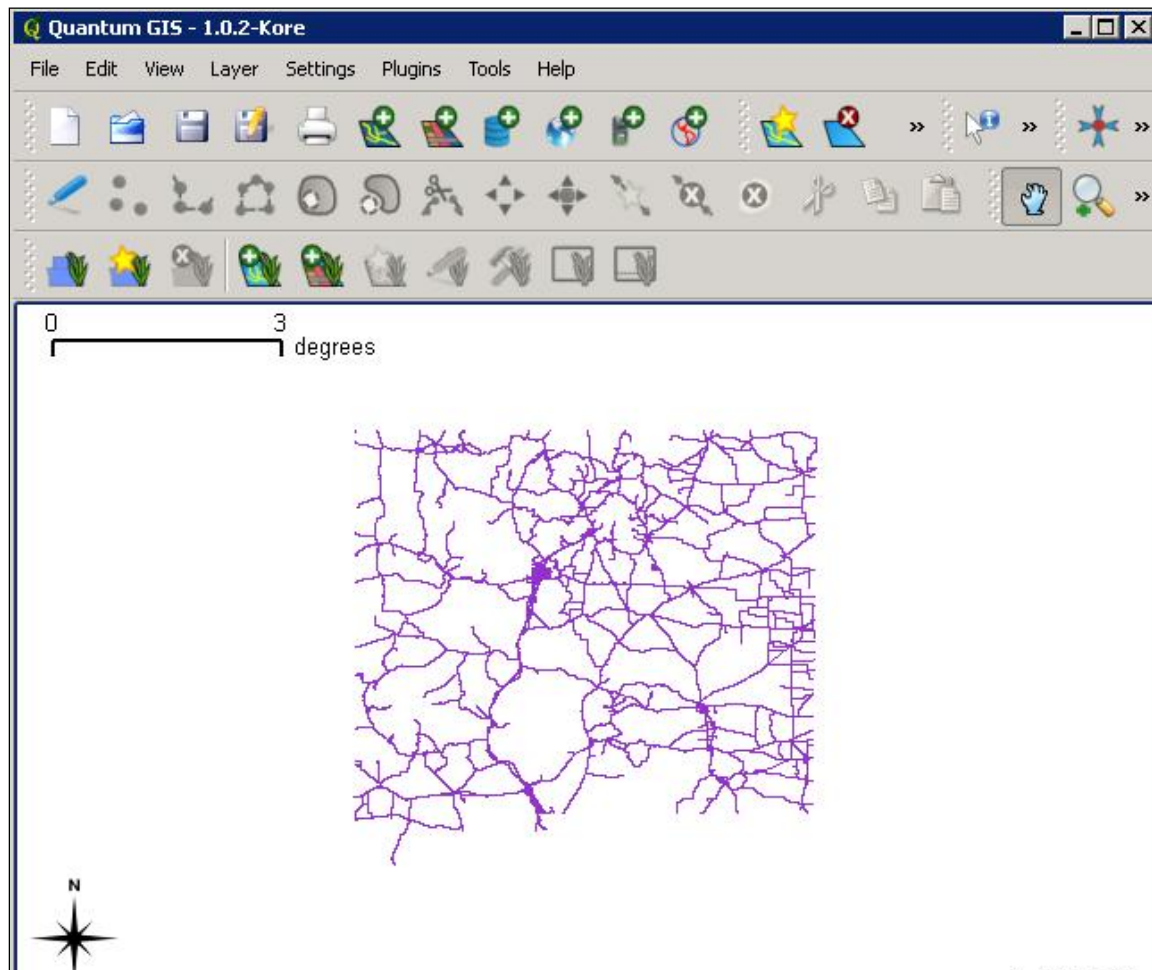
9. Test with QGIS and directly with Apache/WMS service

<http://localhost/cgi-bin/mapserv.exe?map=mapfiles/test.map&service=WMS&request=getmap&version=1.1.1&layers=test&width=200&height=200&bbox=-109,33,-107,35&style=&SRS=EPSG:4326&format=image/jpeg>

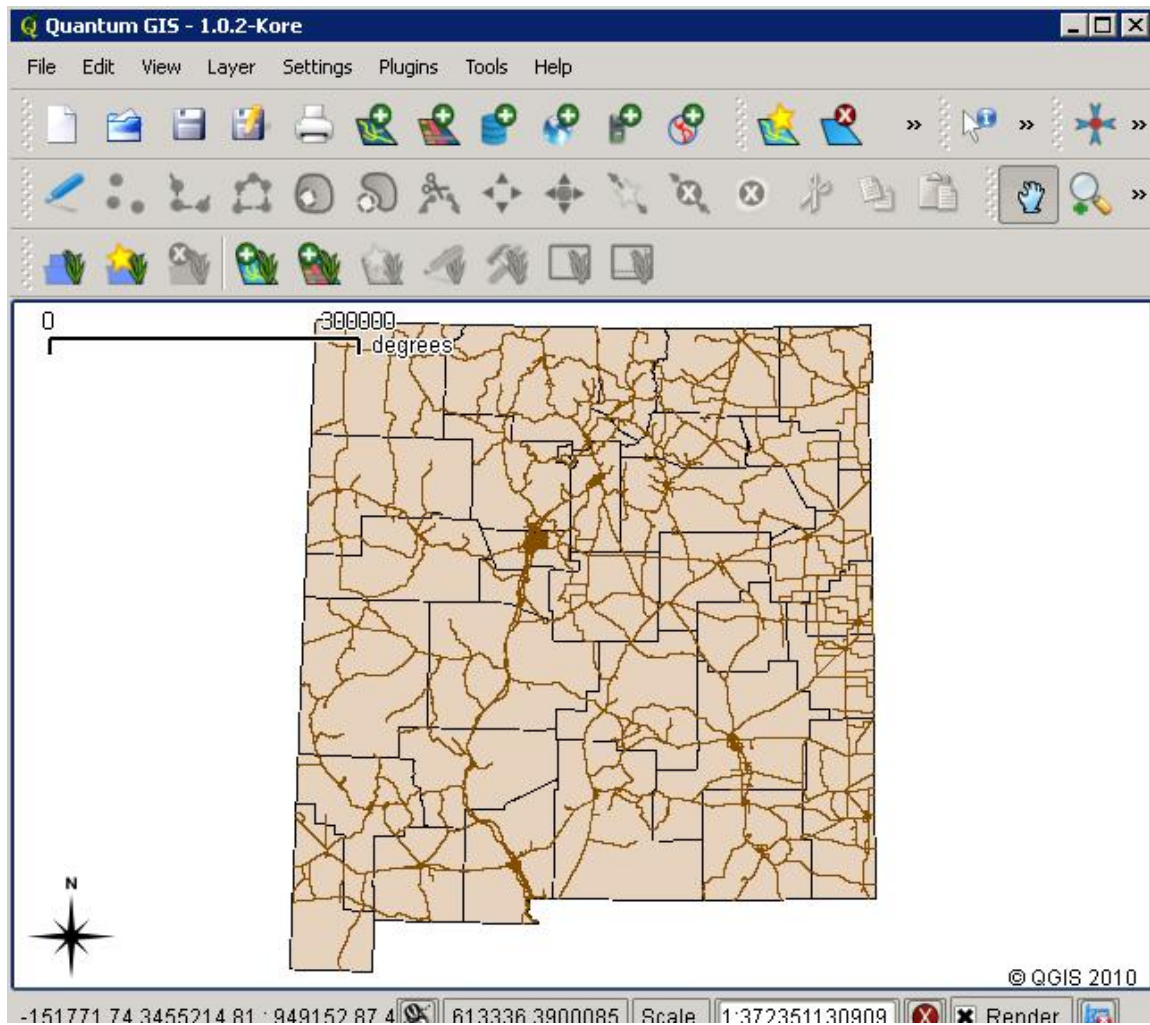
Screenshot of County GIS Map



## Traffic GIS image



## Intersection Map of County and Traffic



## Chapter 5

### WEB APPLICATIONS OF MEPDG DATABASE

#### INTRODUCTION

In this study, a web application for the MEPDG database was developed. This section describes how to launch a Website in the MEPDG server and how the server acts as Web server. It is also discussed how Website can generate reports by fetching data from respective databases based on queries provided by a user.

The Web coding is done using Hypertext Preprocessor (PHP) and python, which internally uses Oracledb module for database connection. XAMPP, a free software, was used for setting Apache in the MEPDG server. In particular, the following technologies are used for developing the website:

- PHP
- HTML
- CSS
- Oracle Database
- PHP OCI8 module
- Java Script
- Ajax and jQuery API

**PHP: Hypertext Preprocessor** is a widely used, general-purpose scripting language that was originally designed for web development to produce dynamic web pages. In this research, PHP is mainly used for processing the data of HTML Forms. It is also used for validating the user names and passwords. It is also used for validating the sessions of the users using the SESSION variable.

*Sample Code:*

```
<?php
session_start();
//echo "You are logged off from the page";
if($_SESSION['auth'] == true)
{
$_SESSION['auth']= false;
$_SESSION['name']= "";
header('Location: index.html');
}?>
```

**HTML: Hyper Text Markup Language** is a predominant markup language for web pages. HTML forms the main structure of the web page. HTML helps in the creation of forms where the user can enter his data and submit the forms for further processing of the data by the server and for storing of the data by the system at back end.



*Sample Code:*

```
<html>
<head>
<meta http-equiv="Content-Type" content="text/html; charset=iso-8859-1">
<title>Registration Form</title>
<LINK rel="stylesheet" href="style.css" type="text/css">
<SCRIPT type="text/javascript" language="JavaScript src="common_functions.js"></SCRIPT>
</head>
<body>
<FORM action="registration.html" method="post" name="sectionIdForm">
<TABLE border="0" width="90%" align="center" height="100%">
</TABLE>
</body>
</head></html>
```

**CSS: Cascading Style Sheets (CSS)** is a style sheet language used to describe the presentation semantics (that is, the look and formatting) of a document written in a markup language. It's most common application is to style web pages written in HTML and XHTML.

*Sample code:*

```
*{
margin:0px;
padding:0px;
}
img{border:0px}
html{
width:100%;
height:100%;
}
body{
width:700px;
margin:auto;
}
```

**Oracle Database:** Oracle Database is used in this project as a backend for storing the user data such as username and registration details. Oracle database is also used for storing the data regarding the MEPDG project. Users query the oracle database for obtaining the results.

**PHP OCI8 Module:** PHP OCI8 module is used for establishing the connection to oracle in PHP. The PHP OCI8 module is downloaded from internet and later installed on the system to integrate with the PHP and Oracle.

*Sample code:*

```
$conn = oci_connect('dbuser', 'Rafi1234',
'(DESCRIPTION=(ADDRESS_LIST=(ADDRESS=(PROTOCOL=TCP)(HOST=localhost)(PORT=1521)))(CONNECT_DATA=(SID=gismepdg)))');
if (!$conn) {
    $m = oci_error();
    echo $m["message"];
    exit;
}
$query = "Select distinct(rtsys) from trafficcounty";
```

**oci\_connect()** helps in connecting to the database.. The oci\_connect(Name, Password, Connection string) parameters are

Name: Name of the oracle database user. Here it is “dbuser”

Password: Password of oracle database. Here it is “Rafi1234”

Connection string: Connection string is the address of the database. It contains the port number, server name and SID

**oci\_parse():**

oci\_parse() prepares an oracle query for execution. The parameters of oci\_parse(\$conn, \$quer) are

\$conn is the variable containing the output of oci\_connect().

\$query is the variable containing the sql query to be executed.

EX: \$stid = oci\_parse(\$conn,\$query);

**OCI\_EXECUTE():**

Oci\_execute() executes the output of the oci\_parse function.

Example: \$result=oci\_execute(\$stid);

**Java Script:** Java Script is used in this project for validating the web forms submitted by the user. Java script is also used for generating alerts about the inconsistency of the data submitted in the forms.

*Sample code:*

```
function validateRegistrationForm() {  
    var validateFlag = true;  
    if ((document.sectionIdForm.FirstName.value) == "") {  
        alert ("Please enter your name!!");  
        return false;  
    }  
    else if ((document.sectionIdForm.Organization.value) == "") {  
        alert ("Please enter your organization!!");  
        return false;  
    }  
}
```

**AJAX:** AJAX is shorthand for Asynchronous JavaScript and XML is a group of interrelated web development techniques used on the client-side to create interactive web applications. With Ajax, web applications can retrieve data from the server asynchronously in the background without interfering with the display and behavior of the existing page.

*Sample code:*

```
<script src="jquery.js"></script>  
<script type="text/javascript">  
  
$(document).ready(function(){  
    $('#districts').change(function(){  
        $.ajax({  
            type: "GET",  
            url: "send.php",  
            data: "dist="+this.value,  
            success: function(msg){  
  
                document.getElementById("counties1").innerHTML = msg;  
            }  
        });  
    }  
});
```

The detailed description and snapshots of the pages developed for the website are given below:

### INDEX.html

Index.html is the starting page of the website. It contains links for pages such as registration, login and search.

### MEPDG Database Introduction Page



### Registration.html

Registration.html page contains form for the user to enter his registration details. The user will be asked to enter his Name, Organization name, email address , password and conform password.

## Registration Page of MEPDG Database

Development of a Flexible Pavement Database for Local Calibration of MEPDG

 **NEW MEXICO** DEPARTMENT OF  
**TRANSPORTATION**  
MOBILITY FOR EVERYONE

 **THE UNIVERSITY of**  
**NEW MEXICO**

HOME | REGISTRATION | LOGIN | SEARCH | FEEDBACK

**PLEASE CREATE YOUR ACCOUNT**

Name:

Organization:

Email Address:

Password:

Retype Password:

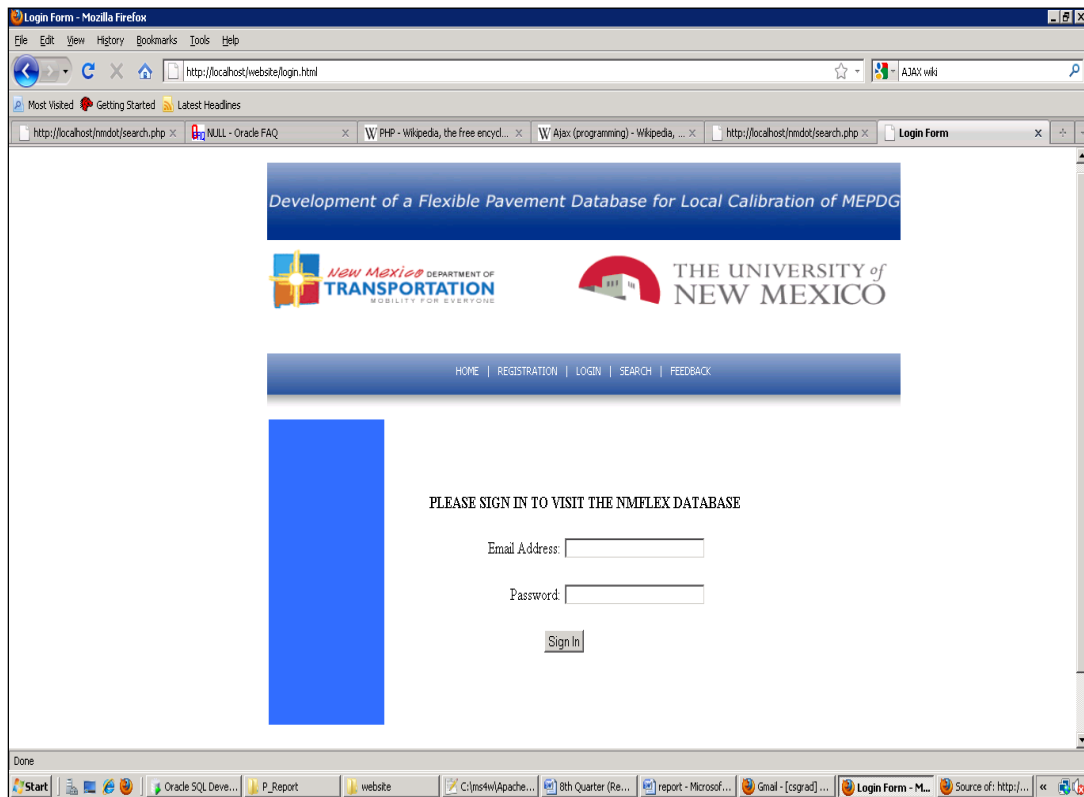
HOME | REGISTRATION | LOGIN | SEARCH | FEEDBACK

Copyright © 2003 NMDOT UNM

## Login.html

Login.html page asks for the login details of the user. Here the user have to provide the email address and the password.

## Login page of MEPDG database



## List of Web Applications

The following Web applications were developed in this study:

1. Provisions for displaying the traffic data, Soil data, Pavement data and axle load spectra data in the website.
2. Provisions for users to download the required data through web interface.
3. Developing protocols for users to upload data to MEPDG data base using web interface.
4. Adding GIS oriented maps to the web interface for easy access of data.

Many features of Webpage such as pages for displaying the section information, traffic details, distress summary, and structure details for a particular section of the road were included. Features such as axle load spectra for the state was included in addition to features for downloading particular sections information. The detailed description and snapshots for the pages developed for the website is given below:

## Search.php

Figure 5.1 shows the final design of the search page, which is to search for details regarding to a particular milepost. This page has been modified as per the suggestions of the technical panel. The search criterion has been changed from road name and section id to road name and milepost. The search contains various selection options. The user initially chooses the type of road such as interstate, state roads, frontage roads etc. Then the different route ID's for that type of road are displayed. The user can also select a particular route ID and the mileposts along that road. The user finally can select particular mileposts along that road and click on submit which directs to different page.

Search Form - Mozilla Firefox

File Edit View History Bookmarks Tools Help

http://mepdg.unm.edu/website/search.php

Most Visited Getting Started Latest Headlines

Search Form

Development of a Flexible Pavement Database for Local Calibration of MEPDG

New Mexico DEPARTMENT OF TRANSPORTATION  
MOBILITY FOR EVERYONE

THE UNIVERSITY of  
NEW MEXICO

welcome sriram [logout](#)

HOME | REGISTRATION | LOGIN | SEARCH | FEEDBACK

Select Road Type: Federal Aid Local

Select Route Id: FL2500

Select Mile Point: 0.000

Submit

HOME | REGISTRATION | LOGIN | SEARCH | FEEDBACK

Copyright © 2003 NMDOT UNM

Done

**FIGURE 5.1 Snapshot of the search.php page**

## Maps.php

The various details for the particular milepost selected by the user are displayed in a page shown in Figure 5.2. The map is in the center of this page and it displays the location of the milepost selected by the user. There is a table below the map, which displays the details of the milepost selected by the user. The information about the selected location such as county name, route

name, milepost, starting and ending point's latitude and longitude are displayed in the table. This page also contains links to various details about the location such as traffic summary, distress summary.

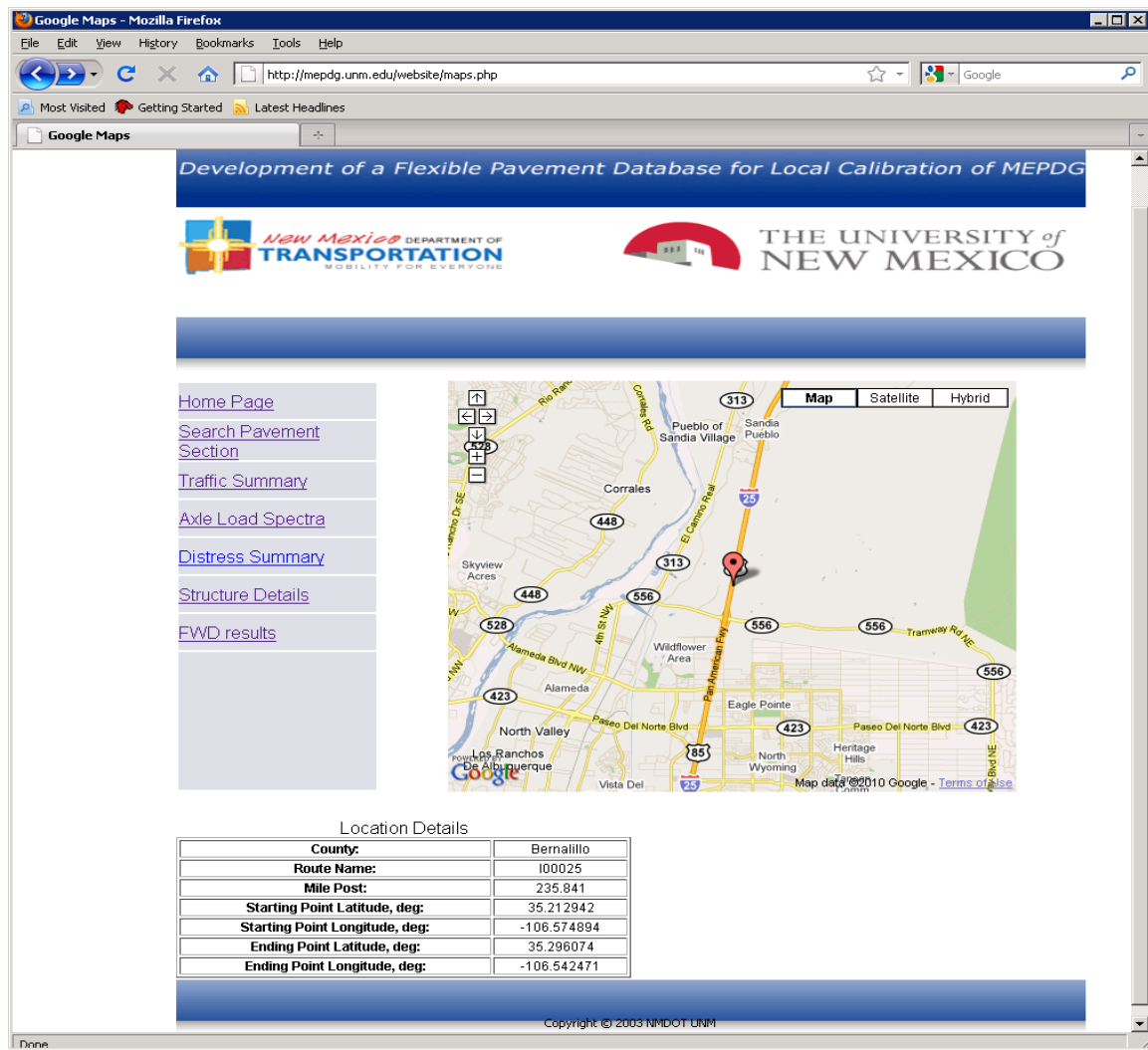


**FIGURE 5.2 Snapshot of the maps.php Showing a Particular Location**

### Traffic Summary.php

Traffic summary page, as shown in Figure 5.3, contains all the details of traffic for the location selected by the user. This page contains a table displaying the traffic for years 2002, 2004, 2005, 2006 and 2007. It also contains a graph displaying the traffic pictorially. This page also provides a button for the user to download all the traffic details of the section in an excel sheet. The snapshot of the traffic summary page is shown below:

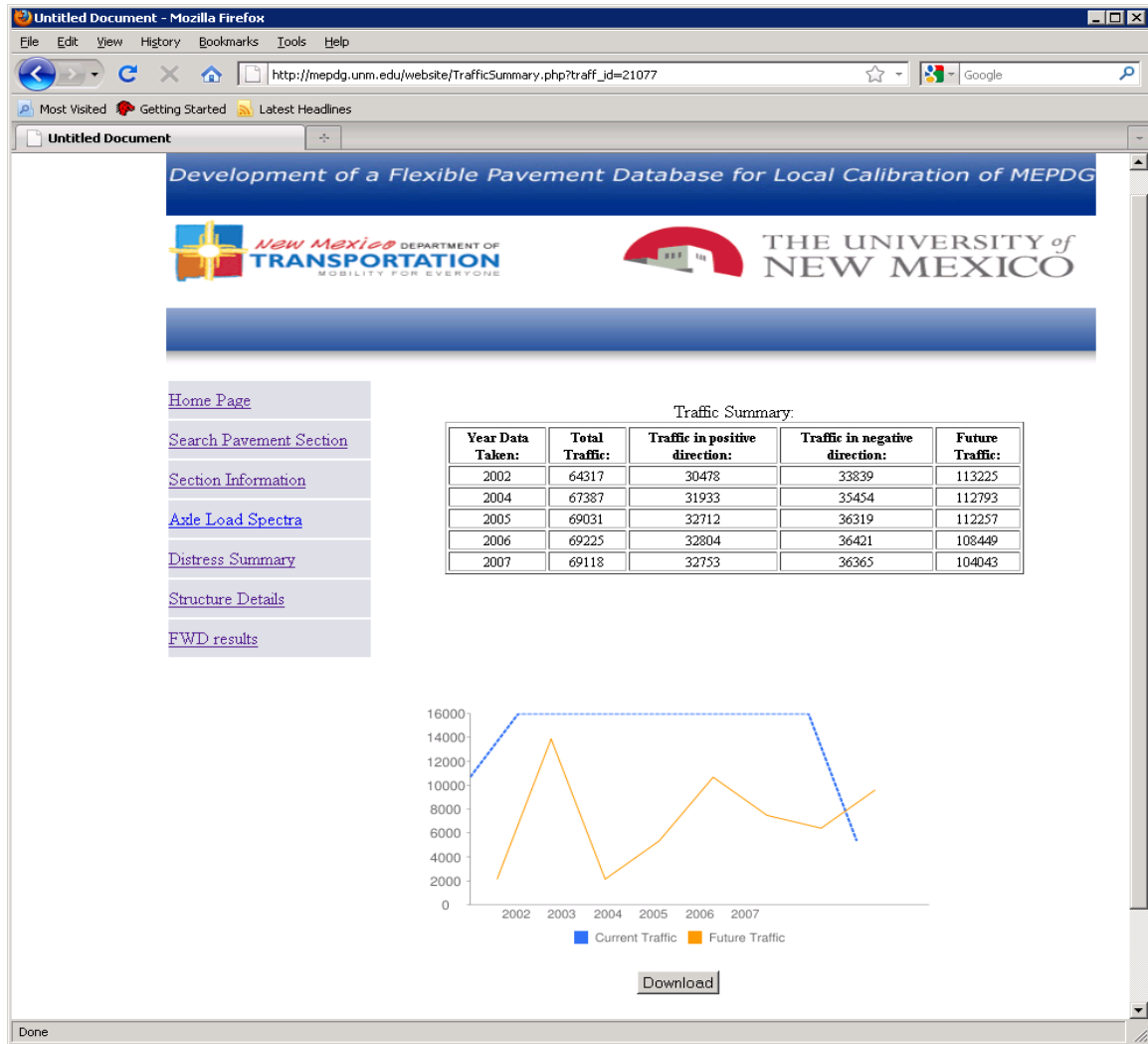


**FIGURE 5.3 Snapshot of Traffic Summary Page**

## Distress Summary

Distress summary contains a table displaying the distress details of the particular section. The details displayed are the alligator crack average value, transverse average value, longitudinal average value, crack length average value and rutting average values. The values displayed are according to the MEPDG standard. The snapshot of the page is shown in Figure 5.4.



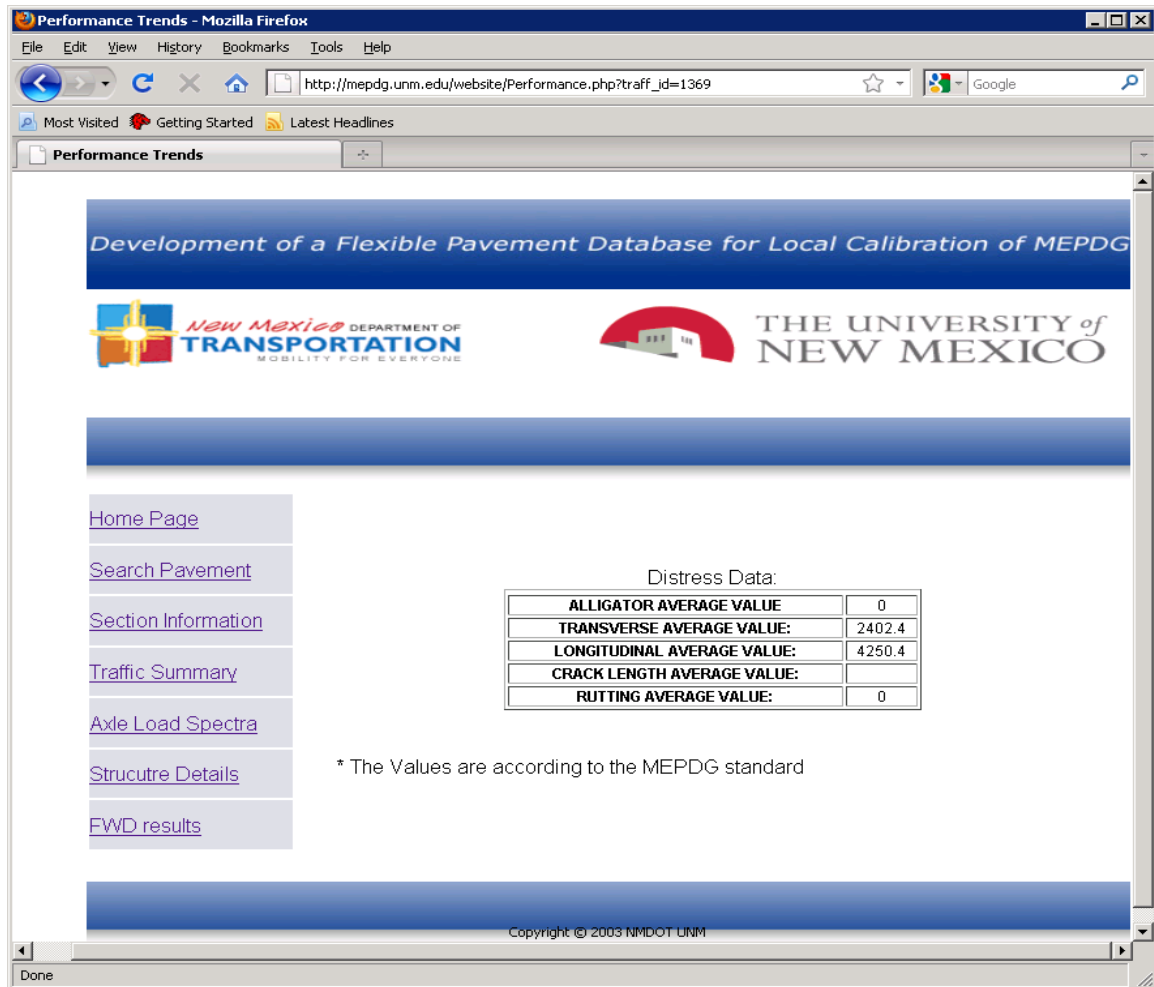


**FIGURE 5.4 Snapshot of the Distress Summary Page**

The user can also get the data in Excel format by clicking on the download button. The excel files contains the distress data for the particular section collected over years 1999-2009. The snapshot of an example excel file are shown in Figure 5.5.

Performance\_Data-8 [Read-Only] - Microsoft Excel

	A	B	C	D	E	F	G	H	I
1									
2	ROUTE_NO	LANE_DIR	MILE_POS	YEAR_DAT	ALLIGATOR_AVG	TRANSVERSE	LONGITUDINAL	CRACK_LEN	RUTTING_AVG
3	I00025	M	42.304	1997	0	0	4250.4		0
4	I00025	M	40.324	1997	0	0	4250.4		0
5	I00025	M	42.304	1997	0	0	4250.4		0
6	I00025	M	38.314	1997	15.5	0	4250.4		0
7	I00025	M	40.324	1997	0	0	4250.4		0
8	I00025	M	38.314	1997	15.5	0	4250.4		0
9	I00025	M	38.424	1998	0	0	0		0
10	I00025	P	40.34	1998	0	0	0		0
11	I00025	M	40.414	1998	0	0	818.4		0
12	I00025	P	38.33	1998	0	0	0		0
13	I00025	M	42.404	1998	0	0	0		0
14	I00025	P	40.34	1999	0	0	0		0
15	I00025	M	39.323	1999	0	0	0		0
16	I00025	P	38.33	1999	0	0	0		0

**FIGURE 5.5 Excel Sheet with Distress Data for a Particular Section**

### FWD.php

Figures 5.6(a) and 5.6(b) are the snapshots of the FWD data. This page contains a table that displays the FWD results of the section. The details displayed are dynamic load, the spacing details of the sensors, and the resilient modulus of the section are displayed.

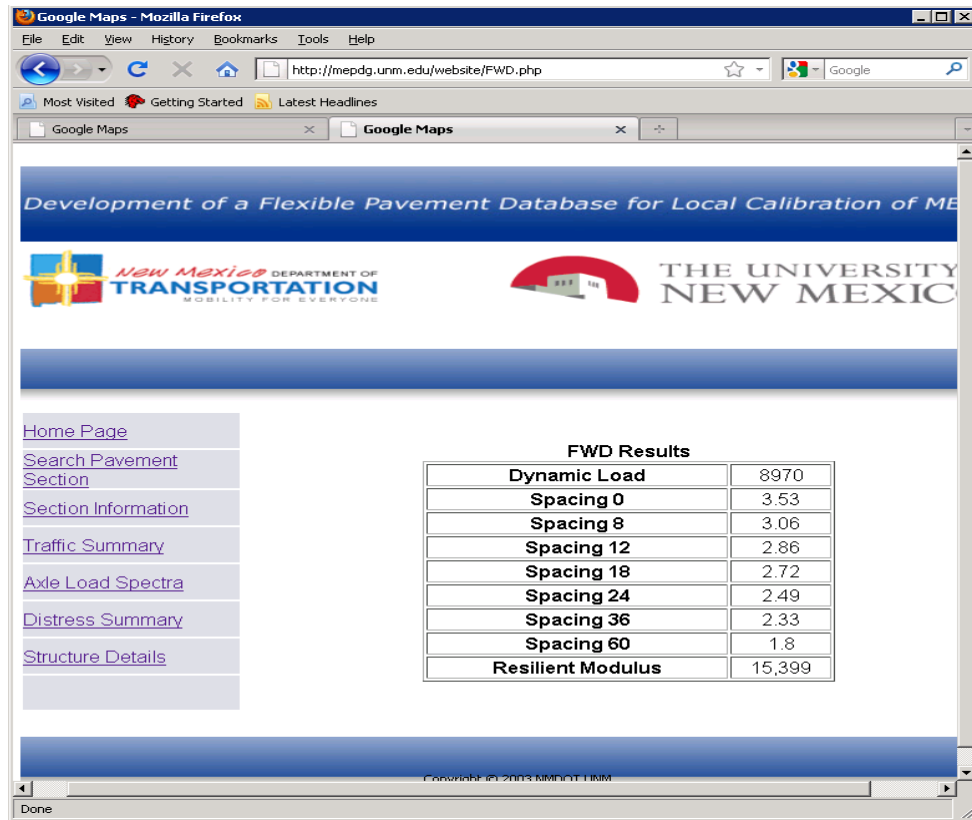


FIGURE 5.6(a) Snapshot of the FWD Page

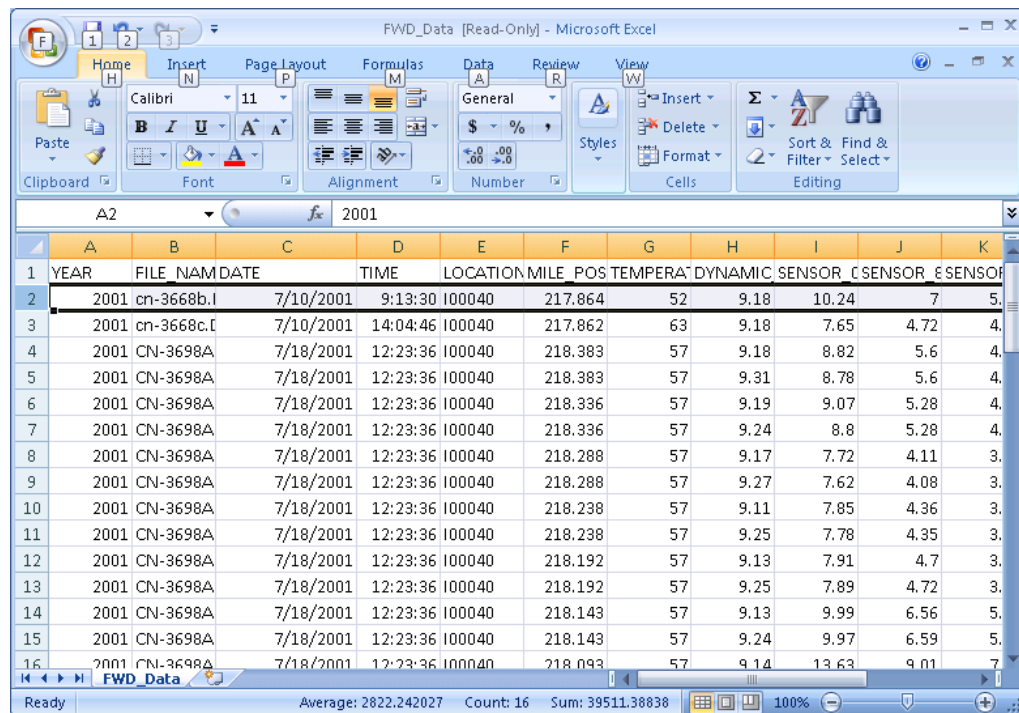


FIGURE 5.6(b) Snapshot of Downloaded Excel Sheet with FWD Data

## Axle Load Spectra

Figure 5.7 displays a screenshot of the axle load spectra graphs. The graphs displayed in this page are vehicle class distribution and class 9 GVW frequency distribution. The snapshots of the axle load spectra page are shown in Figures 5.7(a) to 5.7(c).

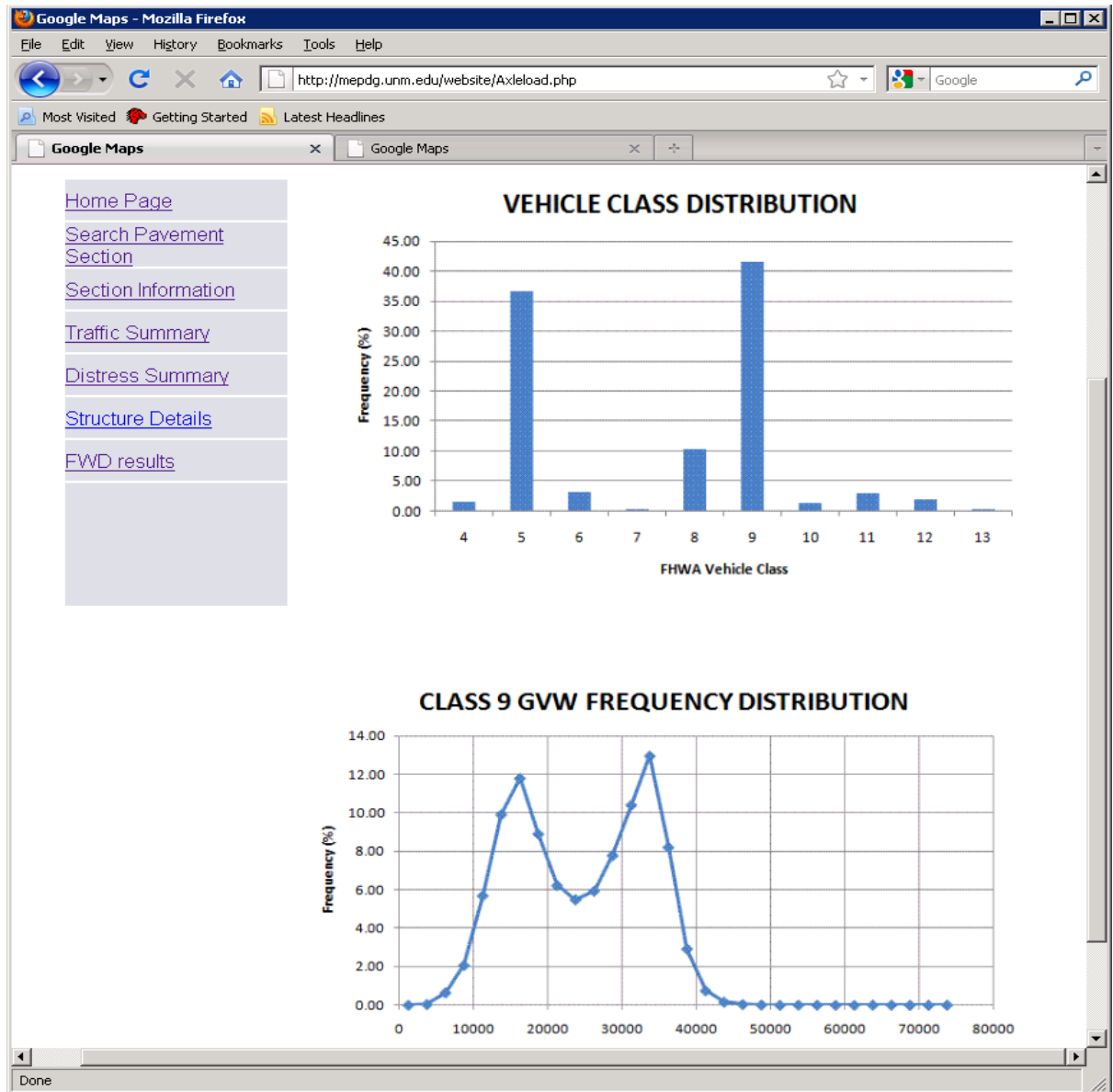
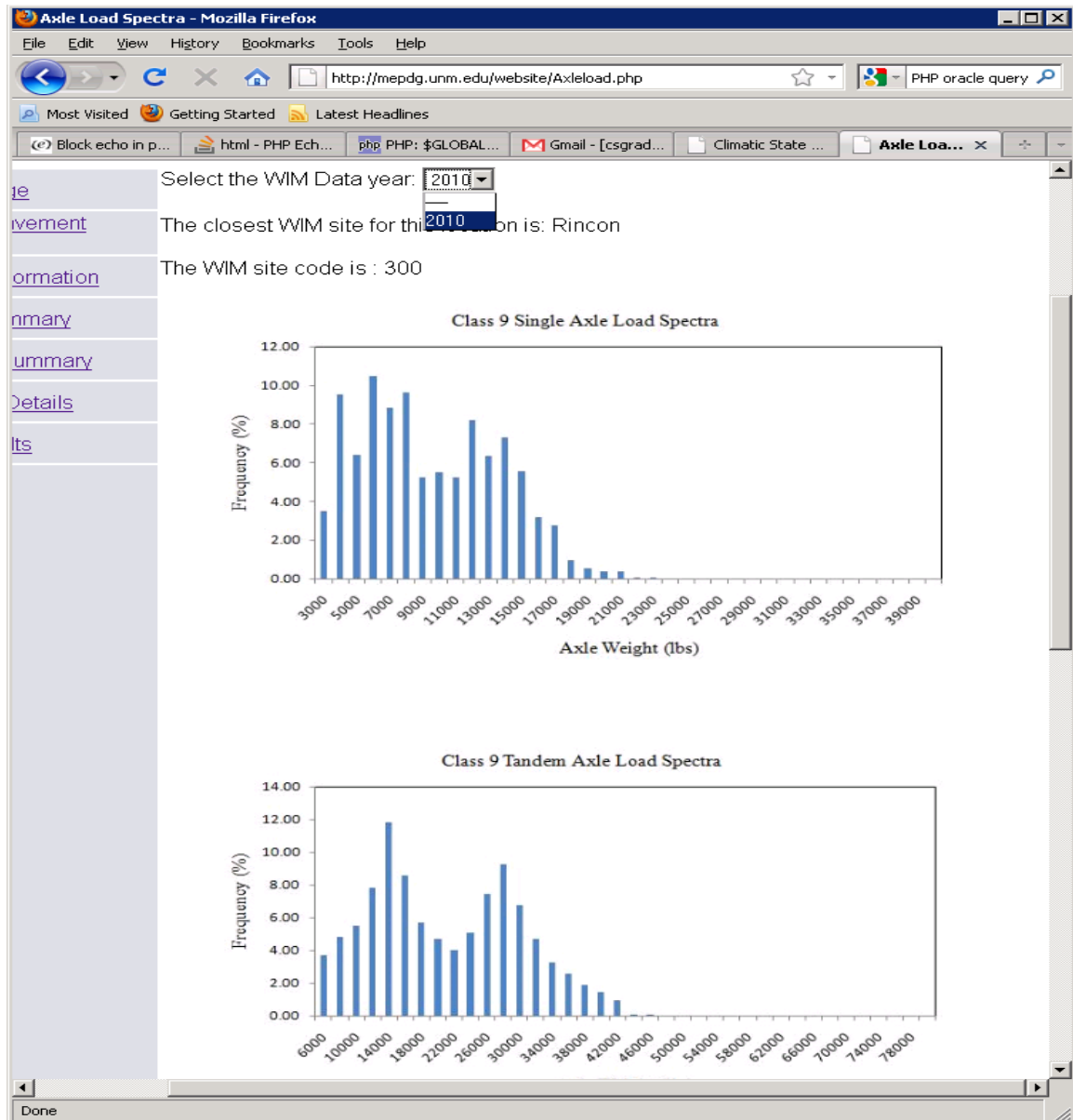


FIGURE 5.7(a) Snapshot Showing the Axle Load Spectra Page



**FIGURE 5.7(b) Snapshot Showing the Axle Load Spectra Page**

The screenshot shows a Microsoft Excel spreadsheet titled "Axle\_Load\_Data [Read-Only] - Microsoft Excel". The ribbon includes Home, Insert, Page Layout, Formulas, Data, Review, and View. The active cell is C34, which contains the text "January".

	A	B	C	D	E	F	G	H	I	J	K	L
22	300	2010	February	Class 11	100	2.78	0.02	2.4	4.18	4.99	8.24	6.39
23	300	2010	February	Class 12	100	0	3.04	1.9	5.32	5.7	10.65	6.84
24	300	2010	February	Class 13	100	0	0	0	0	0	25	0
25	300	2010	January	Class 4	100	7.47	11.26	11.26	14.44	17.5	8.69	4.41
26	300	2010	January	Class 5	100	71.78	14.16	5.88	3.95	1.78	1.27	0.41
27	300	2010	January	Class 6	100	5.44	19.98	14.18	17.66	12.22	11.86	5.71
28	300	2010	January	Class 7	100	0	0	0	33.33	0	0	0
29	300	2010	January	Class 8	100	51.27	17.8	8.79	7.75	4.59	4.27	1.33
30	300	2010	January	Class 9	100	6.86	17.89	11.76	18.81	13.68	10.9	3.85
31	300	2010	January	Class 10	100	4.87	18.73	20.97	14.98	11.24	13.48	5.24
32	300	2010	January	Class 11	100	12.28	0.84	12.69	18.77	13.76	13.22	4.76
33	300	2010	January	Class 12	100	10.92	22.5	15.05	17.84	12.78	9.85	2
34	300	2010	January	Class 13	100	11.11	22.22	0	22.22	11.11	0	0
35												
36	<b>The Tandem Axle spectra data is:</b>											
37	SHRP_ID	YEAR_DAT	MONTH_C	VEHICLE_C	TOTAL	WT_6000	WT_8000	WT_10000	WT_12000	WT_14000	WT_16000	WT_18000
38	300	2010	Average	Class 8	100	30.81	12.73	10.83	7.73	8.21	6.29	3.49
39	300	2010	Average	Class 9	100	3.7	4.82	5.53	7.82	11.81	8.59	5.68
40	300	2010	Average	Class 10	100	1.38	2.17	6.69	9.06	11.02	9.25	5.31
41	300	2010	Average	Class 11	100	6.98	0.08	18.25	14.13	22.14	14.44	2.78
42	300	2010	Average	Class 12	100	5.42	9.27	13.21	15.4	16.97	11.11	3.06
43	300	2010	Average	Class 13	100	3.85	5.77	1.92	1.92	7.69	5.77	7.69
44	300	2010	February	Class 4	100	0.34	0.52	0.86	1.72	3.26	1.72	4.81
45	300	2010	February	Class 5	100	47.86	25.94	16.67	7.4	1.79	0.34	0

**FIGURE 5.7(c) Snapshot Showing the Axle Load Spectra Page**

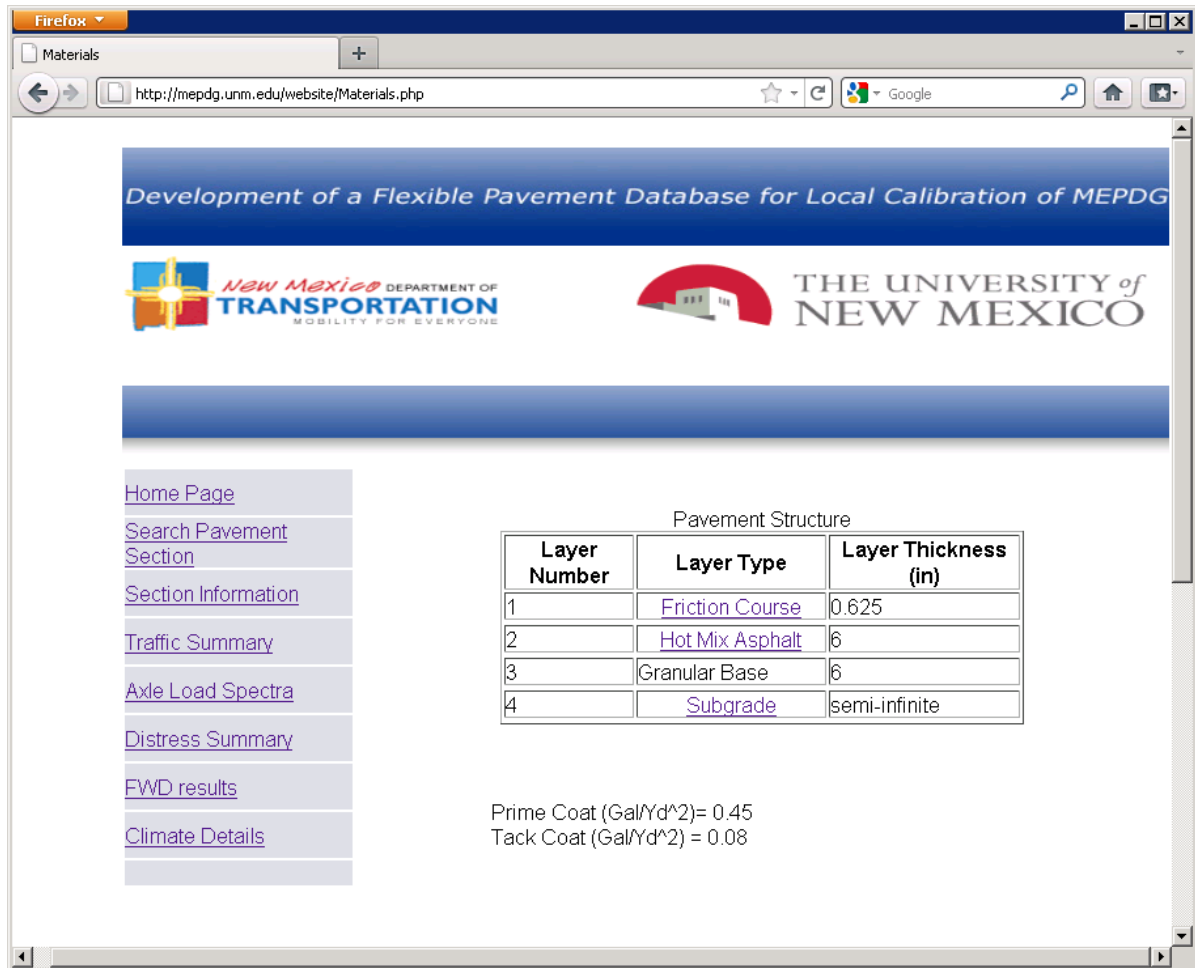
## Pavement Structure Design Data

Research team collected files including the summaries of materials investigation for different projects carried out in the state. Data extracted from these files are related to the pavement structure dimensions, pavement material properties, and subgrade strength. After careful screening and evaluation, the researchers uploaded only relevant data to the MEPDG database. Table 5.1 describes the fields of pavement structure data. Again, the first five fields correspond to several keys for searching such as road name, mileposts, control number, project number, and location. The remaining fields are design and structural inputs for different layers of pavement and subgrade.

**TABLE 5.1 Fields of Pavement Structure**

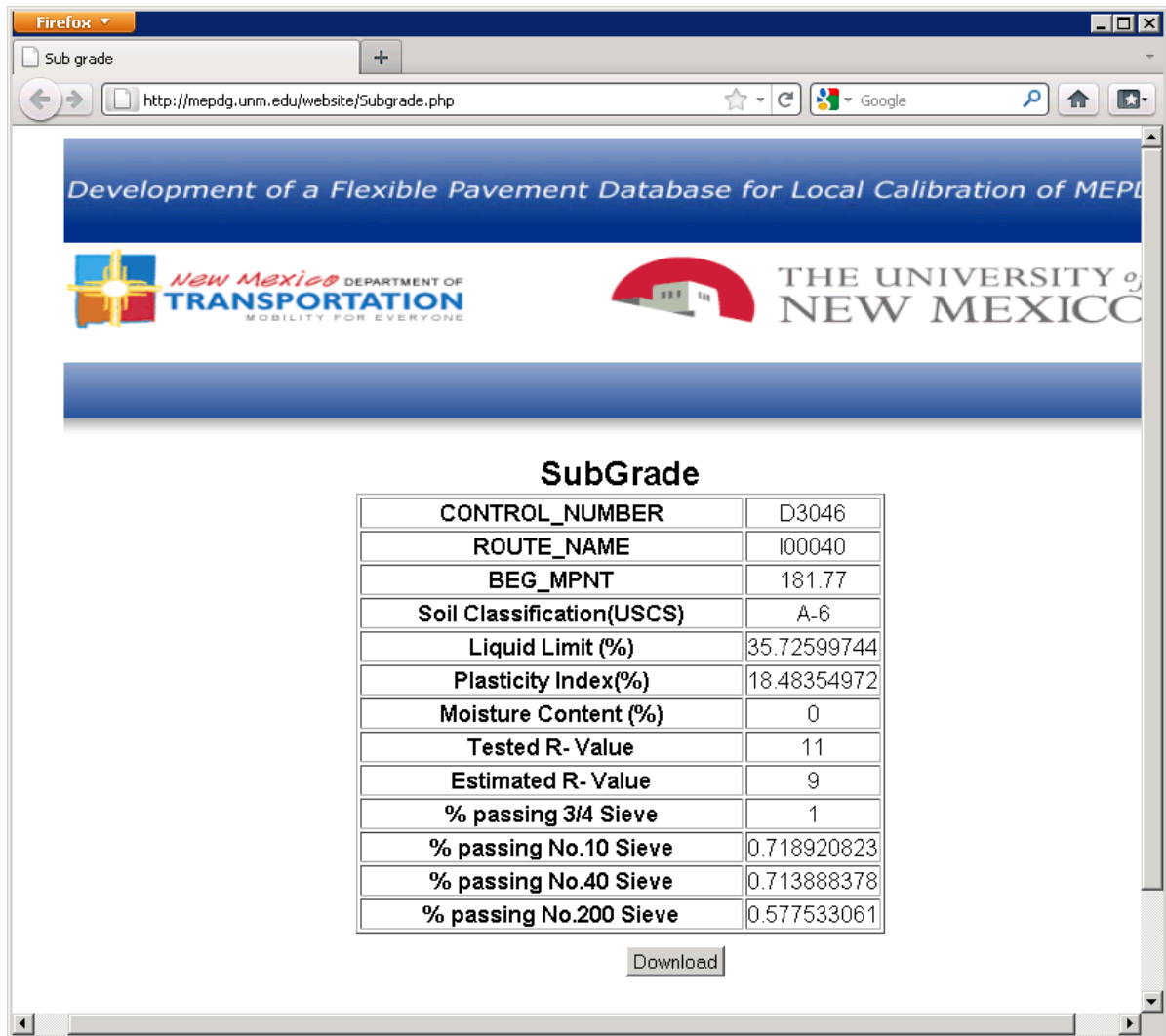
Field	Description
CONTROL_NUMBER	Control Number
PROJECT_NUMBER	Project Number
ROUTE_NAME	Road Name
ROUTE_LOCATION	Location
DISTRICT	District
BEG_MPNT	Beginning Milepost
END_MPNT	Ending Milepost
PROJECT_DATE	Date
LAYER_1_TYPE	Layer 1 Type
LAYER_1_THICKNESS	Thickness (in) of Layer 1
LAYER_1_BINDER	Type of Binder in Layer 1
LAYER_1 ASPHALT	% Asphalt in Layer 1
LAYER_1 DENSITY	Unit Weight (lb/yd3) of Layer 1
LAYER_1_ADDIT_HYD_LIME	% Additive Hydrated Lime in Layer 1
LAYER_2_TYPE	Layer 2 Type
LAYER_2_THICKNESS	Thickness (in) of Layer 2
LAYER_2_BINDER	Type of Binder in Layer 2
LAYER_2 ASPHALT	% Asphalt in Layer 2
LAYER_2 DENSITY	Unit Weight (lb/yd3) of Layer 2
LAYER_2_ADDIT_HYD_LIME	% Additive Hydrated Lime in Layer 2
LAYER_3_TYPE	Layer 3 Type
LAYER_3_THICKNESS	Thickness (in) of Layer 3
LAYER_3_BINDER	Type of Binder in Layer 3
LAYER_3 ASPHALT	% Asphalt in Layer 3
LAYER_3 DENSITY	Unit Weight (lb/yd3) of Layer 3
LAYER_3_ADDIT_HYD_LIME	% of Additive Hydrated Lime in Layer 3
PRIME_COAT	Prime Coat (gal/yd2)
TACK_COAT	Tack Coat (gal/yd2)
SUBGRADE_TREATMENT	Type of Subgrade Treatment
SUBGRADE_TYPE	Subgrade Soil Classification
SUDGRADE_RES_MOD	Subgrade Resilient Modulus (psi)
SUDGRADE_R_VALUE	Subgrade Soil R-Value

Figure 5.8 shows a screenshots of the page that displays type of layers and their thickness at this particular location. The structure details page displays the information related to the section of the route. The script searches for a section which is in the pavement design data table and gives the number of layers in the section and also the details of the layers. Data related to the base course and hot mix asphalt is obtained from the mix design table. The subgrade data is obtained from the soil data table. If there is no data available in the database for the selected location a blank page saying there is no data available for the selected location is displayed. The snapshots of structure details page and the subgrade details page are shown in Figure 5.8(a) to Figure 5.8(c).



**FIGURE 5.8(a) Snapshot of Materials.php page**





**FIGURE 5.8(b) Displaying the Subgrade Details**

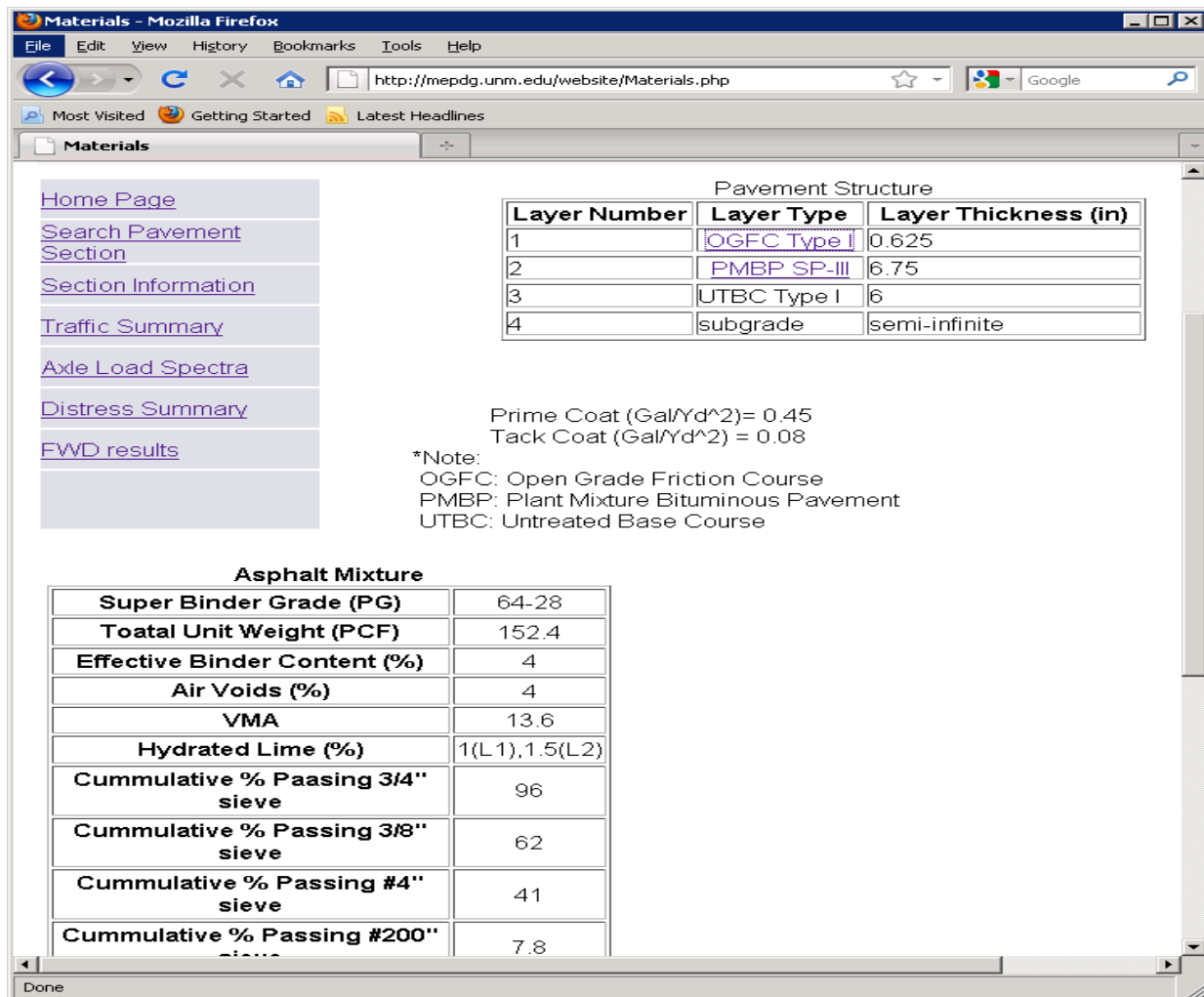


**FIGURE 5.8(c) Snapshot of the Materials page**

## Mix Design Data

Hard copies of the mix design data were collected from NMDOT Materials. The research team sorted and gathered all inputs that are required by MEPDG in a table. The information was then uploaded to the MEPDG database. Table 5.2 describes the fields of the mix design data that were used to populate MEPDG database. The first five fields such as control number, project number, road name, mileposts and location are key information for searching the database. The fields such as binder grade, density, percentage effective binder, percentage air voids, and cumulative percentage retained in the sieves 3/4", 3/8", #4, and #200 are mix design inputs required by MEPDG.

**TABLE 5.2: Fields of mix design**

Table Field	Description
CONTROL NUMBER	Control Number
PROJECT NUMBER	Project Number
PSTD RTE	Road Name
LOCATION	Location
DISTRICT	District
BEG MPNT	Beginning Milepost
END MPNT	Ending Milepost
YEAR DATA	Year
PG GRADE	Binder PG Grade
DENSITY	Density (pcf)
EFFECTIVE AC	Effective Binder (%)
AIR VOIDS PERCENT	Air Voids (%)
VMA	VMA
AG 3 4	Cumulative % Retained in Sieve 3/4"
AG 3 8	Cumulative % Retained in Sieve 3/8"
AG NO 4	Cumulative % Retained in Sieve #4
AG NO 200	Cumulative % Passing Sieve #200

The research team has collected all the required mix design data for MEPDG database into Microsot Excel sheets. Figure 5.9 shows the image of excel sheet into which required mix design data is gathered. From the excel sheets the mix design data is exported to MEPDG database using a python script. The python script for populating mix design data into MEPDG database is shown in Figure 5.10. Figure 5.11 shows the image of the table containing the mix design data in the MEPDG database.

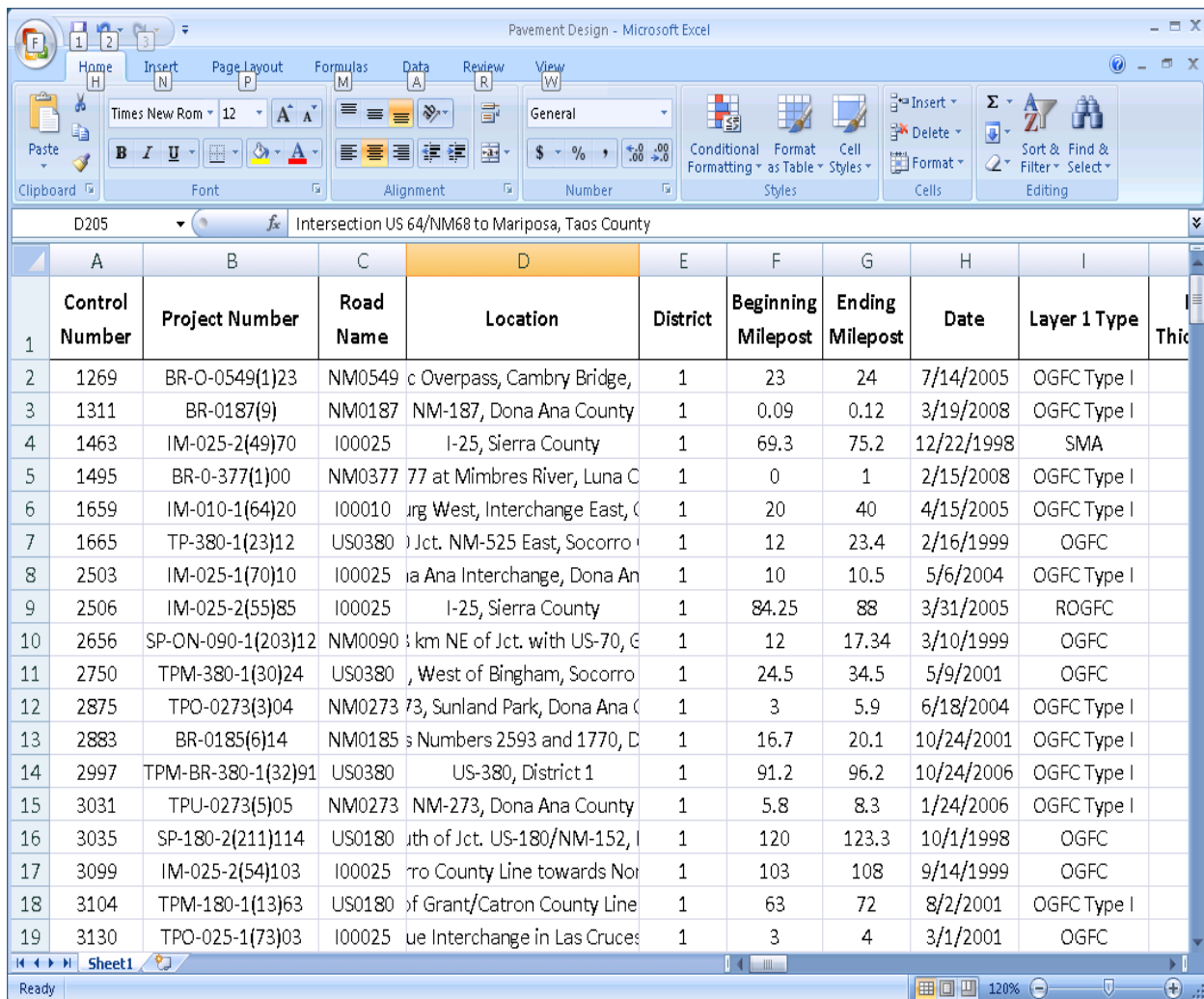
mix design data [Compatibility Mode] - Microsoft Excel

	A	B	C	D	E	F	G	H	I	J
4	3035/9598	NH-TPE-180-2(12)119	US180/NM152, Grant County	1			SP-III	64-16	1/14/2002	5.4
5	2750	AC-TPA-(TPM)-380-1(35)	US380, Socorro County	1			SP-IV	70-22	6/20/2002	4.3
6	2767	NH-BR-062-1(10)34	Hwy62/180, Eddy County	2			SP-III	76-22	3/18/2002	4.7
7	3164	AC-MIP-070-7(28)370	US70, Chavez County	2			SP-III	70-22	4/11/2002	7.65
8	2768	AC-MIP-070-7(20)400	US70, Roosevelt County	2			SP-III	70-22	7/3/2002	7.1
9	2847/3036	AC-MIP-070-7(23)349/(26)359	US70, Chavez County	2			SP-III	70-22	2/19/2002	5
10	3394/3395	AC-MIP-070-5(32)302/310	US70, Chavez/Lincoln County	2			SP-III	70-22	1/17/2002	4.3
11	3398	AC-MIP-070-5(33)397	23 miles SW of Portales	2			SP-III	70-22	2/26/2002	4.4
12	3635	IM-010-2(87)116	I-10, Dona Ana County	1	116	130.3	SP-III	76-16	3/8/2002	5.5
13	3798	IM-025-2(202)108	I25, Socorro County	1			SP-III	70-16	10/3/2002	5.8
14	3874	TPM-082-1(14)	US82, Otero County	2			SP-III	64-22	3/28/2002	4
15	3588	AC-NH-054-2(20)85	US54, Otero County	2			SP-III	64-22	7/29/2002	4.7
16	3042	SP-054-2(206)	US54, Otero County	2			SP-III	64-22	7/29/2002	4.7
17	3277R	NH-060-6(24)387	US60, Curry County	2	386.7	387.2	SP-III	82-22	9/18/2002	4.2
18	3657	MGE-NH-285-1(30)140	US285, Chaves/DeBaca County	2			SP-III	64-28	3/26/2002	4.5
19	3588	AC-NH-MGS-070-7(29)425	Clovis, Roosevelt County	2			SP-III	76-22	7/2/2002	4.2
20	3917	WS-285-1(217)00	US285, Tx State Line, Eddy County	2	0	20.03	SP-IV	70-22	8/7/2002	5.2
21	2685	IM-025-4(97)241	I25/NM473 Interchange, Sandoval County	3			SP-II	70-22	7/29/2002	5.2
22	3248	TPU-4020(7)05	NM528, Sandoval County	3			SP-II	82-16	11/18/2002	4.5
23	3248	TPU-4020(7)05	NM528, Sandoval County	3			SP-III	82-16	11/27/2002	4.8
24	2476R	TPS-054-6(14)323	Logan County	4			SP-III	70-22	10/18/2002	4.6
25	3102	AC-TPM-TPE-039-1(9)42	NM39, Harding County	4	42.05	Mosquero	SP-III	64-22	7/8/2002	7.2
26	3300	SP-040-5(56)276	I40, Guadalupe County	4	276.98	291.41	SP-II	76-22	11/20/2002	4.6
27	3100	MGS-NH-064-9(30)420	US64/87, Union County	4	420.98	430.22	SP-III	64-28	7/1/2002	5.6
28	N/A	Espanola Tansit Mix	Various Locations	5			SP-IV	64-22	7/26/2002	4.3
29	N/A	Various	Taos, County	5			Type I-B	58-28	5/9/2002	5.7
30	N/A	Various	Various Locations	2			Type I-B	70-22	2/11/2002	4.7
31	Various	Various	Bernalillo County	3			SP-IV	76-22	9/16/2002	5.3
32	N/A	Various	Dona Ana County	1			SP-III	82-16	2/18/2002	4.8
33	N/A	Various	Dona Ana County	1			SP-III	76-16	3/21/2002	4.9
34	2403	IM-040-1(114)00	I40, McKinley County	6			SP-II	76-28	4/25/2002	4.3
35	N/A	Commercial Mix Design	Eddy County	2			Type I-C	76-22	3/25/2002	5

FIGURE 5.9 Image of Mix Design Data Excel Sheet

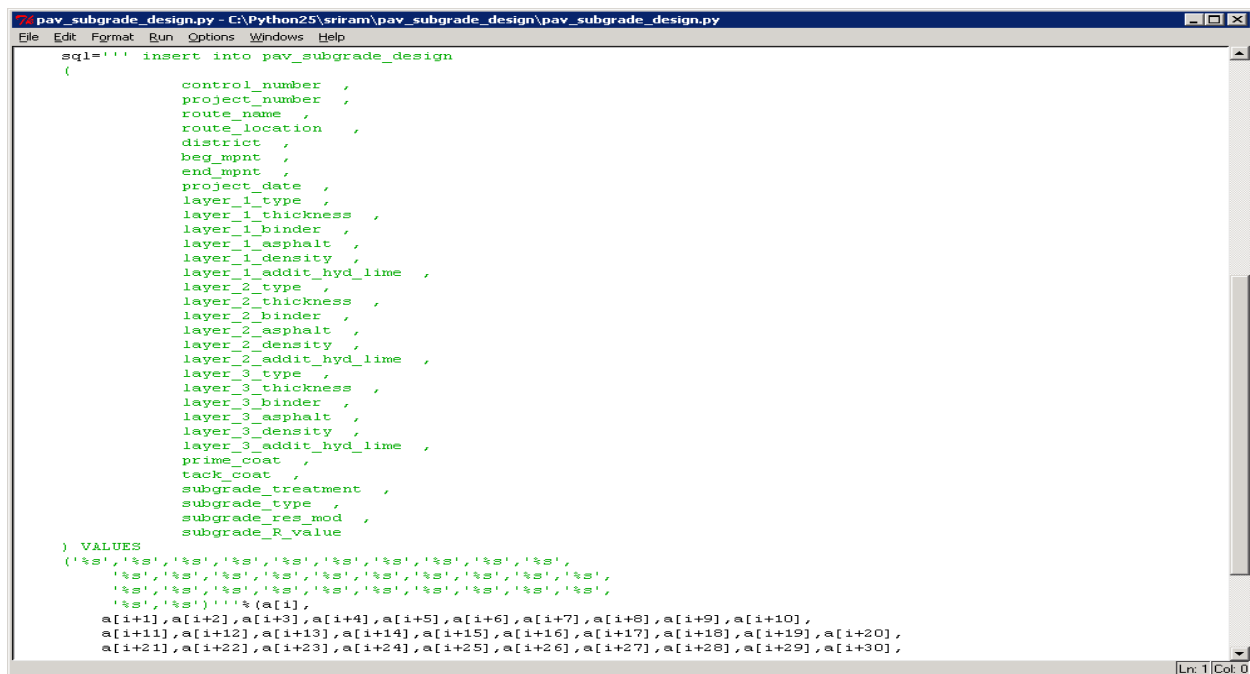


The research team has analyzed the pavement design files and gathered data that are required for MEPDG into Microsoft Excel sheets. Figure 5.12 shows the image of the pavement design data in excel sheets. From excel sheets the research team has uploaded the pavement design data into MEPDG data base using python scripts. Figure 5.13 shows the image of the python script used to populate data into database. Figure 5.14 shows the screen shot of PAV\_DESIGN\_DATA table containing pavement design data in MEPDG database.



	A	B	C	D	E	F	G	H	I	J
	Control Number	Project Number	Road Name	Location	District	Beginning Milepost	Ending Milepost	Date	Layer 1 Type	Thickness
2	1269	BR-O-0549(1)23	NM0549	c Overpass, Cambry Bridge,	1	23	24	7/14/2005	OGFC Type I	
3	1311	BR-0187(9)	NM0187	NM-187, Dona Ana County	1	0.09	0.12	3/19/2008	OGFC Type I	
4	1463	IM-025-2(49)70	I00025	I-25, Sierra County	1	69.3	75.2	12/22/1998	SMA	
5	1495	BR-O-377(1)00	NM0377	77 at Mimbres River, Luna C	1	0	1	2/15/2008	OGFC Type I	
6	1659	IM-010-1(64)20	I00010	urg West, Interchange East, C	1	20	40	4/15/2005	OGFC Type I	
7	1665	TP-380-1(23)12	US0380	Jct. NM-525 East, Socorro	1	12	23.4	2/16/1999	OGFC	
8	2503	IM-025-1(70)10	I00025	ia Ana Interchange, Dona An	1	10	10.5	5/6/2004	OGFC Type I	
9	2506	IM-025-2(55)85	I00025	I-25, Sierra County	1	84.25	88	3/31/2005	ROGFC	
10	2656	SP-ON-090-1(203)12	NM0090	3 km NE of Jct. with US-70, G	1	12	17.34	3/10/1999	OGFC	
11	2750	TPM-380-1(30)24	US0380	, West of Bingham, Socorro	1	24.5	34.5	5/9/2001	OGFC	
12	2875	TPO-0273(3)04	NM0273	73, Sunland Park, Dona Ana C	1	3	5.9	6/18/2004	OGFC Type I	
13	2883	BR-0185(6)14	NM0185	s Numbers 2593 and 1770, D	1	16.7	20.1	10/24/2001	OGFC Type I	
14	2997	TPM-BR-380-1(32)91	US0380	US-380, District 1	1	91.2	96.2	10/24/2006	OGFC Type I	
15	3031	TPU-0273(5)05	NM0273	NM-273, Dona Ana County	1	5.8	8.3	1/24/2006	OGFC Type I	
16	3035	SP-180-2(211)114	US0180	uth of Jct. US-180/NM-152, I	1	120	123.3	10/1/1998	OGFC	
17	3099	IM-025-2(54)103	I00025	ro County Line towards Nor	1	103	108	9/14/1999	OGFC	
18	3104	TPM-180-1(13)63	US0180	of Grant/Catron County Line	1	63	72	8/2/2001	OGFC Type I	
19	3130	TPO-025-1(73)03	I00025	ue Interchange in Las Cruces	1	3	4	3/1/2001	OGFC	

**FIGURE 5.12 Image of Pavement Design Data Excel Sheet**

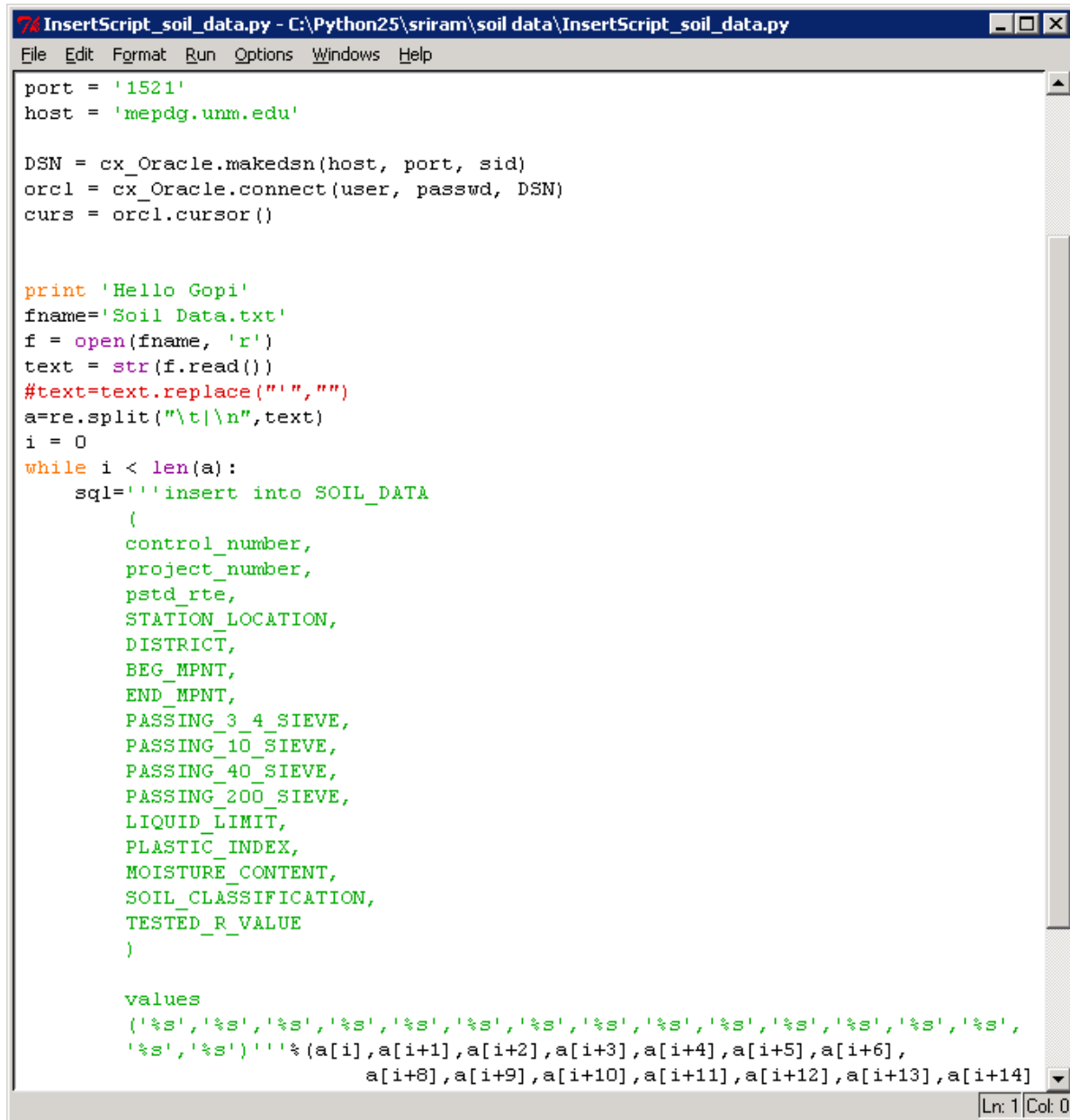


The screenshot shows the Oracle SQL Developer interface. The main window displays the 'PAV\_DESIGN\_DATA' table. The table structure is as follows:

CONTROL_NUMBER	PROJECT_NUMBER	ROUTE_NAME	ROUTE_LOCATION	DISTRICT
15 3590	TPM-0220-1(100)	NM0220	NM-220, Kusunoki, Chavez County	2
16 3595	SP-ET-0128(200)42	NM0128	"NM-128, Jal, Lea County"	2
17 3597	NH-070-2(28)212	US0070	"US-70, Walker to Jct. US-54, Alamogordo, Otero County"	2
18 3616	SD-WPP-285-3(208)156	US0285	"US-285, North of Ramon, De Baca County"	2
19 3637	TPO-9997(10)	NM0523	"NM-523 & Norris Street Intersection, Clovis, Curry County"	2
20 3680	NH-060-6(26)396	US0060	"US-60 at Texico to Texas State Line, Curry County"	2
21 3683	BR-0249(6)	NM0249	"NM-249, Bridge Number 5714 over Pecos River, Chavez County"	2
22 3692	TPS-285-2(26)106	US0285	"US-285 & Brasher Road, Roswell, Chavez County"	2
23 3704	AC-MIP-018-1(25)08	NM0018	"NM-18, Lea County"	2
24 3748	HSP-285-1(31)34	US0285	"US-285 between Callaway and 8th Street, Eddy County"	2
25 3750	NH-054-2(19)130	US0054	"US-54 between Carrizozo and Vaughn, Lincoln County"	2
26 3752	NH-285-1(32)00	US0285	"US-285 From NM/TX State Line North 9 miles, Eddy County"	2
27 3753	TPM-060-5(20)316	US0060	"US-60, 10 miles West of Jct. NM-20 - East, De Baca County"	2
28 3753	TPM-060-5(20)316	US0060	"US-60, 10 miles West of Jct. NM-20 - East, De Baca County"	2
29 3755	TPM-380-1(33)97	US0380	"US-380, 10 miles West of Jct. US-70 East, Lincoln County"	2
30 3757	TPM-0220(1)09	NM0220	"NM-220 by Sierra Airport East, Lincoln County"	2
31 3779	BR-285-3(15)123	US0285	"US-285, Salk Creek and Macho Draw, Chavez County"	2
32 3827	TPO-62-1(7)33	US0062	"US-62, Canal St., Pampa St. to Pierce St., Carlsbad, Eddy County"	2
33 3829	TPO-018-1(32)70	NM0018	"NM-18, Lincoln County"	2
34 3879	TPM-380-1(34)62	US0380	"US-380, Valley of Fires East to NM-37, Lincoln County"	2
35 3882	BR-082-2(9)110	US0082	"US-82, 4.1 miles East of Jct. US-285, Eddy County"	2
36 3927	TPA-TPM-1238-(8)16	NM0002	"NM-2, 0.15 miles South of Jct. NM-249 - N, Chavez County"	2
37 88044	SP-2-08(365)	NM0206	"NM-206, Roosevelt County"	2
38 D2047	TPM-209-1(23)12	NM0209	"NM-209, 7.4 miles Clovis North to Frio Draw, Curry County"	2
39 D2047	TPM-209-1(23)28	NM0209	"NM-209, South of Broadview - West to Quay County Line, Curry County"	2
40 D2077	TPM-082-2(1)126	US0082	"US-82, Eddy County"	2
41 D2255	TPM-0132(3)11	NM0132	"NM-132, Lea County"	2
42 (null)	(null)	(null)	(null)	(null)
43 N/A	SP-3-04(321)	NM0314	"NM-314, at Los Lunas, Valencia County"	3

## Soil data

Soil data were collected in excel sheets and used to populate the MEPDG database. The soil data table has been formatted to include the route ID, Beg\_mpnt to make data to MEPDG standard. The script to include the soil data is shown in **Error! Reference source not found.** and the snapshot of data in database is shown in Figure 5.15.



```
InsertScript_soil_data.py - C:\Python25\sriram\soil data\InsertScript_soil_data.py
File Edit Format Run Options Windows Help

port = '1521'
host = 'mepdg.unm.edu'

DSN = cx_Oracle.makedsn(host, port, sid)
orcl = cx_Oracle.connect(user, passwd, DSN)
curs = orcl.cursor()

print 'Hello Gopi'
fname='Soil Data.txt'
f = open(fname, 'r')
text = str(f.read())
#text=text.replace("'", "")
a=re.split("\t|\n",text)
i = 0
while i < len(a):
    sql='''insert into SOIL_DATA
    (
        control_number,
        project_number,
        pstd_rte,
        STATION_LOCATION,
        DISTRICT,
        BEG_MPNT,
        END_MPNT,
        PASSING_3_4_SIEVE,
        PASSING_10_SIEVE,
        PASSING_40_SIEVE,
        PASSING_200_SIEVE,
        LIQUID_LIMIT,
        PLASTIC_INDEX,
        MOISTURE_CONTENT,
        SOIL_CLASSIFICATION,
        TESTED_R_VALUE
    )

    values
    ('%s','%s','%s','%s','%s','%s','%s','%s','%s','%s','%s','%s','%s','%s',
    '%s','%s')'''%(a[i],a[i+1],a[i+2],a[i+3],a[i+4],a[i+5],a[i+6],
    a[i+8],a[i+9],a[i+10],a[i+11],a[i+12],a[i+13],a[i+14]
```

**FIGURE 5.15(a) Snapshot of Script for Populating Soil Data into MEPDG Database**



CONTR...	LOCATION	PST...	BEG_MP...	DISTRICT	PROJEC...	SAMPLE...	BEG_MPNT	STATION_LOCATION	TOP_OF_LIFT
1 1006	I-40 MP60.0...	100040	0	6 AC-GRIP-04...	2004_4041	0		EAST BOUND LANE	18
2 1006	I-40 MP60.0...	100040	0	6 AC-GRIP-04...	2004_3904	0		EAST BOUND LANE	15
3 1006	I-40 MP60.0...	100040	0	6 AC-GRIP-04...	2004_4227	0		WEST BOUND LANE	13.5
4 1133	(null)	100040	2	3 AC-GRIP(BR...	(null)	2.00		I-40 WASHINGTON BRIDGE	(null)
5 D6027	I-40 MP 40 ...	100040	12	6 IM-040-1(12...	2005_4613	12		EB/ROADWAY	22
6 BR016	(null)	100040	21.3	6 BR-9997-6(...	(null)	21.3		I-40	(null)
7 D6056	I-40 IYANBI ...	100040	36	6 HSP-040-1(...	2005_1281	MP36.00		EAST BOUND LANE	11
8 D6056	I-40 IYANBI ...	100040	36	6 HSP-040-1(...	2005_1282	MP36.00		EAST BOUND LANE	18
9 D6056	I-40 IYANBI ...	100040	36	6 HSP-040-1(...	2005_1300	MP36.00		EAST BOUND LANE	11
10 D6056	I-40 IYANBI ...	100040	36	6 HSP-040-1(...	2005_1297	MP36.00		WEST BOUND LANE	21
11 D6056	I-40 IYANBI ...	100040	36	6 HSP-040-1(...	2005_1310	MP36.00		WEST BOUND LANE	20
12 D6056	I-40 IYANBI ...	100040	36	6 HSP-040-1(...	2005_1299	MP36.00		EAST BOUND LANE	24
13 D6056	I-40 IYANBI ...	100040	36	6 HSP-040-1(...	2005_1298	MP36.00		WEST BOUND LANE	13
14 D6056	I-40 IYANBI ...	100040	36.25	6 HSP-040-1(...	2005_1284	MP36.25		EAST BOUND LANE	26
15 D6056	I-40 IYANBI ...	100040	36.25	6 HSP-040-1(...	2005_1283	MP36.25		EAST BOUND LANE	15
16 D6056	I-40 IYANBI ...	100040	36.3	6 HSP-040-1(...	2005_1295	MP36.30		WEST BOUND LANE	24
17 D6056	I-40 IYANBI ...	100040	36.3	6 HSP-040-1(...	2005_1309	MP36.30		WEST BOUND LANE	13
18 D6056	I-40 IYANBI ...	100040	36.3	6 HSP-040-1(...	2005_1308	MP36.30		WEST BOUND LANE	19
19 D6056	I-40 IYANBI ...	100040	36.3	6 HSP-040-1(...	2005_1296	MP36.30		WEST BOUND LANE	13
20 D6056	I-40 IYANBI ...	100040	36.5	6 HSP-040-1(...	2005_1286	MP36.50		EAST BOUND LANE	21
21 D6056	I-40 IYANBI ...	100040	36.5	6 HSP-040-1(...	2005_1285	MP36.50		EAST BOUND LANE	14
22 D6056	I-40 IYANBI ...	100040	36.5	6 HSP-040-1(...	2005_1301	MP36.50		EAST BOUND LANE	16
23 D6056	I-40 IYANBI ...	100040	36.5	6 HSP-040-1(...	2005_1302	MP36.50		EAST BOUND LANE	13
24 D6056	I-40 IYANBI ...	100040	36.7	6 HSP-040-1(...	2005_1293	MP36.70		WEST BOUND LANE	26
25 D6056	I-40 IYANBI ...	100040	36.7	6 HSP-040-1(...	2005_1294	MP36.70		WEST BOUND LANE	17
26 D6056	I-40 IYANBI ...	100040	36.75	6 HSP-040-1(...	2005_1287	MP36.75		EAST BOUND LANE	14
27 D6056	I-40 IYANBI ...	100040	36.75	6 HSP-040-1(...	2005_1288	MP36.75		EAST BOUND LANE	24

**FIGURE 5.15(b) Snapshot of Soil Data in The MEPDG Database**

## Subgrade Design Data

Research team has collected soils “R-value” summary sheets related to NMDOT road projects. Data was then uploaded to the MEPDG database. Data fields are shown in Table 5.2.

**TABLE 5.2 Fields of subgrade design table**

Field	Description
CONTROL_NUMBER	Control Number
PROJECT_NUMBER	Project Number
ROUTE_NAME	Road Name
ROUTE_LOCATION	Location
DISTRICT	District
BEG_MPNT	Beginning Milepost
END_MPNT	Ending Milepost
PROJECT_DATE	Date
PASSING_SIEVE_3_4	% Passing 3/4" Sieve
PASSING_SIEVE_10	% Passing #10 Sieve
PASSING_SIEVE_40	% Passing #40 Sieve
PASSING_SIEVE_200	% Passing #200 Sieve
LIQUID_LIMIT	Liquid Limit, LL (%)
PLATICITY_INDEX	Plasticity Index, PI (%)
MOISTURE_CONTENT	Moisture Content (%)
SOIL_CLASSIFICATION	Soil Classification
SUBGRADE_R_VALUE	R-value

The research team has created some key fields like road name, mileposts, control number, project number, and location. Other fields represent subgrade properties such as percentage passing through sieves 3/4", #10, #40, and #200, liquid limit, plasticity index, moisture content, classification of the soil, and R-value.

### Soils Data from LIMS

LIMS is a database which contains a variety of material properties of samples tested at NMDOT labs and district labs. UNM researchers have explored the database and came up with 18 tables that might have useful MEPDG pavement design data. Table 5.3 shows the data selected from LIMS database to upload to the MEPDG database. The first two tables contain the control number, project number, and location. The remaining tables include the results of tests such as gradation of coarse and fine aggregates, los Angeles wear, moisture content, liquid limit and plasticity index, R-value, soil classification, specific gravity, etc.

**TABLE 5.3 List of tables uploaded from LIMS to MEPDG database**

TABLE NAME	DESCRIPTION
LIMS_GENERAL	Contains details about the control number, project number, location, district and county of the project.
LIMS_PROJNUM_LABNUM	Relates the control number and test lab number.
LIMS_SOILS_TEST_CLF	Clay lumps, F/A(c 142) test
LIMS_SOILS_TEST_FF	Fractured faces test
LIMS_SOILS_TEST_GCC	Gradation, C/A (T 27) for CON and CMD Reports
LIMS_SOILS_TEST_GFC	Gradation, F/A (T 27) for CON and CMD Reports
LIMS_SOILS_TEST_GSF	Gradation (T 27) for SST,FTR or Rundown Reports
LIMS_SOILS_TEST_LAW	Los Angeles Wear (T 96)
LIMS_SOILS_TEST_MC	Moisture content (T 265)
LIMS_SOILS_TEST_PI	Liquid limit (T 89), plastic limit and plastic index (T 90)
LIMS_SOILS_TEST_RV	R-Value (T 190)
LIMS_SOILS_TEST_SCA	Soil classification
LIMS_SOILS_TEST_SE	Sand equivalent (T 176)
LIMS_SOILS_TEST_SLC	Soundness loss, C/A (T 104)
LIMS_SOILS_TEST_SLF	Soundness loss, F/A (T 104)
LIMS_SOILS_TEST_SPGC	Specific gravity and absorption, C/A (T 85)
LIMS_SOILS_TEST_SPGF	Specific gravity and absorption, F/A (T 84)
LIMS_SOILS_TEST_WG	Wash gradation, soils (T 11)

LIMS is an access database. The selected tables from LIMS are initially exported to excel sheets. From excel, data is uploaded into MEPDG database by using python scripts. Figure 5.16 is an example image of a table in LIMS. Figure 5.17 and Figure 5.18 show the images of the python script used for uploading the data from the TST\_RV\_TEST excel sheet into the LIMS\_SOILS\_TEST\_RV table of MEPDG database. Fig 5.19 is a screen shot of the LIMS\_SOILS\_TEST\_RV table in MEPDG database.

	A	B	C	D	E	F	G	H	I	J	
	ST_LAB_NUMBE	TST_TEST	SIEVE_B1	SIEVE_B2	SIEVE_B3	SIEVE_B4	SIEVE_B5	SIEVE_B6	SIEVE_B7	SIEVE_B8	
2	1993-00320	RV	0.0	0.0	628.0	417.0	296.0	735.0	652.0	1645.0	174
3	1993-00321	RV	0.0	0.0	0.0	0.0	0.0	0.0	0.0	0.0	100
4	1993-00323	RV	0.0	0.0	0.0	1119.0	487.0	705.0	406.0	873.0	896
5	1993-00324	RV	0.0	3006.0	1012.0	1841.0	619.0	579.0	343.0	490.0	390
6	1993-00326	RV	0.0	0.0	0.0	2473.0	703.0	1167.0	598.0	1048.0	101
7	1993-00327	RV	0.0	0.0	0.0	387.0	324.0	582.0	510.0	2112.0	286
8	1993-00329	RV	0.0	0.0	0.0	324.0	338.0	594.0	374.0	707.0	101
9	1993-00332	RV	0.0	0.0	1608.0	2689.0	963.0	1503.0	773.0	1319.0	895
10	1993-00334	RV	0.0	0.0	0.0	0.0	0.0	0.0	0.0	0.0	100
11	1993-00335	RV	0.0	0.0	772.0	876.0	472.0	414.0	369.0	923.0	119
12	1993-00337	RV	0.0	0.0	0.0	199.0	191.0	543.0	443.0	1648.0	209
13	1993-00338	RV	0.0	0.0	0.0	0.0	0.0	0.0	0.0	0.0	100
14	1993-00340	RV	0.0	0.0	0.0	0.0	0.0	0.0	0.0	0.0	100
15	1993-00344	RV	0.0	0.0	0.0	0.0	0.0	0.0	0.0	0.0	100
16	1993-00346	RV	0.0	0.0	0.0	0.0	0.0	0.0	0.0	0.0	100
17	1993-00348	RV	0.0	0.0	0.0	0.0	0.0	0.0	0.0	0.0	100
18	1993-00364	RV	0.0	0.0	0.0	0.0	0.0	0.0	0.0	0.0	100
19	1993-00367	RV	0.0	0.0	0.0	0.0	0.0	0.0	0.0	0.0	100
20	1993-00370	RV	0.0	0.0	0.0	1233.0	656.0	1182.0	853.0	1451.0	100
21	1993-00373	RV	0.0	0.0	0.0	2348.0	1207.0	1687.0	928.0	1327.0	580
22	1993-00378	RV	0.0	0.0	489.0	1582.0	1013.0	1313.0	810.0	1244.0	108
23	1993-00381	RV	0.0	0.0	0.0	926.0	761.0	1409.0	850.0	1311.0	634
24	1993-00384	RV	0.0	0.0	0.0	624.0	573.0	1063.0	845.0	1342.0	632
25	1993-00388	RV	0.0	0.0	0.0	1239.0	627.0	744.0	429.0	621.0	260

FIGURE 5.16 Excel Sheet Image of the TST\_RV\_TESTS File

```

tst_rv_table.py - C:\Python25\sriram\LIMS SCRIPTS\lms tables\table scripts\tst_rv_table.py
File Edit Format Run Options Windows Help

sql1="select count(*) from lms_soils_test_rv"
curs.execute(sql1)
k=curs.fetchall()
for row in k:
    j=int(row[0])
    j=j+1
    print j
    print len(a)

while i < len(a):
    print a[i],"-->"
    sql="'' insert into LIMS_SOILS_TEST_RV
    (
        TST_LAB_NUMBER ,
        TST_TEST ,
        SIEVE_B1 ,
        SIEVE_B2 ,
        SIEVE_B3 ,
        SIEVE_B4 ,
        SIEVE_B5 ,
        SIEVE_B6 ,
        SIEVE_B7 ,
        SIEVE_B8 ,
        SIEVE_B9 ,
        SIEVE_B10 ,
        BTOT ,
        SIEVE_C1 ,
        SIEVE_C2 ,
        SIEVE_C3 ,
        SIEVE_C4 ,
        SIEVE_C5 ,
        SIEVE_C6 ,
        SIEVE_C7 ,
        SIEVE_C8 ,
        SIEVE_C9 ,
        SIEVE_D1 ,
        SIEVE_D2 ,
        SIEVE_D3 ,
        SIEVE_D4 ,

```

FIGURE 5.17 Image of Python Script for LIMS\_SOILS\_TEST\_RV Table

```
tst_rv_table.py - C:\Python25\sriram\LIMS SCRIPTS\lms tables\tst_rv_table.py
File Edit Format Run Options Windows Help

SIEVE_H3 ,
SIEVE_H4 ,
SIEVE_H5 ,
SIEVE_H6 ,
SIEVE_I1 ,
SIEVE_I2 ,
SIEVE_I3 ,
SIEVE_I4 ,
SIEVE_I5 ,
SIEVE_I6 ,
SIEVE_J1 ,
SIEVE_J2 ,
SIEVE_J3 ,
SIEVE_J4 ,
SIEVE_J5 ,
SIEVE_J6 ,
TST_DATE_COMPLETED ,
STAB_PH_200_1 ,
DISPLACEMENT1 ,
R_VALUE1 ,
EXUD_PRESS1 ,
STAB_PH_200_2 ,
DISPLACEMENT2 ,
R_VALUE2 ,
EXUD_PRESS2 ,
STAB_PH_200_3 ,
DISPLACEMENT3 ,
R_VALUE3 ,
EXUD_PRESS3 ,
RESULT_R_VALUE
) VALUES
(' %s', '%s', '%s', '%s', '%s', '%s', '%s', '%s', '%s', '%s',
 '%s', '%s', '%s', '%s', '%s', '%s', '%s', '%s', '%s', '%s',
 '%s', '%s', '%s', '%s', '%s', '%s', '%s', '%s', '%s', '%s',
 '%s', '%s', '%s', '%s', '%s', '%s', '%s', '%s', '%s', '%s',
 '%s', '%s', '%s', '%s', '%s', '%s', '%s', '%s', '%s', '%s',
 '%s', '%s', '%s', '%s', '%s', '%s', '%s', '%s', '%s', '%s') '' % (a[1],
a[1+1], a[1+2], a[1+3], a[1+4], a[1+5], a[1+6], a[1+7], a[1+8], a[1+9], a[1+10],
a[1+11], a[1+12], a[1+13], a[1+14], a[1+15], a[1+16], a[1+17], a[1+18], a[1+19], a[1+20],
a[1+21], a[1+22], a[1+23], a[1+24], a[1+25], a[1+26], a[1+27], a[1+28], a[1+29], a[1+30],
a[1+31], a[1+32], a[1+33], a[1+34], a[1+35], a[1+36], a[1+37], a[1+38], a[1+39], a[1+40],
a[1+41], a[1+42], a[1+43], a[1+44], a[1+45], a[1+46], a[1+47], a[1+48], a[1+49], a[1+50],
a[1+51], a[1+52], a[1+53], a[1+54], a[1+55], a[1+56], a[1+57], a[1+58], a[1+59], a[1+60],
a[1+61], a[1+62], a[1+63], a[1+64], a[1+65], a[1+66], a[1+67], a[1+68], a[1+69])
```

**FIGURE 5.18** Image of Python Script for LIMS SOILS TEST RV Table

[illegible]

**FIGURE 5.19** Image of LIMS SOILS TEST RV Table in Database

## Climate Details

The climate details page displays the climate data at the selected section of the route. The climate data that is displayed is ground water depth at the selected location. The ground water depth data is obtained from a service hosted on the EDAC's server at UNM.

The user collects the coordinates (latitude (X), longitude (Y)) of the selected section from the MEPDG database and this data is used as the input for the map service. The code for accessing the MAP service is given below:

```
// Extract the xml content from EDAC's remote server passing the X and Y parameters (fixed in URL for
this example)
$xml = file_get_contents("http://edacwms.unm.edu/cgi-
bin/mapfiles/gfi?layers=osewells_idw&x=".$row1['X']."&y=".$row1['Y']."");
// Parse the received XML
$xml = new SimpleXMLElement($xml);
// Save the variable / value of interest
$value = $xml->osewells_idw_layer->osewells_idw_feature->value_0;
```

The user will make a request and gets an XML response. The XML response data is then parsed and the required value is extracted from the response data.

In a similar way the temperature data and precipitation data at a particular location will be collected using the map service. The temperature and precipitation data will be included in the website once they are collected.

This page also gives the location details such as the beg\_mpnt, end\_mpnt, traffic\_id and the county details. It also has a provision for downloading all the climate data. The snapshot of the climate page and the snapshot of downloaded excel sheet are given in Figures 5.20 and 5.21, respectively.

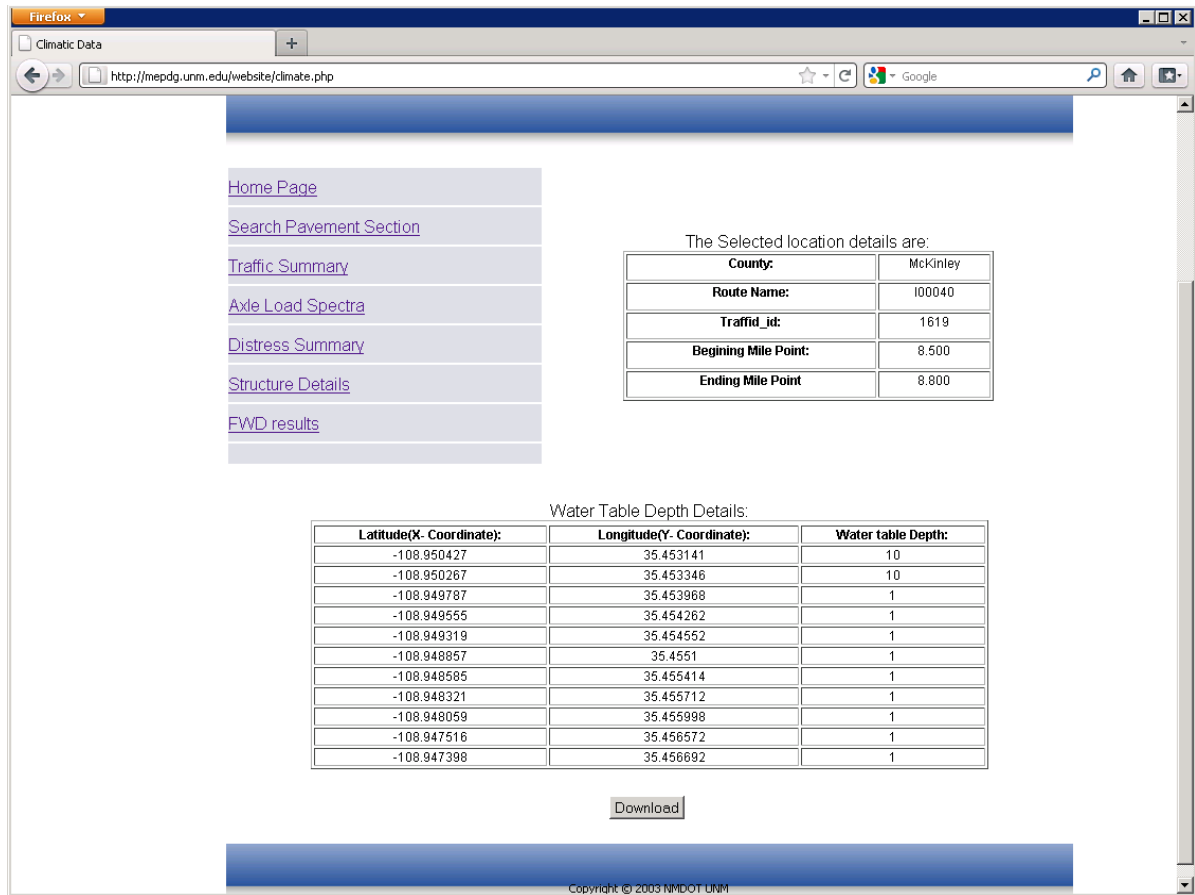


**FIGURE 5.20 Snapshot of the Climate Details Page**

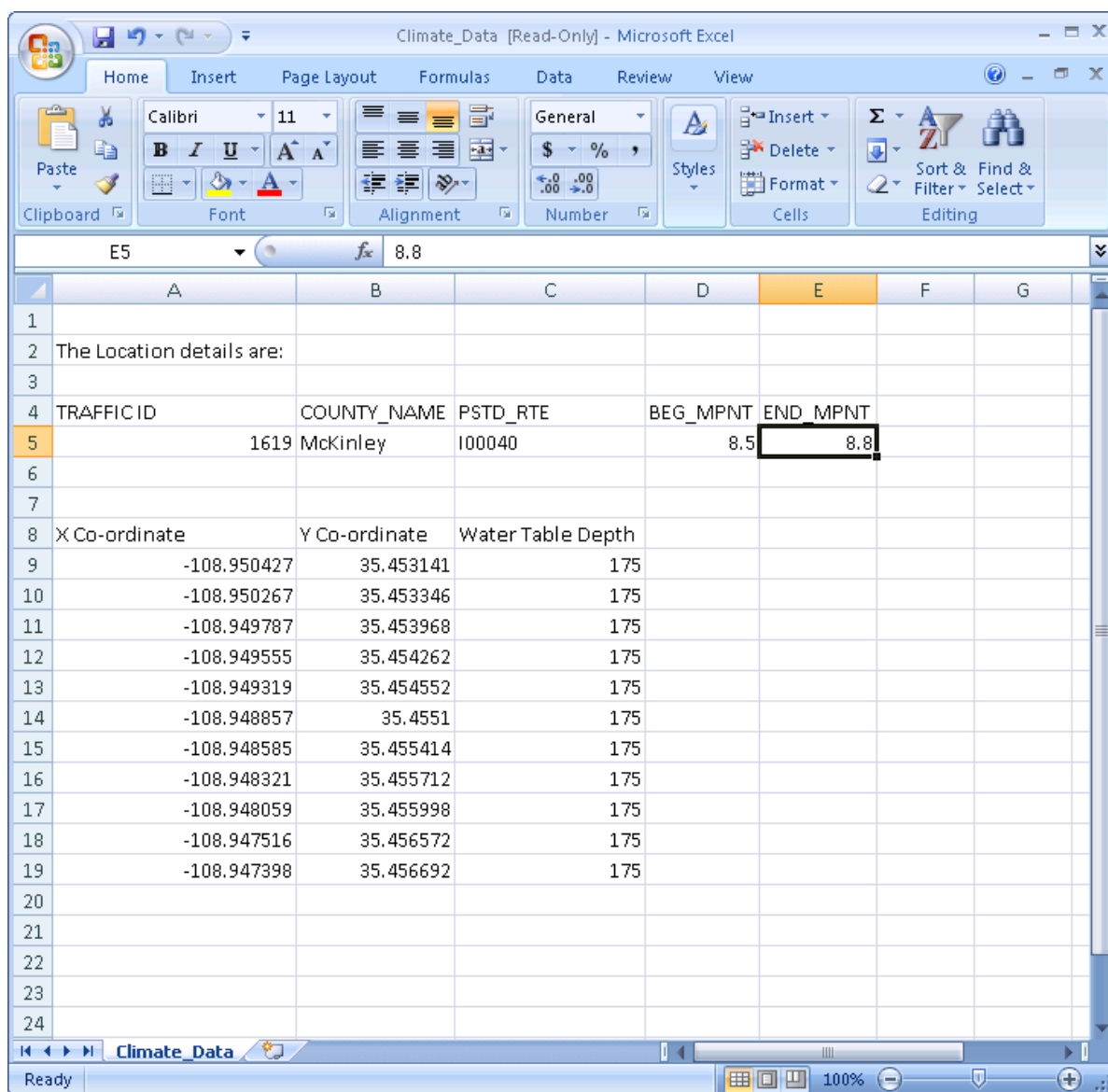


**FIGURE 5.21 Snapshot of the Downloaded Climate Data in Excel Sheet**

## Chapter 6

### DATABASE MAINTENANCE AND INTEGRITY

#### INTRODUCTION

This chapter describes the strategies to protect and maintain the database and the integrity of data therein, and to ensure that data is current and accurate.

#### Database Maintenance

The following standard protocols are recommended for routine maintenance of the MEPDG database:

- Table and index fragmentations
- Schedule backups once a week depending on the criticality of the database updates.
- Schedule jobs to check the free space on Server Disk and Tablespaces and send the report to DBAs
- Check the database growth projection and plan for the space
- Plan for scheduled downtime of the database once in month
- Put the database in archive log mode to restore the point in time, not to lose any of the data.
- Clean-up the unused user accounts frequently

#### Data Integrity

During population of data into MEPDG database tables, source data were checked using python scripts. By observing the data and column definition, data types and ranges for an attribute in a table are checked. Since MEPDG is a relational database, the referential integrity is maintained in the database. The insertion of data followed the primary and foreign key constraints using triggers and procedures.

#### Database Backup

A database backup is done through the execution of database dumps that include both database structure and content backups. Data Pump Utility (EXPDP) was used for taking backup of database. The dump files are copied into external hard drive for storage.

#### Database Security

**Database User:** User name “dbuser” was created which does not give privileges to make changes in data tables.



**Virtual Private Database (VPD):** Enhanced access control, privacy, and performance have been added to the MEPDG database through the Virtual Private Database, a feature of the Oracle 11g Enterprise Edition.

*Column-Level VPD:* Column-level VPD policies were placed to provide fine-grained access controls on data. With Column-level VPD, security policies can be applied only where a particular column or columns are accessed by a user's query. This means that when a user has rights to access the object itself, VPD can limit the individual row-return only if the columns a user accesses contain sensitive information.

*Column-Masking:* The default behavior of column-level VPD restricts the number of rows returned when a query addresses columns containing sensitive data. In contrast, column-masking behavior allows all rows to be returned for a query against data protected by column-level VPD, but the columns that contain sensitive information are returned as NULL values. With Column-masking, users see all the data they are supposed to see, but privacy is not compromised.

### **Data Exchange Protocol**

A goal of this study is to develop an effective means of interaction between the MEPDG database and existing databases maintained by NMDOT for network-level applications. The interaction between MEPDG database and NMDOT's existing databases can be done using database links. Figure 1 shows a database link between MEPDG database and an existing database conceptually. It can be defined as a connection between two physical database servers that allows a client to access them as one logical database. A database link can be private or public. If the link is private, then only the user who created the link has access. If the link is public, then all database users have access.

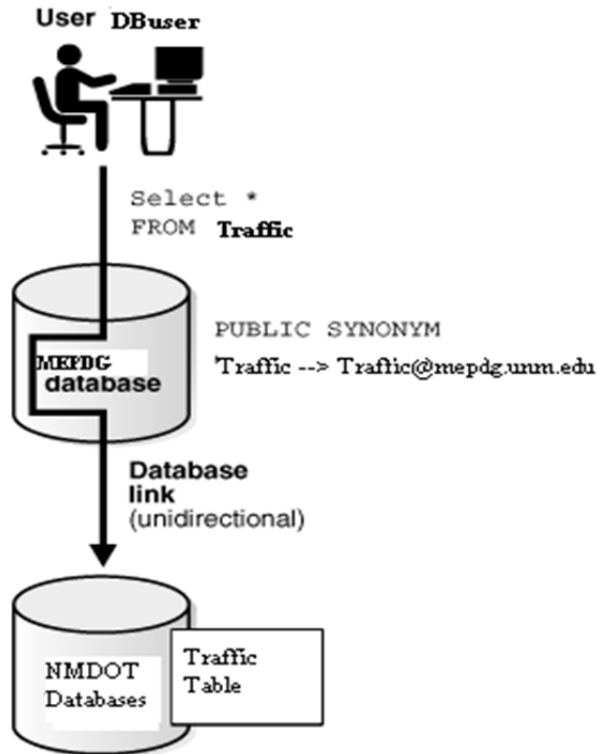


**FIGURE 6.1 Protocols for Data Exchange Among Databases**

The database links have access models, which include authenticated database connections via ODBC (Open Database Connectivity), the standard for cross-platform database access. A sample database link is shown in Figure 2.

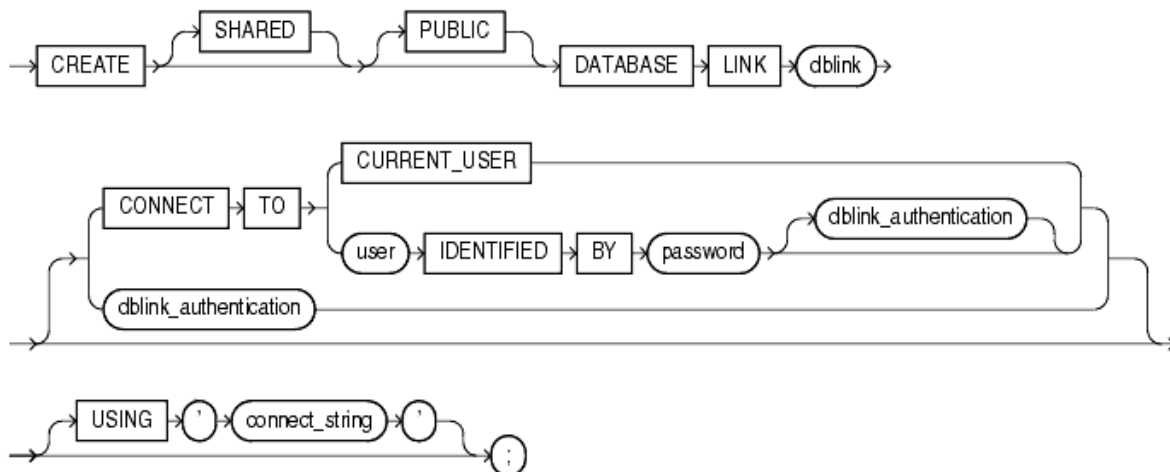


**FIGURE 6.2 Database link**

## Data Reduction

In this study, redundant data were removed to ensure data integrity and to maintain efficiency of the database. Research team adopted different methods for eliminating redundant data. They are:

### *Unique, primary key and foreign key constraints*

During table creation, attributes were made unique or primary key based on the attribute's relation with the table. The foreign key was used to enter only data relating to data in some other table. Thus the redundant data is eliminated from the MEPDG database in the initial stages of populating the data in the database.

### *Distinct Technique*

For some tables, the research team was not able to remove the data redundancy while populating the data. Such kinds of data redundancy are removed with the help of "The Distinct Technique". In this technique a distinct query is first run on the database thus first identifying the unique rows in the tables. Then the unique rows are copied to a temporary table and the original table is deleted. The data from temporary table is copied back to the original table. In this way the duplicate data is removed. To prevent from further insertion of duplicate data, the attributes were made unique and primary key.

## Restoring Database from Backup

### *Requirements:*

Install oracle and restore database from an export file.

### *Tasks:*

Download software for Oracle 11.2.0.2 , Opatch and PSU Jan 2012.

### *Install software:*

- Copy database software to c:\oracle\_software\database
- Copy Opatch software to c:\oracle\_software\patches (it is a zip file)
- Copy PSU software to c:\oracle\_software\patches\13413154
- Install Oracle software at c:\app\Administrator\oracle\11.2.0.2

### *Database configuration:*

- Used configuration assistant to create database mepdg.
  - Datafiles store in c:\oradata\mepdg
- Set up listener.ora
- Set up tnsnames.ora file
- Verify database connectivity through listener

### *Data recovery:*

- Create tablespaces MEPDG\_DATA and MEPDG\_INDEX
- Import data from GISMEPDG\_export.dmp dated 7/11/2011
- Verified import

- Moved objects owned by DBUSER from USER tablespace to MEPDG\_DATA and MEPDG\_INDEX

*Data verification:*

- Login using sys, system and dbuser account information
- Set up connectivity to the database
  - Installed Oracle client
  - Set up tnsnames.ora information for the database

## Database Query Examples

Datasets tables:

- 1) dataset\_general\_info  
This table gives the general information about the datasets. i.e their project numbers, control numbers, location etc.
- 2) Dataset\_soil  
This table contains the soil data for the datasets.
- 3) Dataset\_Structure  
Provides the structural data for the datasets.
- 4) Dataset\_ac\_mixtures  
Provides the asphalt concrete mixtures data.
- 5) Dataset\_trafficdata  
This table contains the traffic data of the locations.

Dataset\_general\_info:

# Command to view the data in Dataset\_general\_info table

Query 1:

```
select * from dataset_general_info
```

# command to view different control numbers of the datasets

Query:2

```
select distinct(control_numbers) from dataset_general_info
```

# command to view data in dataset\_soil table

Query:3

```
select * from dataset_soil
```

# command to view soil data for specific control numbers.

Query:4

```
select * from dataset_soil where control_number='X'
```

'X' is the control number which can be obtained by running query :2

# command to view traffic data

Query:5

```
select * from dataset_trafficdata
```

```

# command to view traffic data of specific control numbers
Query :6
select * from dataset_trafficdata where control_number='X'
'X' is the control number which can be obtained by running query :2

# command to view structures data
Query : 7
select * from dataset_structure

# command to view structures data of specific control numbers
Query :8
select * from dataset_structure where control_number='X'
'X' is the control number which can be obtained by running query :2

# command to view asphalt concrete data
Query : 9
select * from dataset_ac_mixtures

# command to view structures data of specific control numbers
Query :10
select * from dataset_ac_mixtures where control_number='X'
'X' is the control number which can be obtained by running query : 2

```

## **Chapter 7**

### **INITIAL LOCAL CALIBRATION**

#### **INTRODUCTION**

In this study, the MEPDG Oracle database as well as from different NMDOT sources are analyzed for complete data sets. Initially, a total of 29 New Mexico pavement sections are found to have all MEPDG inputs, however data lack from quantitative distress values required for MEPDG calibration. This is because New Mexico has collected qualitative distress data rather than actual measurements of rut depth and crack length over the past years. Instead of using these 29 sections, only 11 sections from the Long Term Pavement Performance (LTPP) database located in New Mexico are used for local calibration. The permanent deformation, alligator cracking, and longitudinal cracking models are calibrated. In calibration methodology, the target is fixed to reduce the residual sum of squared errors, defined by the square of the difference between predicted and measured distress, so that any bias is eliminated and precision is increased.

#### **PAVEMENT SECTIONS FOR INITIAL CALIBRATION**

The internal databases of New Mexico Department of Transportation (NMDOT) are the first source considered for collecting the traffic, climate, structure, materials, and performance data necessary to obtain a sufficient number of local pavement sections. Indeed, all these databases have been consolidated in the new NMDOT Flexible Pavement Database created at the University of New Mexico. A total of 29 sections are completed for a variety of roads across the state but their use is discarded because the corresponding distress data is inconsistent and unreliable. The reason for this is that NMDOT measures pavement performance with qualitative ratings rather than with quantitative measures of distress (depth of rutting or length of cracks). Nonetheless, these sections are kept aside in case that better performance data is obtained in the future. This leaves the LTPP database as the only source of data.

However, the LTPP database created under the Strategic Highway Research Program (SHRP) contains extensive amounts of data and is consistent and reliable being the main resource used by most state agencies in their calibration efforts. There are 11 complete flexible experiments within the state of New Mexico. The code, location, functional class, construction date, and type of each of these sections are contained in Table 7.1. As shown, six sections are new flexible pavements while the other five are rehabilitated asphalt concrete pavements. Figure 7.1 shows the location of these sections across New Mexico.

### TABLE 7.1 LTPP flexible pavement sections in New Mexico

State Code	SHRP Id	Road	Mile Point	Functional Class	Type of Experiment	Construction Date *
35	1002	US-70	310.1	2	GPS-6A	May, 1985
35	1003	US-70	320.9	2	GPS-1	May, 1983
35	1005	I-25	263.8	1	GPS-1	Sep, 1983
35	1022	US-550	125.1	2	GPS-1	Sep, 1986
35	1112	US-62	81.3	2	GPS-1	May, 1984
35	2006	US-550	89.5	2	GPS-2	Jun, 1982
35	2007	US-550	106.2	2	GPS-6A	Jun, 1981
35	2118	I-40	346.2	1	GPS-2	Dec, 1979
35	6033	I-25	159.3	1	GPS-6A	May, 1981
35	6035	I-40	96.7	1	GPS-6A	May, 1985
35	6401	I-40	107.7	1	GPS-6A	May, 1984

*GPS-1: Asphalt Concrete on Unbound Granular Base; GPS-2: Asphalt Concrete on Bound Granular Base  
GPS-6A: Existing AC Overlay on AC Pavement; \* This is the date of last major improvement in the case of  
rehabilitated sections.*



### FIGURE 7.1 LTPP sections in New Mexico

## DATA FOR INITIAL CALIBRATION

### Traffic Data

The traffic information necessary to run the MEPDG is obtained from the following LTPP database tables:

- TRF\_BASIC: Location and number of lanes.
- TRF\_MEPDG\_AADTT\_LTPP\_LN: Annual average daily truck traffic.
- TRF\_MONITOR\_LTPP\_LN: AADTT and vehicle class distribution.
- TRF\_MEPDG\_VEH\_CLASS\_DIST: Vehicle class distribution.
- TRF\_MEPDG\_MONTHLY\_ADJ\_FACTORS: Monthly distribution factors.
- TRF\_MONITOR\_AXLE\_DISTRIB: Axle load spectra.
- TRF\_MEPDG\_AX\_PER\_TRUCK: Number of axles of each type per truck class.

The directional distribution, the lane distribution, and the truck growth rate are obtained from NMDOT sources. Default values are used for other traffic inputs. Table 7.2 shows the AADTT for each section, the truck growth rate at the beginning of the design life, and the percentage of class 5, 8 and 9 trucks.

**TABLE 7.2 AADTT, truck growth, and classes 5, 8 and 9 at LTPP sections**

SHRP Id	Traffic Open Date	Initial two- way AADTT	Growth Rate (%) *	Class 5 (%)	Class 8 (%)	Class 9 (%)
351002	Jun, 1985	736	0.1	14.5	13.1	67.7
351003	Jun, 1983	735	0.1	14.5	13.1	67.7
351005	Oct, 1983	2971	0.3	23.4	17.0	47.9
351022	Oct, 1986	911	1.0	30.4	13.5	42.6
351112	Jun, 1984	559	3.2	32.9	9.9	44.5
352006	Jul, 1982	844	0.4	23.5	17.7	42.8
352007	Jul, 1981	563	2.8	36.8	10.0	39.6
352118	Jan, 1980	831	7.3	4.8	5.6	79.2
356033	Jun, 1981	1885	0.5	39.9	17.9	32.6
356035	Jun, 1985	540	10.4	16.4	7.1	71.6
356401	Jun, 1984	1760	4.7	9.2	5.4	75.9

*\* The truck growth rate is assumed to be compound*

### Climatic Data

The climatic data is obtained by interpolating the MEPDG weather files at the location of each section. The ground water table depth is assumed to be 100 ft as suggested by NMDOT. The following LTPP tables are used to collect the coordinates and elevation of each section:

- CLM\_SITE\_VWS\_LINK: Weather stations.
- CLM\_VWS\_OWS\_LINK: Weather stations and distance to LTPP sections.
- CLM\_OWS\_LOCATION: Longitude, latitude and elevation.

Table 7.3 contains the coordinates and elevation where the climatic data is interpolated and the ground water table depth.



**TABLE 7.3 Coordinates, elevation, and ground water table depth of LTPP sections**

SHRP Id	Latitude (dd.mm)	Longitude (dd.mm)	Elevation (ft)	GWT Depth (ft)
351002	33.22	-104.55	3800	100
351003	33.23	-104.44	3800	100
351005	35.31	-106.14	5523	100
351022	36.22	-107.50	6727	100
351112	32.38	-103.31	3760	100
352006	36.11	-107.20	6742	100
352007	36.15	-107.36	7021	100
352118	35.10	-103.29	3927	100
356033	34.12	-106.55	4662	100
356035	35.50	-107.39	6200	100
356401	35.20	-107.29	5893	100

**Structural Data**

The number of layers, and the thickness and type of each pavement layer are included in Table 7.4. This information has been collected from the following LTPP tables:

- INV\_ID: Location and elevation of sections.
- INV\_AGE: Date of construction.
- INV\_MAJOR\_IMPROV: Date, thickness and type of rehabilitation.
- INV\_LAYER: Number of layers, thickness and type of each layer.

**TABLE 7.4 Layer system of LTPP sections**

SHRP Id	Type and Thickness of Layers
351002	AC Overlay (3.9 in); AC Existing (5.2 in); GB (5 in); SG (semi-infinite)
351003	AC (7.6 in); GB (5 in); SG (semi-infinite)
351005	AC (9.1 in); GB (7 in); SG (semi-infinite)
351022	AC (6.6 in); GB (10 in); SG (semi-infinite)
351112	AC (5.6 in); GB (4 in); SG (semi-infinite)
352006	AC (6.1 in); GB (11.5 in); SG (semi-infinite)
352007	AC Overlay (2.1 in); AC Existing (7.1 in); GB (6 in); SG (semi-infinite)
352118	AC (11.1 in); GB (18 in); SG (semi-infinite)
356033	AC Overlay (3.1 in); AC Existing (4.8 in); GB (4 in); GB (8 in); SG (semi-infinite)
356035	AC Overlay (3.1 in); AC Existing (5.1 in); GB (16 in); SG (semi-infinite)
356401	AC Overlay (3.7 in); AC Existing (3.5 in); GB (12 in); SG (semi-infinite)

- AC: Asphalt Concrete, GB: Granular Base, SG: Subgrade

## Materials Data

In the flexible pavement sections used in this study, there are mainly three types of materials: asphalt concrete, engineered granular soil, and natural soil. The properties of these materials are extracted from the following LTPP tables:

- INV\_GRADATION: Gradation analysis of layers.
- INV\_PMA\_ASPHALT: Binder grade of asphalt.
- INV\_PMA\_ORIG\_MIX: Asphalt content and air voids of mixture.
- INV\_UNBOUND: Properties of unbound granular soil.
- INV\_SUBGRADE: Properties of natural soil.
- TST\_AG04: Gradation of AC mixture aggregates.
- TST\_AC05: Asphalt content, air voids, and specific gravity of mixture.
- TST\_SS04\_UG08: AASHTO class of soil.
- TST\_SS01\_UG01\_UG02: Gradation of soil.
- TST\_UG04\_SS03: Plasticity index (PI) and liquid limit (LL).
- TST\_UG05\_SS05: Moisture content and maximum dry unit weight.

Tables 7.5(a) and 7.5(b) contains the binder grade, asphalt content, air voids percent, unit weight, and aggregate gradation of the AC mixtures used in these sections. Tables 7.6 and 7.7 shows the AASHTO class, PI, LL, sieve analysis, maximum dry unit weight, optimum gravimetric water content, and R-value of the soils used for the granular base and the subgrade respectively.

**TABLE 7.5(a) Asphalt concrete properties of LTPP sections**

SHRP Id	Binder Viscosity Grade	Effective Binder Content (%)	Air Voids (%)	Total Unit Weight (pcf)
351002	Pen 85-100	5.5	4.1	143.65
351003	Pen 85-100	5.9	4.8	143.8
351005	Pen 85-100	5.3	3.9	146
351022	Pen 85-100	5.9	3.7	147
351112	Pen 85-100	5.05	4.4	151.63
352006	AC 10	5.5	5.8	142.7
352007	Pen 85-100	6.1	4.6	145.95
352118	Pen 120-150	4.8	4.4	147.8
356033	Pen 85-100	6.1	3.2	143.8
356035	Pen 85-100	5.5	8.1	149
356401	Pen 85-100	5.4	4	153

**TABLE 7.5(b) AC aggregate gradation**

SHRP Id	Cum. Retained 3/4 in (%)	Cum. Retained 3/8 in (%)	Cum. Retained #4 (%)	Passing #200 (%)
351002	0	20	43	5.8
351003	0	23	39.5	10.2
351005	0	27	48	6
351022	0	26	44	6
351112	0	20	36.5	7.75
352006	3.5	41	56	7.85
352007	0	30.5	44	5
352118	6	35.5	51	5
356033	0	21.7	43.3	6
356035	0	30	50	3
356401	1	20	42	8.5

**TABLE 7.6 Granular base properties of LTPP sections**

SHRP Id	AASHTO Class	PI	LL	Passing #4 (%)	Passing #40 (%)	Passing #200 (%)	$\gamma_{dry}$ (pcf)	$W_{opt}$ (%)	R- value*
351002	A-1-a	0.5	12	42	23.5	12.3	131.0	8.5	-
351003	A-2-4	10.5	28.5	41	18.5	12.3	139.5	6	-
351005	A-1-a	0	6	49.5	21	6.1	135	7.4	61
351022	A-1-b	0	6	59.5	35	9.3	138	6	-
351112	Gravel	5.5	23.5	70	48.5	16.8	121	10	61
352006	A-2-4	0	14	99	88.5	14.4	122.5	10.5	54
352007	A-3	1.5	22	99	77.5	28.4	122	10	-
352118	A-1-a	0	6	42.5	21.5	6.9	138.5	5.5	-
356033	A-1-b	1	11	59	23	8	119	11.5	77
356033	A-1-a	1	21	62.5	24.5	11.2	131.5	7.5	75
356035	Gravel	0	6	59.5	23.5	8	133	8	-
356401	A-1-b	6.5	23.5	47.5	20.5	12.8	142	5	-

*The layer modulus is estimated from ICM inputs (Level 3). \* The layer modulus is estimated from the R-value (Level 2).*

**TABLE 7.7 Subgrade properties of LTPP sections**

SHRP Id	AASHTO Class	PI	LL	Passing #4 (%)	Passing #40 (%)	Passing #200 (%)	$\gamma_{dry}$ (pcf)	$W_{opt}$ (%)	R-value*
351002	A-1-b	2.5	23	52.5	32	21.4	120.5	11.5	48
351003	A-2-4	6	23.5	52.5	34.5	27.6	130	9.5	-
351005	A-2-4	3	22.5	95.5	73.5	28.7	118	14	30
351022	A-2-4	2	19.5	97.5	73.5	8.4	122	11.5	49
351112	A-2-4	0	0	99.5	84	13.7	106	12.5	59
352006	A-2-4	0	14	100	82.5	25.6	122.5	10	53
352007	A-4	5	21	93	83	37	123	9.3	52
352118	A-2-4	2	14	93.5	85.5	21.4	114.5	12.5	51
356033	A-2-4	2.5	22	79	60.5	41	126	9.5	71
356035	A-4	3.5	23	91	78	43.7	121	11.5	24
356401	A-2-4	2	14	98.5	96	23.1	120	11.5	37

*The layer modulus is estimated from ICM inputs (Level 3). \* The layer modulus is estimated from the R-value (Level 2).*

## Performance Data

Measures of total rutting, alligator cracking, longitudinal cracking, transverse cracking and international roughness index (IRI) at the LTPP sections are obtained from the following tables:

- MON\_T\_PROFILE\_INDEX\_SECTION: Total rutting.
- MON\_DIS\_AC\_REV: Alligator, longitudinal, and transverse cracking.
- MON\_PROFILE\_MASTER: IRI.

Tables 7.8, 7.9, and 7.10 contains the measurements of total rutting, alligator cracking, and longitudinal cracking respectively that were taken between 1989 and 2007 at the LTPP experiments.

**TABLE 7.8 Total rutting (in) measured in LTPP sections**

Yr	SHRP Id										
	1002	1003	1005	1022	1112	2006	2007	2118	6033	6035	6401
89	0.1969	0.1969	0.6299	0.1969	0.1969	0.4724	0.2362		0.2362	0.4724	0.2756
90								0.1969	0.2756	0.3543	0.3150
91	0.1575	0.1969	0.6693	0.1575	0.1969	0.6299	0.1969	0.1575	0.2362	0.3543	0.3543
92			0.5512	0.1969		0.4724			0.2362	0.3937	0.3937
93	0.1969	0.1181			0.1575			0.1575			
94											
95	0.3937	0.1969	0.6693	0.2756	0.2165		0.1969	0.2362	0.2756	0.4331	0.4331
96											
97	0.3543	0.1575	0.6693	0.2362	0.1969		0.1575	0.2756	0.5118	0.4331	0.4724
98											
99	0.3543	0.1969	0.7283	0.1969	0.1969		0.1575	0.3150	0.4724		0.4724
00					0.1969			0.3543			

01	0.3543		0.8268		0.2362				0.0394		
02	0.2756		0.7480		0.1772			0.2756			
03			0.8268		0.1969						
04					0.1969				0.1969		
05			0.8268								
06											
07								0.3543	0.2362		

**TABLE 7.9 Alligator cracking (%) measured in LTPP sections**

Yr	SHRP Id										
	1002	1003	1005	1022	1112	2006	2007	2118	6033	6035	6401
1991	0.00	0.00	0.00	0.00	0.00	0.00		0.00	0.00		3.17
1992											
1993											
1994	0.00	0.00	0.00	0.00	0.00		0.00	0.00	13.00	9.95	1.26
1995		1.77			0.00						
1996					0.00						
1997	0.00	0.02	0.00	0.00	0.00		0.00	0.12	13.00	7.07	4.24
1998											
1999	0.05	0.00	0.00	0.00	0.00		0.61	0.27	13.00		6.51
2000					0.00						
2001								3.97	12.63		
2002	0.75		0.00		0.00			0.00	25.70		
2003					0.00						
2004					0.00				0.00		
2005			0.00								
2006											
2007								0.00	0.00		

**TABLE 7.10 Longitudinal cracking (ft/mi) measured in LTPP sections**

Yr	SHRP Id										
	1002	1003	1005	1022	1112	2006	2007	2118	6033	6035	6401
1989											
1990											
1991	0.00	706.77	0.00	0.00	0.00	0.00		0.00	5442.83		1773.86
1992											
1993											
1994	0.00	491.97	0.00	0.00	0.00		398.43	0.00	381.10	1087.87	5855.12
1995		225.20			0.00						
1996					0.00						
1997	48.50	460.79	0.00	0.00	0.00		845.35	76.22	401.89	543.94	2885.98
1998											
1999	0.00	363.78	0.00	0.00	0.00		696.38	69.29	381.10		1739.21
2000					0.00						
2001								0.00	381.10		
2002	69.29		0.00		0.00			0.00			
2003					0.00						
2004					0.00				0.00		
2005			0.00								
2006											
2007								0.00	0.00		

## INITIAL CALIBRATION

The possibility of using numerical nonlinear optimization techniques was explored but its application would be too difficult since the MEPDG prediction of distress is a very complex iterative process. Therefore, the only way to proceed is to run the MEPDG multiple times for different combinations of the calibration coefficients and calculate the corresponding sum of squared errors.

The distress values measured in the field are compared to those predicted by the MEPDG and the residual error is calculated at five particular times per section equally distributed through the pavement design life. Calibration of the performance prediction models is achieved by varying the coefficients such that the residual sum of squared errors is reduced.

The split-sample approach is used in the calibration-validation process: 9 out of 11 LTPP sections are chosen randomly for use in the calibration of each distress model while the other 2 sections are kept aside to check whether the calibrated pavement performance model can reduce the error in the MEPDG prediction of distress for cases different to those used during calibration.

## Permanent Deformation Model

### Prediction of Permanent Deformation in the MEPDG

This section describes the empirical model used in the MEPDG to predict the permanent deformation occurring in the pavement layers (*MEPDG Documentation, 2004*).

The plastic strain of the asphalt concrete layer is given by the following equations:

$$\frac{\varepsilon_p}{\varepsilon_r} = k_z \beta_{r1} 10^{k_1} T^{k_2 \beta_{r2}} N^{k_3 \beta_{r3}}$$

$$k_z = (C_1 + C_2 d) 0.328196^d$$

$$C_1 = -0.1039 h_{AC}^2 + 2.4868 h_{AC} - 17.342$$

$$C_2 = 0.0172 h_{AC}^2 - 1.7331 h_{AC} + 27.428$$

where  $\varepsilon_p$  = Plastic strain of the asphalt concrete layer (in/in)  
 $\varepsilon_r$  = Resilient strain of the asphalt concrete layer (in/in)  
 $T$  = Asphalt concrete layer temperature (°F)  
 $N$  = Number of axle load repetitions  
 $d$  = Depth of the point where strain is being determined (in)  
 $h_{AC}$  = Thickness of the asphalt concrete layer (in)  
 $k_1 = -3.35412$ ,  $k_2 = 1.5606$ ,  $k_3 = 0.4791$   
 $\beta_{r1}$ ,  $\beta_{r2}$ ,  $\beta_{r3}$  = calibration coefficients to be optimized

This plastic strain value multiplied by the AC thickness provides the permanent deformation occurring at the asphalt concrete layer. The permanent deformation for granular bases and the subgrade is obtained using the following formula:

$$\delta_a = \beta_{s1} k_1 \varepsilon_v h \frac{\varepsilon_0}{\varepsilon_r} e^{-\left(\frac{\rho}{N}\right)^\beta}$$

where  $\delta_a$  = Permanent deformation of the unbound layer (in)  
 $N$  = Number of axle load repetitions  
 $\varepsilon_v$  = Average vertical strain in the unbound layer (in/in)  
 $h$  = Thickness of the unbound layer (in)  
 $\varepsilon_r$  = Resilient strain in the unbound layer (in/in)  
 $\varepsilon_0$ ,  $\beta$ ,  $\rho$  = Material properties  
 $k_1 = 2.03$  for granular base and 1.35 for subgrade  
 $\beta_{s1}$  = Calibration coefficient to optimize for both base and subgrade

The total permanent deformation of the section is the summation of the permanent deformation occurring in every single layer:

$$PD = \sum_{i=1}^{layers} \varepsilon_p^i h^i$$

$$= h_{AC} \varepsilon_r k_z \beta_{r1} 10^{k_1} T^{k_2 \beta_{r2}} N^{k_3 \beta_{r3}}$$

$$+ \beta_{GB} k_{GB} \varepsilon_v h_{GB} \frac{\varepsilon_0}{\varepsilon_r} e^{-\left(\frac{\rho}{N}\right)^\beta}_{GB}$$

$$+ \beta_{SG} k_{SG} \varepsilon_v h_{SG} \frac{\varepsilon_0}{\varepsilon_r} e^{-\left(\frac{\rho}{N}\right)^\beta}_{SG}$$

where PD = Total permanent deformation (in)  
 $\varepsilon_p^i$  = Total plastic strain of layer i (in/in)  
 $h^i$  = Thickness of layer i (in)

In the previous equation, there are five calibration coefficients:  $\beta_{r1}$ ,  $\beta_{r2}$ , and  $\beta_{r3}$  for the asphalt concrete layer,  $\beta_{GB}$  for the granular base layer, and  $\beta_{SG}$  for the subgrade. These coefficients cannot be calibrated separately for each layer since individual rutting data of each pavement layer is not available. Therefore, only the total permanent deformation prediction can be calibrated. Measurement of rutting at each pavement layer would require cutting trenches in the pavement sections but it would make the local calibration process much easier and more accurate.

### *Calibration of the Permanent Deformation Model*

LTPP sections 2006 and 6033 are chosen randomly to be kept aside for validation while the nine remaining sections are used in the calibration process.

In the total rutting equation,  $\beta_{r2}$  and  $\beta_{r3}$  are respectively exponents to the AC temperature and the number of axle loads which are large numbers. Therefore,  $\beta_{r2}$  and  $\beta_{r3}$  are nonlinear calibration coefficients and the two most sensitive parameters of this model. The remaining calibration coefficients  $\beta_{r1}$ ,  $\beta_{GB}$ , and  $\beta_{SG}$  are linear calibration factors.

It is decided to optimize  $\beta_{r2}$  and  $\beta_{r3}$  in a first iterative run. This is done by varying and permuting the two nonlinear calibration coefficients while the other three,  $\beta_{r1}$ ,  $\beta_{GB}$ , and  $\beta_{SG}$  are set to the default value 1.0. The residual sum of squared errors which is the target to reduce is calculated for every set of  $\beta_{r2}$  and  $\beta_{r3}$  values.

Table 7.11 contains the sets of calibration coefficients considered in this first step and the corresponding sum of squared errors (SSE) and mean residual error (MRE) per section. As shown, the set of calibration coefficients  $\beta_{r2} = 0.9$  and  $\beta_{r3} = 1.2$  reduces the SSE from 0.9107 to 0.6724. Similarly the MRE per section is reduced from 0.1060 to 0.0911.

In a second iterative run, the calibration coefficients  $\beta_{r2}$  and  $\beta_{r3}$  are fixed to 0.9 and 1.2 respectively, while the values of  $\beta_{r1}$ ,  $\beta_{GB}$ , and  $\beta_{SG}$  are varied and permuted. Table 7.12 shows the SSE and the MRE per section for every set of coefficients. It is observed that the set  $\beta_{r1} = 1.0$ ,  $\beta_{r2} = 0.9$ ,  $\beta_{r3} = 1.2$ ,  $\beta_{GB} = 0.8$ , and  $\beta_{SG} = 0.8$  reduces the sum of squared errors to 0.6217 and the mean residual error per section to 0.0876.

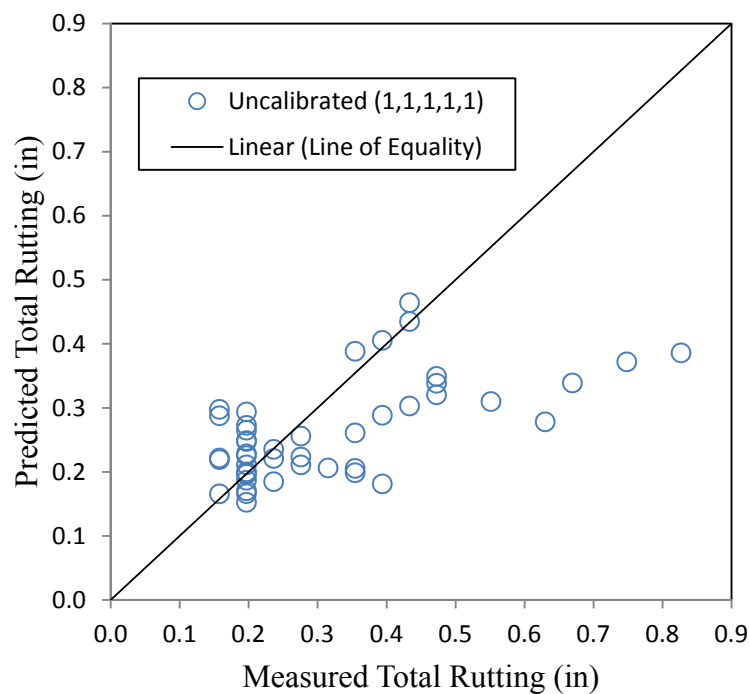
A total of 476 MEPDG runs were initially made but more were performed in order to refine the calibration coefficients and reduce the SSE even more.



Figure 7.2 plots measured total rutting versus predicted total rutting with default MEPDG settings. There is significant bias. Most of the data points fall on the right side of the line of equality suggesting that MEPDG tends to under-predict rutting.

**TABLE 7.11 SSE and MRE of the rutting model for different  $\beta_{r2}$  and  $\beta_{r3}$**

Set #	$\beta_{r2}$	$\beta_{r3}$	SSE	MRE
1	0.8	0.8	2.0613	0.1595
2	0.8	0.9	1.9586	0.1555
3	0.8	1	1.7671	0.1477
4	0.8	1.1	1.4305	0.1329
5	0.8	1.2	0.9309	0.1072
6	0.9	0.8	1.9448	0.1550
7	0.9	0.9	1.7495	0.1470
8	0.9	1	1.4121	0.1320
9	0.9	1.1	0.9248	0.1069
<b>10</b>	<b>0.9</b>	<b>1.2</b>	<b>0.6724</b>	<b>0.0911</b>
11	1	0.8	1.7237	0.1459
12	1	0.9	1.3834	0.1307
<b>13</b>	<b>1</b>	<b>1</b>	<b>0.9107</b>	<b>0.1060</b>
14	1	1.1	0.7289	0.0949
15	1	1.2	3.3398	0.2031
16	1.1	0.8	1.3433	0.1288
17	1.1	0.9	0.8906	0.4719
18	1.1	1	0.8148	0.1003
19	1.1	1.1	3.7853	0.2162
20	1.1	1.2	21.9508	0.5206
21	1.2	0.8	0.8685	0.1035
22	1.2	0.9	0.9518	0.1084
23	1.2	1	4.4849	0.2353
24	1.2	1.1	24.3645	0.5484
25	1.2	1.2	110.2678	1.1668



**FIGURE 7.2 Predicted Versus Measured Total Rutting Before Calibration**

**TABLE 7.12 SSE and MRE of the rutting model for different  $\beta_{r1}$ ,  $\beta_{GB}$ , and  $\beta_{SG}$**

Set #	$\beta_{r1}$	$\beta_{r2}$	$\beta_{r3}$	$\beta_{GB}$	$\beta_{SG}$	SSE	MRE
1	0.8	0.9	1.2	0.8	0.8	0.7150	0.0940
2	0.8	0.9	1.2	0.8	1	0.6510	0.0896
3	0.8	0.9	1.2	0.8	1.2	0.6335	0.0884
4	0.8	0.9	1.2	1	0.8	0.6944	0.0926
5	0.8	0.9	1.2	1	1	0.6500	0.0896
6	0.8	0.9	1.2	1	1.2	0.6524	0.0897
7	0.8	0.9	1.2	1.2	0.8	0.6823	0.0918
8	0.8	0.9	1.2	1.2	1	0.6596	0.0902
9	0.8	0.9	1.2	1.2	1.2	0.6818	0.0917
<b>10</b>	<b>1</b>	<b>0.9</b>	<b>1.2</b>	<b>0.8</b>	<b>0.8</b>	<b>0.6217</b>	<b>0.0876</b>
11	1	0.9	1.2	0.8	1	0.6391	0.0888
12	1	0.9	1.2	0.8	1.2	0.7033	0.0932
13	1	0.9	1.2	1	0.8	0.6352	0.0886
14	1	0.9	1.2	1	1	0.6724	0.0911
15	1	0.9	1.2	1	1.2	0.7564	0.0966
16	1	0.9	1.2	1.2	0.8	0.6592	0.0902
17	1	0.9	1.2	1.2	1	0.7163	0.4232
18	1	0.9	1.2	1.2	1.2	0.8202	0.1006
19	1.2	0.9	1.2	0.8	0.8	0.6899	0.0923
20	1.2	0.9	1.2	0.8	1	0.7890	0.0987
21	1.2	0.9	1.2	0.8	1.2	0.9350	0.1074
22	1.2	0.9	1.2	1	0.8	0.7376	0.0954
23	1.2	0.9	1.2	1	1	0.8566	0.1028
24	1.2	0.9	1.2	1	1.2	1.0225	0.1124
25	1.2	0.9	1.2	1.2	0.8	0.7961	0.0991
26	1.2	0.9	1.2	1.2	1	0.9348	0.1074
27	1.2	0.9	1.2	1.2	1.2	1.1203	0.1176

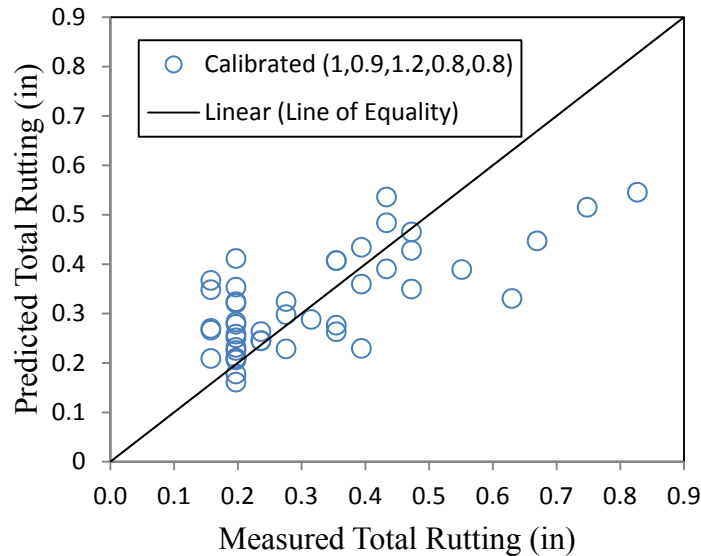


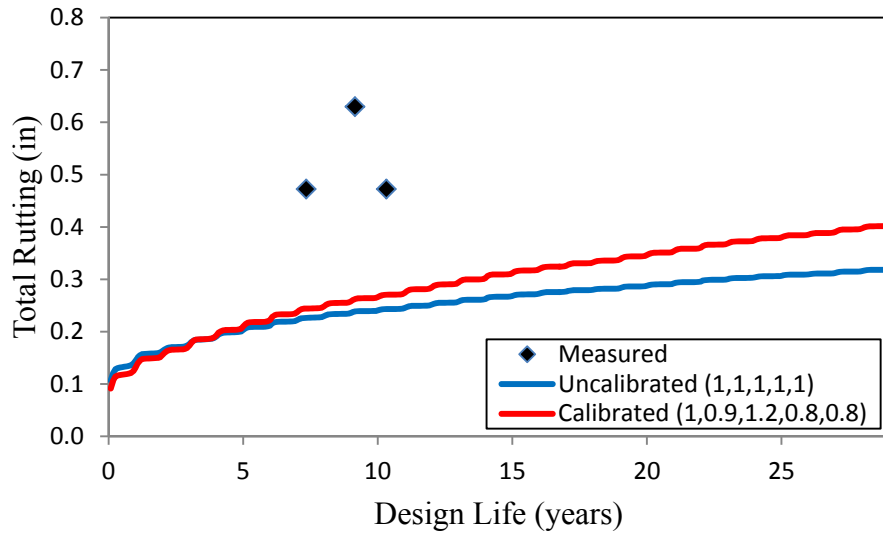
**FIGURE 7.3 Predicted Versus Measured Total Rutting After Calibration**

With calibration, bias is eliminated. Now the line of equality is around the middle of the scatter plot. This is evident from Figure 7.3 which plots the measured total rutting versus the corresponding prediction with calibrated MEPDG.

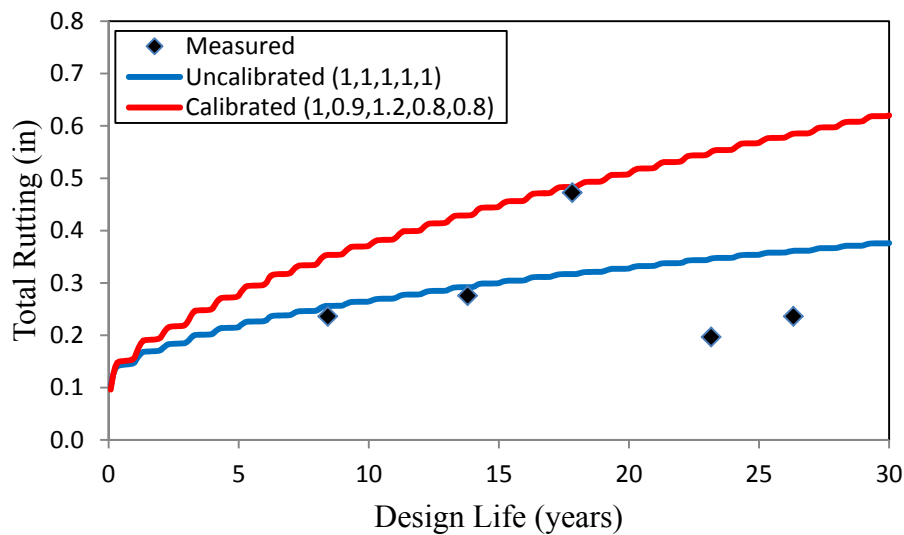
#### *Validation of the Permanent Deformation Model*

Validation of the calibrated permanent deformation model requires running the MEPDG for LTPP sections 2006 and 6033 using the new set of calibration coefficients. Then, the corresponding SSE and MRE are calculated to check whether the new model reduces the residual error for the validation sections as well.

Figures 7.4(a) and 7.4(b) compare the field measurements of total rutting and the un-calibrated and calibrated MEPDG predictions through the pavement design life of sections 2006 and 6033, respectively. The new model improves the MEPDG prediction for section 2006 but it does not for section 6033. The SSE of these two sections increases from 0.3291 to 0.5121. If the squared error of the validation sections is added to that of the calibration sections, the new model still reduces the SSE from 1.2398 to 1.1338. This validation is considered acceptable, but more sections are needed for a better calibration.



(a) LTPP Section 2006



(b) LTPP Section 6033

**FIGURE 7.4 Validation of the Calibrated Permanent Deformation Model**

### Alligator (Bottom-Up) Cracking Model

#### *Prediction of Alligator Cracking in the MEPDG*

The approach used in the MEPDG to model fatigue cracking is based on the calculation of fatigue damage at the surface for top-down (longitudinal) cracking and at the bottom of the asphaltic layer for bottom-up (alligator) cracking (*MEPDG Documentation, 2004*).

The fatigue damage is estimated using the following relationship known as Miner's Law:

$$D = \sum_{i=1}^T \frac{n_i}{N_i}$$

where  
D = Fatigue damage  
T = Total number of periods  
n<sub>i</sub> = Actual number of axle load repetitions applied during period i  
N<sub>i</sub> = Number of load repetitions to fatigue cracking

The following mathematical relationship is used for predicting the number of load repetitions to fatigue cracking:

$$N_f = 0.00432 C \beta_{f1} k_1 \left( \frac{1}{\varepsilon_t} \right)^{k_2 \beta_{f2}} \left( \frac{1}{E} \right)^{k_3 \beta_{f3}}$$

$$C = 10^M$$

$$M = 4.84 \left( \frac{V_b}{V_a + V_b} - 0.69 \right)$$

where  
N<sub>f</sub> = Number of load repetitions to fatigue cracking  
ε<sub>t</sub> = Tensile strain at the critical location (in/in)  
E = Stiffness modulus of the asphalt concrete (psi)  
k<sub>1</sub> = 0.007566, k<sub>2</sub> = 3.9492, k<sub>3</sub> = 1.281  
V<sub>b</sub> = Effective binder content (%)  
V<sub>a</sub> = Percent of air voids (%)  
β<sub>f1</sub>, β<sub>f2</sub>, β<sub>f3</sub> = Calibration coefficients to be optimized

The critical location may be at the surface for top-down cracking or at the bottom of the asphalt concrete layer for bottom-up cracking. The final transfer function provides bottom-up fatigue cracking from the fatigue damage and is expressed as:

$$FC_{bottom} = \frac{1}{60} \left( \frac{C_3}{1 + e^{C_1 C'_{11} + C_2 C'_{22} \log_{10}(100 D)}} \right)$$

$$C'_{22} = -2.40874 - 39.748 (1 + h_{AC})^{-2.856}$$

$$C'_{11} = -2 C'_{22}$$

where  
FC<sub>bottom</sub> = Bottom-up fatigue cracking (% of the lane area)  
D = Bottom-up fatigue damage  
h<sub>AC</sub> = Thickness of the asphalt concrete layer  
C<sub>1</sub>, C<sub>2</sub>, C<sub>3</sub> = Calibration coefficients to be optimized

### *Calibration of the Alligator Cracking Model*

Sections 1002 and 1022 are randomly chosen for validation. The remaining nine sections are used in the calibration process.

The coefficients β<sub>f1</sub>, β<sub>f2</sub>, and β<sub>f3</sub> of the fatigue damage prediction equation cannot be calibrated because there is no available data to compare with. Calibration of these factors would require performing lab testing on the asphalt concrete mixtures used in the sections to determine the

number of load repetitions necessary to initiate fatigue cracking. Therefore, the calibration coefficients  $\beta_{f1}$ ,  $\beta_{f2}$ , and  $\beta_{f3}$  are set to default value 1.0.

In the bottom-up cracking transfer function, the calibration coefficients  $C_1$  and  $C_2$  are varied and permuted in order to find a combination of values that will reduce the SSE. The coefficient  $C_3$  is fixed at the default value 6000. Table 7.13 shows the sum of squared errors and the mean residual error per section for several sets of calibration coefficients. It is found that  $C_1 = 0.625$  and  $C_2 = 0.25$  reduces the SSE from 1383.58 to 1227.87 and the MRE per section from 4.13 to 3.89.

The calibration is refined by varying the three coefficients and performing more MEPDG runs. The combination of coefficients  $C_1 = 0.73$ ,  $C_2 = 0.09$ , and  $C_3 = 7200$  further reduces the SSE to 1133.13 and the MRE to 3.74.

The graph predicted versus measured alligator cracking before calibration is plotted in Figure 7.5. It is observed that the alligator cracking predicted by MEPDG with default settings is almost zero. The measurements vary from zero to some high values. It seems that MEPDG tends to under-predict alligator cracking as well.

**TABLE 7.13 SSE and MRE of the alligator cracking model for different C1 and C2**

Set #	$C_1$	$C_2$	$C_3$	SSE	MRE
1	0.25	0.25	6000	8355.94	10.16
2	0.25	0.625	6000	7447.21	9.59
3	0.25	1	6000	8579.38	10.29
4	0.25	1.5	6000	11181.53	11.75
5	0.25	2	6000	14527.67	13.39
6	0.625	0.25	6000	1227.87	3.89
7	0.625	0.625	6000	1400.68	4.16
8	0.625	1	6000	1547.42	4.37
9	0.625	1.5	6000	1833.23	4.76
10	0.625	2	6000	2383.02	5.42
11	1	0.25	6000	1335.85	4.06
12	1	0.625	6000	1370.69	4.11
13	1	1	6000	1383.58	4.13
14	1	1.5	6000	1395.21	4.15
15	1	2	6000	1414.60	4.18
16	1.5	0.25	6000	1401.18	4.16
17	1.5	0.625	6000	1403.89	4.16
18	1.5	1	6000	1405.28	4.17
19	1.5	1.5	6000	1405.64	4.17
20	1.5	2	6000	1405.69	4.17
21	2	0.25	6000	1407.68	4.17
22	2	0.625	6000	1407.68	4.17
23	2	1	6000	1407.68	4.17
24	2	1.5	6000	1407.68	4.17
25	2	2	6000	1407.68	4.17

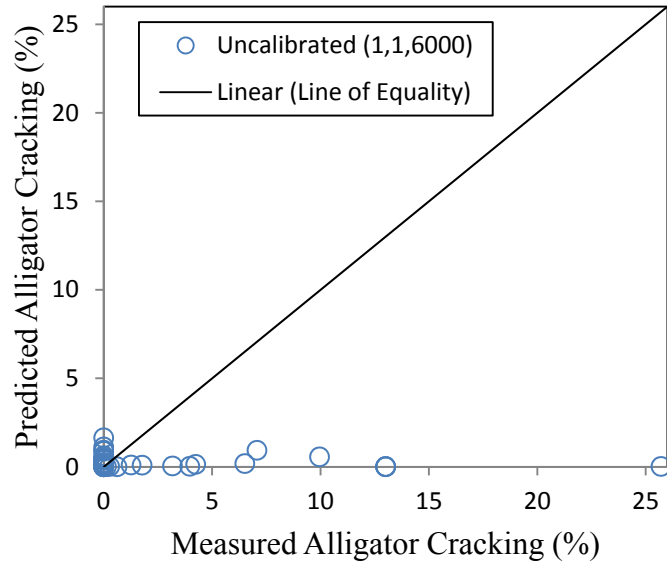


**FIGURE 7.5 Predicted Versus Measured Alligator Cracking Before Calibration**

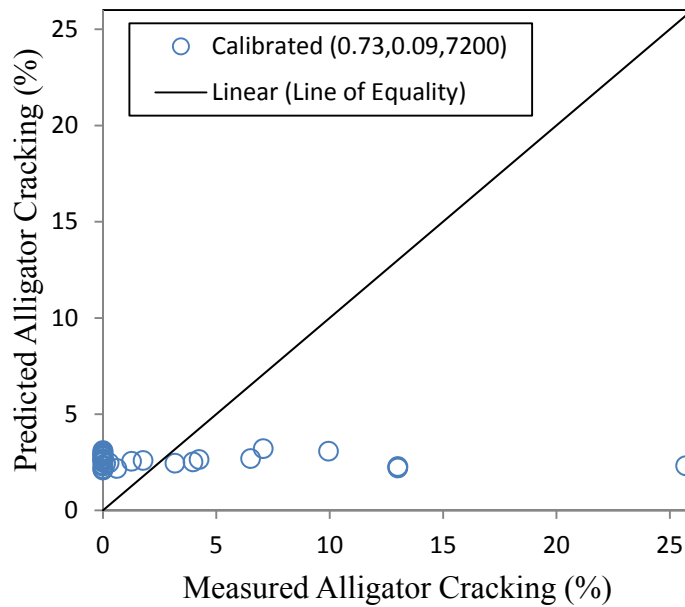
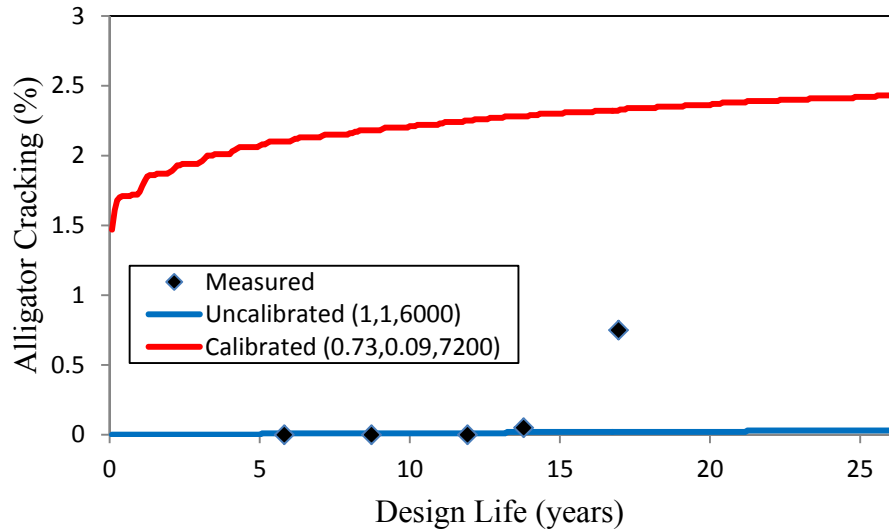


**FIGURE 7.6 Predicted Versus Measured Alligator Cracking After Calibration**

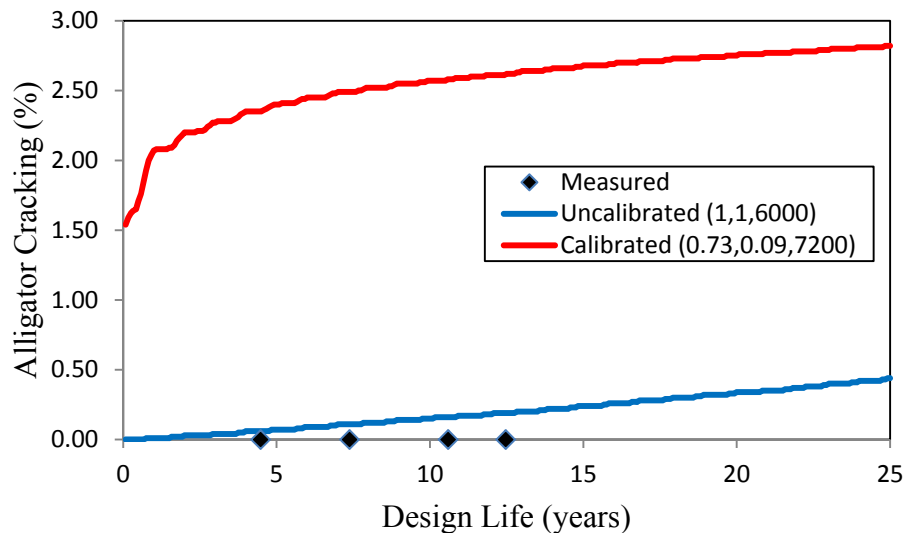
Figure 7.6 compares predicted versus measured alligator cracking after performing calibration. It is shown that the calibration process brings many data points closer to the line of equality. Prediction can still be improved with additional MEPDG runs.

### *Validation of the Alligator Cracking Model*

In the validation process, sections 1002 and 1022 are run in the MEPDG with the calibrated alligator cracking model. Figures 7.7(a) and 7.7(b) compare the uncalibrated and calibrated MEPDG predictions with the measurements taken in the field during the design life of sections 1002 and 1022, respectively. Default MEPDG does not predict any alligator cracking at all for section 1002, in consequence the new calibration coefficients improve the prediction of future distress.



**(a) LTPP Section 1002**



**(b) LTPP Section 1022**

**FIGURE 7.7 Validation of the Calibrated Alligator Cracking Model**



In the case of section 1022, it seems that the default MEPDG prediction is more accurate but probably the new model will match better the distress measured in the future. The SSE of these two sections increases from 0.61 to 46.92 with the new model. But considering the eleven sections, the new calibration coefficients reduce the SSE from 1384.19 to 1180.05.

### **Longitudinal (Top-Down) Cracking Model**

#### *Prediction of Longitudinal Cracking in the MEPDG*

The approach used in the MEPDG to predict longitudinal cracking is based on the estimation of the fatigue damage that was described previously in detail (*MEPDG Documentation, 2004*). The next transfer function calculates the longitudinal fatigue cracking:

$$FC_{top} = 10.56 \left( \frac{C_3}{1 + e^{C_1 - C_2 \log_{10}(100 D)}} \right)$$

where  $FC_{top}$  = Top-down fatigue cracking (ft/mile)

$D$  = Top-down fatigue damage

$C_1, C_2, C_3$  = Calibration coefficients to be optimized

#### *Calibration of the Longitudinal Cracking Model*

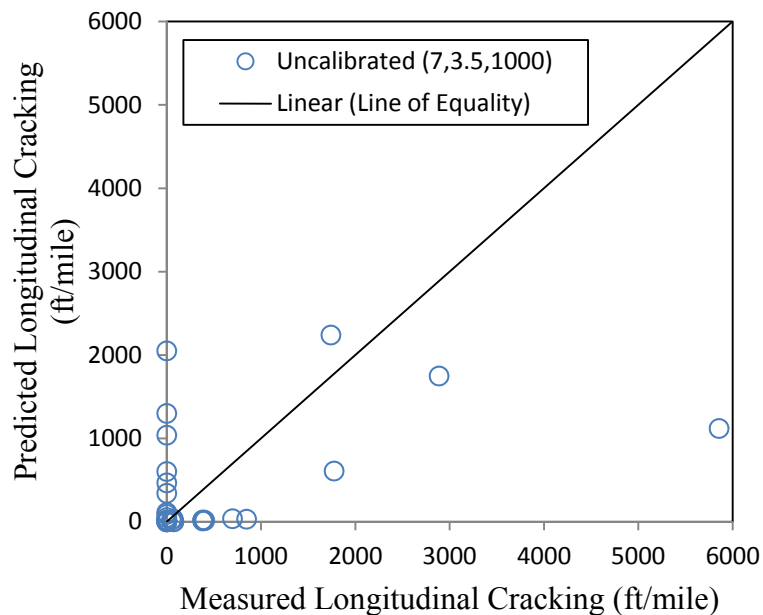
Sections 1003 and 6035 are reserved for validation. In the calibration of the longitudinal cracking model, the numerator of the corresponding transfer function ( $C_3$ ) is kept constant at the default value 1000. The calibration coefficients  $C_1$  and  $C_2$  are varied and the MEPDG is run for different combinations of these parameters.

Table 7.14 shows the SSE and the MRE per section for different values of the  $C_1$  and  $C_2$  coefficients. The calibration coefficients  $C_1 = 5$  and  $C_2 = 2.25$  reduce the SSE from 34,814,457.96 to 33,612,603.89 and the MRE from 655.60 to 644.18. The improvement is not significant, and therefore, more MEPDG runs are performed varying the three coefficients. Finally, the set  $C_1 = 5.5$ ,  $C_2 = 2.56$ , and  $C_3 = 1000$  reduces the SSE to 26,601,745.13 and the MRE to 573.08.

Figures 7.8 and 7.9 illustrate the predicted versus measured longitudinal cracking values before and after calibration, respectively. Even though the top-down cracking data is too scattered, calibration still brings some data points closer to the line of equality, and thus, bias is reduced.

**TABLE 7.14 SSE and MRE of the longitudinal cracking model for different C1 and C2**

Set #	C <sub>1</sub>	C <sub>2</sub>	C <sub>3</sub>	SSE	MRE
1	1	0.3	1000	277,227,886.44	1850.02
2	1	1	1000	491,663,106.44	2463.72
3	1	2.25	1000	1,003,746,096.80	3520.22
4	1	3.5	1000	1,319,859,564.48	4036.65
5	1	5	1000	1,548,756,568.03	4372.69
6	3	0.3	1000	40,133,542.18	703.90
7	3	1	1000	40,118,158.96	703.77
8	3	2.25	1000	222,374,099.13	1656.91
9	3	3.5	1000	640,972,187.17	2813.05
10	3	5	1000	953,108,144.95	3430.27
11	5	0.3	1000	47,770,755.93	767.96
12	5	1	1000	43,879,446.01	736.02
<b>13</b>	<b>5</b>	<b>2.25</b>	<b>1000</b>	<b>33,612,603.89</b>	<b>644.18</b>
14	5	3.5	1000	164,075,443.56	1423.24
15	5	5	1000	585,830,659.05	2689.33
16	7	0.3	1000	50,320,260.83	788.19
17	7	1	1000	49,690,503.44	783.24
18	7	2.25	1000	45,177,197.42	746.82
<b>19</b>	<b>7</b>	<b>3.5</b>	<b>1000</b>	<b>34,814,457.96</b>	<b>655.60</b>
20	7	5	1000	189,775,193.08	1530.65
21	10	0.3	1000	50,734,102.16	791.42
22	10	1	1000	50,702,029.07	791.17
23	10	2.25	1000	50,445,318.17	789.17
24	10	3.5	1000	48,883,159.46	776.85
25	10	5	1000	39,310,112.68	696.64



**FIGURE 7.8 Predicted Versus Measured Longitudinal Cracking Before Calibration**

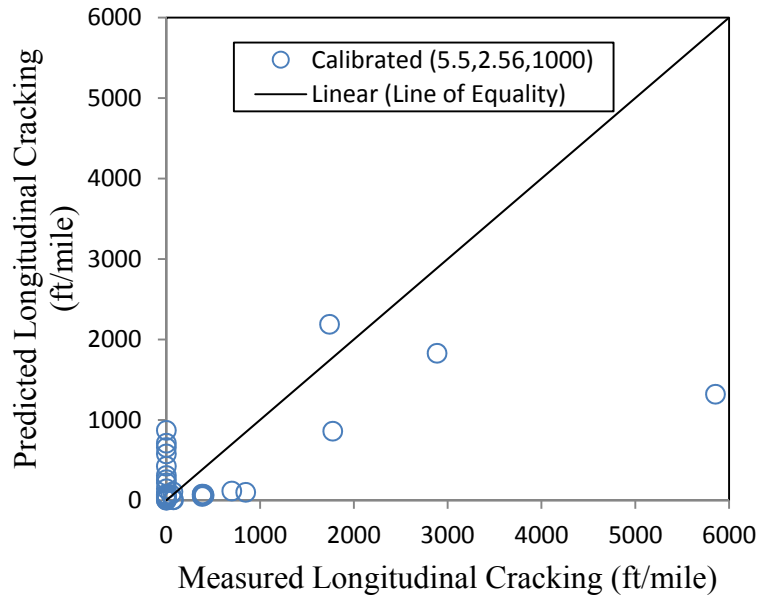
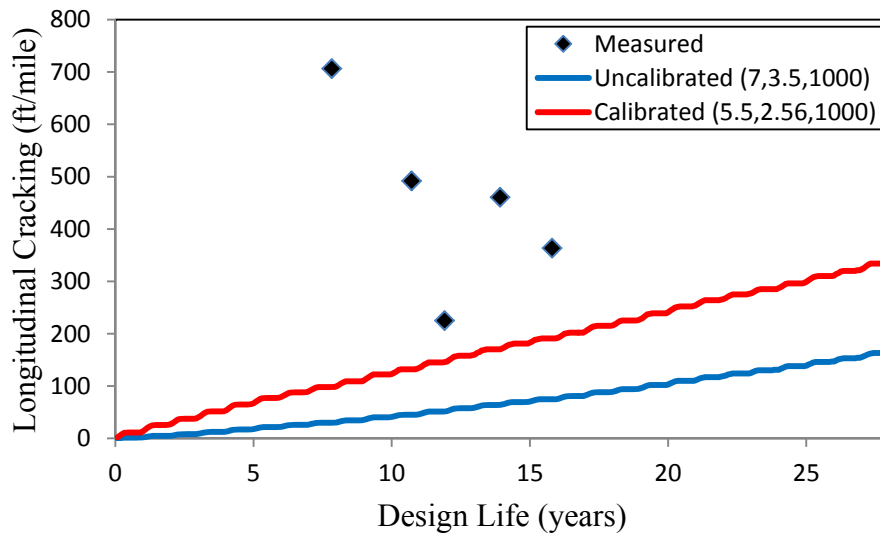


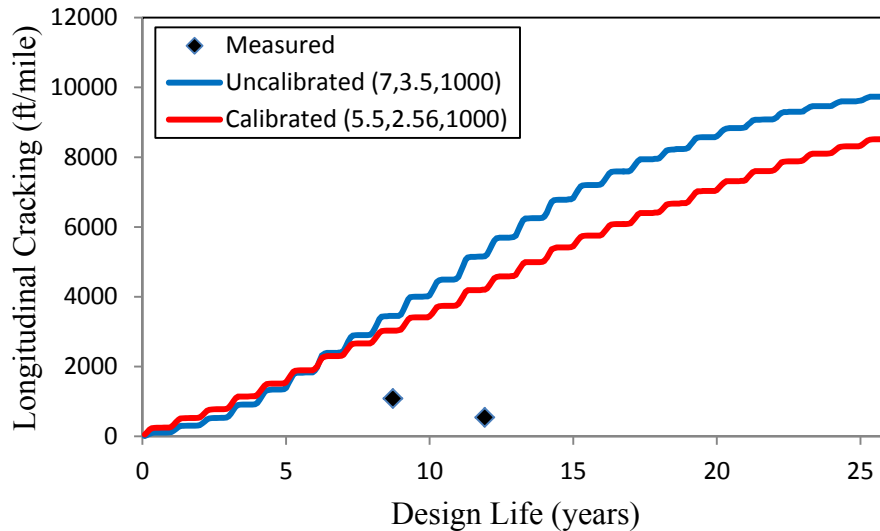
**FIGURE 7.9 Predicted Versus Measured Longitudinal Cracking After Calibration**

*Validation of the Longitudinal Cracking Model*

Sections 1003 and 6035 are run with the calibrated longitudinal cracking model for validation. Figures 7.10(a) and 7.10(b) compare the uncalibrated and calibrated MEPDG predictions with the values measured in the field for sections 1003 and 6035, respectively. The new calibration factors improve the longitudinal cracking prediction of both sections. The SSE is reduced from 27,816,784.48 to 17,759,263.90 for the validation sections and from 62,631,242.44 to 44,361,009.03 for the eleven LTPP sections. This validation is considered successful.



**a) LTPP section 1003**



**b) LTPP section 6035**

**FIGURE 7.10 Validation of the calibrated longitudinal cracking model**

#### Remarks

- Initial verification runs suggest that there is significant bias in the permanent deformation prediction of default MEPDG. Only total rutting can be calibrated since there is no rut depth data for individual layers. Local calibration of the rutting calibration coefficients  $\beta_{r1}$ ,  $\beta_{r2}$ ,  $\beta_{r3}$ ,  $\beta_{GB}$ , and  $\beta_{SG}$  is successfully achieved. The standard error of the estimate is low and bias is eliminated.
- The plot showing measured versus predicted alligator cracking before calibration indicates that the default MEPDG prediction does not match the observed values particularly well. Many field measurements have a value of zero which makes the local calibration process of this particular distress more difficult. Nonetheless, the alligator cracking calibration coefficients  $C_1$ ,  $C_2$ , and  $C_3$  are optimized such that the sum of squared errors is reduced and thus many data points are brought closer to the line of equality.
- The longitudinal cracking model is even more challenging because many data points fall very close to the origin (the values are almost zero). Calibration of the longitudinal cracking coefficients  $C_1$ ,  $C_2$ , and  $C_3$  does not produce as good results as those obtained for rutting and alligator cracking. However, the positive effect of calibration is noticed with some points moving closer to the line of equality and the sum of squared errors being reduced.

## Chapter 8

### SENSITIVITY STUDY BY PARAMETRIC TECHNIQUES

#### INTRODUCTION

The MEPDG includes a large number of input variables of different categories such as traffic, material, and climate. As a result, it becomes challenging for a pavement designer to use MEPDG for generating alternative pavement design scenarios. If the most important inputs can be identified from the large pool of MEPDG inputs, it is possible for the pavement designers to come up with few design scenarios using only the most important inputs. MEPDG generates six outputs that represent pavement distresses such as rutting, cracking and roughness. Literally a designer can work with a set of inputs to reduce one or few distresses among those six outputs. If a set of input variables contributing to a certain distress can be identified, then it becomes very useful for the pavement designers to deal with that particular distress. In this study, sensitivity is examined through the identification of a set of inputs potentially responsible for rutting, cracking and International Roughness Index (IRI).

Several researches have performed MEPDG sensitivity analysis to understand the impacts and relationships of the hundreds of input variables contained in the MEPDG (NCHRP 2004a, NCHRP 2004b, and NCHRP 2004c, Masad and Little 2004, Coree 2005, Li et al. 2007, Swan et al. 2008, Rabab'ah and Liang 2008, Chehab 2008, Daniel and Chehab 2008, Li et al. 2009a, 2009b, Ahn et. al 2009, Aguiar-Moya et al. 2009). Most of the sensitivity analysis performed so far by changing one factor at a time (OAT or Morris method) and showed how output changes due to that input. None of the previous studies included a large number of inputs for sensitivity analysis nor did they employ Latin Hypercube Sampling (LHS) sampling with advanced statistical method rather than OAT analysis.

The fact is, MEPDG includes more than 100 input variables, which makes traditional Monte-Carlo based sensitivity analysis impractical to use. Alternatively, parametric procedures such as tests for non-randomness in scatter plots, linear and nonlinear regression analyses can be used for MEPDG sensitivity analysis, which is presented in this chapter. In particular, LHS combined with advanced statistical approach based on scatter plot tests and parametric regressions are employed to study a large number of MEPDG inputs and ranking based on their contributions to outputs. Employing a four-layer pavement geometry consisting of two asphalt concrete (AC) layers, a base layer and a subgrade layer, thirty inputs are used to generate 750 pavement scenarios using LHS. Simulations are run using MEPDG software to produce time series of pavement distresses such as roughness, rutting, and cracking. Based on the results of statistical tests, the effect of MEPDG inputs on the distress values are evaluated.

## OBJECTIVES

The objective of this study is to identify a set of inputs that are highly sensitive to MEPDG outputs. Specific objectives are to:

- Identify the range of inputs based on the New Mexico LTPP pavement sections and NMDOT materials, traffic and climate data representing the local practice of NMDOT.
- Identify a set of MEPDG inputs that are significant to a particular distress using parametric regression techniques.
- Ranking significant MEPDG inputs using Rank regression.

## DEFINING INPUTS-OUTPUTS

### Inputs

Based on previous studies, a total of 30 inputs listed in Table 8.1 are considered. Their ranges are calculated based on New Mexico pavement data from LTPP database and MEPDG database. LTPP data includes 39 LTPP sections of which 12 GPS and 27 SPS test sections in New Mexico (FHWA 2004). The MEPDG database has 23 complete datasets and many incomplete datasets in regards to MEPDG requirements.

**TABLE 8.1 Inputs for Sensitivity Analysis**

No	Type	Input Name	Variabl e	Range of Inputs	Numeric Values Assigned	Variable Type	Data Source
1	TRAFFIC	Initial two-way AADTT	X <sub>1</sub>	300 to 6000		Integer	LTPP
2		Number of Lanes in Design Direction	X <sub>2</sub>	1 to 3		Integer	LTPP
3		Percent of Trucks in Design Direction (%)	X <sub>3</sub>	40 to 60		Non Integer	Design Guide
4		Percent of Trucks in Design Lane (%)	X <sub>4</sub>	6 to 94		Non Integer	Huang, 2004
5		Operational Speed (mph)	X <sub>5</sub>	35 to 75		Non Integer	NMDOT
6		AADTT Distribution by Vehicle Class 9 (%)	X <sub>6</sub>	2 to 85		Non Integer	LTPP
7		AADTT Distribution by Vehicle Class 11 (%)	X <sub>7</sub>	0.1 to 7		Non Integer	LTPP
8		Traffic Growth Factor	X <sub>8</sub>	3 to 9		Non Integer	LTPP
9		Design Lane Width (ft)	X <sub>9</sub>	10 to 12		Non Integer	LTPP
10		Tire Pressure (psi)	X <sub>10</sub>	90 to 150		Non Integer	Design Guide
11	CLIMATE	Depth of Water Table (ft)	X <sub>11</sub>	5 to 20		Non Integer	NMDOT
12		Climatic Zones	X <sub>12</sub>	1 to 5	1=SouthEast	Discrete	Design Guide
					2=SouthWest		
					3=NorthWest		
					4=NorthEast		
					5=Central		

**TABLE 8.1 Inputs for Sensitivity Analysis (cont.)**

No	Type	Input Name	Variable	Range of Inputs	Numeric Values Assigned	Variable Type	Data Source
13	STRUCTURE	Layer Thickness (in)	X <sub>13</sub>	1.5 to 3		Non Integer	NMDOT
14		Aggregate Gradation	X <sub>14</sub>	1 to 2	1=SP-III 2=SP-IV	Discrete	NMDOT
15		Effective Binder Content (%)	X <sub>15</sub>	9 to 12		Non Integer	NMDOT
16		Superpave Binder Grade	X <sub>16</sub>	1 to 3	1=PG 64-22 2=PG 70-28 3=PG 76-28	Discrete	NMDOT
17		Air Voids (%)	X <sub>17</sub>	4 to 7		Non Integer	LTPP
18		Layer Thickness (in)	X <sub>18</sub>	2 to 8		Non Integer	NMDOT
19		Aggregate Gradation	X <sub>19</sub>	1 to 3	1=SP-II 2=SP-III 3=SP-IV	Discrete	NMDOT
20		Effective Binder Content (%)	X <sub>20</sub>	9 to 12		Non Integer	NMDOT
21		Superpave Binder Grade	X <sub>21</sub>	1 to 3	1=PG 64-22 2=PG 70-28 3=PG 76-28	Discrete	NMDOT
22		Air Voids (%)	X <sub>22</sub>	4 to 7		Non Integer	LTPP
23		Layer Thickness (in)	X <sub>23</sub>	6 to 10			NMDOT
24		Material Type	X <sub>24</sub>	1 to 5	1=Crushed Gravel 2=A-1-b 3=A-2-6 4=A-3 5=A-2-4	Discrete	LTPP
25		Modulus (psi)	X <sub>25</sub>	20,000 to 40,000		Non integer	NMDOT
26		Material Type	X <sub>26</sub>	1 to 5	1=CL 2=CL-ML 3=ML 4=SM 5=SP	Discrete	LTPP
27		Modulus (psi)	X <sub>27</sub>	5000 to 20,000		Non integer	LTPP
28	Subgrade	Plastic Limit (PL)	X <sub>28</sub>	10 to 24		Non integer	NMDOT
29		Liquid Limit (LL)	X <sub>29</sub>	25 to 90		Non integer	NMDOT
30		Optimum Gravimetric Water Content (%)	X <sub>30</sub>	12 to 60		Non integer	NMDOT

To perform MEPDG design simulations, the flexible pavement structure considered for this study consists of four layers shown in Figure 8.1. The top layer is a thin Asphalt Concrete (AC) layer with thickness varies from 1.5 to 3 inch. The second layer is a thick AC layer with thickness varies from 2 to 8 inches. Rests of the layers are base (6 to 10 inch) and subgrade.

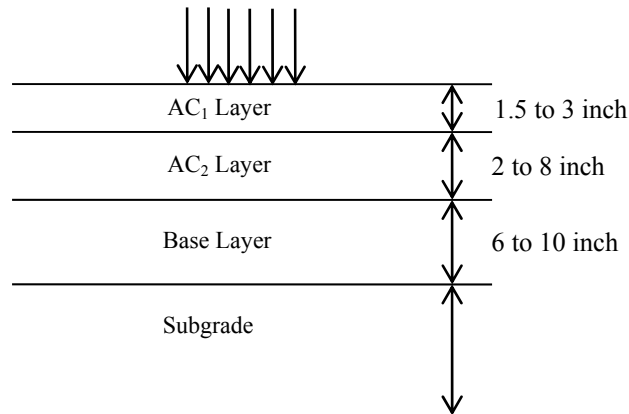


**FIGURE 8.1 Pavement Structure Information for the Analysis**

The collected data are organized into three input category: traffic inputs, climate inputs and structural inputs. Among traffic inputs, average daily truck traffic (ADTT), number of lanes, percent of trucks and vehicle class distribution are obtained from LTPP database. Operational Speed data is obtained from NMDOT database for all the routes located in NM. Rests of the categories are kept as default values of MEPDG. Pavement design files obtained from NMDOT contain structural information, i.e., layer thickness, HMA mix type, gradation of subgrade materials and used in this study. There are total 13 weather stations in New Mexico included in the Integrated Climatic Model (ICM) of MEPDG. To get the proper impact of climate in sensitivity analysis, NM is divided in five zones according to the locations to create 5 virtual weather stations. They are zone 1 to zone 5. Details of these zones are presented in Figure 8.2. To achieve the real climatic behavior, some weather stations also taken from New Mexico border. These stations are also shown in Figure 8.2. These stations are located in Colorado, Arizona and Texas. Ground Water Table (GWT) depth values were obtained from NMDOT and LTPP database. First 10 inputs ( $X_1$  to  $X_{10}$ ) are related to traffic. Inputs  $X_{11}$  and  $X_{12}$  represent climatic inputs. Rest of the inputs is related to structural properties.

### Latin Hypercube Sampling (LHS)

LHS is employed to generate 750 input scenarios using the above 30 inputs. A snapshot of LHS sampled test matrix is shown in Table 8.2. The highlighted part presents only a segment of the test matrix. Each column contains one specific input variable, which are denoted by  $X_1$ ,  $X_2$ ,  $X_3$ , ..... $X_{30}$ . Each row represents one data set, generated by LHS method. The spread of LHS data are plotted in sample spaces as shown in Figure 8.3. It can be seen that AADTT varies from 300 to 6000. Unlike random sampling, LHS method ensures a more uniform coverage of the range of input space. In fact, LHS method produces equal probability of data in sample space and is very useful for sensitivity study. Figure 8.3(b) shows the distribution of climatic zone input, which is discrete type. From Figure 8.3(b), five climatic zones of New Mexico can be seen to produce five axis-aligned hyper planes.



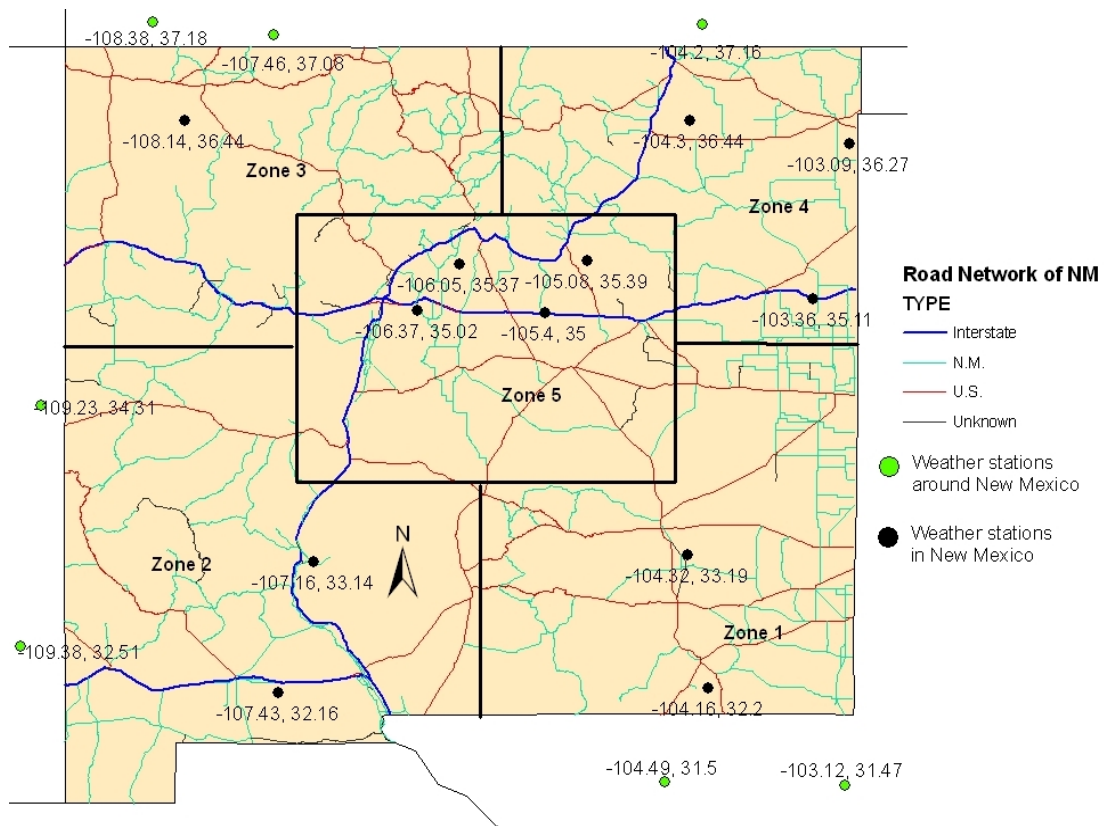
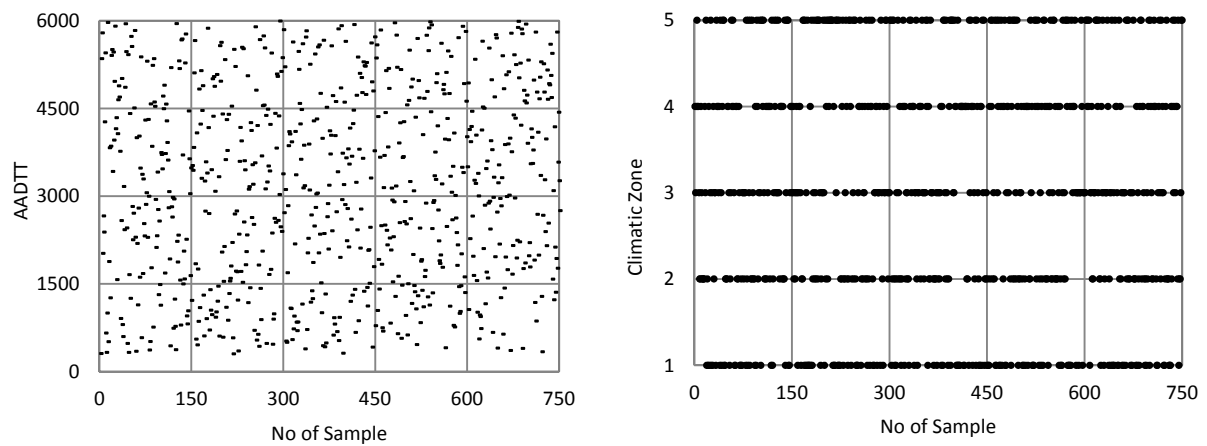


**FIGURE 8.2 Climatic Zones in New Mexico**



(a) AADTT (Variable Type: Integer)

(b) Climatic Zones (Variable Type: Discrete)

**FIGURE 8.3 Latin Hypercube Sampling of Inputs**

**TABLE 8.2 A Snapshot of LHS Sampling of Traffic Inputs**

Input	Initial two-way AADTT	Number of Lanes in Design Direction	Percent of Trucks in Design Direction (%)	Percent of Trucks in Design Lane (%)	Operational Speed (mph)	AADTT Distribution by Vehicle Class 9 (%)	AADTT Distribution by Vehicle Class 11 (%)	Traffic Growth Factor	Design Lane Width (ft)	Tire Pressure (psi)
Variable	X <sub>1</sub>	X <sub>2</sub>	X <sub>3</sub>	X <sub>4</sub>	X <sub>5</sub>	X <sub>6</sub>	X <sub>7</sub>	X <sub>8</sub>	X <sub>9</sub>	X <sub>10</sub>
Lower Limit	300	1	40	6	35	2	0.1	3	10	90
Upper Limit	6000	3	60	94	75	85	7	9	12	150
1	312	3	43.43	58.62	70.31	50.93	3.483	3.491	11.34	106.6
2	5354	1	55.4	75.22	59.56	73.87	4.504	6.295	11.67	128
3	5796	1	46.43	86.31	63.03	75.88	5.041	5.68	11.45	119.3
4	2025	2	59.86	88.66	58.05	58.33	6.813	8.913	10.19	128.5
5	2665	2	48.34	51.8	42.25	80.7	4.653	4.216	10.36	124.2
6	2389	1	42.33	39.6	50.92	74.42	3.819	7.786	10.77	92.6
7	4273	2	50.61	10.46	55.79	22.72	1.652	8.276	11.97	104.1
8	5454	1	53.11	25.71	55.42	57.57	0.99	7.805	10.68	130
9	662	2	52.59	25.22	44.13	52.64	4.967	7.941	11.47	125.6
10	330	1	56.25	30.48	65.15	39.52	6.115	4.263	10.24	146.5
11	1003	1	55.66	21.41	43.1	50.42	0.231	4.489	10.24	98.47
12	5974	1	41.13	46.24	51.5	53.37	0.168	3.148	10.76	101.5
13	512	1	44.24	57.72	49.34	42.47	2.733	5.091	10.52	133.3
14	1885	2	40.15	23.66	73.26	62.83	3.944	5.504	11.92	118.2
15	3830	3	45.34	11.96	44.33	17.34	3.064	5.272	10.66	133.1
16	1264	2	51.9	66.84	68.98	10.95	5.377	5.307	11.10	136.2
17	3857	3	45.89	13.54	60.19	46.3	0.8	7.665	10.25	132.9
18	5408	1	47.17	7.218	41.64	38.11	5.434	4.194	10.32	112.5
19	5510	3	59.52	23.15	36.99	61.78	0.471	6.405	10.13	149.3
20	3426	1	51.31	63.53	63.36	40.78	5.829	7.071	10.88	142

## MEPDG Outputs

Using 750 input scenarios, simulations are run using MEPDG software to predict six distresses namely IRI, AC rut, total rut, longitudinal cracking, transverse cracking and alligator cracking. These output variables are identified as Y<sub>1</sub> to Y<sub>6</sub> and shown in Table 8.3. After required number of MEPDG simulation, results for the output variables (Y<sub>1</sub> to Y<sub>6</sub>) are summarized and full factorial output matrix is developed (750x36). This matrix is used in the next steps for advanced statistical analysis to determine sensitivity.

TABLE 8.3 Outputs (predicted) for Sensitivity Analysis

Serial No	Output (Predicted)	Variable
1	Terminal IRI (inch/mile)	$Y_1$
2	Longitudinal Cracking (ft/mile)	$Y_2$
3	Alligator Cracking (%)	$Y_3$
4	Transverse Cracking (ft/mile)	$Y_4$
5	AC Rutting (in)	$Y_5$
6	Total Rutting (in)	$Y_6$

## PARAMETRIC STATISTICAL TECHNIQUES

In this study, seven parametric statistical techniques are used to perform sensitivity analysis, that is, to identify the significant inputs. These seven techniques fall into two categories: one based on gridding and the other based on grid free tests. Each method has underlying assumptions and drawbacks. These methods are implemented by writing subroutines in the R statistical computing environment (R 2010). The reason for using seven approaches is to examine whether the outcome of the study is consistent rather than method dependent.

### Tests Based On Gridding

Assuming  $Y$  is a dependent variable and function of input variable  $X_j$ , where  $j$  varies from 1 to 30. Analyses based on correlation (Partial Correlation Coefficient, Standardized Regression Coefficient) can fail when the underlying relationships between the  $X_j$  and  $Y$  are nonlinear and nonmonotonic. On the contrary, grids can be placed on the scatter plot of  $Y$  and  $X_j$  and then various statistical tests can be performed to examine if the distribution of points across the grid cells appears to be nonrandom (Helton 2006). Appearance of a nonrandom pattern indicates that  $X_j$  has effects on  $Y$ . In this study, three methods based on gridding are employed to determine nonrandom distribution of points across grid cells. They are common means (CMNs), common locations (CLs) and statistical independence (SI).

### Common Means (CMN)

The CMNs test is based on dividing the values of  $X_j$  ( $j=1, 2, \dots, n$ ) into  $n$  classes and then testing to determine if  $Y$  has a CMN across these classes (Helton et al. 2006; Scheffe, H. 1959). The required classes are obtained by dividing the range of  $X_j$  into a sequence of mutually exclusive and exhaustive subintervals containing equal numbers of sampled values. If  $X_j$  is discrete, individual classes are defined for each of the distinct values. Then an analysis of variance (ANOVA) is performed to determine if  $Y$  has a different mean across these classes. The F-test is used to test for the equality of the mean values of  $Y$  for the classes into which the values of  $X_j$  have been divided.

$$F^* = \frac{\frac{[\sum_{c=1}^M (\bar{y}_c - \bar{y})^2]}{(M-1)}}{\frac{[\sum_{c=1}^M \sum_{i \in X_c} (y_i - \bar{y}_c)^2]}{(n-M)}} \quad (1)$$

where

$X_{ij}$  = observed values of  $X_j$  and  $Y$  and  $i=1, 2, \dots, n$ ;

$c = 1, 2, \dots, M$  number of individual classes into which the values of  $X_j$  have been divided,

$X_c$  = the set of  $X_j$  values such that  $i \in X_c$  ( $X_{ij}$  belongs to class  $c$ );

$M_c$  = number of elements contained in  $X_c$ .

Typical ANOVA assumptions are assuming  $Y_i$  are independent and  $Y_i = N(\mu_c, \sigma^2)$  for  $i \in X_c$ , which are likely violated in our case. However, the ANOVA procedure is known to be fairly robust to departures from these assumptions. The ANOVA procedure is a test of the hypothesis

$$H_0: \mu_1 = \mu_2 = \dots = \mu_M \quad (2)$$

versus the alternative that  $H_0$  is not true. If  $H_0$  is assumed to be true, then Eqn. 1 will follow an F-distribution with  $(M - 1, n - M)$  degrees of freedom, where  $Y = \sum_{i=1}^n \frac{Y_i}{n}$

and  $\bar{Y}_c = \sum_{i \in X_c} \frac{Y_i}{m_c}$ .

The p-value for the test of the null hypothesis  $H_0$  is given by

$$p = P[F_{M-1, n-M} > F^*] \quad (3)$$

A small p-value suggests that at least one of the  $\mu_c$  is not equal to the rest. Hence, the observed pattern involving  $X_j$  and  $Y$  did not arise by chance and  $X_j$  has an effect on the behavior of  $Y$ . A level of significance  $\alpha$  is specified a-priori (e.g.,  $\alpha = .05$ ). If  $p < \alpha$ , then it can be concluded like that  $x_j$  has an effect on the behavior of  $Y$ . Relative importance of the  $X_j$ 's can be assessed by ranking them according to their respective p-values (smaller the p-value, the more important).

For CMN test used here, the values of  $X_j$  are divided into  $M=5$  disjoint classes. In Figure 8.4(a), one example is shown. Figure 8.4 shows that x axis is divided into 5 equal parts which are spaced at 1.2 inch interval for plotting AC Thickness ( $X_{18}$ ). No portioning is done for vertical axis, which presents total rutting ( $Y_6$ ). The result obtained from CMN test is presented in Table 8.4 for each output variable ( $Y_1$  to  $Y_6$ ). Only p-values are shown. A level of significance,  $\alpha = 0.05$  is used. if p-value is less than  $\alpha$ , then the hypothesis made in Eq. 2 is rejected and it is confirmed that  $X_j$  has an effect on the behavior of  $Y$ . Relative importance of the  $X_j$ 's, are measured and ranked according to their respective p-values. Generally speaking, the smaller the p-value, the more important the input variable is. Table 8.4 is organized based on an ordering of p-value from smallest to largest for output  $Y_1$  to  $Y_6$ .

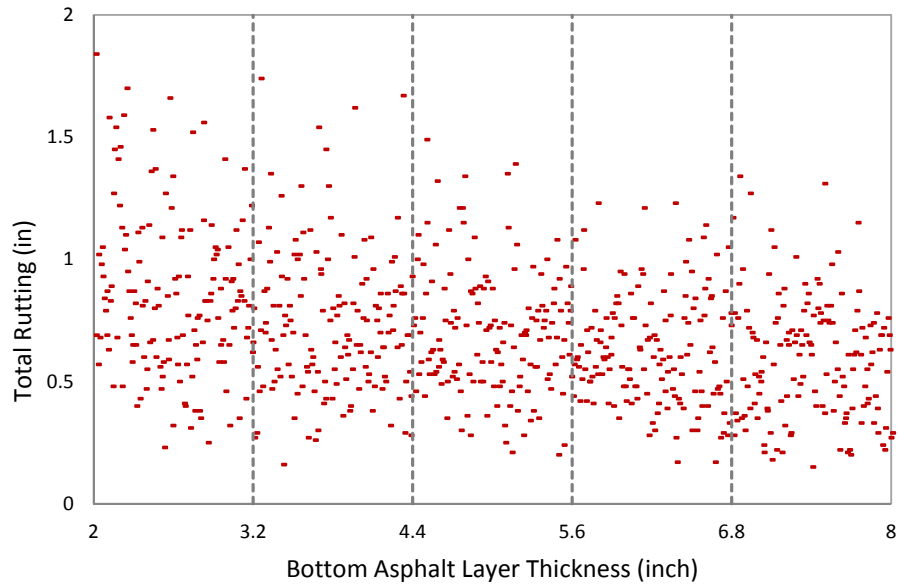


**FIGURE 8.4 Partitioning of  $X_j$  (AC Thickness) for Gridding Tests (CMN and CL)**

It can be seen that from Table 8.4, for  $Y_1$  (terminal IRI), a total of twelve inputs have significant p-values (less than 0.05) out of thirty. Four input have p-value=0 which means that they are most important. They are AADTT ( $X_1$ ), percent of trucks in design lane ( $X_4$ ), top and bottom asphalt layer thickness ( $X_{13}$  and  $X_{18}$ ). For  $Y_2$  (longitudinal cracking), 10 inputs have been identified. Among them, six inputs are most significant with zero p-value. They are AADTT ( $X_1$ ), percent of trucks in design lane ( $X_4$ ), percent air void of top AC layer ( $X_{17}$ ), bottom asphalt layer thickness ( $X_{18}$ ), base material ( $X_{24}$ ) and base modulus ( $X_{25}$ ). Alligator cracking or  $Y_3$  has 10 important factors among the thirty inputs. Among them, six inputs have zero p-value. They are AADTT ( $X_1$ ), percent of trucks in design lane ( $X_4$ ), top and bottom asphalt layer thickness ( $X_{13}$  and  $X_{18}$ ), percent air void of bottom AC layer ( $X_{22}$ ) and base modulus ( $X_{25}$ ). No inputs have been identified for  $Y_4$  or transverse cracking. Transverse cracking ( $Y_4$ ) is mainly occurs by environmental variables such as moisture, freeze thaw, temperature and precipitation. Some of these factors were kept constant and the others do not very too much for New Mexico weather condition.

Total 13 inputs have been identified for significantly contributing to AC rutting ( $Y_5$ ) and 14 inputs for identified for affecting total rutting ( $Y_6$ ). For both type of rutting, 5 inputs have zero p-value. Four input variables are common for both cases. They are: AADTT ( $X_1$ ), percent of trucks in design lane ( $X_4$ ), design lane width ( $X_9$ ) and bottom asphalt layer thickness ( $X_{18}$ ). Traffic growth factor ( $X_8$ ) is very significant for  $Y_5$  (p-value = 0.0) but not that much for total rutting ( $Y_6$ ). Subgrade modulus ( $X_{27}$ ) is very significant for total rutting ( $Y_6$ ) (p value = 0.0) but not even expected for AC rutting ( $Y_5$ ). Three input variables AADTT ( $X_1$ ), percent of trucks in design lane ( $X_4$ ) and bottom asphalt layer thickness ( $X_{18}$ ) are obtained (zero p value) as most important for all predicted pavement distresses.

**TABLE 8.4 Significant inputs based on p-value from CMN test result**

Input Name	Variable No	Terminal IRI (in/mile)	Longitudinal Cracking (ft/mile)	Alligator Cracking (%)	Transverse Cracking (ft/mile)	AC Rutting (in)	Total Rutting (in)
Initial two-way AADTT	X <sub>1</sub>	<b>0.00</b>	<b>0.00</b>	<b>0.00</b>		<b>0.00</b>	<b>0.00</b>
Percent of Trucks in Design Direction (%)	X <sub>3</sub>	0.0056	0.0152			0.0251	0.0015
Percent of Trucks in Design Lane (%)	X <sub>4</sub>	<b>0.00</b>	<b>0.00</b>	<b>0.00</b>		<b>0.00</b>	<b>0.00</b>
Operational Speed (mph)	X <sub>5</sub>					0.0141	0.0063
Traffic Growth Factor	X <sub>8</sub>	0.0234				<b>0.00</b>	0.0002
Design Lane Width (ft)	X <sub>9</sub>	0.0479	0.0011	0.0186			
Tire Pressure	X <sub>10</sub>	0.0368				<b>0.00</b>	<b>0.00</b>
Climatic Zones	X <sub>12</sub>					0.0002	0.0234
AC Mix 1	Layer Thickness (in)	X <sub>13</sub>	<b>0.00</b>	0.0005	<b>0.00</b>	0.0008	0.0002
	Effective Binder Content (%)	X <sub>15</sub>		0.0217			
	Superpave Binder Grade	X <sub>16</sub>				0.0495	
	Air Voids (%)	X <sub>17</sub>		<b>0.00</b>		0.0378	
AC Mix 2	Layer Thickness (in)	X <sub>18</sub>	<b>0.00</b>	<b>0.00</b>	<b>0.00</b>	<b>0.00</b>	<b>0.00</b>
	Effective Binder Content (%)	X <sub>20</sub>				0.0281	0.0137
	Air Voids (%)	X <sub>22</sub>	0.0031	<b>0.00</b>			
Base	Material Type	X <sub>24</sub>		<b>0.00</b>	0.0458		
	Modulus (psi)	X <sub>25</sub>	0.0003	<b>0.00</b>	<b>0.00</b>		0.0258
Subgrade	Material Type	X <sub>26</sub>	0.0001				0.0023
	Modulus (psi)	X <sub>27</sub>	0.0001		0.0488		<b>0.00</b>
	Optimum Gravimetric Water Content (%)	X <sub>30</sub>			0.0209	0.0092	0.0026

**Common Locations (CL)**

The CLs test employs the Kruskal–Wallis test statistic  $T$ , which is based on rank-transformed data and uses the same classes of  $X_j$  values as the F-statistic in Eq. 1 (Helton et al. 2006, Conover 1980). Assuming,  $Y_i$ 's are independent and identically distributed with median  $(Y_i) = \eta_c$ . For,  $i \in X_c$ ,  $c = 1, \dots, M$ . It is also assumed that the shape and scale of the distribution of the  $Y_i$ 's is the same across all  $M$  groups. The CL procedure is then a test of the hypothesis

$$H_0: \eta_1 = \eta_2 = \dots = \eta_M \quad (4)$$

versus the alternative that  $H_0$  is not true. The test statistic  $T^*$  for the CL test is based on

rank-transformed data. Specifically,

$$T^* = (n - 1) \frac{\sum_{c=1}^M m_c (\bar{r}_c - \bar{r})^2}{\sum_{c=1}^M \sum_{i \in X_c} (r(Y_i) - \bar{r}_c)^2} \quad (5)$$

$$\text{where } \bar{r}_c = \left( \frac{1}{m_c} \right) \sum_{i \in X_c} r(Y_i) \quad (6)$$

$$\bar{r} = \left( \frac{1}{n} \right) \sum_{i \in X_c}^n r(Y_i) \quad (7)$$

where

$X_{ij}$  = observed values of  $X_j$  and  $Y$  and  $i=1, 2, \dots, n$ ;

$c = 1, 2, \dots, M$  number of individual classes into which the values of  $X_j$  have been divided,

$X_c$  = the set of  $X_j$  values such that  $i \in X_c$  ( $X_{ij}$  belongs to class  $c$ );

$M_c$  = number of elements contained in  $X_c$ .

$r(y_i)$  = rank of  $Y_i$ .

If all of the  $y$  values have same distribution, then  $T^*$  approximately follows a  $\chi^2_{M-1}$  distribution.

The p-value of the test is

$$p = P[\chi^2_{M-1} > T^*] \quad (8)$$

A small p-value indicates that  $y$  has a different distribution depending on which of the groups  $X_j$  is in. Since it was assumed that the shape and scale of the distribution of  $y$  across each of the  $M$  groups is the same, the difference must be between the locations (medians). Even without the shape and scale assumption though, a small p-value indicates that  $X_j$  has some effect on  $Y$  (location shift or otherwise).

For CL test, the values of  $X_j$  are divided into  $M=5$  disjoint classes which is same as CMN test. No portioning is done for vertical axis. Table 8.5 presents the CL test result for output  $Y_1$  to  $Y_6$ . For Terminal IRI ( $Y_1$ ), total eleven inputs have significant p-value among all the thirty. Five input variable has lowest p value (zero). They are AADTT ( $X_1$ ), percent of trucks in design lane ( $X_4$ ), bottom AC layer thickness ( $X_{18}$ ), subgrade material ( $X_{26}$ ) and subgrade modulus ( $X_{27}$ ).

For Longitudinal Cracking ( $Y_2$ ), twelve inputs have been identified. Among them, seven inputs are most significant with zero p-value. They are AADTT ( $X_1$ ), percent of trucks in design lane ( $X_4$ ), percent air void of top AC layer ( $X_{17}$ ), top and bottom asphalt layer thickness ( $X_{13}$  and  $X_{18}$ ), base material ( $X_{24}$ ) and base modulus ( $X_{25}$ ).

Alligator Cracking ( $Y_3$ ) has eleven important factors among the thirty variables. Among them, AADTT ( $X_1$ ), percent of trucks in design lane ( $X_4$ ), top and bottom asphalt layer thickness ( $X_{13}$  and  $X_{18}$ ), percent air void of bottom AC layer ( $X_{22}$ ) have zero p-value. Only two variables have been identified for Transverse Cracking ( $Y_4$ ). They are climatic zone ( $X_{12}$ ) and Superpave binder grade of top AC layer ( $X_{16}$ ). None of them has zero p-value.

Total twelve variables have been identified for AC Rutting ( $Y_5$ ). Five significant inputs are identified with zero p-value. They are: AADTT ( $X_1$ ), percent of trucks in design lane ( $X_4$ ), traffic growth factor ( $X_8$ ), tire pressure ( $X_{10}$ ) and bottom asphalt layer thickness ( $X_{18}$ ). For Total Rutting ( $Y_6$ ), thirteen inputs are identified as important. Among them, five input variables can be said as very important as they have obtained zero p-value, they are: AADTT ( $X_1$ ), percent of trucks in

design lane ( $X_4$ ), tire pressure ( $X_{10}$ ), bottom asphalt layer thickness ( $X_{18}$ ) and subgrade modulus ( $X_{30}$ ). Four very important input variables are common for both rutting. They are AADTT ( $X_1$ ), percent of trucks in design lane ( $X_4$ ), tire pressure ( $X_{10}$ ) and bottom asphalt layer thickness ( $X_{18}$ ). Three input variables are obtained as very important in CL test for all pavement distresses. They are AADTT ( $X_1$ ), percent of trucks in design lane ( $X_4$ ) and bottom AC layer thickness ( $X_{18}$ ).

**TABLE 8.5 Significant Inputs Based on p-value from CL Test Result**

Input Name		Variable No	Terminal IRI (in/mile)	Longitudinal Cracking (ft/mile)	Alligator Cracking (%)	Transverse Cracking (ft/mile)	AC Rutting (in)	Total Rutting (in)
Initial two-way AADTT		$X_1$	0.00	0.00	0.00		0.00	0.00
Percent of Trucks in Design Direction (%)		$X_2$	0.0020	0.0449	0.0074		0.0295	0.0013
Percent of Trucks in Design Lane (%)		$X_3$	0.00	0.00	0.00		0.00	0.00
Operational Speed (mph)		$X_4$	0.0031	0.0301			0.0060	0.0024
Traffic Growth Factor		$X_8$	0.0032	0.0373	0.0135		0.00	0.0001
Design Lane Width (ft)		$X_9$		0.0094				
Tire Pressure		$X_{10}$	0.0005				0.00	0.00
Depth of Water table (ft)		$X_{11}$			0.0279			
Climatic Zones		$X_{12}$				0.0127	0.0001	0.0026
AC Mix 1	Layer Thickness (in)	$X_{13}$	0.0002	0.00	0.00		0.0027	0.0006
	Superpave Binder Grade	$X_{16}$				0.0010	0.0428	
	Air Voids (%)	$X_{17}$		0.0001				
AC Mix 2	Layer Thickness (in)	$X_{18}$	0.00	0.00	0.00		0.00	0.00
	Effective Binder Content (%)	$X_{20}$					0.0398	0.0181
	Air Voids (%)	$X_{22}$			0.00			
Base	Material Type	$X_{24}$		0.00	0.0037			
	Modulus (psi)	$X_{25}$		0.00	0.0002			
Subgrade	Material Type	$X_{26}$	0.00					0.0003
	Modulus (psi)	$X_{27}$	0.00	0.00				0.00
	Optimum Gravimetric Water Content (%)	$X_{30}$	0.0166		0.0066		0.0244	0.0012



## Statistical Independence (SI)

A Statistical Independence (SI) test uses the  $\chi^2$  test to examine nonrandomness of a pattern appearing in a scatter plot (Helton et al. 2006). The SI test uses the same partitioning of  $X_j$  values as used for the CMN, CL tests. In addition, the  $Y$  values are also partitioned in a manner analogous to that used for the  $X_j$  values (Helton et al. 2006). The SI procedure is a test of the hypothesis

$$H_0: Y \text{ is dependent of } X_j \quad (9)$$

versus the alternative that  $H_0$  is not true. Under the assumption of  $H_0$ ,  $Y$  has the same distribution in each of the  $X_j$  classes. If  $X_j$  and  $Y$  are independent,

$$E_{r,c} = \frac{I_r m_c}{n} \quad (10)$$

is an estimate of the expected number of observations ( $X_j$ ,  $Y$ ) that should fall in class ( $r$ ,  $c$ ), where

$r$  = number of individual classes into which the values of  $Y$  are divided ( $r=1,2,.. L$ );

$Y_r$  = set of  $Y$  values, such that  $i \in Y_r$  only if  $Y_i$  belongs to class  $r$ ;

$I_r$  = number of elements contained in  $Y_r$ .

The partitioning of  $x_j$  and  $y$  into  $M$  and  $L$  classes, respectively, in turn partitions ( $X_j$ ,  $Y$ ) into  $M \times L$  classes. The test statistic

$$T^* = \sum_{c=1}^M \sum_{r=1}^L \frac{(k_{r,c} - E_{r,c})^2}{E_{r,c}} \quad (11)$$

where

$O_{r,c}$  = set of value such that  $i \in O_{r,c}$  only if  $i \in X_c$  and also  $i \in Y_r$ ;

$k_{r,c}$  = the number of elements contained in  $O_{r,c}$ .

Asymptotically,  $T^*$  follows approximately follows a  $\chi^2_{(M-1)(L-1)}$  distribution when  $X_j$  and  $Y$  are independent.. The p-value of the test is defined by

$$p = P[\chi^2_{(M-1)(L-1)} > T^*] \quad (12)$$

A small p-value indicates that  $X_j$  and  $Y$  are likely not independent. Appearance of a nonrandom pattern indicates that  $x_j$  has an effect on  $y$ .

Figure 8.5 represents the partitioning used for SI test for the same input and output variable ( $X_{18}$  and  $Y_6$ ). The horizontal axis partitioning is same as CL and CMN test. In addition, the  $Y$  values are also partitioned in a manner analogous to that used for the  $X_j$  values.

SI test results are presented in Table 8.6 for output  $Y_1$  to  $Y_6$ . Similar trend like CMN and CL test is also obtained in this test. Overall two input variables AADTT ( $X_1$ ), percent of trucks in design lane ( $X_4$ ) have captured (zero p value) for all predicted pavement distresses.

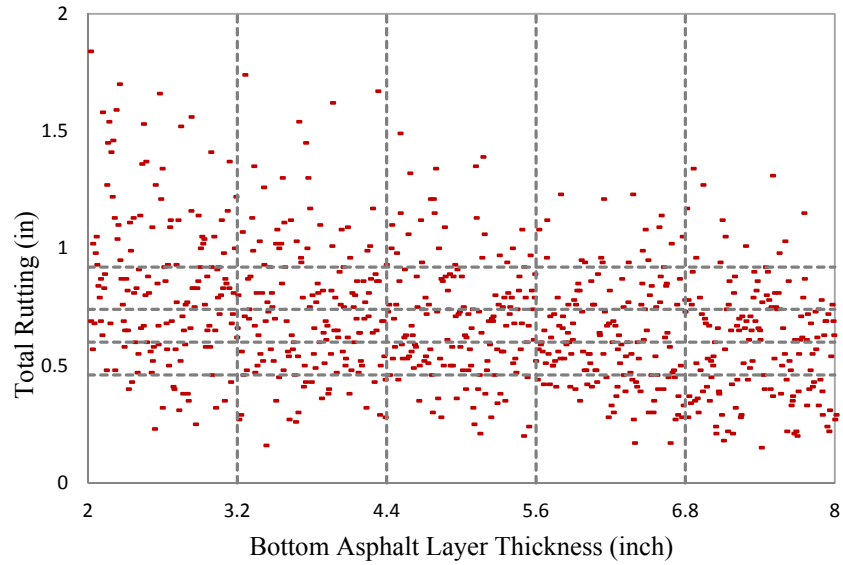


**FIGURE 8.5 Partitioning of Y (Total Rutting) for Gridding Tests (SI)**

### **FLEXIBLE GRID FREE TESTS**

Four grid free tests are performed and they are: Linear regression analysis (REG), Quadratic regression analysis (QREG), Rank Correlation Coefficient test (RCC) and Squared Rank Differences Test (SRD).

### **Simple Linear Regression (LREG)**

The regression (REG) test for nonrandomness is performed by fitting simple linear regression of the Y on  $X_j$  (Helton et al. 2006). Simple Linear regression is the most commonly used approach to model a relationship between two variables. It is assumed that, the variables have linear relationship. Specifically, a simple linear regression model for each input takes the form

$$Y_i = b_0 + b_j x_{ij} + \varepsilon_i, \quad j = 1, 2, \dots, k \quad (13)$$

where  $b_j$ =regression coefficients,  $\varepsilon_i$ =residual error p-value is obtained from Linear Regression test for all input variables and presented in Table 8.7. A total of fourteen inputs are identified as important for predicted distress Terminal IRI ( $Y_1$ ). Among these, six variables can be said as very important as they have obtained zero p-value. they are AADTT ( $X_1$ ), percent trucks in design lane ( $X_4$ ), top and bottom AC layer thickness ( $X_{13}$  and  $X_{18}$ ), base and subgrade modulus ( $X_{25}$  and  $X_{27}$ ) and subgrade material ( $X_{26}$ ). For Longitudinal Cracking ( $Y_2$ ), eleven inputs are identified among 30 variables. A total of five variables are identified as very important with zero p-value. They are ADTT ( $X_1$ ), percent trucks in design lane ( $X_4$ ), top and bottom AC layer thickness ( $X_{13}$  and  $X_{18}$ ), base modulus ( $X_{25}$ ).

**TABLE 8.6 Significant inputs based on p-value from SI test result**

Input Name		Variable No	Terminal IRI (in/mile)	Longitudinal Cracking (ft/mile)	Alligator Cracking (%)	Transverse Cracking (ft/mile)	AC Rutting (in)	Total Rutting (in)
Initial two-way AADTT		X <sub>1</sub>	<b>0.00</b>	<b>0.00</b>	<b>0.00</b>		<b>0.00</b>	<b>0.00</b>
Number of Lanes in Design Direction		X <sub>2</sub>				<b>0.00</b>		
Percent of Trucks in Design Direction (%)		X <sub>3</sub>			0.0214			
Percent of Trucks in Design Lane (%)		X <sub>4</sub>	<b>0.00</b>	<b>0.00</b>	<b>0.00</b>		<b>0.00</b>	<b>0.00</b>
Operational Speed (mph)		X <sub>5</sub>	0.0400					0.0346
Traffic Growth Factor		X <sub>8</sub>	0.0089	0.0453			0.0034	0.0140
Design Lane Width (ft)		X <sub>9</sub>		0.0020		0.0029		
Tire Pressure		X <sub>10</sub>	0.0005			0.0278	0.00	0.0007
Depth of Water Table (ft)		X <sub>11</sub>			0.0075			
Climatic Zones		X <sub>12</sub>					0.0014	0.0039
AC Mix 1	Layer Thickness (in)	X <sub>13</sub>	0.0003	0.0002	0.0023		0.0132	0.0012
	Aggregate Gradation	X <sub>14</sub>				<b>0.00</b>		
	Superpave Binder Grade	X <sub>16</sub>				<b>0.00</b>		
	Air Voids (%)	X <sub>17</sub>	0.0400	0.0080				
AC Mix 2	Layer Thickness (in)	X <sub>18</sub>	<b>0.00</b>	<b>0.00</b>	<b>0.00</b>		0.0001	<b>0.00</b>
	Aggregate Gradation	X <sub>19</sub>				<b>0.00</b>		
	Effective Binder Content (%)	X <sub>20</sub>		0.0462				
	Superpave Binder Grade	X <sub>21</sub>				<b>0.00</b>		
	Air Voids (%)	X <sub>22</sub>			<b>0.00</b>			
Base	Material Type	X <sub>24</sub>		0.0002	0.0198	0.0003		
	Modulus (psi)	X <sub>25</sub>		0.0006	0.0007			
Subgrade	Material Type	X <sub>26</sub>	<b>0.00</b>					<b>0.00</b>
	Modulus (psi)	X <sub>27</sub>	0.0033	<b>0.00</b>				<b>0.00</b>
	Liquid Limit	X <sub>29</sub>	0.0495					
	Optimum Gravimetric Water Content (%)	X <sub>30</sub>						0.0015

Seven important variables are identified for Alligator Cracking ( $Y_3$ ). Among them, five are very significant and same as for  $Y_2$ . No variables are identified in a linear regression test for Transverse Cracking ( $Y_4$ ). A total of sixteen variables are captured in linear regression test result for AC Rutting ( $Y_5$ ), which is highest among all predicted distresses. The six of them with zero p value can be considered as very significant among all.

**TABLE 8.7 Significant inputs based on p-value from linear regression test result**

Input Name		Variable No	Terminal IRI (in/mile)	Longitudinal Cracking (ft/mile)	Alligator Cracking (%)	Transverse Cracking (ft/mile)	AC Rutting (in)	Total Rutting (in)
Initial two-way AADTT		$X_1$	0.00	0.00	0.00		0.00	0.00
Percent of Trucks in Design Direction (%)		$X_3$	0.0009	0.0307			0.0073	0.0002
Percent of Trucks in Design Lane (%)		$X_4$	0.00	0.00	0.00		0.00	0.00
Operational Speed (mph)		$X_5$	0.0492	0.0167			0.0031	0.0013
AADTT Distribution by Vehicle Class 9 (%)		$X_6$					0.0054	
Traffic Growth Factor		$X_8$	0.0040				0.00	0.00
Tire Pressure		$X_{10}$	0.0037				0.00	0.00
Depth of Water Table (ft)		$X_{11}$		0.0202				0.0285
Climatic Zones		$X_{12}$					0.0011	0.0134
Asphalt Mix 1	Layer Thickness (in)	$X_{13}$	0.00	0.00	0.00		0.00	0.00
	Effective Binder Content (%)	$X_{15}$		0.0062				
	Superpave Binder Grade	$X_{16}$					0.0009	
	Air Voids (%)	$X_{17}$	0.0203	0.00			0.0005	0.0012
Asphalt Mix 2	Layer Thickness (in)	$X_{18}$	0.00	0.00	0.00		0.00	0.00
	Effective Binder Content (%)	$X_{20}$					0.0029	0.0024
	Superpave Binder Grade	$X_{21}$					0.0083	0.0208
	Air Voids (%)	$X_{22}$	0.0001		0.00		0.0267	0.0319
Base Modulus (psi)		$X_{25}$	0.00	0.00	0.00			0.0097
Subgrade	Material Type	$X_{26}$	0.00					0.0002
	Modulus (psi)	$X_{27}$	0.00	0.0086	0.0035			0.00
	Optimum Gravimetric Water Content (%)	$X_{30}$	0.0292				0.0013	0.0001

They are AADTT ( $X_1$ ), percent trucks in design lane ( $X_4$ ),  $X_8$  (Traffic growth factor),  $X_{10}$  (tire pressure), top and bottom AC layer thickness ( $X_{13}$  and  $X_{18}$ ). These inputs have obtained zero p-value in case of Total Rutting ( $Y_6$ ). the same six inputs with the addition of subgrade modulus( $X_{27}$ ) also have zero p value for  $Y_6$ . Including these seven, a total of 15 variables are obtained for  $Y_6$  in linear regression test. Four input variables have zero p value for all predicted distresses except for  $Y_4$ . They are AADTT ( $X_1$ ), percent trucks in design lane ( $X_4$ ), top and bottom AC layer thickness ( $X_{13}$  and  $X_{18}$ ).

### Quadratic Regression (QREG)

The quadratic regression (QREG) test performs a quadratic regression of  $Y$  on  $X_j$ . Specifically, it is estimated that

$$Y_i = \beta_0 + \beta_1 X_i + \beta_2 X_i^2 + \varepsilon_i \quad (14)$$

The p-value is obtained by testing significance of the model. Detailed result for this test is shown in Table 8.8. A total of three variables have zero p-value for all outputs. They are AADTT ( $X_1$ ), percent trucks in design lane ( $X_4$ ), bottom AC layer thickness ( $X_{18}$ ). Fifteen variables are identified for Terminal IRI ( $Y_1$ ) and AC Rutting ( $Y_5$ ). For Longitudinal Cracking ( $Y_2$ ), Alligator Cracking ( $Y_3$ ) and Total Rutting ( $Y_6$ ), number of variables are identified are 13, 10 and 16 respectively. For Transverse Cracking ( $Y_4$ ) only one input is identified as significant which is plastic limit ( $X_{28}$ ). There are six very significant variables for  $Y_1$  and  $Y_3$ . For  $Y_1$ , the inputs are  $X_1$ ,  $X_4$ ,  $X_{13}$ ,  $X_{18}$ ,  $X_{26}$  and  $X_{27}$ . For  $Y_3$  the inputs are  $X_1$ ,  $X_4$ ,  $X_{13}$ ,  $X_{18}$ ,  $X_{22}$  and  $X_{25}$ . For  $Y_2$  and  $Y_5$ , there are five very important inputs. For  $Y_2$ , the inputs are  $X_1$ ,  $X_4$ ,  $X_{17}$ ,  $X_{18}$  and  $X_{25}$ .  $X_1$ ,  $X_4$ ,  $X_8$ ,  $X_{10}$  and  $X_{18}$  are very significant for output  $Y_5$ . Among sixteen inputs identified for  $Y_6$ , seven inputs can be considered as very significant. They are  $X_1$ ,  $X_4$ ,  $X_8$ ,  $X_{10}$ ,  $X_{13}$ ,  $X_{18}$  and  $X_{27}$ .

### Rank Correlation Coefficient (RCC)

The rank correlation coefficient (RCC) test is based on the rank correlation coefficient (Helton et al. 2006) which is defined below:

$$r = \frac{\sum_{i=1}^n \left[ r(X_{ij}) - \frac{n+1}{2} \right] \left[ r(Y_i) - \frac{n+1}{2} \right]}{\left\{ \sum_{i=1}^n \left[ r(X_{ij}) - \frac{n+1}{2} \right]^2 \right\}^{1/2} \left\{ \sum_{i=1}^n \left[ r(Y_i) - \frac{n+1}{2} \right]^2 \right\}^{1/2}} \quad (15)$$

where  $r(X_{ij})$  = ranks associated  $X_j$  for sample element  $i$ ;  
 $r(Y_i)$  = ranks associated  $Y$  for sample element  $i$ .

The null hypothesis is made as there is no monotonic relationship between  $X_j$  and  $Y$ . The absolute value of  $r$  is used to calculate a p-value. A large value of  $|r|$  means the underlying rank correlation may be different from zero and there is a relationship between  $X_j$  and  $Y$ . Thus, the p-value to test the null hypotheses is given by

$$p = P(|t_{n-2}| > |r|) \quad (16)$$

**TABLE 8.8 Significant inputs based on p-value from QREG test result**

Input Name		Variable No	Terminal IRI (in/mile)	Longitudinal Cracking (ft/mile)	Alligator Cracking (%)	Transverse Cracking (ft/mile)	AC Rutting (in)	Total Rutting (in)
Initial two-way AADTT		X <sub>1</sub>	<b>0.00</b>	<b>0.00</b>	<b>0.00</b>		<b>0.00</b>	<b>0.00</b>
Percent of Trucks in Design Direction (%)		X <sub>3</sub>	0.0033	0.0320			0.0246	0.0007
Percent of Trucks in Design Lane (%)		X <sub>4</sub>	<b>0.00</b>	<b>0.00</b>	<b>0.00</b>		<b>0.00</b>	<b>0.00</b>
Operational Speed (mph)		X <sub>5</sub>	0.0039	0.0369	0.0412		0.0015	0.0003
AADTT Distribution by Vehicle Class 9 (%)		X <sub>6</sub>					0.0208	
Traffic Growth Factor		X <sub>8</sub>	0.0076				<b>0.00</b>	<b>0.00</b>
Design Lane Width (ft)		X <sub>9</sub>	0.0272	0.0024	0.0163			
Tire Pressure (psi)		X <sub>10</sub>	0.0114				<b>0.00</b>	<b>0.00</b>
Depth of Water Table (ft)		X <sub>11</sub>						0.0332
Climatic Zones		X <sub>12</sub>					0.0043	0.0458
Asphalt Mix 1	Layer Thickness (in)	X <sub>13</sub>	<b>0.00</b>	0.0001	<b>0.00</b>		0.0001	<b>0.00</b>
	Effective Binder Content (%)	X <sub>15</sub>		0.0092				
	Superpave Binder Grade	X <sub>16</sub>					0.0028	
	Air Voids (%)	X <sub>17</sub>	0.0445	<b>0.00</b>			0.0007	0.0024
Asphalt Mix 2	Layer Thickness (in)	X <sub>18</sub>	<b>0.00</b>	<b>0.00</b>	<b>0.00</b>		<b>0.00</b>	<b>0.00</b>
	Effective Binder Content (%)	X <sub>20</sub>		0.0366			0.0057	0.0049
	Superpave Binder Grade	X <sub>21</sub>					0.0301	
	Air Voids (%)	X <sub>22</sub>	0.0003		<b>0.00</b>			
	Material Type	X <sub>24</sub>		0.0002				
	Modulus (psi)	X <sub>25</sub>	0.0001	<b>0.00</b>	<b>0.00</b>			0.0257
Subgrade	Material Type	X <sub>26</sub>	<b>0.00</b>					0.0004
	Modulus (psi)	X <sub>27</sub>	<b>0.00</b>	0.0148	0.0114			<b>0.00</b>
	Plastic Limit	X <sub>28</sub>				0.0301		
	Optimum Gravimetric Water Content (%)	X <sub>30</sub>	0.0182		0.0093		0.0048	0.0004

A summary of RCC test result is shown in Table 8.9. Sixteen inputs are identified as important for output Terminal IRI ( $Y_1$ ). Among them, seven inputs have zero p-value and can be considered as very important for  $Y_1$ . They are AADTT ( $X_1$ ), Percent of Trucks in Design Lane ( $X_4$ ), Tire pressure ( $X_{10}$ ), top and bottom AC layer thickness ( $X_{13}$ ,  $X_{18}$ ), subgrade material and modulus ( $X_{26}$  and  $X_{27}$ ). For Longitudinal Cracking ( $Y_2$ ), twelve inputs are identified in this test. A total seven inputs have zero p-value. They are  $X_1$ ,  $X_4$ ,  $X_{13}$ ,  $X_{18}$ ,  $X_{17}$ ,  $X_{25}$ , and  $X_{27}$ . Eleven

important inputs are identified for  $Y_3$ , and six of them have zero p-value. They are  $X_1$ ,  $X_4$ ,  $X_{13}$ ,  $X_{18}$ ,  $X_{22}$  and  $X_{25}$ . Only one input is identified for  $Y_4$  and that is Superpave binder grade of top AC layer ( $X_{16}$ ). Total 16 and 15 inputs are identified for AC rut and total rut respectively. Number of very significant inputs are five for  $Y_5$  and also common for  $Y_6$ . They are  $X_1$ ,  $X_4$ ,  $X_8$ ,  $X_{10}$ , and  $X_{18}$ . In addition to these five,  $Y_6$  has three more inputs that are very significant. They are  $X_{13}$ ,  $X_{26}$  and  $X_{27}$ . In this test, three inputs have zero p-value for all cases. They are  $X_1$ ,  $X_4$ , and  $X_{18}$ .

**TABLE 8.9 Significant Inputs Based on p-value from RCC Test Result**

Input Name		Variable No	Terminal IRI (in/mile)	Longitudinal Cracking (ft/mile)	Alligator Cracking (%)	Transverse Cracking (ft/mile)	AC Rutting (in)	Total Rutting (in)
Initial two-way AADTT		$X_1$	<b>0.00</b>	<b>0.00</b>	<b>0.00</b>		<b>0.00</b>	<b>0.00</b>
Percent of Trucks in Design Direction (%)		$X_3$	0.0009				0.0151	0.0002
Percent of Trucks in Design Lane (%)		$X_4$	<b>0.00</b>	<b>0.00</b>	<b>0.00</b>		<b>0.00</b>	<b>0.00</b>
Operational Speed (mph)		$X_5$	0.0013	0.0068	0.0172		0.0014	0.0010
AADTT Distribution by Vehicle Class 9 (%)		$X_6$					0.0390	
Traffic Growth Factor		$X_8$	0.0003	0.0389	0.0024		<b>0.00</b>	<b>0.00</b>
Tire Pressure (psi)		$X_{10}$	<b>0.00</b>				<b>0.00</b>	<b>0.00</b>
Depth of Water Table (ft)		$X_{11}$	0.0242	0.0146	0.0132			0.0262
Climatic Zones		$X_{12}$	0.0126		0.0408		0.0003	0.0021
Asphalt Mix 1	Layer Thickness (in)	$X_{13}$	<b>0.00</b>	<b>0.00</b>	<b>0.00</b>		<b>0.0001</b>	<b>0.00</b>
	Superpave Binder Grade	$X_{16}$		0.0257		0.0029	0.0007	
	Air Voids (%)	$X_{17}$	0.0083	<b>0.00</b>			0.0028	0.0034
Asphalt Mix 2	Layer Thickness (in)	$X_{18}$	<b>0.00</b>	<b>0.00</b>	<b>0.00</b>		<b>0.00</b>	<b>0.00</b>
	Effective Binder Content (%)	$X_{20}$					0.0046	0.0038
	Superpave Binder Grade	$X_{21}$					0.0095	
	Air Voids (%)	$X_{22}$	0.0120		<b>0.00</b>		0.0177	
Base	Material Type	$X_{24}$		0.0444				
	Modulus (psi)	$X_{25}$	0.0232	<b>0.00</b>	<b>0.00</b>			
Subgrade	Material Type	$X_{26}$	<b>0.00</b>					<b>0.00</b>
	Modulus (psi)	$X_{27}$	<b>0.00</b>	<b>0.00</b>	0.0027			<b>0.00</b>
	Optimum Gravimetric Water Content (%)	$X_{30}$	0.0033				0.0016	0.0001

### Squared Rank Differences (SRD)

In this method, no parametric model is considered between inputs and outputs. The SRD test is based on a quantity  $Q$  defined by:

$$Q = \sum_{i=1}^{n-1} (r_{i+1,j} - r_{i,j})^2 \quad (17)$$

where  $r_{i,j}$ =rank of  $y$  obtained with the sample element in which  $X_j$  has rank  $i$ . Under the null hypothesis of no relationship between  $X_j$  and  $Y$ , the test statistic is defined by

$$S^* = \frac{Q - n \frac{(n^2 - 1)}{6}}{\frac{n^{5/2}}{6}} \quad (18)$$

where  $S^*$  approximately follows a standard normal distribution for  $n > 40$ . Small values of  $Q$  (and subsequently small values of  $S$ ) indicate similar ranks among  $Y$  values with similar  $X_j$  values. This is inconsistent with the null hypothesis of independence between  $X_j$  and  $Y$ . Thus, a  $p$ -value can be obtained as

$$p = P(Z < S^*) \quad (19)$$

where  $Z$  is a standard normal random variable.

Summary of SRD test results is presented in Table 8.10. There is no single input obtained in this test which is very significant for all predicted pavement distresses. There are three inputs which are significant for Terminal IRI ( $Y_1$ ). They are AADTT ( $X_1$ ), percent trucks in design lane ( $X_4$ ), bottom AC layer thickness ( $X_{18}$ ). Input  $X_1$  and  $X_4$  have zero  $p$  value and can be considered as very important. Longitudinal Cracking ( $Y_2$ ) has six input variables, which are identified as significant. Among these six, only one can be said as very important which is  $X_{18}$  or bottom AC layer thickness. A total of inputs are significant for Alligator Cracking ( $Y_3$ ) and three of them have zero  $p$ -value. They are AADTT ( $X_1$ ), percent trucks in design lane ( $X_4$ ), and bottom AC layer thickness ( $X_{18}$ ). No input variable is identified as significant in this test for Transverse Cracking ( $Y_4$ ). AC Rutting ( $Y_5$ ) has six input variables in the list and two of them have zero  $p$ -value. They are AADTT ( $X_1$ ), percent trucks in design lane ( $X_4$ ). Four input variables are identified as significant for Total Rutting ( $Y_6$ ) and two of them are with zero  $p$ -value. They are AADTT ( $X_1$ ) and percent trucks in design lane ( $X_4$ ). It can be noted that SRD test has resulted 10 out of 30 inputs as significant inputs. Like RCC and other tests, AADTT ( $X_1$ ), percent trucks in design lane ( $X_4$ ), bottom AC layer thickness ( $X_{18}$ ) are the most significant inputs.



**TABLE 8.10 Significant inputs based on p-value from SRD test result**

Input Name		Variable No	Terminal IRI (in/mile)	Longitudinal Cracking (ft/mile)	Alligator Cracking (%)	Transverse Cracking (ft/mile)	AC Rutting (in)	Total Rutting (in)
Initial two-way AADTT		X <sub>1</sub>	<b>0.00</b>	0.0007	<b>0.00</b>		<b>0.00</b>	<b>0.00</b>
Percent of Trucks in Design Lane (%)		X <sub>4</sub>	<b>0.00</b>		<b>0.00</b>		<b>0.00</b>	<b>0.00</b>
AADTT Distribution by Vehicle Class 9 (%)		X <sub>6</sub>			0.0247			
Traffic Growth Factor		X <sub>8</sub>					0.0094	0.0283
Tire Pressure (psi)		X <sub>10</sub>					0.0488	
AC Mix	AC Mix 1	Effective Binder Content (%)	X <sub>15</sub>		0.0070			
	AC Mix 2	Layer Thickness (in)	X <sub>18</sub>	0.0001	<b>0.00</b>	<b>0.00</b>	0.0156	0.0240
		Aggregate Gradation	X <sub>19</sub>		0.0176	0.0354		
Base	Material Type		X <sub>24</sub>		0.0136			
	Modulus (psi)		X <sub>25</sub>		0.0454		0.0203	

## SUMMARY OF INPUT IDENTIFICATION

Table 8.11 represents a summary of the above seven parametric tests (gridding and grid free). It includes inputs that have shown zero p-value for a specific output ( $Y_1, Y_2, \dots, Y_6$ ). For model Terminal IRI ( $Y_1$ ),  $X_1$  (AADTT) and  $X_4$  (Percent of Trucks in Design Lane) is common for all test. So, it can be said that these two inputs are most important factor for  $Y_1$  without any doubt. Next,  $X_{13}$  (top AC layer thickness),  $X_{18}$  (bottom AC layer Thickness),  $X_{26}$  (subgrade modulus) are obtained in several tests.  $X_{10}$  (tire pressure) is obtained as significant only in two tests.  $X_{25}$  (base modulus) is obtained as significant only in linear regression result.

For  $Y_2$  (longitudinal Cracking),  $X_{18}$  (bottom AC layer Thickness) is found in all test result.  $X_1$  (AADTT) and  $X_4$  (Percent of Trucks in Design Lane) are also obtained from all but one test. Among all 7 test,  $X_{25}$  (base modulus) is obtained in 6 test result.  $X_{17}$  (percent air void of top AC layer) is captured by five tests. Both  $X_{27}$  (subgrade modulus) and  $X_{13}$  (top AC layer thickness) are obtained in four test result.

For  $Y_3$  (alligator cracking), three input variables are common to all test results and can be said as vary important factor for alligator cracking. They are  $X_1$  (AADTT),  $X_4$  (Percent of Trucks in Design Lane) and  $X_{18}$  (bottom AC layer Thickness). Among all seven test,  $X_{22}$  (percent air void

of bottom AC layer) is obtained in 6 test results except SRD test.  $X_{13}$  (top AC layer thickness) is common for all test result except SI and SRD test. Without these, another variable is obtained for  $Y_3$  which is  $X_{25}$  (Base modulus) which is captured by four test results.

For  $Y_4$  or transverse cracking, no input variable is obtained with zero p-values except SI test. For SI test, total five input variables are found with zero p-values. Among them, two are  $X_{14}$  and  $X_{19}$  (aggregate gradation of top and bottom AC layer). Superpave binder grade of both layers ( $X_{16}$  and  $X_{21}$ ) are also captured in this test. So, it is clear that mix properties affect transverse cracking significantly.

**TABLE 8.11 Summary of most significant inputs (p-value = 0)**

Output/ Predicted Distress	CMN	CL	SI	LREG	QREG	RCC	SRD
$Y_1$	$X_{18}$ $X_1$ $X_4$ $X_{13}$	$X_1$ $X_4$ $X_{18}$ $X_{26}$ $X_{27}$	$X_1$ $X_4$ $X_{18}$ $X_{26}$	$X_{18}$ $X_1$ $X_4$ $X_{13}$ $X_{27}$ $X_{26}$ $X_{25}$	$X_1$ $X_4$ $X_{18}$ $X_{13}$ $X_{26}$ $X_{27}$	$X_1$ $X_4$ $X_{18}$ $X_{26}$ $X_{27}$ $X_{13}$ $X_{10}$	$X_4$ $X_1$
$Y_2$	$X_{18}$ $X_4$ $X_1$ $X_{24}$ $X_{25}$ $X_{17}$	$X_{18}$ $X_1$ $X_4$ $X_{27}$ $X_{24}$ $X_{25}$ $X_{13}$	$X_{18}$ $X_4$ $X_1$ $X_{27}$	$X_{18}$ $X_4$ $X_1$ $X_{25}$ $X_{17}$ $X_{13}$	$X_{18}$ $X_4$ $X_1$ $X_{25}$ $X_{17}$	$X_{18}$ $X_4$ $X_1$ $X_{27}$ $X_{25}$ $X_{13}$ $X_{17}$	$X_{18}$
$Y_3$	$X_{18}$ $X_1$ $X_4$ $X_{22}$ $X_{13}$ $X_{25}$	$X_{18}$ $X_4$ $X_1$ $X_{22}$ $X_{13}$	$X_{18}$ $X_1$ $X_4$ $X_{22}$	$X_{18}$ $X_1$ $X_4$ $X_{22}$ $X_{13}$ $X_{25}$	$X_{18}$ $X_1$ $X_4$ $X_{22}$ $X_{13}$ $X_{25}$	$X_{18}$ $X_4$ $X_1$ $X_{22}$ $X_{13}$ $X_{25}$	$X_{18}$ $X_4$ $X_1$
$Y_4$	None	None	$X_{14}$ $X_{19}$ $X_{21}$ $X_{16}$ $X_2$	None	None	None	None
$Y_5$	$X_1$ $X_4$ $X_{10}$ $X_{18}$ $X_8$	$X_1$ $X_4$ $X_{10}$ $X_{18}$ $X_8$	$X_1$ $X_4$ $X_{10}$	$X_1$ $X_4$ $X_{10}$ $X_{18}$ $X_8$ $X_{13}$	$X_1$ $X_4$ $X_{10}$ $X_{18}$ $X_8$	$X_1$ $X_4$ $X_{10}$ $X_{18}$ $X_8$	$X_1$ $X_4$
$Y_6$	$X_1$ $X_4$ $X_{18}$ $X_{27}$ $X_{10}$	$X_1$ $X_4$ $X_{18}$ $X_{27}$ $X_{10}$	$X_1$ $X_4$ $X_{18}$ $X_{26}$ $X_{27}$	$X_1$ $X_4$ $X_{18}$ $X_{27}$ $X_{10}$ $X_{13}$ $X_8$	$X_1$ $X_4$ $X_{18}$ $X_{27}$ $X_{10}$ $X_{13}$ $X_8$	$X_1$ $X_4$ $X_{18}$ $X_{27}$ $X_{10}$ $X_{13}$ $X_8$ $X_{26}$	$X_1$ $X_4$

For  $Y_5$  (AC rutting), excellent result is obtained from scatter plot test result.  $X_1$  (AADTT) and  $X_4$  (Percent of Trucks in Design Lane) can be categorized as most important factor.  $X_{10}$  (tire pressure),  $X_{18}$  (bottom AC layer thickness) and  $X_8$  (traffic growth factor) are important because

they are captured in almost of the test cases. In case of model  $Y_6$  or total rutting, similar results are observed from all test results. Like AC rutting, most important factors are  $X_1$  (AADTT) and  $X_4$  (Percent of Trucks in Design Lane) as they are obtained for all tests.  $X_{18}$ ,  $X_{27}$  and  $X_{10}$  can be categorized as important as they are common to almost all cases.  $X_8$  (traffic growth factor) and  $X_{13}$  (top Ac layer thickness) should be part of attention as they are also obtained as significant.

From Table 8.11, it is evident that SRD method produces only a few but very significant inputs. On the contrary, RCC and LREG produce relatively a large number of inputs. Therefore, depending on available resources, one may decide whether a large or small significant inputs for detailed study and pavement design. Another observation can be made from Table 8.11 is that factors for transverse cracking ( $Y_4$ ) can be seen only from SI test results. Therefore, inclusion of seven methods for MEPDG sensitivity is justified. Each methods has drawbacks and advantages, which are not discussed in this study. Irrespective of that, it can be said that sensitivity study using these few methods is rigorous.

In the next section an attempt is made to rank the input factors based on their relative contributions to a specific output. In particular, stepwise regression is employed to rank the significant inputs shown in Table 8.11. For example,  $Y_1$  (terminal IRI) model considers all the input factors obtained as significant from all tests (Table 8.4 to 8.10). That is,  $Y=f(X_1, X_4, X_{18}, X_{26}, X_{27}, X_{10}, X_{30}, X_{13}, X_8, X_3, X_{29}, X_5, X_{22}, X_{12}, X_{17}, X_{11}, X_{25})$ .

## RANKING OF INPUTS BY RANK REGRESSION

In this section, calculation of sensitivity is performed using stepwise rank regression method. To avoid the problem of nonlinearity, this test is chosen. It is always difficult to fit a nonparametric regression model with a large number of input variables. Therefore, stepwise variable selection is used for this regression model.

In the previous section, the determination of the coefficients  $b_j$  of Eq. 13 was not necessary for input identification purpose (Draper, N. R. 1981). However, if  $b_j$  can be calculated, they can be used to indicate the importance of individual input variables  $X_j$  with respect to the uncertainty in output  $Y$  (Saltelli et al. 2004). In that case, the regression model can be written as:

$$\frac{Y - \bar{Y}}{\hat{s}} = \sum_j \frac{b_j \hat{s}_j}{\hat{s}} \times \frac{X_j - \bar{X}_j}{\hat{s}_j} \quad (20)$$

where,

$$\bar{Y} = \sum_i \frac{Y_i}{N} \text{ and } \bar{X}_j = \sum_i \frac{X_{ij}}{N} ;$$

$$\hat{s} = \left[ \sum_i \frac{(Y_i - \bar{Y})^2}{N - 1} \right]^{1/2} \text{ and } \hat{s}_j = \left[ \sum_i \frac{(X_{ij} - \bar{X}_j)^2}{N - 1} \right]^{1/2}$$

The coefficients  $\frac{b_j \hat{s}_j}{\hat{s}}$  are called standardized regression coefficients (SRC). Another important measure from regression analysis is partial correlation coefficient (PCC). It can be obtained by

using a sequence of regression model between output and input variables. First, the following two models are constructed

$$\hat{Y} = b_0 + \sum_{h \neq 1} b_h x_h \quad (21)$$

$$\hat{X}_j = c_0 + \sum_{h \neq 1} c_h x_h \quad (22)$$

Then the results of these two regression are used to define the new variables:  $Y - \hat{Y}$  and  $X_j - \hat{X}_j$ . The partial correlation between Y and  $X_j$  is defined as the correlation coefficients between  $Y - \hat{Y}$  and  $X_j - \hat{X}_j$  (Helton et al, 1993). Rank regression works very well to identify the strength of relationships between inputs and output in nonlinear situations as long the relationships between inputs and output are approximately monotonic (Helton et al. 2006; Iman, R. L, 1979). The procedure for rank regression involves replacing the data with their corresponding ranks.

$$Y = (Y_1, Y_2, \dots, Y_N) \quad (23)$$

where Y is vector of N values is generated by repeatedly evaluating the model for a set of N sampled vector

$$(X_{11}, X_{12}, \dots, x_{N1k}); \dots (X_{N1}, X_{N2}, \dots, X_{Nk})$$

The observations are then replaced by their corresponding ranks. This is followed from highest values (rank 1) to lowest values (rank N).

## Results of Ranking

The p-value provides the criterion for assessing the importance of input variables. Bootstrap confidence intervals are created for PCC<sup>2</sup> based on a bootstrap sample of size 1000 (Storlie et al., 2009). Number of bootstrap is 1000 for each model. In this method, the relationship of an output variable and one or more input variables are determined. Results of the statistical analysis of the regression models are presented in Table 8.12(a) to Table 8.12(f). The corresponding R<sup>2</sup> value of each model indicates the proportion of uncertainty of model is accounted.

### ***Output Y<sub>1</sub> (Terminal IRI)***

Table 12(a) presents the model summary of output variable Y<sub>1</sub> (Terminal IRI). The R<sup>2</sup> of this model is 0.85. This is a very good model because about 90 percent uncertainties are captured in this model. This model is summarized with 15 significant input variables obtained from previous section. R<sup>2</sup>, SRC, PCC, and CI are determined as summary result of rank regression method, which are described in this table. In the first and second column of the table, the input variables and their explanation are given. R<sup>2</sup> value for regression model is calculated and shown in the third column in cumulative terms. In the next column to this, increment of R<sup>2</sup> is presented which the individual R<sup>2</sup> value for each input variable.

**TABLE 8.12 Result of Rank Regression Analysis for Output Y1 (Terminal IRI)**

Input	Name	R <sup>2</sup>	Increment R <sup>2</sup> (%)	SRC	PCC <sup>2</sup>	95% PCC <sup>2</sup> CI
X <sub>1</sub>	AADTT	0.2670	27	0.5020	0.5950	(0.539, 0.644)
X <sub>4</sub>	Percent of Trucks in Design Lane (%)	0.4930	23	0.4620	0.5500	(0.492, 0.607)
X <sub>18</sub>	Bottom AC Layer Thickness	0.6350	14	-0.3710	0.4440	(0.383, 0.509)
X <sub>26</sub>	Subgrade Material	0.6840	5	0.2100	0.1970	(0.146, 0.259)
X <sub>27</sub>	Subgrade Modulus	0.7120	3	-0.1650	0.1370	(0.093, 0.191)
X <sub>10</sub>	Tire Pressure	0.7390	3	0.1680	0.1370	(0.093, 0.191)
X <sub>30</sub>	Optimum Gravimetric Water Content (%)	0.7640	3	-0.1510	0.1150	(0.075, 0.163)
X <sub>13</sub>	Top AC layer Thickness	0.7860	2	-0.1420	0.1050	(0.065, 0.151)
X <sub>8</sub>	Traffic Growth Factor	0.8010	2	0.1350	0.0950	(0.059, 0.140)
X <sub>3</sub>	Percent of Trucks in Design Direction (%)	0.8090	1	0.0840	0.0390	(0.018, 0.070)
X <sub>29</sub>	Liquid Limit	0.8160	1	0.0850	0.0400	(0.016, 0.074)
X <sub>5</sub>	Operational Speed (mph)	0.8240	1	-0.0890	0.0430	(0.018, 0.077)
X <sub>22</sub>	Percent Air Void of Bottom AC Layer	0.8280	0	0.0670	0.0250	(0.009, 0.050)
X <sub>12</sub>	Climatic Zones	0.8280	0	-0.0090	0.0000	(0.000, 0.010)
X <sub>17</sub>	Percent Air Void of Top AC Layer	0.8290	0	0.0270	0.0040	(0.000, 0.017)

For rank regression, R<sup>2</sup> value is very informative. The highest R<sup>2</sup> value is obtained for input variable X<sub>1</sub> (AADTT) and the value is 0.267. It means that 26.7% of the variance is explained by this input only. The second highest R<sup>2</sup> value is obtained by X<sub>4</sub> (percent of trucks in design lane) and the value is 0.226. About 23% of the variance captured by X<sub>4</sub>. The R<sup>2</sup> value (0.493) tells that 49% of the variance is explained by both X<sub>1</sub> and X<sub>4</sub>. Input variable X<sub>18</sub> (bottom AC layer thickness) has captured 14% uncertainties by itself. These three input variable mentioned above have captured 63.5% of uncertainties altogether among all the input variables used in these model. Then X<sub>26</sub> (type of subgrade material) explains 5% of the uncertainties. Both X<sub>27</sub> (subgrade modulus), X<sub>10</sub> (tire pressure) and X<sub>30</sub> (optimum gravimetric water content) has captured 3% of uncertainties individually. Rest of the input variables has increment R<sup>2</sup> value either 2% or 0%.

From the R<sup>2</sup> value discussed above, it can be said that first two parameters (X<sub>1</sub> and X<sub>4</sub>) are very important as they have explained at least 20% of the variance and altogether accounted almost half of the variance. Next parameter X<sub>18</sub> is important as itself explained at least 10% of the variance. The next parameters (X<sub>26</sub>, X<sub>27</sub>, X<sub>10</sub> and X<sub>30</sub>) are somewhat important as they explained at least 2% of the variance and altogether 14% of the variance. Rest of the parameters is not very important because they explain less than 10% of the variance altogether.

According to SRC value, importance of the variables can be measured. The SRC sign represent whether the parameter has a positive or negative influence on the output. The highest SRC value

obtained for  $X_1$  and  $X_4$ , which are 0.502 and 0.462 respectively. This means that, model  $Y_1$  will increase if  $X_1$  increases and vice versa.  $X_4$  has also positive influence like  $X_1$  on model  $Y_1$ .  $X_{18}$  has negative SRC value which is -0.371. The negative sign means that if  $X_{18}$  increases then  $Y_1$  will decrease and vice versa. Another variable  $X_{26}$  has SRC value 0.210, which has also the same positive effect like  $X_1$  and  $X_4$ .  $X_{27}$ ,  $X_{10}$  and  $X_{30}$  has the same  $R^2$  value individually but they have different SRC value with different sign. Among these three,  $X_{27}$  and  $X_{30}$  has negative influence on  $Y_1$ . That means if any of these two variable increase then  $Y_1$  will decrease.  $X_{10}$  has positive influence that means  $Y_1$  will increase or decrease if  $X_{10}$  increase or decreases.

The impact of  $X_1$  is approximately 8% larger than the impact of  $X_4$  (i.e.,  $(0.502-0.465)/0.465=0.082$ ). In this table, the lowest positive SRC value is obtained for  $X_{17}$  (percent air void of top AC layer) and the value is 0.027.  $PCC^2$  value is also provided in this table in a separate column. The ranking of importance between SRC and PCC is the same here, which means that there is no strong correlation between the inputs is working in this model  $Y_1$ . The confidence interval column given here, helps testing the stability of the result. So for  $X_1$ , the estimated value for  $PCC^2$  is 0.595, but 95% of the time, the true value of  $PCC^2$  would be between 0.539 and 0.644. However, for  $X_4$ , calculated  $PCC^2$  is 0.550 but 95% of the time, the true value of  $PCC^2$  would be between 0.492 to 0.607.

### ***Output Y2 (Longitudinal Cracking)***

Rank Regression analysis has done for Model  $Y_2$  (Longitudinal Cracking) and presented in Table 8.13. This is a very good model because the  $R^2$  value of this model is 0.83. About 90 percent uncertainties are captured in this model so this method is appropriate for this model. This model is summarized with 15 significant input variables.  $R^2$ , SRC, PCC, and CI are determined as summary result of rank regression method, which are described in this table. In the first and second column of the table, the input variables and their explanation are given.  $R^2$  value for all input variables used in this model  $Y_2$  is calculated and shown in the third column in cumulative terms. In the next column to this, increment of  $R^2$  is presented which the individual  $R^2$  value for each input variable.

The highest  $R^2$  value is obtained for  $X_{18}$  (bottom AC layer thickness) is 0.485. It means that 49% of the variance is explained by this input only. From this  $R^2$  value, it can be said this parameter ( $X_{18}$ ) is very important as itself explained almost half of the variance. SRC value for this input variable is obtained 0.679, which is negative. It means that, if  $X_{18}$  decreases then model  $Y_2$  will increase. If  $Y_2$  need to decrease then  $X_{18}$  needs to be increased. The PCC value obtained for this variable is 0.714. This is the highest value among all other input variables. Therefore, it is decided that this is the most important factor for this model. However, the calculated PCC value for this input is 0.714, but 95% of the time this value will be within 0.671 to 0.751.

In this table, three input variables can be categorized as slightly less important. These are  $X_1$  (AADTT),  $X_4$  ((percent of trucks in design lane) and  $X_{27}$  (subgrade modulus).  $R^2$  value obtained for these three input variables are almost close to each other (7%, 6% and 6% respectively). These three input variables explain at least 5% of the variance individually and altogether around 20%. SRC values of these variables are also close to each other. From SRC value, it can be said

that these all three have positive influence on model  $Y_2$ .  $Y_2$  will increase if any of these value increases and vice versa.

Total four input variables can be categorized as somewhat important for model  $Y_2$ . They explain at least 2% of the variance and altogether 13% of the variance). They are  $X_{24}$ ,  $X_{25}$ ,  $X_{13}$  and  $X_{17}$ . Among these,  $X_{24}$  and  $X_{25}$  represent base material type and base modulus.  $X_{24}$  (base material type) has positive influence on  $Y_2$  but  $X_{25}$  (base modulus) has negative effect.  $X_{13}$  and  $X_{17}$  indicate top AC layer properties, which are thickness and percent air void.  $X_{13}$  and  $X_{17}$  have almost same SRC value but of opposite sign. If AC layer thickness or  $X_{13}$  increases then  $Y_2$  or long crack will be reduced. Again,  $Y_2$  will increase if percent air void or  $X_{17}$  increases. Rest of the parameters mentioned in the model is not important because they explain less than 10% of the variance altogether.

**TABLE 8.13 Result of Rank Regression Analysis for Output  $Y_2$  (Longitudinal Cracking)**

Input	Name	$R^2$	Increment $R^2$ (%)	SRC	$PCC^2$	95% $PCC^2$ CI
$X_{18}$	Bottom AC Layer Thickness	0.485	49	-0.679	0.714	(0.671, 0.751)
$X_1$	AADTT	0.555	7	0.252	0.255	(0.199, 0.319)
$X_4$	Percent of Trucks in Design Lane (%)	0.615	6	0.235	0.230	(0.171, 0.287)
$X_{27}$	Subgrade Modulus	0.676	6	0.254	0.260	(0.208, 0.318)
$X_{24}$	Base Material	0.712	4	0.193	0.163	(0.111, 0.216)
$X_{13}$	Top AC Layer Thickness	0.746	3	-0.175	0.143	(0.097, 0.199)
$X_{17}$	Percent Air void of top AC layer	0.777	3	0.172	0.138	(0.094, 0.193)
$X_{25}$	Base Modulus	0.805	3	-0.158	0.118	(0.078, 0.164)
$X_{15}$	Effective Binder Content (%) of Top AC Layer	0.810	1	-0.072	0.027	(0.008, 0.058)
$X_8$	Traffic Growth Factor	0.814	0	0.072	0.027	(0.007, 0.058)
$X_{16}$	Superpave Binder Grade of Top AC Layer	0.815	0	0.035	0.006	(0.000, 0.022)
$X_{11}$	Depth of Water Table (ft)	0.817	0	0.035	0.006	(0.000, 0.025)
$X_{19}$	Aggregate Gradation of Bottom AC Layer	0.817	0	0.005	0.000	(0.000, 0.007)
$X_3$	Percent of Trucks in Design Direction (%)	0.817	0	0.026	0.004	(0.000, 0.017)
$X_5$	Operational Speed (mph)	0.818	0	-0.025	0.003	(0.000, 0.017)

The impact of  $X_{18}$  (thickness of 2<sup>nd</sup> AC layer) is approximately 280% larger than the impact of  $X_{13}$  (thickness of top AC layer) (i.e.,  $(0.680-0.175)/0.175=2.8$ ) which seems interesting in this result. The impact of  $X_{27}$  (subgrade modulus) and the impact of  $X_{25}$  (base modulus) are opposite which is also remarkable.

$PCC^2$  value is also provided in this table in a separate column. The ranking of importance between SRC and PCC is the same here, which means that there is no strong correlation between

the inputs is working in this model  $Y_2$ . The confidence interval column given here, helps testing the stability of the result.

### ***Output Y3 (Alligator Cracking)***

Table 8.14 presents the model summary of output variable  $Y_3$  (alligator cracking). This can be said as an excellent model because the  $R^2$  of this model is 0.87. About 90 percent uncertainties are captured in this model. This method is appropriate for modeling alligator crack. This model is summarized with 14 significant input variables among 30 input variables.  $R^2$ , SRC, PCC and CI are determined for all these 14 input variables, which are described in this table. For all variables in each row,  $R^2$  value for regression model is calculated and shown in the third column in cumulative terms. In the next column to this, increment of  $R^2$  is presented which is the individual  $R^2$  value for each input variable.

**TABLE 8.14 Result of rank regression analysis for output Y3 (alligator cracking)**

Input	Name	$R^2$	Increment $R^2$ (%)	SRC	PCC <sup>2</sup>	95% PCC <sup>2</sup> CI
$X_{18}$	Bottom AC Layer Thickness	0.466	47	-0.656	0.755	(0.711, 0.795)
$X_4$	Percent of Trucks in Design Lane (%)	0.610	14	0.356	0.477	(0.403, 0.548)
$X_1$	AADTT	0.736	13	0.355	0.478	(0.420, 0.536)
$X_{22}$	Percent Air Void of Bottom AC Layer	0.790	5	0.218	0.253	(0.188, 0.317)
$X_{13}$	Top AC Layer Thickness	0.818	3	-0.166	0.166	(0.115, 0.217)
$X_{25}$	Base Modulus	0.830	1	-0.091	0.056	(0.030, 0.088)
$X_{24}$	Base Material	0.839	1	0.105	0.070	(0.037, 0.113)
$X_8$	Traffic Growth Factor	0.849	1	0.108	0.077	(0.041, 0.122)
$X_{27}$	Subgrade Modulus	0.855	1	-0.074	0.038	(0.015, 0.069)
$X_3$	Percent of Trucks in Design Direction (%)	0.860	1	0.063	0.028	(0.009, 0.053)
$X_{30}$	Optimum Gravimetric Water Content (%)	0.861	0	-0.040	0.011	(0.000, 0.030)
$X_{12}$	Climatic Zones	0.861	0	0.002	0.000	(0.000, 0.007)
$X_5$	Operational Speed (mph)	0.862	0	-0.034	0.008	(0.000, 0.025)

The highest value is obtained for  $X_{18}$  (second AC layer thickness) is 0.466. It means that 47% of the variance is explained by this input only. The next  $R^2$  value (0.610) tells that 61 % of the variance is explained by both  $X_{18}$  and  $X_4$  (percent of trucks in design lane). The  $R^2$  value (0.736) tells that 74 % of the variance is explained by  $X_{18}$ ,  $X_4$  and  $X_1$  (AADTT).  $X_4$  itself explains 14% uncertainties of the model. Then  $X_1$  explains 13% of the uncertainties. Both  $X_{22}$  (percent air void of second AC layer) and  $X_{13}$  (top AC layer thickness) has captured 5% and 3% of uncertainties individually. Rest of the input variables has increment  $R^2$  value either 1% or 0%. Therefore, the most important factor for model  $Y_3$  is  $X_{18}$ . The SRC value for this parameter is -0.656, which



helps to understand the influence type of this factor.  $X_{18}$  has negative effect on  $Y_3$ . It means that if  $Y_3$  value needs to be minimized, than at first  $X_{18}$  value needs to be increase and vice versa.  $X_{18}$  also has highest PCC value among this table, which also helps to categorize this input as most important. For  $X_{18}$ , the estimated value for  $PCC^2$  is 0.755, but 95% of the time; the true value of  $PCC^2$  would be between 0.711 and 0.795.

Both  $X_4$  and  $X_1$  can be considered as important factor for the model  $Y_3$  because they explain at least 10% of the variance. These two parameters have also same type of effect with same SRC value. This means that  $Y_3$  will increase if any of these parameter value increases. The next two parameters ( $X_{22}$  and  $X_{13}$ ) are somewhat important as they explained at least 2% of the variance and altogether 8% of the variance.  $X_{22}$  has positive effect on  $Y_3$  with SRC value 0.218.  $X_{13}$  has negative effect on  $Y_3$  with SRC value 0.166. Rest of the parameters is not very important because they explain 1% or less of the variance individually. In addition to this, they altogether explained less than 10% of the variance. The impact of  $X_{18}$  (second AC layer thickness) is approximately 300% larger than the impact of  $X_{13}$  (top AC layer thickness) (i.e.,  $(0.656-0.166)/0.166=2.92$ ).  $PCC^2$  value is also provided in this table in a separate column. The ranking of importance between SRC and PCC is the same here, which means that there is no strong correlation between the inputs is working in this model  $Y_3$ .

#### ***Output Y4 (Transverse Cracking)***

Table 8.15 presents the model summary of output variable  $Y_4$  (transverse cracking). The  $R^2$  of this model is 0.04. This is a not a very good model because only 4 percent uncertainties are captured in this model. Therefore, any other method may be appropriate for this model. Among 10 significant input variables, this model is summarized with two input variables by following stepwise addition/deletion.  $R^2$ , SRC, PCC and CI are determined for all these input variables, which are described in this table.

**TABLE 8.15 Result of regression analysis for output Y4 (transverse cracking)**

Input	Name	$R^2$	Increment $R^2$ (%)	SRC	$PCC^2$	95% $PCC^2$ CI
$X_{16}$	Superpave Binder Grade of top AC Layer	0.015	1.5	0.027	0.015	(0.000, 0.031)
$X_{12}$	Climatic zones	0.021	0.6	-0.017	0.007	(0.000, 0.027)

For all variables in each row,  $R^2$  value for regression model is calculated and shown in the third column in cumulative terms. In the next column to this, increment of  $R^2$  is presented which the individual  $R^2$  value for each input variable is. The highest value is obtained for  $X_{16}$  (Superpave binder grade of top AC layer) is 0.015. It means that 2% of the variance is explained by this input only. The next  $R^2$  value (0.021) tells that 2.1 % of the variance is explained by both  $X_{16}$  and  $X_{12}$  (Climatic zones).  $X_{12}$  itself explains 1% uncertainties of the model.

SRC provides the measure of importance of the variables. The highest SRC value obtained for  $X_{16}$  which is 0.027. This means that, model  $Y_4$  will increase if  $X_{16}$  increases and vice versa. The

next SRC value obtained for  $X_{12}$  and the value is -0.017. The negative sign means that  $X_{12}$  has negative effect on model  $Y_4$ .

The ranking of importance between SRC and PCC is the same here, which means that there is no strong correlation between the inputs is working in this model  $Y_4$ . The confidence interval column given here, helps testing the stability of the result. So for  $X_{16}$ , the estimated value for  $PCC^2$  is 0.015, but 95% of the time, the true value of  $PCC^2$  would be between 0.000 and 0.031. However, for  $X_{12}$ , calculated  $PCC^2$  is 0.007 but 95% of the time, the true value of  $PCC^2$  would be between 0 to 0.027.

### ***Output Y5 (AC Rut)***

Table 8.16 presents the model summary of output variable  $Y_5$  (AC rutting). The  $R^2$  of this model is 0.87, which means almost 90% of uncertainties are captured in this model. Therefore, this is a very good model and this method is appropriate for this model, too. Among 30 input variables, this model is summarized with 15 significant input variables.  $R^2$ , SRC, PCC are determined for all these input variables, which are described in this table. In the first two column of this table, name and explanation of these input variables are given.  $R^2$  value for this regression model is calculated and shown in the third column in cumulative terms. In the next column to this, increment of  $R^2$  is given which is the individual  $R^2$  value for each input variable. In this model the first two input variable can be categorized as most important factor because they explain at least 10% of the variance and altogether more than half of the variance. Among them, one is  $X_1$  (AADTT). The highest  $R^2$  value in this model is obtained for  $X_1$  and the value is 0.389. It means that 39% of the variance is explained by this input only. Another most important factor for this model is  $X_4$  (percent of trucks in design lane).  $X_4$  explains 26% of the total uncertainties. The  $R^2$  value (0.645) tells that 65 % of the variance is explained by both  $X_1$  and  $X_4$ . Then  $X_{10}$  (tire pressure) explains 8% of the uncertainties. Therefore it can be categorized as slightly less important as less than 10% of the variance are captured by this input. Both  $X_{18}$  (second AC layer thickness) and  $X_8$  (traffic growth factor) has captured 4% and 3% of uncertainties individually. These two parameters are somewhat important as they explained at least 2% of the variance and altogether 7% of the variance. Rest of the input variables has increment  $R^2$  value either 2% or less. They are not very important because they explain 2% or less of the variance individually. In addition to this, they altogether explained less than 10% of the variance.

The SRC number and sign gives the importance and influence type on the output. The highest SRC value obtained for  $X_1$ , which is 0.571. This means that, model  $Y_5$  will increase if  $X_1$  increases and vice versa.  $X_4$  has also SRC value 0.509 which is almost close to  $X_1$ . It has the same positive effect like  $X_1$ .  $X_{10}$  has SRC value 0.29 and has the same positive effect like  $X_1$  and  $X_4$ .  $X_{18}$  has negative SRC value of 0.188. The negative sign means that if  $X_{18}$  increases then  $Y_5$  will decrease and vice versa. The impact of  $X_1$  is approximately 11% larger than the impact of  $X_4$  (i.e.,  $(0.571-0.509)/0.509=0.12$ ). In this table, the lowest positive SRC value is obtained for  $X_{20}$  (effective binder content of bottom AC Layer) and the value is 0.044. The impact of  $X_1$  is 1200% larger than  $X_{22}$ .

Usually PCC works out the same as SRC. The ranking of importance between SRC and PCC is the same here, which means that there is no strong correlation between the inputs is working in

this model  $Y_5$ . The confidence interval column given here, helps testing the stability of the result. So for  $X_1$ , the estimated value for  $PCC^2$  is 0.715, but 95% of the time, the true value of  $PCC^2$  would be between 0.676 and 0.753. However, for  $X_4$ , calculated  $PCC^2$  is 0.663 but 95% of the time, the true value of  $PCC^2$  would be between 0.616 to 0.707.

**TABLE 8.16 Result of rank regression analysis for output  $Y_5$  (permanent deformation, AC only)**

Input	Name	$R^2$	Increment $R^2$ (%)	SRC	$PCC^2$	95% $PCC^2$ CI
$X_1$	AADTT	0.389	39	0.571	0.715	(0.676, 0.753)
$X_4$	Percent of Trucks in Design Lane (%)	0.645	26	0.509	0.663	(0.616, 0.707)
$X_{10}$	Tire Pressure	0.728	8	0.29	0.387	(0.330, 0.443)
$X_{18}$	Bottom AC layer Thickness	0.765	4	-0.188	0.213	(0.160, 0.271)
$X_8$	Traffic Growth factor	0.793	3	0.165	0.172	(0.124, 0.222)
$X_{12}$	Climatic Zones	0.813	2	0.133	0.114	(0.071, 0.163)
$X_{13}$	Top AC Layer	0.827	1	-0.115	0.093	(0.053, 0.140)
$X_5$	Operational Speed (mph)	0.836	1	-0.094	0.062	(0.031, 0.098)
$X_{16}$	Superpave Binder Grade of Top AC Layer	0.844	1	0.098	0.061	(0.029, 0.101)
$X_3$	Percent of Trucks in Design Direction (%)	0.85	1	0.087	0.054	(0.027, 0.092)
$X_{30}$	Optimum Gravimetric Water Content (%)	0.856	1	0.084	0.051	(0.025, 0.086)
$X_{21}$	Superpave Binder Grade of Bottom AC Layer	0.86	0	0.066	0.029	(0.011, 0.056)
$X_6$	AADTT Distribution by Vehicle Class 9 (%)	0.865	1	0.07	0.036	(0.013, 0.070)
$X_{22}$	Percent Air Void of Bottom AC Layer	0.869	0	0.058	0.025	(0.007, 0.056)
$X_{20}$	Effective Binder Content (%) of Bottom AC Layer	0.87	0	0.044	0.014	(0.000, 0.036)

### **Output $Y_6$ (Total Rut)**

Table 8.17 presents the model summary of output variable  $Y_6$  for total rut. The  $R^2$  of this model is 0.86. This is a very good model because almost 90 percent uncertainties are captured in this model. This model is summarized with 15 significant input variables by following stepwise addition/deletion. For all variables in each row,  $R^2$  value for regression model is calculated and shown in the third column in cumulative terms. In the next column to this, increment of  $R^2$  is presented which the individual  $R^2$  value for each input variable is.

**TABLE 8.17 Result of Rank Regression Analysis for Output Y6 (Permanent Deformation (Total Pavement))**

Input	Name	R <sup>2</sup>	Increment R <sup>2</sup> (%)	SRC	PCC <sup>2</sup>	95% PCC <sup>2</sup> CI
X <sub>1</sub>	AADTT	0.317	32	0.534	0.648	(0.603, 0.690)
X <sub>4</sub>	Percent of Trucks in Design Lane (%)	0.554	24	0.475	0.588	(0.531, 0.640)
X <sub>18</sub>	Bottom AC layer Thickness	0.635	8	-0.289	0.349	(0.287, 0.404)
X <sub>10</sub>	Tire Pressure	0.674	4	0.202	0.203	(0.149, 0.263)
X <sub>27</sub>	Subgrade Modulus	0.712	4	-0.189	0.187	(0.132, 0.247)
X <sub>30</sub>	Optimum Gravimetric Water Content (%)	0.747	4	-0.18	0.171	(0.121, 0.224)
X <sub>8</sub>	Traffic Growth Factor	0.772	3	0.154	0.131	(0.085, 0.184)
X <sub>26</sub>	Subgrade Material	0.79	2	0.139	0.107	(0.066, 0.151)
X <sub>13</sub>	Top AC layer Thickness	0.809	2	-0.137	0.108	(0.071, 0.158)
X <sub>12</sub>	Climatic Zones	0.824	1	0.116	0.077	(0.040, 0.124)
X <sub>3</sub>	Percent of Trucks in Design Direction (%)	0.834	1	0.095	0.054	(0.027, 0.088)
X <sub>5</sub>	Operational Speed (mph)	0.841	1	-0.087	0.046	(0.022, 0.081)
X <sub>21</sub>	Superpave Binder Grade of Bottom AC Layer	0.843	0	0.051	0.014	(0.000, 0.035)
X <sub>22</sub>	Percent Air Void of Bottom AC Layer	0.845	0	0.035	0.008	(0.000, 0.026)
X <sub>17</sub>	Percent Air Void of Top AC Layer	0.846	0	0.035	0.008	(0.000, 0.023)

The highest value is obtained for X<sub>1</sub> (AADTT) is 0.317. It means that 32% of the variance is explained by this input only. The next R<sup>2</sup> value (0.554) tells that 55.5 % of the variance is explained by both X<sub>1</sub> and X<sub>4</sub> (percent of trucks in design lane). X<sub>4</sub> itself explains 24% uncertainties of the model. Then X<sub>18</sub> (AC layer thickness of bottom layer) explains 8% of the uncertainties. The next three parameters X<sub>10</sub> (tire pressure), X<sub>27</sub> (subgrade modulus) and X<sub>30</sub> (optimum gravimetric water content) captured 4% of uncertainties individually. Rest of the input variables has increment R<sup>2</sup> value either 3% or less. Therefore, it can be said that first two parameters are very important as they have explained at least 10% of the variance and altogether accounted almost half of the variance. The next parameters (X<sub>18</sub>) is important as it explained 8% of the variance. The next three parameters are somewhat important (they explain at least 4% of the variance and altogether 12% of the variance). Rest of the parameters is not very important because they explain 2% or less of the variance individually. In addition to this, they altogether explained 10% of the variance.

SRC provides the measure of importance of the variables and type of the influence on the output. The highest SRC value obtained for X<sub>1</sub> and X<sub>4</sub>, which are 0.534 and 0.475 respectively. This means that, model Y<sub>6</sub> will increase if X<sub>1</sub> increases and vice versa. The same condition also applies for X<sub>4</sub>. Another variable X<sub>18</sub> has SRC value -0.289 which has opposite effect of X<sub>1</sub> and X<sub>4</sub>. The impact of X<sub>1</sub> is approximately 12% larger than the impact of X<sub>4</sub> (i.e., (0.534-0.475)/0.475=0.12). PCC<sup>2</sup> value is also provided in this table in a separate column. The ranking

of importance between SRC and PCC is the same here, which means that there is no strong correlation between the inputs is working in this model  $Y_6$ . The confidence interval column given here, helps testing the stability of the result. So for  $X_1$ , the estimated value for  $PCC^2$  is 0.648, but 95% of the time, the true value of  $PCC^2$  would be between 0.603 and 0.690. However, for  $X_4$ , calculated  $PCC^2$  is 0.588 but 95% of the time, the true value of  $PCC^2$  would be between 0.531 to 0.640.

## SUMMARY OF RANKING

Rank regression results are summarized and presented in Table 8.18. The  $R^2$  of the models are shown.  $R^2$  is 0.85 means that only 85% of the variance can be explained using rank regression. A true non-linear model including further of MEPDG inputs may yield a higher  $R^2$  value, however  $R^2$  value of 0.85 suffices the purpose of this study. This is adequate to describe the general behavior of the output and hence identify the important inputs.

For  $Y_1$  (terminal IRI),  $Y_2$  (longitudinal cracking) and  $Y_3$  (alligator cracking),  $Y_5$  (rutting of AC layer) and  $Y_6$  (rutting of total pavement) good  $R^2$  values are obtained from rank regression method (more than 0.8). It indicates that, these models are sufficient to get an idea about the input variables which have significant effect on flexible pavement performance. In case of model  $Y_4$  (Transverse cracking), this method failed to provide any reasonable  $R^2$  value. Any A more flexible method is required to study the sensitivity of  $Y_4$ .

The inputs are categorized in three groups based on their individual  $R^2$  value. This is based on a rule of thumb some statisticians have used previously. In order to classify the input variables in groups of importance (high importance, medium importance, low importance), some cut off values are used in the incremental  $R^2$ . Usually,  $R^2$  increment of more than 10% is visible on a scatter plot. Between 2% and 10%,  $R^2$  value requires log transform values to be visible). Below 2%, it looks like randomness. Based on this, the following discretization, which seems reasonable and appropriate in the context of the analysis is used in this study to categorize importance.

- If the variance in an input parameter explains at least 10% of the variance of the output of interest, then it is considered of high importance. Based on this, IRI ( $Y_1$ ) is highly sensitive to  $X_1$  (AADTT),  $X_4$  (percent of trucks in design lane), and  $X_{18}$  (bottom AC layer thickness).
- If the variance in a input parameter explains between 2% and 9% of the variance of the output of interest, then it is considered of medium importance. Due to this, IRI ( $Y_1$ ) is medium sensitive to  $X_{26}$  (subgrade material),  $X_{27}$  (subgrade Modulus),  $X_{10}$  (tire pressure),  $X_{30}$  (water content),  $X_{13}$  (top AC layer thickness),  $X_8$  (Traffic growth factor).
- Finally, if the variance of an input parameter explains less than 2% of the variance of the output of interest or if the parameter is not selected by the stepwise algorithm, it is considered of low importance. Therefore, IRI ( $Y_1$ ) is low sensitive to  $X_3$  (percent of Trucks in Design Direction (%)),  $X_{29}$  (Liquid Limit),  $X_5$  (Operational Speed (mph)),  $X_{22}$  (Percent Air Void of Bottom AC Layer),  $X_{12}$  (Climatic Zones),  $X_{17}$  (Percent Air Void of Top AC Layer).

**TABLE 8.18 Summary of Rank Regression Analysis**

Model	Name	R <sup>2</sup>	High	Medium	Low
Y <sub>1</sub>	Terminal IRI	<b>0.85</b>	X <sub>1</sub> X <sub>4</sub> X <sub>18</sub>	X <sub>26</sub> X <sub>27</sub> X <sub>10</sub> X <sub>30</sub> X <sub>13</sub> X <sub>8</sub>	X <sub>3</sub> X <sub>29</sub> X <sub>5</sub> X <sub>22</sub> X <sub>12</sub> X <sub>17</sub>
Y <sub>2</sub>	Longitudinal Cracking	<b>0.83</b>	X <sub>18</sub>	X <sub>1</sub> X <sub>4</sub> X <sub>27</sub> X <sub>24</sub> X <sub>13</sub> X <sub>17</sub> X <sub>25</sub>	X <sub>15</sub> X <sub>8</sub> X <sub>16</sub> X <sub>11</sub> X <sub>19</sub> X <sub>3</sub> X <sub>5</sub>
Y <sub>3</sub>	Alligator Cracking	<b>0.87</b>	X <sub>18</sub> X <sub>4</sub> X <sub>1</sub>	X <sub>22</sub> X <sub>13</sub>	X <sub>25</sub> X <sub>24</sub> X <sub>8</sub> X <sub>27</sub> X <sub>3</sub> X <sub>30</sub> X <sub>12</sub> X <sub>5</sub>
Y <sub>4</sub>	Transverse Cracking	<b>.04</b>	None	None	X <sub>16</sub> X <sub>12</sub>
Y <sub>5</sub>	AC Rutting	<b>0.87</b>	X <sub>1</sub> X <sub>4</sub>	X <sub>10</sub> X <sub>18</sub> X <sub>8</sub> X <sub>12</sub>	X <sub>13</sub> X <sub>5</sub> X <sub>16</sub> X <sub>3</sub> X <sub>30</sub> X <sub>21</sub> X <sub>6</sub> X <sub>22</sub>
Y <sub>6</sub>	Total Rutting	<b>0.86</b>	X <sub>1</sub> X <sub>4</sub>	X <sub>18</sub> X <sub>10</sub> X <sub>27</sub> X <sub>30</sub> X <sub>8</sub> X <sub>26</sub> X <sub>13</sub>	X <sub>12</sub> X <sub>3</sub> X <sub>5</sub> X <sub>21</sub> X <sub>22</sub> X <sub>17</sub>

## CONCLUSIONS

Based on parametric statistical procedures, the most sensitive inputs are given below.

- The most sensitive variables for Terminal IRI are AADTT, percent of trucks in design lane and bottom AC layer thickness.
- For Longitudinal Cracking, the most sensitive variable is bottom AC layer thickness.
- Alligator cracking is highly sensitive to bottom AC layer thickness, percent of trucks in design lane and AADTT.

- No inputs were determined as significant for Transverse cracking
- AC Rutting is highly sensitive to AADTT and percent of trucks in design lane.
- Total Rutting is highly sensitive to AADTT and percent of trucks in design lane.

Compared to other pavement performance measures, the predicted AC rutting and total rutting are influenced by a large number of input parameters. Traffic input variables, such as Annual Average Daily Truck Traffic (AADTT) and percent of trucks in design lane are obtained to be the most critical input parameter. AC mix properties and AC thickness are very important for roughness, longitudinal crack and fatigue crack. Base properties (modulus and thickness) have significant impact on longitudinal and fatigue cracking. Bottom AC layer thickness has most interacting effects with other input variables for all type of distresses.

## **Chapter 9**

### **SENSITIVITY BY NONPARAMETRIC REGRESSIONS**

#### **INTRODUCTION**

The MEPDG includes numerous inputs; therefore, a sensitivity analysis using Monte Carlo approach is not practical because it requires thousands of MEPDG runs. Instead, nonparametric regression procedures can be very useful to perform MEPDG sensitivity analysis. In this study, nonparametric regression procedures such as Multivariate Adaptive Regression Spline (MARS) and Gradient Boosting Machine (GBM) are employed for identifying inputs that contribute significantly to the outputs. This chapter presents the sensitivity analysis results in three groups of inputs, to which the output is (i) highly sensitive, (ii) moderately sensitive and (iii) minimally sensitive. The list of significant inputs can be useful to pavement engineers to optimize pavement designs and analyze performances as well as for local calibration of MEPDG.

Parametric regression, which was presented in the last chapter, is the most popular choice for sensitivity analysis because of its simplicity. Parametric regression procedures give good results when the output is approximately linear to the inputs. However, these procedures fail to appropriately identify the importance of input variables that have nonlinear effects on the analysis results. In these situations, nonparametric regression procedures provide better results. The use of nonparametric regression for estimating sensitivity measures can be more accurate than the use of standard Monte Carlo methods. This is especially true for estimating sensitivity measures with small to moderate sample sizes (Storlie et al. 2009). Nonparametric regression procedures can account for the interactions among the key inputs and account for the nonlinearity in the outputs. In this study, nonparametric regression procedures are implemented to estimate sensitivity indices and quantify the sensitivity of MEPDG inputs.

Again, the main objective is to identify a set of inputs that are most sensitive to MEPDG outputs for flexible pavement design. Specific objectives are to: determine a set of input variables and their suitable range for New Mexico pavement conditions, rank a set of MEPDG inputs that are significant to the prediction of outputs, and quantify interactions of the important inputs using nonparametric regression procedures. In this study, 30 inputs are selected based on the findings of the previous studies (NCHRP 2004a; NCHRP 2004b; NCHRP 2004c).

#### **RECENT SENSITIVITY STUDIES**

Coree (2005) evaluated the relative sensitivity of MEPDG input parameters to asphalt concrete (AC) material properties, traffic, and climatic conditions based on field data from two existing Iowa flexible pavement systems. Twenty-three key input parameters were studied. Corey (2005) found that longitudinal cracking is influenced by most input parameters. Subbase resilient modulus and aggregate thermal coefficient are insensitive to pavement rutting, cracking and smoothness.



Li et al. (2009) developed a sensitivity chart of the design input values to predict their applicability in the state of Washington. They found that longitudinal cracking is mostly influenced by binder properties and asphalt layer thickness. Climate or temperature is the most essential input to transverse cracking. The hot mix asphalt (HMA) mix stiffness heavily influences the development of alligator cracking. Climate, base type and traffic loading have significant impacts on HMA rutting and roughness.

Ahn et al. (2009) studied the sensitivity of the traffic inputs on the pavement performance predicted by the MEPDG for the state of Arizona. The traffic input parameters were annual average daily truck traffic (AADTT), monthly adjustment factors (MAF) and axle load distribution factors. It was shown that, longitudinal and alligator cracking increases nonlinearly with increases in AADTT. The use of default monthly adjustment factors (uniform throughout months) did not have significant impact on pavement performance (Ahn et. al 2009).

Aguiar-Moya et al. (2009) studied the sensitivity of the MEPDG using probability distributions of pavement layer thickness on performance. Long Term Pavement Performance (LTPP) SPS-1 sections located in the state of Texas were used to determine the thickness distribution associated with the HMA surface layer, the HMA binder course and the granular base layer. It was found that there is a significant increase in fatigue distress at the design life as the HMA surface layer thickness decreases within the given range. Total rutting, roughness and fatigue cracking appear to be unaffected by changes in the granular base layer thickness.

Masad and Little (2004) conducted a sensitivity analysis of MEPDG (version 0.8) performance models to the properties of the unbound pavement layers. It was shown that the base modulus and thickness have significant influence on the International Roughness Index (IRI) and the longitudinal cracking. The influence of base properties on alligator cracking is about half of the influence of base properties on longitudinal cracking. Their analysis results show that the base properties have almost no influence on permanent deformation (Masad and Little, 2004).

Manik et al. (2009) presented a strategy for determining optimal values for the desired design variables. The researchers considered three significant variables: asphalt layer thickness, base and subbase thickness (together), and base modulus.

Swan et al. (2008) conducted a sensitivity analysis of the predicted pavement performance varies only traffic input parameters. Their study showed that the number and type of trucks, followed by the axle load spectra, have a significant influence on the MEPDG predicted pavement performance. Hourly traffic volume adjustment factors and axle spacing have little influence on the predicted performance (Swan et al. 2008).

Rabab'ah and Liang (2008) showed that subgrade resilient modulus influence total rutting more than the base resilient modulus. The influence of unbound materials on performance as predicted by the MEPDG methodology is less pronounced than the influence of the AC layer thickness on MEPDG predicted performances.

Daniel and Chehab (2008) performed a study on reclaimed asphalt pavement (RAP) materials using MEPDG. They found that the number of AC layers affect the predicted performance, even

though the total thickness of the AC layers is the same (Daniel and Chehab 2008). Li et al. (2007) showed that roughness, rutting and cracking are medium to highly sensitive to axle load distribution. Hourly distribution and number of axles per truck do not have any influence on roughness, rutting and cracking.

## DATA

Two different data sources are used for this study. They are LTPP Database and NMDOT's MEPDG Databases. There are 39 LTPP sections with 12 General Pavement Study (GPS) and 27 Specific Pavement Study (SPS) test sections located in New Mexico (NM) (FHWA, 2004). The collected data are organized into three fundamental types of inputs: traffic inputs, climate inputs and structural inputs. There are 13 weather stations in New Mexico included in the Integrated Climatic Model (ICM). To study the sensitivity of climate on MEPDG outputs, NM is divided in five zones according to the locations to create 5 virtual weather stations. They are zone 1 to zone 5. Details of these zones are presented in previous chapter. Ground water table (GWT) depth values are collected from NMDOT and LTPP database. Pavement design files obtained from NMDOT contain structural information, i.e., layer thickness, HMA mix type and gradation of subgrade materials.

**TABLE 9.1 Inputs for sensitivity analysis**

No	Type	Input Name	Variable	Range of Inputs	Numeric Values Assigned	Variable Type	Data Source
1	TRAFFIC	Initial two-way AADTT	$X_1$	300 to 6000		Integer	LTPP
2		Number of Lanes in Design Direction	$X_2$	1 to 3		Integer	LTPP
3		Percent of Trucks in Design Direction (%)	$X_3$	40 to 60		Non Integer	Design Guide
4		Percent of Trucks in Design Lane (%)	$X_4$	6 to 94		Non Integer	Huang, 2004
5		Operational Speed (mph)	$X_5$	35 to 75		Non Integer	NMDOT
6		AADTT Distribution by Vehicle Class 9 (%)	$X_6$	2 to 85		Non Integer	LTPP
7		AADTT Distribution by Vehicle Class 11 (%)	$X_7$	0.1 to 7		Non Integer	LTPP
8		Traffic Growth Factor	$X_8$	3 to 9		Non Integer	LTPP
9		Design Lane Width (ft)	$X_9$	10 to 12		Non Integer	LTPP
10		Tire Pressure (psi)	$X_{10}$	90 to 150		Non Integer	Design Guide
11	CLIMATE	Depth of Water Table (ft)	$X_{11}$	5 to 20		Non Integer	NMDOT
12		Climatic Zones	$X_{12}$	1 to 5	1=SouthEast 2=SouthWest 3=NorthWest 4=NorthEast 5=Central	Discrete	Design Guide

The variables selected for the sensitivity study ( $X_1$  to  $X_{30}$ ) are shown in Table 9.1. To conduct a detailed sensitivity analysis, a flexible pavement structure is considered consisting of four layers.

The top layer is a thin AC layer with thickness varies from 1.5 to 3 inch. The second layer is a thick AC layer with thickness varying from 2 to 8 inches. The rest of the layers are base (6 to 10 inch) and subgrade. In order to find the true distributions of input variable a number of inputs are required. Therefore, random Latin Hypercube Sampling (LHS) method is followed to generate sample data for the variables of Table 9.1 (number of samples = 750) for each variable.

**TABLE 9.1 Inputs for sensitivity analysis (cont.)**

No	Type	Input Name	Variable	Range of Inputs	Numeric Values Assigned	Variable Type	Data Source
13	Asphalt Mix 1	Layer Thickness (in)	X <sub>13</sub>	1.5 to 3		Non Integer	NMDOT
14		Aggregate Gradation	X <sub>14</sub>	1 to 2	1=SP-III 2=SP-IV	Discrete	NMDOT
15		Effective Binder Content (%)	X <sub>15</sub>	9 to 12		Non Integer	NMDOT
16		Superpave Binder Grade	X <sub>16</sub>	1 to 3	1=PG 64-22 2=PG 70-28 3=PG 76-28	Discrete	NMDOT
17		Air Voids (%)	X <sub>17</sub>	4 to 7		Non Integer	LTPP
18	Asphalt Mix 2	Layer Thickness (in)	X <sub>18</sub>	2 to 8		Non Integer	NMDOT
19		Aggregate Gradation	X <sub>19</sub>	1 to 3	1=SP-II 2=SP-III 3=SP-IV	Discrete	NMDOT
20		Effective Binder Content (%)	X <sub>20</sub>	9 to 12		Non Integer	NMDOT
21		Superpave Binder Grade	X <sub>21</sub>	1 to 3	1=PG 64-22 2=PG 70-28 3=PG 76-28	Discrete	NMDOT
22		Air Voids (%)	X <sub>22</sub>	4 to 7		Non Integer	LTPP
23	Base	Layer Thickness (in)	X <sub>23</sub>	6 to 10			NMDOT
24		Material Type	X <sub>24</sub>	1 to 5	1=Crushed Gravel 2=A-1-b 3=A-2-6 4=A-3 5=A-2-4	Discrete	LTPP
25		Modulus (psi)	X <sub>25</sub>	20,000 to 40,000		Non integer	NMDOT
26		Material Type	X <sub>26</sub>	1 to 5	1=CL 2=CL-ML 3=ML 4=SM 5=SP	Discrete	LTPP
27		Modulus (psi)	X <sub>27</sub>	5000 to 20,000		Non integer	LTPP
28	Subgrade	Plastic Limit (PL)	X <sub>28</sub>	10 to 24		Non integer	NMDOT
29		Liquid Limit (LL)	X <sub>29</sub>	25 to 90		Non integer	NMDOT
30		Optimum Gravimetric Water Content (%)	X <sub>30</sub>	12 to 60		Non integer	NMDOT

MEPDG version 1.00 (MEPDG 2010) is used in this study. There are a total of 750 simulations. Six distress measures are taken as output variables for the sensitivity study. They are IRI, rut (total and AC) and cracking (longitudinal, transverse and alligator). These output variables are identified as  $Y_1$  to  $Y_6$ . After the required number of MEPDG simulation, results for the output variables ( $Y_1$  to  $Y_6$ ) are summarized and full factorial test matrix is developed ( $750 \times 36$ ). This resulting matrix is used in the next steps for advanced statistical analysis to determine the sensitivity of various pavement performances. These methods are implemented by writing subroutines in the R statistical computing environment (R 2010). The reason for using two approaches is to examine whether the outcome of the study is consistent.

## NONPARAMETRIC REGRESSION PROCEDURE

Nonparametric regression is a type of regression analysis. In this procedure, the output function does not take any predetermined form. According to the information derived from the data, the model is constructed. Nonparametric regression requires larger sample sizes than conventional regression based parametric models because the data must supply the model structure as well as the model estimates. Nonparametric regression procedures are applied to quantify the sensitivity of predicted outputs for each input. In nonlinear situations, nonparametric regression methods can be used to achieve a better approximation than can be obtained with the linear regression model (Storlie et al. 2009). There are several nonparametric regression methods which are popular and effective for modeling complex behavior including: Multivariate Adaptive Regression Splines (MARS), Random Forest (RF), Gradient Boosting Machine (GBM) and Adaptive Component Selection and Smoothing Operator (ACOSSO). Gaussian Process (GP) models have also become popular meta-models. Two different types of methods are applied in this study.

### Multivariate Adaptive Regression Splines (MARS)

Multivariate adaptive regression splines (MARS) is a combination of spline regression, stepwise model fitting, and recursive partitioning. With this procedure, a curve is fitted by adding (usually linear spline) basis functions to a model in a stepwise manner and then linear regression model is fitted. MARS procedure also considers stepwise deletion of basic functions. The process of MARS can be described as follows (Storlie et al. 2009): if observed data is  $(x_1, y_1), \dots, (x_n, y_n)$  and  $g_j$  is a generic linear spline function of the input variable  $x_j$  with knots at all the distinct values of  $x_j$ , the function can be presented in Eq (1).

$$g_j(x_j) = \sum_{l=0}^{n+1} b_{j,l} \phi_{j,l}(x_j) \quad (1)$$

These functions can be constructed as the tensor product of two univariate spline spaces as Eq 2.

$$g(x) = [\text{constant}] + [\text{main effects}] + [2\text{-way interactions}] + [\text{higher interactions}] \quad (2)$$

Three way and higher order interaction models can be ignored. After specifying the order of the interaction desired for the resulting model, MARS first fits the model with only the intercept term. Then MARS fits all possible models with two basic functions:

$$\hat{f}_{2,k}(x) = d_0 + d_k \phi_{j,l}(x_j) \quad (3)$$

for  $j = 1, \dots, p$ ,  $l = 1, \dots, n + 1$  via least squares. The model that gives the smallest Sum of Square Error (SSE) is chosen to be the one that enters the model. Once this basis function is included, MARS looks for the next basis function to add and so on. Once  $M$  basis functions have been added, MARS starts to remove basis functions that will result in the smallest increase in SSE. In the end, there are  $2M + 1$  possible models and the one with the lowest  $GCV$  score is chosen as the MARS estimate.

$$GCV_l = \frac{SSE_l}{(1 - (vm_1 + 1)) / n} \quad (4)$$

### Gradient Boosting Machine (GBM)

The general idea behind gradient boosting machine (GBM) is to compute a sequence of simple trees, where each successive tree is built for the prediction of the residuals from the preceding tree. These trees are then put together in an additive expansion to produce the final estimator. Boosting was originally developed for classification purposes. The underlying idea is to combine the output from many “weak” classifiers into a more powerful committee. The general idea behind boosting trees is to compute a sequence of simple regression trees, where each successive tree is built for the prediction of the residuals from the preceding tree (Storlie et al. 2009). For a given GBM, each constituent regression tree is restricted to have only  $J$  terminal nodes (regions that allow for more complex interactions). There is also an  $N_t$  parameter corresponding to the number of trees in the expansion. This can be considered a tuning parameter in the sense that  $R^2$  increases as  $N_t$  increases. The specific algorithm to fit the boosting tree is as follows (Storlie et al. 2009):

- Fit a regression tree with  $J$  nodes to the original data set
- For  $k = 2, \dots, N_t$ , fitting a regression tree with  $J$  nodes to the data set and call this estimate  $\hat{f}_k$ .
- The final estimate is given as

$$\hat{f}(x) = \sum_{k=1}^{N_t} \hat{f}_k(x) \quad (5)$$

### Sensitivity Measure

The statistical quantity used to quantify sensitivity is Total Variance Index (T). This index gives quantitative measure of sensitivity which is not possible by p-value.

### ***Total Variance Index (T)***

$T_j$ , that is  $T_j$ , corresponds to the fraction of the uncertainty in  $Y$  due to  $x_j$  and its interactions with other variables. It can be defined by the following equation (Homma and Saltelli 1996).

$$T_j = \frac{E(Var[f(x)|x_j])}{Var(f(x))} = \frac{Var(f(x)) - Var(E[f(x)|x_{(-j)}])}{Var(f(x))} \quad (6)$$

where  $x_{-j} = \{x_1, \dots, x_{j-1}, x_{j+1}, \dots, x_p\}$ . The calculation of  $T_j$  requires the evaluation of  $p$ -dimensional integrals (Storlie et al. 2009).

It is a very good single number summary of the overall importance of an input variable.  $T_j$  is variance index for the true model. To calculate  $T_j$  for every input, it requires a large number of simulation runs which would be infeasible for this study. The estimated value or calculated value of  $T_j$  according to the regression model approximation is denoted by  $\hat{T}_j$ . For the remaining sections of this study,  $\hat{T}_j$  will be considered instead of  $T_j$ . In addition, confidence intervals (CI) for true  $T_j$  based on the regression approximation are determined.

### ***Confidence Intervals (CI)***

For a given sample size, accuracy of estimation is the main concern for sensitivity analysis.  $\hat{T}_j$  is estimated from 750 simulations run data. For this reason, it is very important to know how confident we have been in measuring the importance and rankings for the individual input variables. By definition, 95% CI for  $T_j$  should contain the true value in 95% of repeated experiments. For example, model evaluation is done on a sample of size  $n$  ( $n = 750$  in this case). These  $n$  values are used to create a CI for  $T_j$ . We should expect that 95% of the CI's would contain true value.

## **RESULTS AND DISCUSSION**

MARS and GBM are implemented on output  $Y_1$ - $Y_6$ . In order to classify the input variables in groups of importance, for example: high importance, medium importance, low importance, it is easier to determine some cut-off values in the variances ( $\hat{T}_j$ ). The following discretization is used for grouping inputs according to their contributions to outputs uncertainty. If the variance of an input parameter explains at least 10% of the variance of a specific output, then it is considered highly important for that output. If the variance of an input parameter explains between 2% and 9% of the variance of specific output, then it is considered of medium importance for that output. Finally if the variance of an input parameter explains less than 2% of the variance of the output or if the parameter is not selected by the stepwise algorithm, it is considered of low important.

### **Output Y1 (Terminal IRI)**

Table 9.2 represents the result summary for Model  $Y_1$  (Terminal IRI). MARS model has a  $R^2$  value of 0.76, which means that 76% of uncertainties are captured in this model. Therefore, this

model can be said to be a less confident model. Rows of Table 9.2 are organized by T.hat values. The first total variance index obtained for this parameter is 0.418 which means that  $X_{18}$  alone and its interaction with all other inputs together explains 41.8% of the uncertainties. Total interaction of this input contributes to 13% uncertainties in output. The CI of T is presented in Table 9.2. It indicates that, 95% of the time  $X_{18}$  and its corresponding interaction can be high as 48.8%. In some cases, this influence can be low up to 35.5%.

**TABLE 9.2 Results for Y1 (Terminal IRI)**

No	Input	Name	T (Estimated)	T-Value Range (95% Confidence Interval)
<b>Model: MARS (<math>R^2=0.763</math>)</b>				
1	$X_{18}$	Bottom AC Layer Thickness	0.418	(0.355, 0.488)
2	$X_1$	AADTT	0.249	(0.169, 0.287)
3	$X_4$	Percent of Trucks in Design Lane (%)	0.218	(0.178, 0.285)
4	$X_{13}$	Top AC Layer Thickness	0.069	(0.033, 0.132)
5	$X_{22}$	Air Void (%) (Bottom AC Layer)	0.066	(0.016, 0.110)
6	$X_{16}$	Superpave Binder Grade (Top AC Layer)	0.020	(0.001, 0.040)
<b>Model: GBM (<math>R^2=0.907</math>)</b>				
1	$X_{18}$	Bottom AC Layer Thickness	0.538	(0.442, 0.602)
2	$X_1$	AADTT	0.285	(0.205, 0.342)
3	$X_4$	Percent of Trucks in Design Lane (%)	0.200	(0.156, 0.286)
4	$X_{22}$	Air Void (%) (Bottom AC Layer)	0.035	(0.019, 0.069)
5	$X_8$	Traffic Growth Factor	0.029	(0.007, 0.058)
6	$X_{13}$	Top AC Layer Thickness	0.027	(0.000, 0.058)
7	$X_{14}$	Aggregate Gradation (Top AC Layer)	0.024	(0.003, 0.048)

In the MARS model, the next important input is  $X_1$  (AADTT). According to the T value,  $X_1$  and its corresponding interaction captured 24.9% of the uncertainties. Therefore, the influence of AADTT on MEPDG output is not affected by interactions. The CI for T is 0.169 to 0.287. Influence of  $X_1$  and its interaction can be 16.9% to 28.7% in most of the cases. Similarly, from Table 9.2,  $X_4$  (percent of trucks in design lane) is third most important. Influences of this input variable with interaction with others have estimated 21.8%. 95% of the time, T value will be from 17.8% to 28.5%. These two factors are considered very important as they both have captured more than 10% of the variance individually.

Next is  $X_{13}$ , or top AC layer thickness. It has an estimated T value of 0.07 that also means this input's effect with the interaction among others can explain 7% of the variance. The range of this value is 3.3% to 13.2%.  $X_{22}$  (percent air void of bottom AC layer) can be considered as an

important parameter for model  $Y_1$  because this parameter itself with interaction has explained 6.6% of the uncertainties. These two parameters are somewhat important, as they have explained at least 5% of the uncertainties individually.  $X_{16}$  (Superpave binder grade of top AC layer) can be considered as not a very important factor because it has explained 2% of the uncertainties.

The GBM model has a  $R^2$  value of 0.90, which means that 90% of uncertainties are captured in this model. Therefore, this model can be said as an excellent and usable model. The most important parameter in GBM model is  $X_{18}$  (bottom AC layer thickness).  $T$  obtained for this parameter is 0.538 which means that  $X_{18}$  alone and its interaction with the other inputs combined explains 53.8% of the uncertainties in IRI. The CI of  $T$  is measured and presented in the next column. The estimated  $T$  value for  $X_{18}$  is 0.538 but 95% time the value will be within 0.442 to 0.602. It indicates that, 95% of the time  $X_{18}$  and its corresponding interaction can be within 44% to 60%.

In the GBM model, the next important parameter is  $X_1$  (AADTT). According to the  $T$  value,  $X_1$  and its corresponding interaction altogether captured 28.5% of the uncertainties. The CI for  $T$  is 0.205 to 0.342. Therefore, influence of  $X_1$  and its interaction can be 20.5% to 34.2% in most of the cases.  $X_4$  (percent of trucks in design lane) is also important factor for IRI. Influence of this input variable with its interaction with others has estimated 20%. For most of the cases, this value will be from 16% to 29%. These three parameters,  $X_{18}$ ,  $X_1$ ,  $X_4$ , are considered the most important factors for this model as they all explained more than 20% of the uncertainties individually.  $X_{22}$  (percent air void of bottom AC layer) can be considered as a somewhat important parameter for model  $Y_1$  (terminal IRI) because this parameter itself with interaction has explained 3.5% of the uncertainties.  $X_8$  (traffic growth factor),  $X_{13}$  (top AC layer thickness) and  $X_{14}$  (aggregate gradation of top AC layer) can be considered as not important factors. They all explain with their interactions less than 5% individually.

Figure 9.4 represents graphically the summary result of the most important factors by MARS and GBM Method. From this figure, it can be seen that  $X_{18}$  or bottom AC layer thickness with its interaction among others has captured the highest percentage of uncertainties for both methods. The total uncertainty captured by this input variable is higher in GBM (42%).  $X_1$  (AADTT) has ranked second important factor in both meta-models. The total uncertainties explained by this input variable are almost the same in both cases (25~30%).  $X_4$  or percent of trucks in design lane placed third in the ranking order for both methods. It is very clear from the figures that the effect of this input is the same in all cases (17%~20%).  $X_{13}$  or top AC layer thickness has significant ranking (fourth) in MARS but not in GBM. It is able to explain less than 10% in both methods.  $X_{22}$  or percent air void of bottom AC layer is also common for both methods with almost the same rank. Without these five parameters, GBM has  $X_8$  (traffic growth factor) and  $X_{10}$  (tire pressure) which are not listed by MARS.  $X_{14}$  (aggregate gradation of top AC layer) is ranked in GBM meta-model but not by MARS.



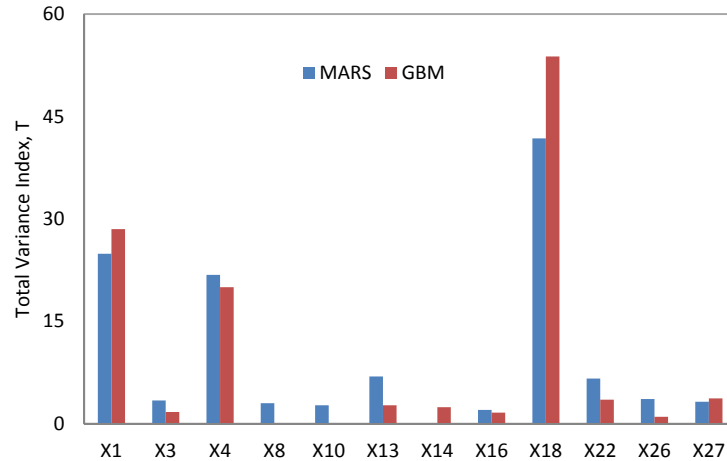


**FIGURE 9.1 Total Variance Index (T) of Input Factors that Affect Terminal IRI ( $Y_1$ )**

### Output Y2 (Longitudinal Cracking)

Table 9.3 represents the result summary for Model  $Y_2$  (Longitudinal Cracking). The MARS model was fitted with  $R^2$  value of 0.79, which means that 79% of uncertainties are captured in this model. Therefore, this model can be said as less confident model but usable. The most important parameter in the MARS model is  $X_{18}$  (bottom AC layer thickness). T obtained for this parameter is 0.60, which means that  $X_{18}$  alone and its interaction with other inputs all together explains 60% of the uncertainties. This can be considered as the most important factor for this model as it includes its interaction and has explained more than 50% of the variance. The CI of T is measured and presented in the next column. The estimated T value for  $X_{18}$  is 0.60 but 95% of the time the value will be within 0.532 to 0.652 and its corresponding interaction can be within 53.2% to 65.2%.

In the MARS model, the next important parameter is  $X_1$  (AADTT). According to the T value,  $X_1$  and its corresponding interaction together captured 14.4% of the uncertainties. The CI for T is 0.092 to 0.180. Therefore, influence of  $X_1$  and its interaction can be 9.2% to 18% in most of the cases.  $X_4$  (percent of trucks in design lane) is also an important factor in this model which has estimated T value almost close to  $X_1$ . Influence of this input variable with its interaction with others is estimated at 13.4%. In most cases (95%), this value will be from 8.5% to 18%. These two parameters can be considered also as very important factors for this model as they explain more than 10% of the variance individually (including interaction).

$X_{17}$  (percent air void of top AC layer) and  $X_{24}$  (base material type) can be categorized as important for this model as they explain 8.6% and 6.5% uncertainties respectively.  $X_{17}$  (percent air void of top AC layer) needs extra attention because most of the case influence can be increased up to 13.4% which is greater than 10%. The same comment is also applicable for  $X_{24}$  as the highest limit of T estimated is 11.3%.  $X_{25}$  (Base Modulus),  $X_{13}$  (top AC layer thickness),  $X_{27}$  (Subgrade Modulus) and  $X_{23}$  (base thickness) have estimated T values from 3.6% to 5.3%. This means that any of these inputs' effects along with the interaction of others can explain

around 5% of the variance. These sets of inputs have a chance to influence up to 9% individually in some cases. Another input variable  $X_3$  (percent of trucks in design direction) is listed in this table with estimated T value of 2.1%. This parameter is not important as it explains 2% of the variance and has a chance of being maximum 4.5%.

**TABLE 9.3 Results for Y2 (Longitudinal Cracking)**

No	Input	Name	T (Estimated)	T-Value Range (95% Confidence Interval)
<b>Model: MARS (<math>R^2=0.791</math>)</b>				
1	$X_{18}$	Bottom AC Layer Thickness	0.600	(0.532, 0.652)
2	$X_1$	AADTT	0.144	(0.092, 0.180)
3	$X_4$	Percent of Trucks in Design Lane (%)	0.134	(0.085, 0.180)
4	$X_{17}$	Percent Air Void (Top AC Layer)	0.086	(0.047, 0.134)
5	$X_{24}$	Base Material Type	0.065	(0.028, 0.113)
6	$X_{25}$	Base Modulus	0.053	(0.000, 0.085)
7	$X_{13}$	Top AC Layer Thickness	0.041	(0.003, 0.081)
8	$X_{27}$	Subgrade Modulus	0.044	(0.001, 0.076)
9	$X_{23}$	Base Thickness	0.036	(0.008, 0.072)
10	$X_3$	Percent of Trucks in Design Direction (%)	0.021	(0.000, 0.045)
<b>Model: GBM (<math>R^2=0.901</math>)</b>				
1	$X_{18}$	Bottom AC Layer Thickness	0.730	(0.605, 0.689)
2	$X_4$	Percent of Trucks in Design Lane (%)	0.148	(0.131, 0.217)
3	$X_1$	AADTT	0.123	(0.100, 0.189)
4	$X_{25}$	Base Modulus	0.054	(0.054, 0.108)
5	$X_{24}$	Base Material Type	0.066	(0.048, 0.104)
6	$X_{17}$	Percent Air voids (Top AC layer)	0.048	(0.031, 0.095)
7	$X_{13}$	Top AC Layer Thickness	0.024	(0.001, 0.041)
8	$X_3$	Percent of Trucks in Design Direction (%)	0.020	(0.007, 0.040)
9	$X_{26}$	Subgrade Material Type	0.016	(0.000, 0.035)

The GBM model has an  $R^2$  value of 0.90, which means that 90% of the uncertainties are captured in this model. Therefore, this model can be said to be an excellent model. The most important parameter in the GBM model is  $X_{18}$  (bottom AC layer thickness). Single variance index for this input is 0.571 which means that sole influence of  $X_{18}$  without any interaction is 57.1%. T obtained for this parameter is 0.73, which means that  $X_{18}$  alone, and its interaction with other inputs explains 73% of the uncertainties. This can be considered as the most important factor for this model as its interaction has explained more than 73% of the variance. The CI of T is measured and presented in the next column. The estimated T value for  $X_{18}$  is 0.73, but 95% of

the time the value will be within 0.605 to 0.689, indicating that 95% of the time  $X_{18}$  and its corresponding interaction can be within 60.5% to 68.9%.

In the GBM model,  $X_4$  (percent of trucks in design lane) is also an important factor in this model which has estimated T value 0.148. Influence of this input variable with its interaction with others has estimated 14.8%. In most cases (95% of the time), this value will be from 13.1% to 21.7%. The next important parameter is  $X_1$  (AADTT). According to the T value,  $X_1$  and its corresponding interaction altogether captured 12.3% of the uncertainties. The CI for T is 0.10 to 0.189. Therefore, influence of  $X_1$  and its interaction can be 10% to 18.9% in most of the cases. These two parameters can be considered very important factors for this model as they explain more than 10% of the variance individually (including interaction).

$X_{25}$  (base modulus),  $X_{24}$  (base material type) and  $X_{17}$  (percent air void of top AC layer) can be categorized as important for this model as they all explain 5% or more than 5% of the variance individually. Estimated T value is 5.4%, 6.6% and 4.8 % respectively. Input variable  $X_{25}$  needs extra attention because most of the case influences can be increased up to 10.8%, which is greater than 10%. The same comment is also applicable for  $X_{24}$  and  $X_{17}$  as the highest limit of T estimated is 10.4% and 9.5% respectively.  $X_{13}$  or top AC layer thickness,  $X_3$  (Percent of Trucks in Design Direction (%)) and  $X_{26}$  (subgrade material type) are also listed in this table. These inputs have effect with the interaction among others can explain less than 5% of the variance. Sometimes, these effects can be negligible (almost 0%) and can be up to 5% in some cases.

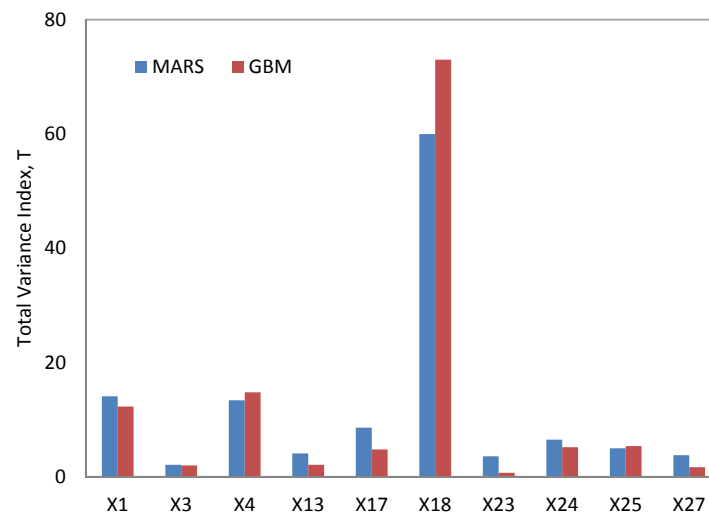


**FIGURE 9.2 Total Variance Index (T) of Input Factors Affecting Longitudinal Cracking (Y2)**

Figure 9.5 represents graphically the summary result of the most important factors of both methods. From this figure, it can be seen that  $X_{18}$  or bottom AC layer thickness with its interaction among others has captured the highest percentage of uncertainties for both methods. The total uncertainty captured by this input variable is 73% in GBM and 60% in MARS. The rest of the inputs for  $Y_2$  model in both meta-models have explained less than 20% of uncertainties individually.  $X_1$  (AADTT) and  $X_4$  or percent of trucks in design lane are also very important factors for output  $Y_2$  and they have explained more than 10% of the uncertainties individually for

both meta-models. All other inputs in these meta-models are considered somewhat important as they all have captured less than 10% of the uncertainties.  $X_{17}$ ,  $X_{24}$  and  $X_{25}$  are almost in same order for both meta-models. These three have explained 5% to 10% of the uncertainties individually.  $X_{13}$  is one of the input variables which is common for the significant list of both methods and has captured 2% to 5% of the uncertainties. The rest of the inputs shown in the graphs are less important as they have explained less than 2% of the variance individually.

### Output Y3 (Alligator Cracking)

Summary of the Model  $Y_3$  (Alligator Cracking) is presented in Table 9.4. MARS is a very good and usable model because the  $R^2$  value is 0.80, which means that 80% of the uncertainties are captured in this model. The most important parameter in the MARS model is  $X_{18}$  (bottom AC layer thickness). T obtained for this parameter is 0.68, which means that  $X_{18}$  alone and its interaction with all other inputs together explains 68% of the uncertainties. This can be considered as the most important factor for this model itself including its interaction has explained more than half of the variance. The CI of T is measured and presented in the next column. The estimated T value for  $X_{18}$  is 0.680, but 95% of the time the value will be within 0.60 to 0.737 and its corresponding interaction can be within 60% to 73.7%.

**TABLE 9.4 Results for Y3 (Alligator Cracking)**

No	Input	Name	T (Estimated)	T-Value Range (95% Confidence Interval)
<b>Model: MARS (<math>R^2=0.800</math>)</b>				
1	$X_{18}$	Bottom AC Layer Thickness	0.680	(0.600, 0.737)
2	$X_1$	AADTT	0.178	(0.094, 0.217)
3	$X_{22}$	Percent Air Void (Bottom AC Layer)	0.133	(0.093, 0.206)
4	$X_4$	Percent of Trucks in Design Lane (%)	0.120	(0.062, 0.166)
5	$X_{13}$	Top AC Layer Thickness	0.080	(0.044, 0.161)
6	$X_{25}$	Base Modulus	0.045	(0.010, 0.089)
7	$X_3$	Percent of Trucks in Design Direction (%)	0.035	(0.000, 0.069)
8	$X_{24}$	Base Material Type	0.022	(0.000, 0.046)
<b>Model: GBM (<math>R^2=0.937</math>)</b>				
1	$X_{18}$	Bottom AC Layer Thickness	0.802	(0.713, 0.787)
2	$X_1$	AADTT	0.166	(0.145, 0.261)
3	$X_4$	Percent of Trucks in Design Lane (%)	0.084	(0.071, 0.169)
4	$X_{22}$	Air Void (%) (Bottom AC Layer)	0.102	(0.055, 0.160)
5	$X_{13}$	Top AC Layer Thickness	0.036	(0.006, 0.073)
6	$X_{25}$	Base Modulus	0.027	(0.000, 0.055)
7	$X_{28}$	Plastic Limit	0.025	(0.000, 0.051)

The next important parameter is  $X_1$  (AADTT) for MARS model. According to the estimated T value,  $X_1$  and its corresponding interaction together captured 17.8% of the uncertainties. The CI for T is 0.094 to 0.217. Therefore, influence of  $X_1$  and its interaction can be 9.4% to 21.7% in most of the cases.  $X_{22}$  (percent air void of second AC layer) and  $X_4$  (percent of trucks in design lane) are also important factors in this model because both have estimated T value of more than 10%. In some cases, the influence of  $X_{22}$  can be up to 20.6% and the influence of  $X_4$  can be up to 16.6%.  $X_{13}$  or top AC layer thickness has a T value of 0.08, which also means that this input's effect with the interaction among others can explain 8% of the variance. The range of this influence can vary from 4.4% to 16.1%. Two input variables,  $X_{25}$  (base modulus) and  $X_3$  (percent of trucks in design direction), can be categorized as somewhat important for this model as they explain more than 2% of the variance individually. Both of these variables have a chance to be influential up to 9%.

The GBM is a very good model because the  $R^2$  value of 0.93, which means that 93% of uncertainties are captured in this model. The most important parameter in GBM model is  $X_{18}$  (bottom AC layer thickness). T obtained for this input is 0.802, which means that  $X_{18}$  and its interaction with other inputs all together explains 80.2% of the uncertainties. This can be considered as the most important factor for this model as it includes its interaction and has explained more than half of the variance. The CI of T is measured and presented in the next column. CI for T value is 0.713 to 0.787, indicating that 95% of the time  $X_{18}$  and its corresponding interaction can be within 71.3% to 78.7%.

The next important parameter is  $X_1$  (AADTT) for the GBM model. According to the estimated T value,  $X_1$  and its corresponding interaction together captured 16.6% of the uncertainties. Total interaction of this input is 2.8%. The CI for T is 0.145 to 0.261. Therefore, influence of  $X_1$  and its interaction can be 14.5% to 26.1% in most of the cases.  $X_{22}$  (percent air void of second AC layer) and  $X_4$  (percent of trucks in design lane) are also important factors in the GBM model. Influence of these input variables with their interaction with others has estimated 8.4% and 10.2% individually. In some cases, the influence of  $X_{22}$  can be up to 16% and the influence of  $X_4$  can be up to 16.9%.

$X_{13}$  or top AC layer thickness has T value of 0.036, which also means that this input's effect with the interaction among others can explain 3.6% of the variance. The range of this influence can vary from 0.6% to 7.3%.  $X_{25}$  (base modulus) and  $X_{28}$  (plastic limit) are ranked in this method. They can be categorized as not very important for this model as they have explained less than 5% of the variance individually. The estimated T values for these variables are 2.7% and 2.5% respectively. In some cases, influence can be increased up to 5%. In some cases, this effect can be negligible (0%).

Figure 9.3 represents graphically the summary result of most important factors by both methods. From this figure, it can be seen that  $X_{18}$  or bottom AC layer thickness with its interaction among others has captured the most percentage of uncertainties for both methods for its sole effect and interaction with others. The total uncertainty captured by this input variable is more than 80% in GBM and 60% in MARS. The rest of the inputs for the  $Y_3$  model in all meta-models have explained less than 20 % of uncertainties individually.  $X_1$  (AADTT) is also considered as a very

important factor for output  $Y_3$  and they have explained more than 10% of the uncertainties individually for all meta-models.

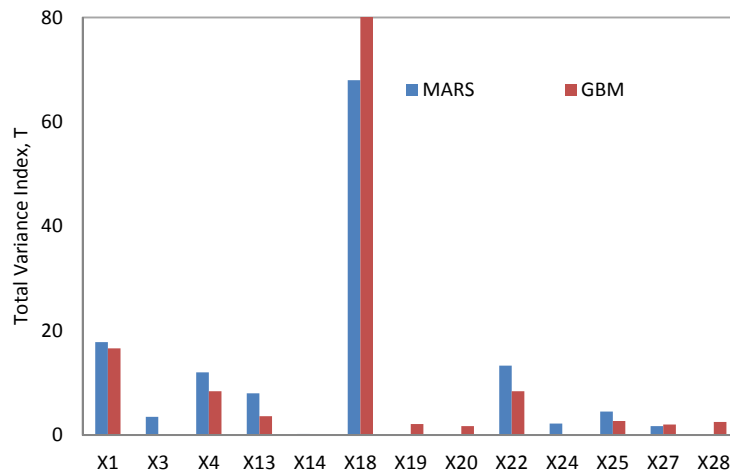


**FIGURE 9.3 Total Variance Index (T) of Input Factors that Affect Alligator Cracking ( $Y_3$ )**

For both methods, the ranking order and percent of variance index are almost identical. Two important factors for output  $Y_3$  have been captured by both of the methods. They are  $X_{22}$  percent air void of bottom AC layer and  $X_4$  or percent of trucks in design lane. The amount of effects obtained for these two variables are almost the same for these two methods. The effect of  $X_{22}$  is greater than the effect of  $X_4$ . All other inputs in these meta-models are considered somewhat important as they all have captured less than 10% of the uncertainties.

$X_{13}$ ,  $X_{24}$  and  $X_{25}$  are almost in the same order for all meta-models. These have explained 5% to 10% of the uncertainties individually.  $X_{13}$  is one of the input variables, which is common for the significant list of all meta-models. It has captured around 10% of the uncertainties in MARS but less than 5% in GBM. The rest of the inputs shown in the graph are less important as they have explained less than 5% of the variance individually. From these three figures, it can be visualized clearly that the ranking order and amount of explainable uncertainties are almost the same for both cases. Therefore, the results obtained for output  $Y_3$  are reliable and consistent.

### Output $Y_4$ (Transverse Cracking)

Table 9.5 represents the result summary for Model  $Y_4$  (Transverse Cracking). The MARS model has a  $R^2$  value of 0.6 which means that only 60% of uncertainties are captured in this model. Therefore, this model may be usable to gain some insight into output sensitivity but cannot be considered as a good model. The most important parameter in the MARS model is  $X_4$  (percent of trucks in design lane). T obtained for this parameter is 0.874, which means that  $X_4$  alone, and its interaction with other inputs all together explains 87.4% of the uncertainties. The CI of T is measured and presented in the next column. The estimated T value for  $X_4$  is 0.874 but 95% of the time the value will be within 0.026 to 1.000, indicating that 95% of the time  $X_4$  and its corresponding interaction can be within 2.6% to 100%. Another input variable,  $X_7$  (AADTT

distribution by vehicle class 11), is considered as important also. Estimated T value is 0.406. According to the T value, its sole influence and interaction with other inputs can explain 40.6% of the uncertainties. The CI for this T value is 0.194 to 0.812.

**TABLE 9.5 Results for Y4 (Transverse Cracking)**

No	Input	Name	T (Estimated)	T-Value Range (95% Confidence Interval)
<b>Model: MARS (<math>R^2=0.602</math>)</b>				
1	X <sub>4</sub>	Percent of Trucks in Design Lane (%)	0.874	(0.026, 1.000)
2	X <sub>7</sub>	AADTT Distribution by Vehicle Class 11 (%)	0.406	(0.194, 0.812)
<b>Model: GBM (<math>R^2=0.382</math>)</b>				
1	X <sub>28</sub>	Plastic Limit	0.872	(0.196, 1.000)
2	X <sub>4</sub>	Percent of Trucks in Design Lane (%)	0.172	(0.000, 0.346)
3	X <sub>12</sub>	Climatic Zones	0.109	(0.115, 0.218)
4	X <sub>23</sub>	Base Thickness	0.085	(0.000, 0.228)
5	X <sub>11</sub>	Depth of Water Table	0.081	(0.000, 0.217)
6	X <sub>21</sub>	Superpave Binder Grade (Bottom AC Layer)	0.048	(0.000, 0.106)

GBM has a  $R^2$  value of 0.39 which means that only 39% of uncertainties are captured in this model. The most important parameter in GBM model is X<sub>28</sub> (plastic limit). T obtained for this parameter is 0.872, which means that X<sub>28</sub> alone, and its interaction with other inputs all together, explains 87.2% of the uncertainties. The CI of T is measured and presented in the next column. The estimated T value for X<sub>28</sub> is 0.872, but 95% of the time the value will be within 0.196 to 1.0. This indicates that 95% of the time X<sub>28</sub> and its corresponding interaction can be within 19.6% to 100%.

Another input variable, X<sub>4</sub> (percent of trucks in design lane), is considered as important. According to T value, 17.2% uncertainties can be explained by X<sub>4</sub> and interaction between X<sub>4</sub> with others. The CI for this T value is 0.0 to 0.346. X<sub>12</sub> (climatic zone) is also important factor in this model like the other two. Influence of this input variable with its interaction with others has estimated 10.9%. Among them all, influence is explained by the interaction of inputs with other inputs. In most of the cases, this value will be from 11.5% to 21.8%. The next three parameters are X<sub>23</sub> (thickness of base layer), X<sub>11</sub> (depth of water table) and X<sub>21</sub> (Superpave binder grade of bottom AC layer) used in this model can be considered as important. They all explain 8.5%, 8.1% and 4.8% of the uncertainties respectively. X<sub>23</sub> and X<sub>11</sub> have a chance to have influence up to 22.8% and 21.7% respectively. X<sub>21</sub> has the chance to have an effect from 0% to 10%.

Figure 9.4 represents graphically the summary result of the most important factors by the MARS and GBM methods. Figure 9.7 represents two significant inputs by MARS. They are X<sub>7</sub> and X<sub>4</sub>. X<sub>7</sub> has captured more than 40% of the uncertainties and X<sub>4</sub> has captured around 90% of uncertainties due to interaction. Figure 9.7 represents that all the significant inputs obtained by

the GBM method are of almost the same importance.  $X_{28}$  has captured more than 80% of the uncertainties. It has ranked first in the input list. The rest of the uncertainties,  $X_4$ ,  $X_{12}$ ,  $X_{23}$ ,  $X_{11}$  and  $X_{21}$ , are considered as significant inputs and presented in the graph.  $X_4$  and  $X_{12}$  explain around 20% of the uncertainties. The rest of them have captured less than 10% of the variance only for interaction.

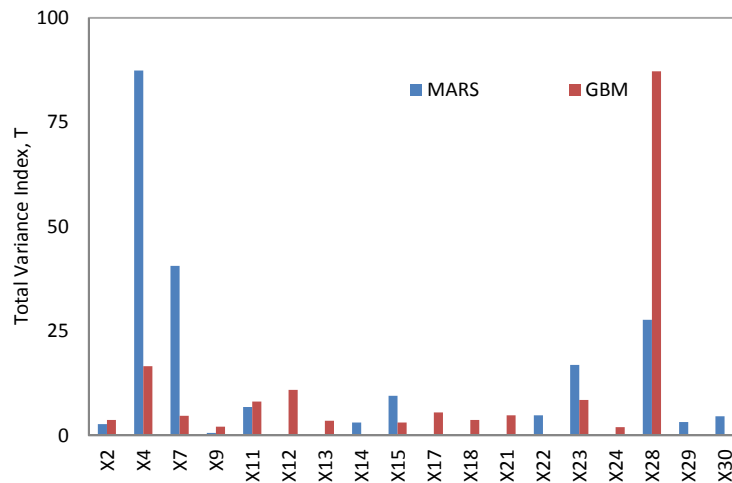


**FIGURE 9.4 Total Variance Index (T) of Input Factors Affecting Transverse Cracking (Y4)**

### Output Y5 (AC Rutting)

Table 9.6 represents the result summary for Model Y<sub>5</sub> (AC Rutting). The MARS model has a  $R^2$  value of 0.94 which means that 94% of uncertainties are captured in this model. Therefore, this model can be said to be a very good and usable model. Two variables can be considered as very important factor for this model as they have explained more than 30% of the uncertainties individually. These inputs are  $X_1$  (AADTT) and  $X_4$  (percent of trucks in design lane). Estimated T value for  $X_1$  and  $X_4$  are 39.5% and 34.7% respectively. The CI of T for  $X_1$  is 0.363 to 0.443. The CI of T for  $X_4$  is 0.305 to 0.386. From the designer's view, these values are very important. The influence of  $X_1$  with its interaction can be up to 44.3% in some cases. The same as  $X_1$ , the effect of  $X_4$  can be up to 38.6%. The influence for these two cases can decrease up to 36.3% and 30.5% respectively.

Another important input in this model is  $X_{10}$  (tire pressure). The estimated T value for  $X_{10}$  is 0.11, but 95% of the time the value will be within 0.081 to 0.139. It indicates that, 95% of the time  $X_{10}$  and its corresponding interaction can be within 8.1% to 13.9%. This parameter is important as it explains at least 10% of the variance.

In this model, the next parameter is  $X_{18}$  (bottom AC layer thickness) and can be considered as quite important. According to the T value,  $X_{18}$  and its corresponding interaction altogether captured 5.3% of the uncertainties. The CI for T is 0.016 to 0.074. Therefore, influence of  $X_{18}$



and its interaction can be 1.6% to 7.4% in most of the cases. Two parameters have captured almost 2% of the uncertainties individually (including their interaction). They are  $X_{30}$  (Optimum gravimetric Water Content) and  $X_{25}$  (Base Modulus). These parameters are not as important as they have captured less than 5% of the variance individually. Overall, this model is an excellent model for  $Y_5$  as it obtained a good  $R^2$  value and the MARS method is good choice for model  $Y_5$ .

**TABLE 9.6 Results for Y5 (AC Rutting)**

No	Input	Name	T (Estimated)	T-Value Range (95% Confidence Interval)
<b>Model: MARS (<math>R^2=0.940</math>)</b>				
1	$X_1$	AADTT	0.395	(0.363, 0.443)
2	$X_4$	Percent of Trucks in Design Lane (%)	0.347	(0.305, 0.386)
3	$X_{10}$	Tire Pressure	0.112	(0.081, 0.139)
4	$X_{18}$	Bottom AC Layer Thickness	0.053	(0.016, 0.074)
5	$X_{30}$	Optimum gravimetric water content	0.019	(0.002, 0.038)
6	$X_{25}$	Base Modulus	0.016	(0.005, 0.032)
<b>Model: GBM (<math>R^2=0.925</math>)</b>				
1	$X_1$	AADTT	0.485	(0.405, 0.501)
2	$X_4$	Percent of Trucks in Design Lane (%)	0.400	(0.340, 0.433)
3	$X_{10}$	Tire Pressure	0.116	(0.099, 0.165)
4	$X_{18}$	Bottom AC Layer Thickness	0.036	(0.019, 0.068)
5	$X_8$	Traffic Growth Factor	0.021	(0.003, 0.042)
6	$X_{13}$	AC Layer Thickness (Top Layer)	0.027	(0.001, 0.031)

The GBM model has a  $R^2$  value of 0.93 which means that 93% of the uncertainties are captured in this model. Therefore, this model can be said to be a very good and usable model. Two variables can be considered as very important factors for GBM model as they have explained more than 30% of the uncertainties individually. This effect includes its interaction with other inputs, too. These inputs are  $X_1$  (AADTT) and  $X_4$  (percent of trucks in design lane). Single variance index for  $X_1$  (AADTT) is 0.424. According to estimated T value for  $X_1$  and  $X_4$  are 48.5% and 40% respectively. The CI of T for  $X_1$  is 0.405 to 0.501. The CI of T for  $X_4$  is 0.34 to 0.433. From the designer's view, these values are very important. The influence of  $X_1$  with its interaction can be up to 50.1% in some cases. The same as  $X_1$ , the effect of  $X_4$  can be up to 43.3%. The influence for these two cases can decrease up to 40.5% and 34% respectively.

Another important parameter in the GBM model is  $X_{10}$  (tire pressure). T obtained for this parameter is 0.116, which means that  $X_{10}$  and its interaction with other inputs together explain 11.6% of the total uncertainties. The estimated T value for  $X_{10}$  is 0.116, but 95% of the time the value will be within 0.099 to 0.165. It indicates that 95% of the time  $X_{10}$  and its corresponding interaction can be within 9.9% to 16.5%. This parameter is important as it explain at least 10% of the variance. In this model, the next parameter,  $X_{18}$  (bottom AC layer thickness), can be considered as quite important. According to T value,  $X_{18}$  solely without corresponding

interaction captured 3.6% of the uncertainties. The CI for T is 0.019 to 0.068. Therefore, influence of  $X_{18}$  and its interaction can be 1.9% to 6.8% in most of the cases.

Two parameters have captured less than 3% of total uncertainties individually (including their interaction). They are  $X_8$  (Traffic growth factor) and  $X_{13}$  (top AC layer thickness). They can have influence up to 4.2% and 3.1% in some cases respectively. Overall, this model is an excellent model for  $Y_5$  as it obtained a good  $R^2$  value. The CI for estimated T is reasonable which indicates reliability ion the result. The GBM method is a good choice for model  $Y_5$ .

Figure 9.5 represents graphically the summary result of most important factors by both the MARS and GBM method. By visual inspection at a glance for both methods, it can be said that the pattern of the bar chart is the same for all cases. The first two parameters are contributing a lot (around 40%) when compared to the other parameters in the bar chart. The rest of the parameters explain 10% or less than 10% of the variances. This is the common trend for both bar charts. From these figures, it can be seen that  $X_1$  or AADTT for its main effect among others has captured the most percentage of uncertainties for both methods. The total uncertainty captured by this input variable is highest in GBM (48%).  $X_4$ , or percent of trucks in design lane, has ranked the second most important factor in all meta-models. The total uncertainties explained by this input's main effect are almost the same in both cases (35~40%).  $X_{10}$ , or tire pressure, placed third in the ranking order for all methods. It is very clear from the figures that the effect of this input is same in all cases (10%~12%).

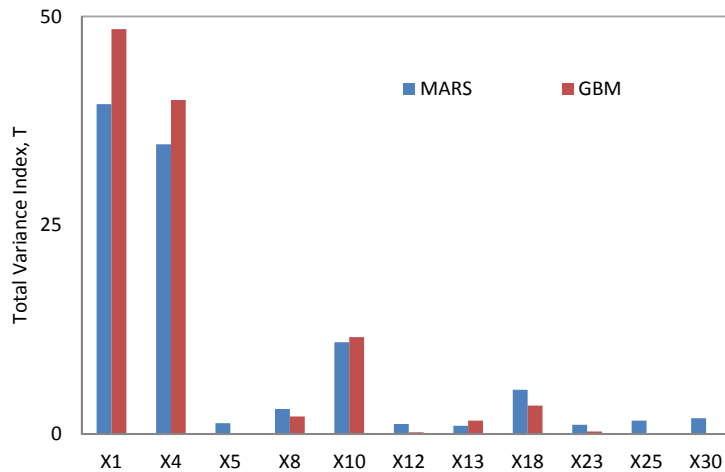


**FIGURE 9.5 Total Variance Index (T) of Input Factors that Effect AC Rutting ( $Y_5$ )**

$X_{18}$ , or bottom AC layer thickness, has almost the same T.hat value in these figures. It ranked fourth in all methods and explains less than 10% of the uncertainties in all cases. Without these parameters, both methods have some less important factors, such as  $X_8$  (traffic growth factor) and  $X_{13}$  (top AC layer thickness). Without all these parameters, some parameters are just captured by one particular method. They are  $X_{12}$ ,  $X_{30}$  and  $X_{25}$ . These are all less important variables as they are not able to explain more than 3% of the uncertainties.

## Output Y6 (Total Rutting)

Table 9.7 represents the result summary for Model Y<sub>6</sub> (Total Rutting). The MARS model has a  $R^2$  value of 0.91, which means that 91% of uncertainties are captured in this model. Therefore, this model can be said to be an excellent and usable model, similar to Y<sub>5</sub>. The most important parameter in MARS model is  $X_1$  (AADTT). T obtained for this parameter is 0.338, which means that  $X_1$ , and its interaction with other input variables explains 33.8% of the uncertainties. Therefore, the total interaction of the input is 3.9%. The CI of T is measured and presented in the next column. The estimated T value for  $X_1$  is 0.338, but 95% of the time the value will be within 0.305 to 0.384. This indicates that 95% of the time  $X_1$  and its corresponding interaction can be within 30.5% to 38.4%.

**TABLE 9.7 Results for Y6 (Total Rutting)**

No	Input	Name	T (Estimated)	T-Value Range (95% Confidence Interval)
<b>Model: MARS (<math>R^2=0.907</math>)</b>				
1	$X_1$	AADTT	0.338	(0.305, 0.384)
2	$X_4$	Percent of Trucks in Design Lane (%)	0.274	(0.234, 0.309)
3	$X_{18}$	Bottom AC Layer Thickness	0.134	(0.083, 0.149)
4	$X_{10}$	Tire Pressure	0.064	(0.047, 0.103)
5	$X_{27}$	Subgrade Modulus	0.052	(0.014, 0.074)
6	$X_{30}$	Optimum gravimetric water content	0.055	(0.000, 0.058)
7	$X_8$	Traffic Growth Factor	0.038	(0.016, 0.071)
8	$X_{13}$	Top AC Layer Thickness	0.030	(0.001, 0.053)
9	$X_3$	Percent of Trucks in Design Direction (%)	0.024	(0.000, 0.053)
10	$X_{26}$	Subgrade Material Type	0.028	(0.001, 0.047)
11	$X_{21}$	Superpave Binder Grade (Bottom AC Layer)	0.016	(0.000, 0.036)
<b>Model: GBM (<math>R^2=0.901</math>)</b>				
1	$X_1$	AADTT	0.446	(0.347, 0.451)
2	$X_4$	Percent of Trucks in Design Lane (%)	0.356	(0.279, 0.384)
3	$X_{18}$	Bottom AC Layer Thickness	0.124	(0.099, 0.169)
4	$X_{10}$	Tire Pressure	0.038	(0.031, 0.076)
5	$X_{27}$	Subgrade Modulus	0.035	(0.015, 0.069)
6	$X_{30}$	Optimum gravimetric water content (%)	0.022	(0.009, 0.044)
7	$X_3$	Percent of Trucks in Design Direction (%)	0.020	(0.013, 0.041)
8	$X_{11}$	Depth of Water Table	0.012	(0.000, 0.025)

In the MARS model, the next important parameter is  $X_4$  (percent of trucks in design lane). According to the T value,  $X_4$  and its corresponding interaction captured 27.4% of the uncertainties. The CI for T is 0.234 to 0.309. Therefore, influence of  $X_4$  and its interaction can be 23.4% to 30.9% in most of the cases.  $X_{18}$ , or bottom AC layer thickness, is also an important factor in this model. Influence of this input variable with its interaction with others has estimated 13.4%. 95% of the time, this value will be from 8.3% to 14.9%. This parameter is important as it explains at least 10% of the variance.  $X_{10}$  (tire pressure) is somewhat important in this model because it has explained 5.3% of sole and 6.4% with interaction of the uncertainties. The CI for T is 0.047 to 0.103. Therefore, influence of  $X_{10}$  and its interaction can be 4.7% to 10.3% in most of the cases.

$X_{27}$  (subgrade modulus) and  $X_{30}$  (optimum gravimetric water content),  $X_8$  (traffic growth factor) and  $X_{13}$  (top AC layer thickness) have captured 2.8% to 5.5% of total uncertainties. In some cases, the effect of subgrade modulus can be up to 7.4% and can be low up to 1.4%. Optimum gravimetric water content can play a role from 0% to 5.8%. For traffic growth factor, the variation is from 1.6% to 7.1%. Top AC layer thickness can have influence from 1% to 5.3%. Three parameters are listed in the table which are not very important but sometimes need extra attention. They are  $X_3$  (percent of trucks in design direction),  $X_{26}$  (type of subgrade material) and  $X_{21}$  (Superpave binder grade of bottom AC layer). They all explain 2% to 3% of the total uncertainties individually. Sometimes their influence is more than 5%.

GBM model has a  $R^2$  value of 0.901 which means that 91% of uncertainties are captured in this model. Therefore, this model can be assigned as an excellent model also like  $Y_5$ . The most important parameter in GBM model is  $X_1$  (AADTT). T obtained for this parameter is 0.446 which means that  $X_1$  and its interaction with other input variables altogether explains 44.6% of the uncertainties. The CI of T is measured and presented in the next column. The estimated T value for  $X_1$  is 0.446 but 95% time the value will be within 0.347 to 0.451. This indicates that 95% of the time  $X_1$  and its corresponding interaction can be within 34.7% to 45.1%.

In GBM model, the next important parameter is  $X_4$  (percent of trucks in design lane). According to the T value,  $X_4$  and its corresponding interaction captured 35.6% of the uncertainties. The CI for T is 0.279 to 0.384. Therefore, influence of  $X_4$  and its interaction can be 27.9% to 38.4% in most of the cases.  $X_{18}$ , or bottom AC layer thickness, is also an important factor in this model. Influence of this input variable with its interaction with others has estimated 12.3%. 95% of time, this value will be from 9.9% to 16.9%. This parameter is important as it explain at least 10% of the variance.

Two input variables are listed in this table and can be considered as not so important factors for this model. They are  $X_{10}$  (tire pressure) and  $X_{27}$  (subgrade modulus). They have captured less than 4% of the uncertainties respectively. In some cases, the effect of subgrade modulus can be up to 6.9% and can be low up to 1.5%. Tire pressure can play role from 3.1% to 7.6%. Three parameters are listed in these tables which are not important because they have captured less than 3% of the uncertainties individually. These are  $X_{30}$  (optimum gravimetric water content),  $X_3$  (percent of trucks in design direction) and  $X_{11}$  (depth of water table).

Figure 9.6 represents graphically the summary results of the most important factors by both methods. By visual inspection at a glance for all the methods, it can be said that the pattern of the bar chart is the same. Two parameters ( $X_1$  and  $X_4$ ) contribute a significant amount (more than 20%) when compared to other parameters in the bar chart. The rest of the parameters are less than 15% of the variances as the main effect. This is the common trend for methods.

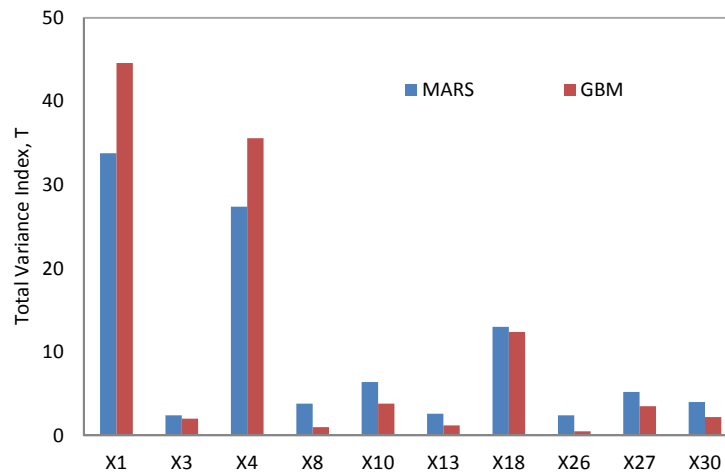


**FIGURE 9.6 Total Variance Index (T) of Input Factors that Effect Total Rutting (Y6)**

From these figures, it can be seen that  $X_1$  or AADTT has captured the highest percentage of uncertainties for all methods. The total uncertainty captured by this input variable is highest in GBM (45%) and the lowest MARS (34%).  $X_4$ , or percent of trucks in design lane, has ranked second in importance factor in the meta-models. The total uncertainties explained by this input variables are almost same in both cases (around 30%).  $X_{18}$ , or bottom AC layer thickness, placed third in the ranking order for both methods. It is very clear from the figures that the effect of this input is also the same in all cases (10%~12%).

$X_{10}$ , or tire pressure placed fourth in the ranking order. It is very clear from the figure that the effect of this input is also the same in all cases (4%~6%).  $X_{27}$  and  $X_{30}$  work like  $X_{10}$  in both methods. Without all the parameters, there are some parameters that are just captured by one or two particular methods. Some of these are  $X_8$ ,  $X_{13}$ , etc. These are all less important variables as they are not able to explain more than 3% of uncertainties.

## REMARKS

Table 9.8 summarizes the analysis results for outputs for both MARS and GBM methods. For terminal IRI ( $Y_1$ ), both models have three common inputs in this group individually. They are  $X_{18}$  (bottom AC layer thickness),  $X_1$  (AADTT) and  $X_4$  (percent of trucks in design lane). Therefore, these three inputs are the most important factors for this output.  $X_{13}$  (top AC layer thickness),  $X_{22}$  (percent air void of bottom AC layer),  $X_8$  (traffic growth factor) and  $X_{27}$  (subgrade modulus) are captured as medium sensitive by both methods.  $X_3$  (percent of trucks in design direction) and  $X_{26}$  (subgrade material) are also considered as medium sensitive in MARS

method but low sensitive in GBM.  $X_{10}$  (tire pressure) is captured as medium sensitive to  $Y_1$  by MARS method but not even captured as significant by GBM.  $X_{15}$  and  $X_{16}$  are also common in low sensitive group for both models. For both of these methods, the top three input ranking is the same. Without these three parameters, the rest of the input variables are also common for both methods and the order also. Therefore, it can be said that the models obtained for output  $Y_1$  are reliable. The same types of results are obtained by the rest of the outputs. For both methods, variables of high and medium importance have almost the same variable list. However, there are some differences for the low important group. It can be concluded that both types of regression methods are able to capture the most important factors for pavement performance.

TABLE 9.8 Summary Result of Outputs

Type	Terminal IRI ( $Y_1$ )		Longitudinal Cracking ( $Y_2$ )		Alligator Cracking ( $Y_3$ )		Transverse Cracking ( $Y_4$ )		AC Rutting ( $Y_5$ )		Total Rutting ( $Y_6$ )	
Model	MARS	GBM	MARS	GBM	MARS	GBM	MARS	GBM	MARS	GBM	MARS	GBM
High	$X_{18}$	$X_{18}$	$X_{18}$	$X_{18}$	$X_{18}$	$X_{18}$	$X_4$	$X_{28}$	$X_1$	$X_1$	$X_1$	$X_1$
	$X_1$	$X_1$	$X_1$	$X_4$	$X_1$	$X_1$	$X_7$	$X_4$	$X_4$	$X_4$	$X_4$	$X_4$
	$X_4$	$X_4$	$X_4$	$X_1$	$X_{22}$		$X_{28}$	$X_{12}$	$X_{10}$	$X_{10}$	$X_8$	$X_{18}$
Medium					$X_4$		$X_{23}$					
	$X_{13}$	$X_{22}$	$X_{17}$	$X_{25}$	$X_{13}$	$X_4$	$X_{15}$	$X_{23}$	$X_{18}$	$X_{18}$	$X_{10}$	$X_{10}$
	$X_{22}$	$X_8$	$X_{24}$	$X_{24}$	$X_{25}$	$X_{22}$	$X_{11}$	$X_{11}$	$X_8$	$X_8$	$X_{27}$	$X_{27}$
	$X_8$	$X_{13}$	$X_{25}$	$X_{17}$	$X_3$	$X_{13}$	$X_{22}$	$X_{17}$			$X_{30}$	$X_{30}$
	$X_3$	$X_{14}$	$X_{13}$	$X_{13}$	$X_{24}$	$X_{25}$	$X_{30}$	$X_{21}$			$X_8$	$X_3$
	$X_{10}$	$X_{27}$	$X_{27}$	$X_3$		$X_{28}$	$X_{29}$	$X_7$			$X_{13}$	
	$X_{27}$		$X_{23}$			$X_{19}$	$X_{14}$	$X_{18}$			$X_3$	
	$X_{26}$		$X_3$			$X_{27}$	$X_2$	$X_2$			$X_{26}$	
	$X_{16}$							$X_{13}$				
								$X_{15}$				
								$X_9$				
								$X_{24}$				
	$X_{24}$	$X_2$	$X_9$	$X_{27}$	$X_7$	$X_{20}$	$X_{25}$	$X_{10}$	$X_{30}$	$X_{13}$	$X_{21}$	$X_{13}$
	$X_{25}$	$X_3$	$X_8$	$X_{26}$	$X_{27}$	$X_{21}$	$X_3$		$X_{25}$	$X_{11}$	$X_5$	$X_{11}$
	$X_{30}$	$X_{16}$	$X_{22}$	$X_{11}$	$X_{21}$	$X_{17}$	$X_9$		$X_5$	$X_{15}$	$X_{16}$	$X_8$
Low	$X_{15}$	$X_{26}$	$X_{15}$	$X_2$	$X_{29}$	$X_{26}$	$X_{10}$		$X_{12}$	$X_3$	$X_9$	$X_{24}$
		$X_{15}$	$X_{30}$	$X_{12}$	$X_5$	$X_5$			$X_{23}$	$X_{20}$	$X_{15}$	$X_{12}$
		$X_{28}$		$X_{22}$	$X_{14}$	$X_9$			$X_{13}$	$X_9$		$X_{20}$
		$X_6$		$X_{23}$	$X_{12}$				$X_{26}$	$X_{21}$		$X_{28}$
									$X_{24}$	$X_{17}$		$X_{26}$
									$X_{19}$	$X_{23}$		
									$X_{28}$	$X_{12}$		

## CONCLUSIONS

Nonparametric regression procedures are employed to determine the sensitivity measures of the input variables in the MEPDG model. A total of two methods were performed in this case study, (i) Multivariate Adaptive Regression Splines (MARS) and (ii) Gradient Boosting Machine (GBM). Results provide an estimate along with CI for the total variance sensitivity index for input variables which considers the interaction effect among them. The T gives the proportion of uncertainty due to a particular input and its interaction with others. Based on this index, significant input variables are categorized into three groups. Input variables are analyzed for six

MEPDG outputs. The significant variables considering interaction with others for MEPDG outputs are given below:

- Terminal IRI
  - High Sensitive: Bottom AC layer thickness, AADTT, Percent of trucks in design lane
  - Medium Sensitive: Top AC layer thickness, Percent air void of bottom AC layer, Traffic growth factor, Subgrade modulus, percent of trucks in design direction, Tire pressure, Subgrade material
  - Low Sensitive: Superpave binder grade of top AC layer, Base material, Base modulus, Optimum gravimetric water content, Effective binder content of top AC layer, Aggregate gradation of top AC layer, Number of lanes in design direction, plastic limit, Percent of Vehicle class 9
  - Insensitive: Operational speed, Percent of Vehicle class 11, Design lane width, Depth of water table, Climate, Percent air void of top AC layer, Aggregate gradation of bottom AC layer, Effective binder content of bottom AC layer, Superpave binder grade of bottom AC layer, base layer thickness, Liquid limit
- Longitudinal Cracking
  - High Sensitive: Bottom AC layer thickness, AADTT, Percent of trucks in design lane
  - Medium Sensitive: Base material, Percent air void of top AC layer, Base modulus, Top AC layer thickness, subgrade modulus, Base layer thickness
  - Low Sensitive: Percent of trucks in design direction, Design lane width, Traffic growth factor, Percent air void of bottom AC layer, Effective binder content of top AC layer, Optimum gravimetric water content, Subgrade material, Depth of water table, Climate, Number of lanes in design direction
  - Insensitive: Operational speed, Percent of Vehicle class 9, Percent of Vehicle class 11, Tire pressure, Aggregate gradation of top AC layer, Superpave binder grade of top AC layer, Aggregate gradation of bottom AC layer, Effective binder content of bottom AC layer, Superpave binder grade of bottom AC layer, Plastic limit, Liquid limit
- Alligator Cracking
  - High Sensitive: Bottom AC layer thickness, AADTT, Percent of trucks in design lane, Percent air void of bottom AC layer
  - Medium Sensitive: Top AC layer thickness, Base modulus, Percent of trucks in design direction, Plastic limit, Subgrade modulus
  - Low Sensitive: Base material, Percent of Vehicle class 11, Superpave binder grade of bottom AC layer, Liquid limit, Operational speed, Aggregate gradation of top AC layer, climate, Aggregate gradation of bottom AC layer, Effective binder content of bottom AC layer, Percent air void of top AC layer, Subgrade material, operational speed, Design lane width
  - Insensitive: Number of lanes in design direction, Percent of Vehicle class 9, Traffic growth factor, Tire pressure, Depth of water table, Aggregate gradation of top AC layer, Effective binder content of top AC layer, Superpave binder grade of

top AC layer, Base layer thickness, Liquid limit, Optimum gravimetric water content

- Transverse cracking
  - High Sensitive: Percent of Trucks in design lane, percent of vehicle class 11, plastic limit, base layer thickness, effective binder content of top AC layer, Climate
  - Medium Sensitive: Depth of water table, top AC layer thickness, Percent air void of top AC layer, Percent air void of bottom AC layer, Optimum gravimetric water content, Liquid limit, Aggregate gradation of top AC layer, Number of lanes in design direction, Superpave binder grade of bottom AC layer, Bottom AC layer thickness
  - Low Sensitive: Base modulus, Percent of Trucks in design direction, Design lane width, Base material, Tire pressure
  - Insensitive: AADTT, Operational speed, Percent of vehicle class 9, Traffic growth factor, Superpave binder grade of top AC layer, Aggregate gradation of bottom AC layer, Effective binder content of bottom AC layer, Subgrade material, Subgrade modulus
- AC Rutting
  - High Sensitive: AADTT, Percent of trucks in design direction, Tire pressure
  - Medium Sensitive: Bottom AC layer thickness, Top AC layer thickness, Traffic growth factor
  - Low Sensitive: Percent of trucks in design direction, Operational speed, Design lane width, Depth of water table, Climate, Effective binder content of top AC layer, Percent air void of top AC layer, Aggregate gradation of top AC layer, Effective binder content of bottom AC layer, Superpave binder grade of bottom AC layer, Base layer thickness, Base modulus, Base material, Subgrade material, Plastic limit, Optimum gravimetric water content
  - Insensitive: Number of lanes in design direction, Percent of vehicle class 9, Percent of vehicle class 11, Aggregate gradation of top AC layer, Superpave binder grade of top AC layer, Percent air void of bottom AC layer, base modulus, Liquid limit
- Total Rutting
  - High Sensitive: AADTT, Percent of trucks in design direction, Bottom AC layer thickness
  - Medium Sensitive: Tire pressure, Optimum gravimetric water content, Subgrade modulus, Top AC layer thickness, Traffic growth factor, Subgrade material,
  - Low Sensitive: Percent of trucks in design direction, Operational speed, Design lane width, Depth of water table, Climate, Effective binder content of top AC layer, Superpave binder grade of top AC layer, Effective binder content of bottom AC layer, Superpave binder grade of bottom AC layer, Base material, Plastic limit
  - Insensitive: Number of lanes in design direction, percent of vehicle class 9, Percent of vehicle class 11, Aggregate gradation of top AC layer, Percent air void



of top AC layer, Aggregate gradation of bottom AC layer, Percent air void of bottom AC layer, Base layer thickness, Base modulus, liquid limit

The sensitivity chart presented in this study can be used to provide an idea about pavement distresses for some specific combinations of input variables. It will also help the designer to pick up the input values that need to be studied to take care of a particular pavement distress.

## Chapter 10

### LOCAL CALIBRATION OF MEPDG

#### INTRODUCTION

The MEPDG is based on both mechanistic and empirical principles. The mechanistic part assumes that pavement can be modeled as a multi-layered elastic structure and performs a time-stepping process. At every time step, structural analysis is done to estimate critical stresses and strains within the structure. Empirical models are then used to compute incremental distresses such as rutting, cracking, and roughness based on the stresses and strains calculated previously. This cycle is repeated through the pavement design life.

The pavement distress prediction models, also called transfer functions, are key components of the mechanistic-empirical procedure. Calibration of these models with local data sets is necessary to obtain an acceptable correlation between levels of distress observed in the field and those levels predicted with the MEPDG. Validation of the performance prediction models is a very important step to establish confidence before adopting them for design purposes. Calibration is the mathematical process in which the total residual error (difference between observed and predicted values of distress) is minimized. Validation is the process to confirm that the calibrated model can predict distresses accurately for other cases not used in the calibration. The calibration-validation process requires the use of precision and bias statistics. The concept of accuracy, or the exactness of a prediction to the actual value, encompasses both precision and bias. A prediction model is said to be precise when it can give repeated estimates that correlate strongly with the observed values. On the other hand, a model that is biased systematically over-predicts or under-predicts observed distresses; this means the prediction is consistently higher or lower than the observed value as distinct from random error.

The standard error of the estimate is a statistic that measures the amount of dispersion of the data points around the line of equality between the observed and predicted values of distress. In calibration, the total standard error of a pavement performance model presents four major components: measurement error, input error, model or lack-of-fit error, and pure error. The measurement error is caused by inaccuracies in the measure of distress along the pavement sections used in the calibration process. The input error is caused by variations in laboratory and field measurements when estimating the MEPDG inputs. Pure error is the random or normal variation due to replication. The model or lack-of-fit error is the portion of the total variance caused by inadequate theory and algorithms or incorrect model form. Understanding the contribution of each of these variance sources to the total standard error is critical in order to have the greatest effectiveness in the calibration refinement process.

Local calibration is performed to reduce bias and increase precision of the MEPDG prediction models. A biased model consistently produces over-designed or under-designed pavements with important cost consequences. A model with lack of precision leads to inconsistency in design

effectiveness. Validation of the MEPDG prediction models is necessary to ensure that the calibrated models produce robust and accurate predictions of pavement distresses for cases other than those used in calibration. Typically, the split sample approach 80/20 is used with 80 percent of the data used for calibration and 20 percent used for validation (randomly chosen). Successful validation requires that the bias and precision statistics of the validation data sets are similar to those obtained from calibration.

The performance models of MEPDG were calibrated nationally at a global scale using a representative number of pavement sections from the LTPP program throughout North America. Local calibration factors are included in the MEPDG to consider the differences in construction practices, maintenance policies, and material specifications across the United States. The objective of the local calibration process is to find appropriate calibration factors such that significant bias is eliminated, standard error is minimized, and precision maximized. In this study, local data related to traffic, climate, pavement structure, materials and distress were collected from different NMDOT sources and stored in the NMDOT's MEPDG database. A total of 24 New Mexico pavement sections were found to have all the MEPDG inputs and quantitative distress values required for MEPDG calibration. Eleven sections were obtained from the LTPP database and the remaining thirteen were collected from NMDOT's MEPDG database. Since NMDOT collected qualitative distress data rather than actual measurements of rut depth and crack length over the past years, distress values of the NMDOT sections were converted to quantitative data in the MEPDG database. Permanent deformation, alligator cracking, longitudinal cracking and roughness models were calibrated using the optimized coefficients. In calibration methodology, the target was fixed to reduce the sum of squared errors, defined by the square of the difference between predicted and measured distress, so that any bias was eliminated and precision was increased.

## **OBJECTIVES**

In this study, the objectives are to:

- Collect data of all MEPDG inputs (traffic, climate, and materials) for a sufficient number of pavement sections throughout New Mexico.
- Determine for every distress model a set of calibration coefficients that minimize the residual error (difference between observed and predicted distresses).
- Validate the effectiveness of these calibration coefficients for a number of pavement sections that were not included in the local calibration process.

## **PAST STUDIES**

Hoegh et al. (2010) conducted research to evaluate and calibrate the MEPDG rutting prediction model using 12 hot mix asphalt (HMA) pavement sections from the full-scale pavement research facility MnROAD in Minnesota. This research project involved the following objectives: identify pavement sections where performance data was known, obtain MEPDG inputs for these MnROAD sections, run MEPDG to predict rutting, compare predicted and measured rutting at every section, and finally adjust the parameters of the MEPDG rutting model to reduce error. All data collected at the MnROAD facility was entered into a database for the Minnesota

Department of Transportation (MnDOT). Rutting was manually measured by MnROAD staff three times per year using the straightedge method. Trenches were cut at the MnROAD sections to study the level of rutting occurring in individual layers of the pavement. It was observed that most of the rutting occurred in the HMA while the granular base and the subgrade were unaffected. The sections were subjected to the same environmental and traffic loading, but the following design variables were different: asphalt binder grade, mix design, air void content, HMA thickness, type and thickness of the base. MEPDG version 1.0 was used to predict the rutting performance of the test sections. The design guide calculates the rutting due to the asphalt concrete (AC) layer, the granular base, and the subgrade; the summation of the three is the total rutting in the pavement:

$$\text{Total Rutting} = \text{Rutting AC} + \text{Rutting Base} + \text{Rutting Subgrade} \quad \text{Eq. (1)}$$

The measured total rutting was compared to the MEPDG predicted value for all MnROAD pavement sections and it was observed that the predicted total rutting was always greater than the measured total rutting. In some sections, the predicted AC rutting was similar to the measured total rutting. Considering that forensic studies found that most of the measured rutting occurred in the AC layer, the MEPDG predicts accurately the rutting due to the AC, but the base and subgrade predictive models overestimate total rutting, and therefore, they should be modified. It was noticed that during the first month of the pavement design life, the MEPDG consistently predicts a huge accumulation of rutting in the base and subgrade layers which is not realistic. Therefore, it was recommended to subtract the base and subgrade rutting accumulated during the first month of pavement life from the MEPDG rutting prediction:

$$\begin{aligned} \text{Total Rutting} = & \text{Rutting AC} + (\text{Rutting Base} - \text{Rutting Base } 1^{\text{st}} \text{ month}) \\ & + (\text{Rutting Subgrade} - \text{Rutting Subgrade } 1^{\text{st}} \text{ month}) \end{aligned} \quad \text{Eq. (2)}$$

With the application of the locally calibrated rutting prediction model, bias and the residual error were reduced significantly.

Li et al. (2009) performed calibration of the MEPDG new flexible pavement distress models to Washington State local conditions using data obtained from the Washington State Pavement Management System (WSPMS). The sensitivity of required input data was analyzed as well. The researchers proposed an implementation plan for MEPDG that could replace the 1993 AASHTO Design Guide. Level 2 MEPDG inputs of traffic, climate, and pavement structure data were collected from a variety of sources. It seems that MEPDG software does not work properly with Level 1 inputs. More than 30 years of distress data were available from the WSPMS. The split-sample and the jackknife testing approaches were combined in the calibration process. The sensitivity of the design parameters was checked by varying the inputs and performing iterative runs. The following key observations were made:

- AC rutting is mostly influenced by climate, traffic loading, AC thickness and base type.
- Longitudinal cracking is strongly influenced by Performance Graded (PG) binder and AC thickness.
- Alligator cracking is mainly affected by the stiffness of the hot mix asphalt (HMA).
- Temperature is the most important factor in transverse cracking prediction.

- Roughness is influenced by climate, traffic loading, and base type.

From analyses, it was observed that default MEPDG tends to under predict AC rutting, longitudinal cracking, and alligator cracking. Trenches in WSDOT routes have shown that very limited rutting occurs in the subgrade, therefore, the corresponding calibration coefficients were set to 0. The MEPDG transverse cracking prediction under default settings matched the WSPMS performance data, and thus, it was not necessary to calibrate this model. An elasticity analysis was conducted to describe the effects of the different calibration factors on the pavement distress predictions. Elasticity is an econometric parameter which is defined as follows:

$$E_{distress}^{C_i} = \frac{\partial(distress)/distress}{\partial(C_i)/C_i} \quad \text{Eq. (3)}$$

where  $E_{distress}^{C_i}$  is the elasticity of the calibration factor  $C_i$  for the associated distress. The elasticity can be zero, positive or negative. Zero indicates that the calibration factor has no influence on the prediction; positive implies that the estimation increases as the factor increases, and negative means that the prediction decreases as the factor increases. The results showed the following conclusions: in the rutting model, the calibration factors  $\beta_{r2}$  and  $\beta_{r3}$  have more impact than  $\beta_{r1}$ ; in the AC fatigue model,  $\beta_{f2}$  and  $\beta_{f3}$  are more influent than  $\beta_{f1}$ ;  $C_2$  is the most important factor in longitudinal cracking and  $C_1$  in alligator cracking. During the calibration process, the user varies the calibration factors until the MEPDG distress prediction matches the actual pavement performance. Only one pavement section can be evaluated at a time in MEPDG software, therefore, a few sections were carefully chosen to represent a larger group of WSDOT's pavements. The calibration factors were adjusted in order of high to low elasticity. The set of calibration factors with the least error between the MEPDG prediction and the WSPMS measurements on all calibration and validation sections was selected as the final result:

- *Rutting:*  $\beta_{r1} = 1.05; \beta_{r2} = 1.109; \beta_{r3} = 1.1; \beta_{s1} = 0$
- *Fatigue:*  $\beta_{f1} = 0.96; \beta_{f2} = 0.97; \beta_{f3} = 1.03$
- *Longitudinal Cracking:*  $C_1 = 6.42; C_2 = 3.596; C_3 = 0; C_4 = 1,000$
- *Alligator Cracking:*  $C_1 = 1.071; C_2 = 1; C_3 = 6,000$

The International Reference Ionosphere (IRI) model could not be calibrated because of bugs in the MEPDG software. These calibration factors can be used to predict more accurately flexible pavement performance.

Banerjee et al. (2009) carried out an extensive local effort with the objective of calibrating the MEPDG permanent deformation performance model for five different regions in the state of Texas. The focus of this study was to find a set of two calibration factors of the AC permanent deformation model per region by minimizing the sum of squared errors (SSE) between observed and predicted pavement distresses. A joint optimization approach was adopted to obtain Level 2 calibration factors for every region. At the end, all of them would be averaged to come up with a set of Level 3 calibration factors for the state of Texas. If this approach were used with all the pavement sections at once, the results obtained would be more accurate, but the computational process would require more time. A total of 18 sections were obtained from the LTPP database. These experiments were representative of five regions with different environmental conditions: wet-warm, wet-cold, dry-warm, dry-cold and mixed. The number is not sufficient and the

researchers recommend monitoring at least 100 new sections and storing the data in the Texas Flexible Pavement Database. The data required to simulate the 18 pavement sections in MEPDG (traffic, layers, materials and performance) was obtained from the LTPP database. The MEPDG analysis was initiated with default calibration parameters and then adjusted such that the difference between the observed and the predicted distress values were reduced progressively. The optimal solution minimizes the SSE. For this calibration, the factor  $\beta_{r2}$  was kept constant. The calibration coefficient  $\beta_{r1}$  that captures the influence of the HMA layer thickness and  $\beta_{r3}$  that captures the impact of the number of load repetitions were optimized. The calibration factor  $\beta_{s1}$  controlling the rutting in the subgrade was preset to regional defaults (0.3 for West Texas and 0.7 for East Texas) that were determined on the basis of average moisture content of the subgrade soil. It was observed that the distress predictions were more sensitive to  $\beta_{r3}$  than  $\beta_{r1}$ , and for this reason a higher precision was used for  $\beta_{r3}$ . The final Level 3 calibration coefficients obtained for the state of Texas were:  $\beta_{r1} = 2.39$ ,  $\beta_{r3} = 0.856$ , and  $\beta_{s1} = 0.5$ . The standard error of the calibrated permanent deformation model was found to be less than 0.1 in. which was a good result.

Muthadi and Kim (2008) performed research to calibrate the MEPDG permanent deformation and alligator cracking models for local materials, conditions, and practices used in the flexible pavements of North Carolina. A total of 53 pavement sections were selected: 30 from the LTPP database (16 new flexible and 14 rehabilitated) and 23 from the North Carolina Department of Transportation (NCDOT) databases. The data collection effort included the gathering of MEPDG inputs related to materials, traffic, climate, and pavement structure. The performance data obtained from the Pavement Management Unit used a nonnumeric rating format which consisted of none, low, medium or severe level of distress. Therefore, this data was converted to MEPDG format to be able to compare measured and predicted distress values. The first step of the local calibration process was to perform verification runs on the pavement sections with default MEPDG models. It was observed that NCDOT sections introduced significant error and inconsistency because of their nonnumeric distress measurement technique. Thus, only LTPP sections were used in the calibration of the permanent deformation model. The second step was to calibrate the model coefficients to reduce the bias and the standard error. For the permanent deformation model, Microsoft Excel Solver program was used to optimize the coefficients  $\beta_{r1}$ ,  $\beta_{GB}$ , and  $\beta_{SG}$  ( $\beta_{r2}$  and  $\beta_{r3}$  were not calibrated) separately for each layer. Since pavement trenches and cores were not available, the total measured rutting was distributed to each layer according to the ratio of predicted total rutting to the predicted permanent deformation in each layer. For the bottom-up cracking model, the coefficients  $C_1$  and  $C_2$  of the corresponding transfer function were optimized using Microsoft Excel Solver. Both LTPP and NCDOT sections were used for the alligator cracking calibration. In the final step, validation was performed to check for the reasonableness of the performance predictions. The split-sample approach was used where 80% of the sections were randomly selected for calibration and 20% were kept aside for validation. The following calibration factors were obtained and proposed to use until a more robust calibration process with more sections is achieved in the future:

- *Rutting:*  $\beta_{r1} = 1.017$ ,  $\beta_{r2} = 1$ ,  $\beta_{r3} = 1$ ,  $\beta_{GB} = 0.778$ ,  $\beta_{SG} = 0.818$
- *Alligator Cracking:*  $C_1 = 0.437$ ;  $C_2 = 0.151$ ;  $C_3 = 6,000$

The standard error of the calibrated permanent deformation model was reduced from 0.154 to 0.109. Similarly, the standard error of the calibrated alligator cracking model was reduced from 6.02 to 3.64. The last model presented a poor precision, possibly because the NCDOT sections

were included in its calibration. The researchers recommended the use of the LTPP distress identification manual for the measurement of distress in the pavement sections.

Hall et al. (2010) conducted the calibration and validation of the Arkansas MEPDG performance prediction models to local traffic, climate, materials and practices. A total of 26 pavement sections were obtained from two sources: the LTPP database and the Pavement Management System (PMS) of the Arkansas State Highway and Transportation Department (AHTD). All pavement sections were distributed across the five different regions of Arkansas. The PMS sections were chosen to have a construction date later than 1996 when the Superpave HMA mixture design system was implemented. 20 sites (80%) were randomly selected for calibration and the other 6 (20%) were preserved for validation. The data required such as traffic, climate, structure, materials, and pavement performance were collected from LTPP and AHTD databases. Verification runs were performed with default calibration coefficients and it was observed that measured and predicted distresses did not match well for longitudinal and alligator cracking. The calibration coefficients were obtained by minimizing the sum of squared error between predicted and measured distresses. The Microsoft Excel Solver function was used to optimize the coefficients of the alligator cracking and longitudinal cracking models. Iterative runs of MEPDG were performed with different combinations of coefficients to optimize the rutting model. It was assumed that rutting would occur only in the HMA layer and in the subgrade, thus the coefficient  $\beta_{GB}$  for the granular base was not calibrated. The transverse cracking model was not calibrated because its MEPDG prediction is zero when properly selected PG binders are used. The IRI model was not calibrated either because it is a function of other predicted distresses. The following calibration coefficients were obtained:

- *Rutting:*  $\beta_{r1} = 1.2, \beta_{r2} = 1, \beta_{r3} = 0.8, \beta_{base} = 1, \beta_{subgrade} = 0.50$
- *Alligator Cracking:*  $C_1 = 0.688, C_2 = 0.294, C_3 = 6000$
- *Longitudinal Cracking:*  $C_1 = 3.016, C_2 = 0.216, C_3 = 0, C_4 = 1000$

The calibrated models were validated by running MEPDG on the remaining sites and it was evident that local calibration reduces the difference between predicted and measured distress.

The next sections provide necessary background for calibration of MEPDG. Firstly, brief review of the efforts on implementation of MEPDG made by some other state agencies is provided. Secondly, some advanced statistical methods for local calibration of MEPDG discussed. Finally, some promising methodologies which can be applied to get more precise calibration of MEPDG are discussed briefly.

## **Calibration Practice Performed in NCHRP Projects**

### *National Calibration Procedure (NCHRP 1-37A)*

The calibration method used in project NCHRP 1-37A in general involves four steps:

1. Collection of the calibration data for each field section from the LTPP database.
2. Simulation runs using the MEPDG software and different sets of calibration coefficients in the performance model.

3. Comparison of the predicted damage to the measured cracking observed in the field obtained from each calibration coefficient combination.

4. Correlation of the predicted damage with the measured cracking in the field by minimizing the square of errors, as the final step.

The main goal of calibration is to minimize the total sum of squared errors and to eliminate the bias and scatter in the predictions. The methodology of calibration used in this project is based on a simple goodness-of-fit statistical method. The optimization techniques for each single performance may vary a little.

### *NCHRP Project 1-40B*

The NCHRP 1-37A project deliveries a uniform basis for design of flexible, rigid, and composite pavements. The distress prediction models were calibrated on a national level which implemented data from Long-Term Pavement Performance (LTPP). Therefore, it employs an array of common parameters for traffic, subgrade, environment, and reliability. As widely recognized, in order to make those models fully applicable to particular materials, environmental conditions and construction practices, the calibration of these distress prediction models should be based on the data directly from local. NCHRP 1-40 project report provides the recommendations and basic guidelines to conduct the local calibration of MEPDG in 11 steps. In this report, two models were calibrated as examples, which are permanent deformation model and alligator cracking model for local conditions and materials.

As to the calibration of distress prediction model, the methodology implemented in 1-40B is based on goodness-of-fit criteria to determine the best sets of values for the parameters. Two approaches are recommended in 1-40B project report, one is an analytical process for linear models. Another one is using numerical optimization for non-linear models. As to linear models, the method is based on the least square regression line analysis, stepwise regression analysis, principal components analysis, or principal component regression analysis. Numerical optimization for non-linear models mainly includes the steepest descent or pattern search analysis.

There are two approach implemented in the NCHRP Project 1-40B to increase the accuracy of calibration of distress prediction models. They are traditional split-sample approach and jackknifing approach, which is an alternative method.

### *Split-Sample Approach*

The traditional split-sample approach is splitting the sample into two parts. Usually half or more than half as a portion is for calibration. And remainders are for validation.

However, there is a shortcoming of this approach. Generally, the sample of pavement performance data usually are limited, therefore the sample size is small. The half of the sample would be even smaller. If we use this to conduct calibration, it may come out inaccurate coefficients, therefore reducing the reliability of distress performance models.



### *Jackknifing Approach*

Suppose there is a sample matrix which has  $n$  rows and  $n$  columns. The alternative approach, jackknifing approach, is to randomly pick up one set of values and leave it for upcoming validation. Then using the remaining  $n-1$  sets of values to conduct the calibration.

The advantage of this method is that the data used for validation is totally independent from the data from calibration, which increase the reliability of validation process. About jackknifing experiment, it will be reviewed more in next section.

### *Findings from NCHRP Project 9-30*

The NCHRP Project 9-30 aims to develop a detailed, statistically sound, and practical experimental plan to refine the calibration and validation of the performance models incorporated in the pavement design guide (2002 Design Guide). It was pointed out that “Development of pavement performance models for M-E pavement design methods requires a rational procedure for performing calibration and validation.” (NCHRP, 2003) Considering that the distress data are expensive and time-consuming to get, it is more rational to calibrate and validate the distress prediction models using one database. Jackknifing’s goodness-of-fit statistics are based on predictions rather than the data used for fitting the model parameters (Miller, 1974; Mosteller and Tukey, 1977). There are three advantages of Jackknifing testing. The key advantage is that the goodness-of-fit statistics are based on the predictions from the data that are totally independent from the data used for calibration process. It increases the accuracy of model calibration. Moreover, multiple jackknifing can be used to assess the stability of the prediction models. Another advantage is that it is easy to apply.

### **The Local Calibration by State Agencies**

The basic objective of local calibration of MEPDG is minimizing the difference between the MEPDG predicted output values

#### *North Carolina Study*

The calibration of the MEPDG for flexible pavements was conducted in North Carolina. Two pavement distress prediction models were selected for this research: permanent deformation and bottom-up fatigue cracking. The methodology North Carolina Department of Transportation (NCDOT) used for local calibration is under the guidelines and recommendations provided by NCHRP Project 1-40B Draft report. The whole process includes three main steps for local calibration of MEPDG to the condition in North Carolina. The first step is using the national factors developed under the NCHRP Project 1-37 to perform the verification runs on each section. The second step is to calibrate the pavement distress prediction model to pursue the goal of minimizing the standard error between measured values and predicted values and try to eliminate the bias. The final step is validating the calibrated model to check if it is reasonable.

The methodology used by NCDOT is split-sample approach. Approximately 80 % of the sections were selected randomly for calibration purposes and 20% for the validation process (Naresh and Y. Richard 2007). As to the software, MEPDG version 1.0 (DG 2002) was used to perform the verification, calibration and validation. During the calibration, first of all, a t-test was performed to determine the bias of the verification results from verification process. After calibrating the

performance models, a chi-square test was used in validation stage to check if there is significance difference between the local standard error and national standard error.

### *Texas Study*

A local calibration of MEPDG pavement permanent performance models was performed in Texas using LTPP database. This effort was an extensive local calibration undertaken to calibrate the pavement distress prediction models in MEPDG for five different regions in Texas and for Texas in general (state defaults) (Ambarish and Jose and Jorge, 2009). The objective of this study is to determine a new set of local calibration coefficients, focusing on Level 2 and Level 3. There are two approaches used for minimizing the sum of squared errors between the predicted values and measured distresses. The first one is a joint optimization approach. Another approach is determining the Level 1 calibration factors for each region first and then averaging them to get the Level 2 calibration factors. As the findings from this study, the former approach is more sound than the latter one in both theoretical and statistical point of view and produces calibration factor with more desirable statistical properties (Ambarish and Jose and Jorge, 2009). With the same approach, the Level 3 calibration factors can be determined either using a joint optimization approach for each region, or just averaging Level 2 calibration coefficients for each of the regions to come up with a Level 3 calibration factors.

The calibration procedure conducted by TXDOT is similar to NCDOT. The calibration is done by comparing the bias between measured distresses and predicted values of pavement performance over time. The local calibration was first conducted with set of national factors and then adjusted some of the factors to reach the goal of bias reduction, trying to minimize the difference between observed distresses and predicted values. The models output and best fit were estimated in terms of the sum of squared errors (SSE).

$$SSE = \sum_{i=1}^N (Y_i - Y_{observed})^2$$

$Y_i$  = Output from the MEPDG

$Y_{observed}$  = Observed Distress Value as obtained from LTPP database

where

$N$  = Number of observed data points/distress measurements

$SSE$  = Sum of Squared Errors

During the whole calibration process, TXDOT using the joint optimization approach to calibrate the pavement distress prediction models for each of the five regions involved to obtain a set of regional calibration factors which jointly minimize the SSE for all the sections. Considering the enormous calculation efforts need to be made using joint optimization approach, TXDOT were just averaging the Level 2 factors to determine Level 3 calibration factors.

As stated in the results of this study, those two approaches used by TXDOT are both have the advantages to the certain aspects. The joint optimization approach is mathematically more sound and statistically efficient, but it requires an considerable amount of calculation if the number of section is increased by a certain amount. While using averaging of Level 2 calibration factors to

get Level 3 calibration factors needs less calculation efforts. Moreover, when it comes to determining Level 3 calibration factors, either approach can come up with the close values.

#### *Kansas Study*

KSDOT has published the *Recommended Practice for Local Calibration of the M E Pavement Design Guide*. This study described the standard procedure MEPDG calibration from limited data. This report focussed on flexible pavements and common rehabilitation strategies for flexible pavements such as hot mix asphalt (HMA) overlays. Two data sources are mainly used to demonstrate the steps, the pavement management systems (PMS) and LTPP test sections (SPS-1 and SPS-5 experiments). Both data sets were used in KSDOT report to demonstrate the steps and potential difference between measures of distress, quality and quantity of input data and to establish regional as well as local calibration factors for each performance measure.

Input level 2 and 3 were used for all input parameters for the PMS segments. Data needed to determine level 1 input were unavailable for the PMS segments. KSDOT had an insufficient number of LTPP sections that was not sufficient to execute local calibration project. So, LTPP sections within Kansas State and some of the nearby states were used for the purpose.

#### *Florida Study*

FDOT sponsored a research project with TTI in Florida to conduct a cooperative effort to establish and characterize field test sections for compiling a database of materials, geometric and traffic related design variables to verify the predictions from the MEPDG program and perform local model calibrations as warranted.

To simulate the current pavement condition criteria used by the department, researchers ran the MEPDG program for different levels of HMAC modules to simulate good, fair and poor pavement conditions by varying the binder and volumetric properties of the existing material, binder viscosity and air voids content. Based on the results of the sensitivity analyses, researchers came up with some selections of variables to generate the design tables for flexible pavements based on the MEPDG. The researchers recommended that, a structured database is required for storing data for calibration over the next 5-10 years.

## **PAVEMENT SECTIONS FOR CALIBRATION**

The internal databases of New Mexico Department of Transportation (NMDOT) were the first source considered for collecting the traffic, climate, structure, materials, and performance data necessary to obtain a sufficient number of local pavement sections. Indeed, all these databases have been consolidated in the new NMDOT Flexible Pavement Database. A total of 13 sections from this database are used in the local calibration process. NMDOT measures pavement performance with qualitative ratings rather than with quantitative measures of distress (depth of rutting or length of cracks), therefore the NMDOT performance data has to be converted.

The LTPP database created under the Strategic Highway Research Program (SHRP) contains extensive amounts of data and is consistent and reliable being one of the main resources used by most state agencies in their calibration efforts. There are 11 complete flexible experiments within the state of New Mexico. The code, location, functional class, construction date, and type of each

of these sections are contained in Table 10.1. As shown, six sections are new flexible pavements while the other five are rehabilitated asphalt concrete pavements. Table 10.2 shows the location, functional class, construction date and type of the NMDOT sections.

**TABLE 10.1 LTPP flexible pavement sections in New Mexico**

State Code	SHRP ID	Road	Mile point	Functional Class	Type of Experiment	Construction Date *
35	1002	US-70	310.1	2	GPS-6A	May 1985
35	1003	US-70	320.9	2	GPS-1	May 1983
35	1005	I-25	263.8	1	GPS-1	Sep 1983
35	1022	US-550	125.1	2	GPS-1	Sep 1986
35	1112	US-62	81.3	2	GPS-1	May 1984
35	2006	US-550	89.5	2	GPS-2	Jun 1982
35	2007	US-550	106.2	2	GPS-6A	Jun 1981
35	2118	I-40	346.2	1	GPS-2	Dec 1979
35	6033	I-25	159.3	1	GPS-6A	May 1981
35	6035	I-40	96.7	1	GPS-6A	May 1985
35	6401	I-40	107.7	1	GPS-6A	May 1984

*GPS-1: Asphalt Concrete on Unbound Granular Base; GPS-2: Asphalt Concrete on Bound Granular Base; GPS-6A: Existing AC Overlay on AC Pavement;*

*\* This is the date of last major improvement in the case of rehabilitated sections*

**TABLE 10.2 NMDOT flexible pavement sections in New Mexico**

Section #	Road	Mile point	Functional Class	Type of Section	Construction Date *
NMDOT 2	I-10	148.0	1	Rehabilitated	07/1984
NMDOT 4	I-40	183.0	1	New	06/1999
NMDOT 5	I-40	187.0	1	New	06/1999
NMDOT 6	I-40	243.0	1	Rehabilitated	06/1986
NMDOT 10	I-25	252.0	1	New	07/1982
NMDOT 12	US-54	82.0	2	New	06/1977
NMDOT 15	US-62	35.0	2	New	05/1992
NMDOT 19	US-64	97.0	2	Rehabilitated	10/1983
NMDOT 20	US-64	205.0	2	New	10/1971
NMDOT 21	US-70	254.0	2	New	10/1986
NMDOT 23	US-82	135.0	2	New	09/1994
NMDOT 25	US-84	183.0	2	Rehabilitated	07/1985
NMDOT 27	US-180	114.0	2	New	09/1994

*\* This is the date of last major improvement in the case of rehabilitated sections*

## CALIBRATION-VALIDATION METHODOLOGY

Calibration of the performance prediction models are achieved by varying the coefficients such that the residual sum of squared errors is reduced. The distress values measured in the field are compared to those predicted by the MEPDG and the residual error is calculated at five particular times per section equally distributed through the pavement design life.

The possibility of using numerical nonlinear optimization techniques was explored but its application would be too difficult since the MEPDG prediction of distress is a very complex iterative process. Therefore, the only way to proceed was to run the MEPDG multiple times for different combinations of the calibration coefficients and calculate the corresponding sum of squared errors.

The split-sample approach is used in the calibration-validation process; 19 out of 24 sections are chosen randomly for use in the calibration of each distress model while the other 5 sections are kept aside to check whether the calibrated pavement performance model can reduce the error in the MEPDG prediction of distress for cases different to those used during calibration.

## PERMANENT DEFORMATION MODEL

### Prediction of Permanent Deformation in the MEPDG

This section describes the empirical model used in the MEPDG to predict the permanent deformation occurring in the pavement layers (MEPDG Documentation 2004).

The plastic strain of the asphalt concrete layer is given by the following equations:

$$\begin{aligned}\frac{\varepsilon_p}{\varepsilon_r} &= k_z \beta_{r1} 10^{k_1} T^{k_2 \beta_{r2}} N^{k_3 \beta_{r3}} \\ k_z &= (C_1 + C_2 d) 0.328196^d \\ C_1 &= -0.1039 h_{AC}^2 + 2.4868 h_{AC} - 17.342 \\ C_2 &= 0.0172 h_{AC}^2 - 1.7331 h_{AC} + 27.428\end{aligned}\tag{Eq. (4)}$$

where  $\varepsilon_p$  = Plastic strain of the asphalt concrete layer (in/in),  $\varepsilon_r$  = Resilient strain of the asphalt concrete layer (in/in),  $T$  = Asphalt concrete layer temperature (°F),  $N$  = Number of axle load repetitions,  $d$  = Depth of the point where strain is being determined (in),  $h_{AC}$  = Thickness of the asphalt concrete layer (in),  $k_1 = -3.35412$ ,  $k_2 = 1.5606$ ,  $k_3 = 0.4791$ , and  $\beta_{r1}$ ,  $\beta_{r2}$ ,  $\beta_{r3}$  = calibration coefficients to be optimized.

This plastic strain value multiplied by the AC thickness provides the permanent deformation occurring at the asphalt concrete layer. The permanent deformation for granular bases and the subgrade is obtained using the following formula:

$$\delta_a = \beta_{s1} k_1 \varepsilon_v h \frac{\varepsilon_0}{\varepsilon_r} e^{-\left(\frac{\rho}{N}\right)^\beta}\tag{Eq. (5)}$$

where  $\delta_a$  = Permanent deformation of the unbound layer (in),  $N$  = Number of axle load repetitions,  $\varepsilon_v$  = Average vertical strain in the unbound layer (in/in),  $h$  = Thickness of the unbound layer (in),  $\varepsilon_r$  = Resilient strain in the unbound layer (in/in),  $\varepsilon_0$ ,  $\beta$ ,  $\rho$  = Material properties,  $k_1 = 2.03$  for granular base and 1.35 for subgrade, and  $\beta_{s1}$  = Calibration coefficient to optimize for both base and subgrade.

The total permanent deformation of the section is the summation of the permanent deformation occurring in every single layer:

$$PD = \sum_{i=1}^{layers} \varepsilon_p^i h^i\tag{Eq. (6)}$$

$$\begin{aligned}
&= h_{AC} \varepsilon_r k_z \beta_{r1} 10^{k1} T^{k2 \beta_{r2}} N^{k3 \beta_{r3}} \\
&+ \beta_{GB} k_{GB} \varepsilon_v h_{GB} \frac{\varepsilon_0}{\varepsilon_r} e^{-\left(\frac{\rho}{N}\right)^\beta}^{GB} \\
&+ \beta_{SG} k_{SG} \varepsilon_v h_{SG} \frac{\varepsilon_0}{\varepsilon_r} e^{-\left(\frac{\rho}{N}\right)^\beta}^{SG}
\end{aligned}$$

where,  $PD$  = Total permanent deformation (in),  $\varepsilon_p^i$  = Total plastic strain of layer  $i$  (in/in),  $h^i$  = Thickness of layer  $i$  (in).

In the previous equation (Eq. 18), there are five calibration coefficients:  $\beta_{r1}$ ,  $\beta_{r2}$ , and  $\beta_{r3}$  for the asphalt concrete layer,  $\beta_{GB}$  for the granular base layer, and  $\beta_{SG}$  for the subgrade. These coefficients cannot be calibrated separately for each layer since individual rutting data of each pavement layer is not available. Therefore, only the total permanent deformation prediction can be calibrated. Measurement of rutting at each pavement layer would require cutting trenches in the pavement sections but it would make the local calibration process much easier and more accurate.

### Calibration of the Permanent Deformation Model

Sections 2006, 6033, NMDOT 15, NMDOT 21, and NMDOT 25 are chosen randomly to be kept aside for validation while the nineteen remaining sections are used in the calibration process.

In the total rutting equation,  $\beta_{r2}$  and  $\beta_{r3}$  are respectively exponents to the AC temperature and the number of axle loads which are large numbers. Therefore,  $\beta_{r2}$  and  $\beta_{r3}$  are nonlinear calibration coefficients and the two most sensitive parameters of this model. The remaining calibration coefficients  $\beta_{r1}$ ,  $\beta_{GB}$ , and  $\beta_{SG}$  are linear calibration factors.

It is decided to optimize  $\beta_{r2}$  and  $\beta_{r3}$  in a first iterative run. This is done by varying and permuting the two nonlinear calibration coefficients while the other three,  $\beta_{r1}$ ,  $\beta_{GB}$ , and  $\beta_{SG}$  are set to the default value 1.0. The residual sum of squared errors which is the target to reduce is calculated for every set of  $\beta_{r2}$  and  $\beta_{r3}$  values.

Table 10.3 contains the sets of calibration coefficients considered in this first step and the corresponding sum of squared errors (SSE) and mean residual error (MRE). As shown, the set of calibration coefficients  $\beta_{r1} = 1.1$ ,  $\beta_{r2} = 1.1$  and  $\beta_{r3} = 0.8$  reduces the SSE from 4.7713 to 3.7842. Similarly the MRE per section is reduced from 0.0248 to 0.0221.

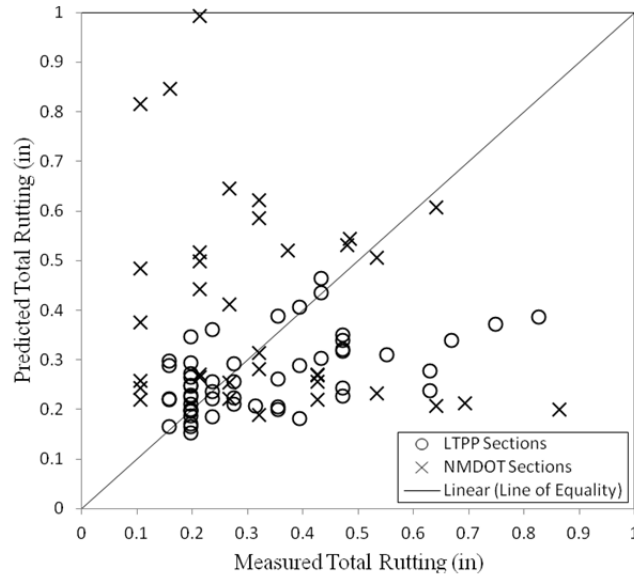
**TABLE 10.3 SSE and MRE of the rutting model for different  $\beta_{r2}$  and  $\beta_{r3}$** 

Set #	$\beta_{r2}$	$\beta_{r3}$	SSE	MRE
1	0.8	0.8	4.5047	0.0241
2	0.8	0.9	4.3604	0.0237
3	0.8	1	4.1495	0.0231
4	0.8	1.1	4.0597	0.0229
5	0.8	1.2	5.3874	0.0264
6	0.9	0.8	4.3367	0.0237
7	0.9	0.9	4.1106	0.0230
8	0.9	1	3.9686	0.0226
9	0.9	1.1	5.0355	0.0255
10	0.9	1.2	13.3237	0.0415
11	1	0.8	4.0628	0.0229
12	1	0.9	3.8808	0.0224
13	1	1	4.7713	0.0248
14	1	1.1	12.0744	0.0395
15	1	1.2	47.5539	0.0784
16	1.1	0.8	3.7917	0.0221
17	1.1	0.9	5.8508	0.0275
18	1.1	1	11.2647	0.0381
19	1.1	1.1	44.7627	0.0760
20	1.1	1.2	145.9079	0.1373
21	1.2	0.8	4.4497	0.0240
22	1.2	0.9	10.8591	0.0374
23	1.2	1	43.2231	0.0747
24	1.2	1.1	144.0629	0.1364
25	1.2	1.2	371.8553	0.2191
26	1.1	0.75	3.8665	0.0223
27	1.05	0.75	4.0342	0.0228
28	1.05	0.8	3.9040	0.0225
29	1.05	0.85	3.8364	0.0223

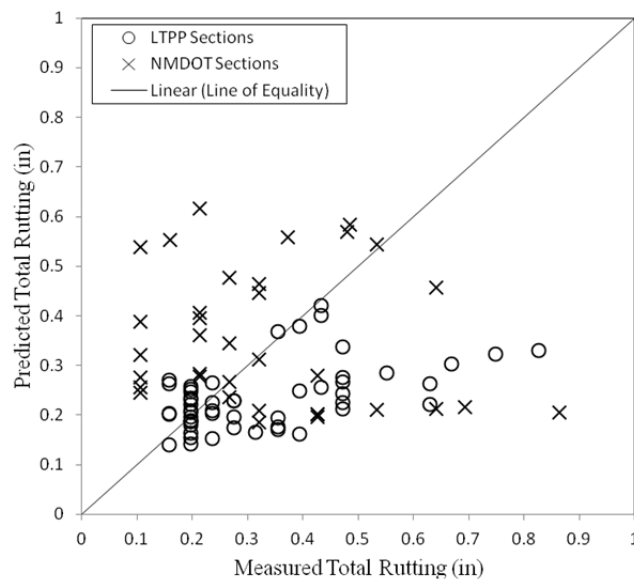
In a second iterative run, the calibration coefficients  $\beta_{r2}$  and  $\beta_{r3}$  are fixed to 1.1 and 0.8 respectively, while the values of  $\beta_{r1}$ ,  $\beta_{GB}$ , and  $\beta_{SG}$  are varied and permuted. It is observed that the set  $\beta_{r1} = 1.1$ ,  $\beta_{r2} = 1.1$ ,  $\beta_{r3} = 0.8$ ,  $\beta_{GB} = 0.8$ , and  $\beta_{SG} = 1.2$  reduces the sum of squared errors to 3.6415 and the mean residual error to 0.0217.

Figure 10.1 plots measured total rutting versus predicted total rutting with default MEPDG settings. Most of the LTPP data points fall on the right side of the line of equality while most of the NMDOT data points fall on the left side. This is due to differences in the distress measurement procedures used by LTPP and NMDOT.

After calibration, data is less scattered; data points are closer to the line of equality. This is evident from Figure 10.2 which plots the measured total rutting versus the corresponding prediction with calibrated MEPDG.



**FIGURE 10.1 Predicted Versus Measured Total Rutting Before Calibration**



**FIGURE 10.2 Predicted Versus Measured Total Rutting After Calibration**



## Validation of the Permanent Deformation Model

Validation of the calibrated permanent deformation model requires running the MEPDG for sections 2006, 6033, NMDOT 15, NMDOT 21, and NMDOT 25 using the new set of calibration coefficients. Then, the corresponding SSE and MRE are calculated to check whether the new model reduces the residual error for the validation sections as well.

Figure 10.3 compares the field measurements of total rutting and the uncalibrated and calibrated MEPDG predictions through the pavement design life of section NMDOT 25 respectively. The new model improves significantly the MEPDG prediction and the SSE decreases from 0.3064 to 0.1142. The validation is considered satisfactory.

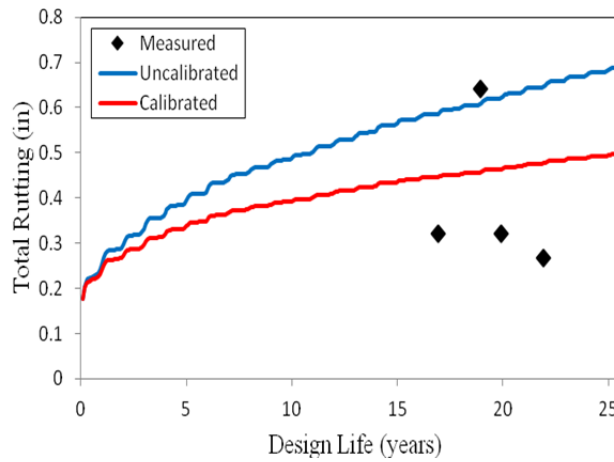


**FIGURE 10.3 Validation of the Calibrated Rutting Model (Section NMDOT 25)**

## ALLIGATOR (BOTTOM-UP) CRACKING MODEL

### Prediction of Alligator Cracking in the MEPDG

The approach used in the MEPDG to model fatigue cracking is based on the calculation of fatigue damage at the surface for top-down (longitudinal) cracking and at the bottom of the asphaltic layer for bottom-up (alligator) cracking (MEPDG Documentation 2010).

The fatigue damage is estimated using the following relationship known as Miner's Law:

$$D = \sum_{i=1}^T \frac{n_i}{N_i} \quad \text{Eq. (7)}$$

where  $D$  = Fatigue damage,  $T$  = Total number of periods,  $n_i$  = Actual number of axle load repetitions applied during period  $i$ , and  $N_i$  = Number of load repetitions to fatigue cracking.

The following mathematical relationship is used for predicting the number of load repetitions to fatigue cracking:

$$N_f = 0.00432 C \beta_{f1} k_1 \left( \frac{1}{\epsilon_t} \right)^{k_2 \beta_{f2}} \left( \frac{1}{E} \right)^{k_3 \beta_{f3}} \quad \text{Eq. (8)}$$

$$C = 10^M$$

$$M = 4.84 \left( \frac{V_b}{V_a + V_b} - 0.69 \right)$$

where  $N_f$  = Number of load repetitions to fatigue cracking,  $\varepsilon_t$  = Tensile strain at the critical location (in/in),  $E$  = Stiffness modulus of the asphalt concrete (psi),  $k_1 = 0.007566$ ,  $k_2 = 3.9492$ ,  $k_3 = 1.281$ ,  $V_b$  = Effective binder content (%),  $V_a$  = Percent of air voids (%), and  $\beta_{f1}$ ,  $\beta_{f2}$ ,  $\beta_{f3}$  = Calibration coefficients to be optimized.

The critical location may be at the surface for top-down cracking or at the bottom of the asphalt concrete layer for bottom-up cracking. The final transfer function provides bottom-up fatigue cracking from the fatigue damage and is expressed as:

$$FC_{bottom} = \frac{1}{60} \left( \frac{C_3}{1 + e^{C_1 C'_1 + C_2 C'_2 \log_{10}(100 D)}} \right) \quad \text{Eq. (9)}$$

$$C'_2 = -2.40874 - 39.748 (1 + h_{AC})^{-2.856}$$

$$C'_1 = -2 C'_2$$

where  $FC_{bottom}$  = Bottom-up fatigue cracking (% of the lane area),  $D$  = Bottom-up fatigue damage,  $h_{AC}$  = Thickness of the asphalt concrete layer, and  $C_1$ ,  $C_2$ ,  $C_3$  = Calibration coefficients to be optimized.

### Calibration of the Alligator Cracking Model

Sections 1002, 1022, NMDOT 19, NMDOT 20, and NMDOT 27 are randomly chosen for validation. The remaining nineteen sections are used in the calibration process.

The coefficients  $\beta_{f1}$ ,  $\beta_{f2}$ , and  $\beta_{f3}$  of the fatigue damage prediction equation cannot be calibrated because there is no available data to compare with. Calibration of these factors would require performing lab testing on the asphalt concrete mixtures used in the sections to determine the number of load repetitions necessary to initiate fatigue cracking. Therefore, the calibration coefficients  $\beta_{f1}$ ,  $\beta_{f2}$ , and  $\beta_{f3}$  are set to default value 1.0.

In the bottom-up cracking transfer function, the calibration coefficients  $C_1$  and  $C_2$  are varied and permuted in order to find a combination of values that will reduce the SSE. The coefficient  $C_3$  is fixed at the default value 6000. Table 10.4 shows the sum of squared errors and the mean residual error for several sets of calibration coefficients. It is found that  $C_1 = 0.625$  and  $C_2 = 0.25$  reduces the SSE from 4861.47 to 3537.84 and the MRE per section from 0.92 to 0.78.

The graph predicted versus measured alligator cracking before calibration is plotted in Figure 10.4. It is observed that the alligator cracking predicted by MEPDG with default settings is almost zero. The measurements vary from zero to some high values.

**TABLE 10.4 SSE and MRE of the alligator cracking model for different C1 and C2**

Set #	C <sub>1</sub>	C <sub>2</sub>	C <sub>3</sub>	SSE	MRE
1	0.25	0.25	6000	15082.72	1.62
2	0.25	0.625	6000	18217.61	1.78
3	0.25	1	6000	27329.87	2.18
4	0.25	1.5	6000	39688.19	2.62
5	0.25	2	6000	48542.23	2.90
6	0.625	0.25	6000	3537.84	0.78
7	0.625	0.625	6000	4184.23	0.85
8	0.625	1	6000	5729.43	1.00
9	0.625	1.5	6000	12219.83	1.45
10	0.625	2	6000	23157.53	2.00
11	1	0.25	6000	4876.49	0.92
12	1	0.625	6000	4918.98	0.92
13	1	1	6000	4861.47	0.92
14	1	1.5	6000	4977.75	0.93
15	1	2	6000	7220.50	1.12
16	1.5	0.25	6000	5219.85	0.95
17	1.5	0.625	6000	5223.26	0.95
18	1.5	1	6000	5211.96	0.95
19	1.5	1.5	6000	5163.09	0.95
20	1.5	2	6000	5044.81	0.93
21	2	0.25	6000	5251.35	0.95
22	2	0.625	6000	5251.13	0.95
23	2	1	6000	5249.79	0.95
24	2	1.5	6000	5245.37	0.95
25	2	2	6000	5231.29	0.95

Figure 10.5 compares predicted versus measured alligator cracking after performing calibration. It is shown that the calibration process brings many data points closer to the line of equality.

### Validation of the Alligator Cracking Model

In the validation process, sections 1002, 1022, NMDOT 19, NMDOT 20, and NMDOT 27 are run in the MEPDG with the calibrated alligator cracking model. Figure 10.6 compares the uncalibrated and calibrated MEPDG predictions with the measurements taken in the field during the design life of section NMDOT 27. Default MEPDG does not predict any alligator cracking at all for this section, in consequence the new calibration coefficients improve the prediction of future distress. The SSE of section NMDOT 27 decreases from 183.60 to 76.16 with the new model.

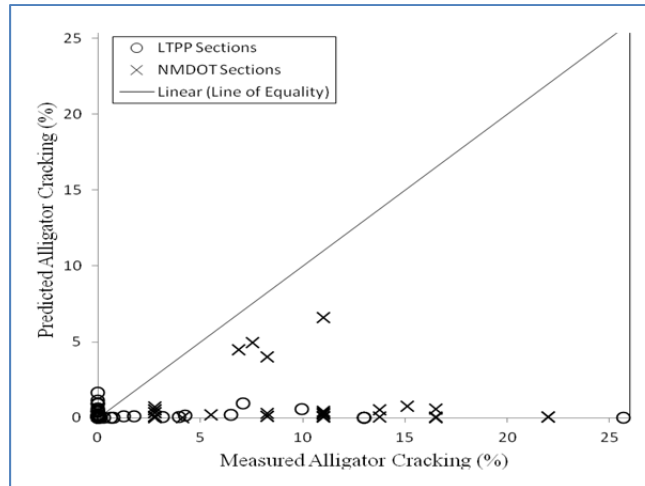


**FIGURE 10.4 Predicted versus measured alligator cracking before calibration**

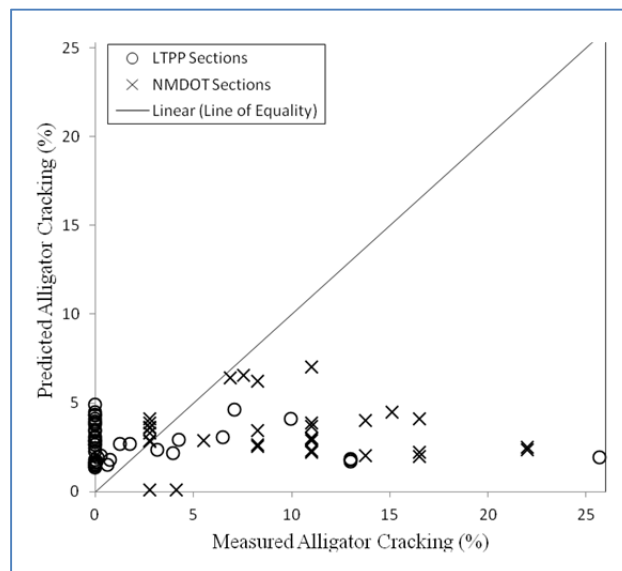


**FIGURE 10.5 Predicted versus measured alligator cracking after calibration**

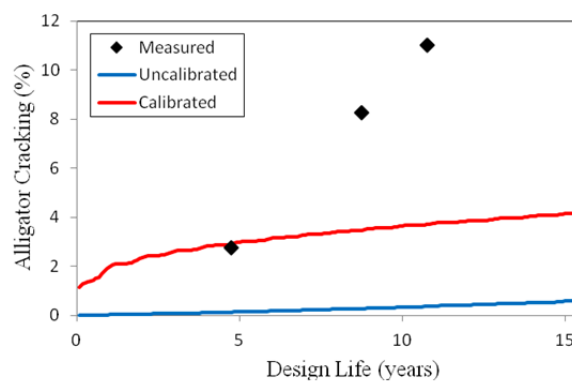


**FIGURE 10.6 Validation of the calibrated alligator cracking model (section NMDOT 27)**

## LONGITUDINAL (TOP-DOWN) CRACKING MODEL

### Prediction of Longitudinal Cracking in the MEPDG

The approach used in the MEPDG to predict longitudinal cracking is based on the estimation of the fatigue damage that was described previously in detail (MEPDG 2010). The next transfer function calculates the longitudinal fatigue cracking:

$$FC_{top} = 10.56 \left( \frac{C_3}{1 + e^{C_1 - C_2 \log_{10}(100 D)}} \right) \quad \text{Eq. (10)}$$

where  $FC_{top}$  = Top-down fatigue cracking (ft/mile),  $D$  = Top-down fatigue damage, and  $C_1$ ,  $C_2$ ,  $C_3$  = Calibration coefficients to be optimized.

### Calibration of the Longitudinal Cracking Model

Sections 1003, 6035, NMDOT 2, NMDOT 12, and NMDOT 23 are reserved for validation. In the calibration of the longitudinal cracking model, the numerator of the corresponding transfer function ( $C_3$ ) is kept constant at the default value 1000. The calibration coefficients  $C_1$  and  $C_2$  are varied and the MEPDG is run for different combinations of these parameters.

Table 10.5 shows the SSE and the MRE for different values of the  $C_1$  and  $C_2$  coefficients. The calibration coefficients  $C_1 = 3$  and  $C_2 = 0.3$  reduce the SSE from 603,101,012.34 to 58,406,192.29 and the MRE from 275.93 to 85.87. The improvement is very significant.

Figures 10.7 and 10.8 illustrate the predicted versus measured longitudinal cracking values before and after calibration, respectively. Calibration brings data points closer to the line of equality, and therefore, bias is reduced.

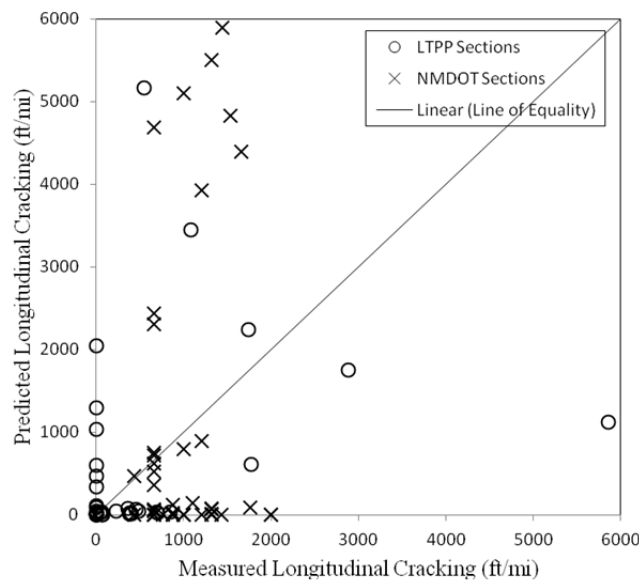


**FIGURE 10.7 Predicted versus measured longitudinal cracking before calibration**

**TABLE 10.5 SSE and MRE of the longitudinal cracking model for different C1 and C2**

Set #	C <sub>1</sub>	C <sub>2</sub>	C <sub>3</sub>	SSE	MRE
1	1	0.3	1000	645,006,970.17	285.36
2	1	1	1000	1,660,586,371.17	457.87
3	1	2.25	1000	3,306,382,014.97	646.08
4	1	3.5	1000	4,131,306,348.15	722.19
5	1	5	1000	4,704,069,017.36	770.63
6	3	0.3	1000	58,406,192.29	85.87
7	3	1	1000	164,870,343.26	144.27
8	3	2.25	1000	1,369,715,531.19	415.84
9	3	3.5	1000	2,569,406,002.47	569.54
10	3	5	1000	3,365,469,711.99	651.83
11	5	0.3	1000	94,519,508.65	109.24
12	5	1	1000	82,731,955.85	102.20
13	5	2.25	1000	385,880,672.89	220.72
14	5	3.5	1000	1,370,064,827.49	415.89
15	5	5	1000	2,462,362,046.06	557.55
16	7	0.3	1000	104,188,084.77	114.69
17	7	1	1000	101,542,737.84	113.22
18	7	2.25	1000	112,599,922.33	119.23
19	7	3.5	1000	603,101,012.34	275.93
20	7	5	1000	1,545,935,462.19	441.78
21	10	0.3	1000	1,545,935,462.19	115.54
22	10	1	1000	105,597,022.35	115.46
23	10	2.25	1000	103,391,480.45	114.25
24	10	3.5	1000	147,298,191.72	136.37
25	10	5	1000	646,631,817.72	285.72

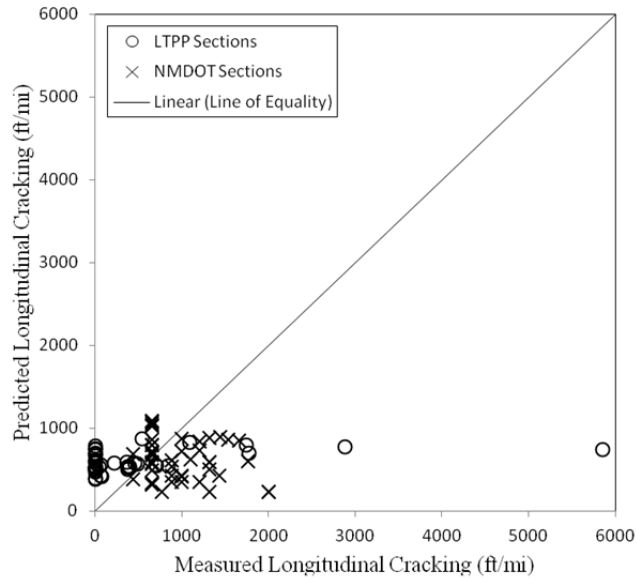


**FIGURE 10.8 Predicted versus measured longitudinal cracking after calibration**

### Validation of the Longitudinal Cracking Model

Sections 1003, 6035, NMDOT 2, NMDOT 12, and NMDOT 23 are run with the calibrated longitudinal cracking model for validation. Figure 10.9 compares the uncalibrated and calibrated MEPDG predictions with the values measured in the field for section NMDOT 2. The new calibration factors improve significantly the longitudinal cracking prediction. The SSE in this section is reduced from 407,098,600.00 to 802,600.00. This validation is considered successful.

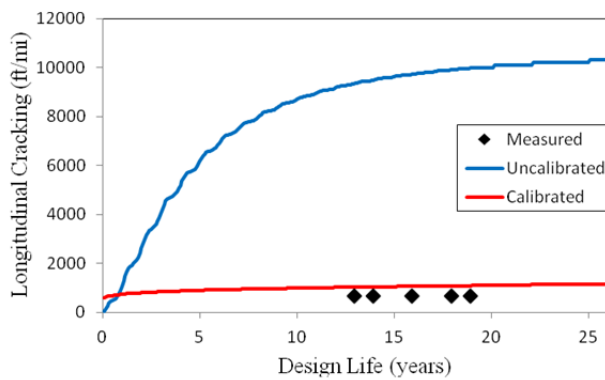


**FIGURE 10.9 Validation of the Calibrated Longitudinal Cracking Model (section NMDOT 2)**

## INTERNATIONAL ROUGHNESS INDEX (IRI) MODEL

### Prediction of IRI in the MEPDG

The smoothness of flexible pavements is affected significantly by rutting, rut depth variance and fatigue cracking. Therefore, the model used in the MEPDG for predicting smoothness is based on correlation with load and climate related distresses such as fatigue cracking, permanent deformation, and thermal cracking which are determined through mechanistic-empirical modeling techniques. However, there are other distresses affecting smoothness that cannot be modeled using mechanistic-empirical principles such as potholes, block cracking, soil depression, frost heave and settlement. These important factors are considered in the MEPDG smoothness prediction through a "site factor" term.

The model for predicting IRI for use in new and rehabilitated flexible pavement design is a function of the base type as described below (MEPDG Documentation 2010):

$$IRI = IRI_0 + 0.0463 \left[ SF \left( e^{\frac{age}{20}} - 1 \right) \right] + 0.00119(TC_L)_T + 0.1834(COV_{RD}) + 0.00384(FC)_T + 0.00736(BC)_T + 0.00115(LC_{SNWP})_{MH} \quad \text{Eq. (11)}$$

where:  $IRI$  = IRI at any given time (m/km),  $IRI_0$  = Initial IRI (m/km),  $SF$  = Site factor,  $e^{\frac{age}{20}} - 1$  = Age term (age is expressed in years),  $COV_{RD}$  = Coefficient of variation of the rut depths, assumed to be 20% (%),  $(TC_L)_T$  = Total length of transverse cracks (m/km),  $(FC)_T$  = Fatigue cracking in wheel path (% of the lane area),  $(BC)_T$  = Area of block cracking, (% of the lane area), and  $(LC_{SNWP})_{MH}$  = Length of sealed longitudinal cracks outside the wheel path (m/km).

The site factor is given by:

$$SF = \left( \frac{(R_{SD})(P_{0.075}+1)(PI)}{2 \times 10^4} \right) + \left( \frac{\ln(FI+1)(P_{0.02}+1)[\ln(R_m+1)]}{10} \right) \quad \text{Eq. (12)}$$

where  $R_{SD}$  = Standard deviation of the monthly rainfall (mm),  $P_{0.075}$  = Fraction passing the 0.075 mm sieve (%),  $PI$  = Plasticity index of the soil (%),  $FI$  = Average annual freezing index ( $^{\circ}\text{C}$ -days),  $P_{0.02}$  = Fraction passing the 0.02 mm sieve (%), and  $R_m$  = Average annual rainfall (mm).

The predicted IRI for HMA pavements over unbound granular bases and subbases at the desired level of reliability is obtained as follows:

$$IRI_P = IRI + STD_{IRI} \times Z_P \quad \text{Eq. (13)}$$

where  $IRI_P$  = Predicted IRI at the reliability level  $P$  (m/km),  $IRI$  = Predicted IRI based on 50% reliability (m/km),  $STD_{IRI}$  = Standard deviation of IRI at the predicted level of mean IRI (m/km), and  $Z_P$  = Standard normal deviate.

### Calibration of the IRI Model

Sections 1112, 2007, NMDOT 5, NMDOT 6, and NMDOT 10 are reserved for validation. In the calibration of the IRI model, the new calibration coefficients are used for the rutting and fatigue cracking models, and the site factor is varied and the MEPDG is run.

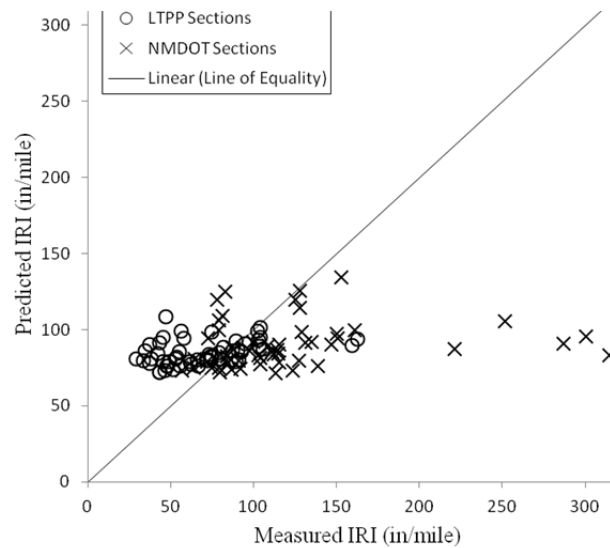


Table 10.6 shows the SSE and the MRE for different values of the site factor. It is observed that the default value of 0.015 provides the lowest SSE and MRE which are 268,903.98 and 4.99 respectively. If the MEPDG is run using the default distress models, then the prediction is slightly better with a SSE of 265,638.14 and a MRE of 4.96.

**TABLE 10.6 SSE and MRE of the IRI model for different "site factors"**

Set #	Site Factor	SSE	MRE
1	default	265,638.14	4.96
2	0.001	308,583.03	5.34
3	0.015	268,903.98	4.99
4	0.1	919,555.57	9.22
5	1	101,768,736.60	97.00
6	0.01	278,288.97	5.07

Figure 10.10 shows the predicted versus measured IRI value when default MEPDG distress models are used. Whereas, Figure 10.11 illustrates the predicted versus measured IRI when the new distress prediction models and a site factor of 0.015 are used. This model shows a good agreement between prediction and observation.



**FIGURE 10.10 Predicted versus measured IRI with default MEPDG models**

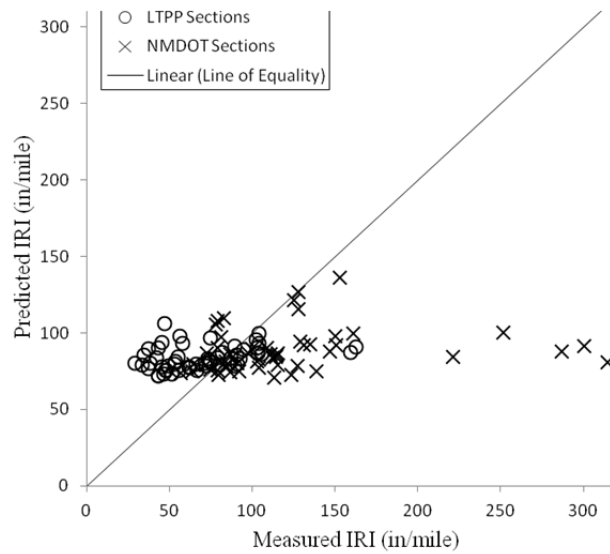


**FIGURE 10.11 Predicted versus measured IRI with the new distress models**

### Validation of the IRI Model

Sections 1112, 2007, NMDOT 5, NMDOT 6, and NMDOT 10 are run with the calibrated IRI model for validation. Figure 10.12 compares the uncalibrated and calibrated MEPDG predictions with the values measured in the field for section NMDOT 6. The SSE in this section is increased from 7,472.85 to 8,106.65.

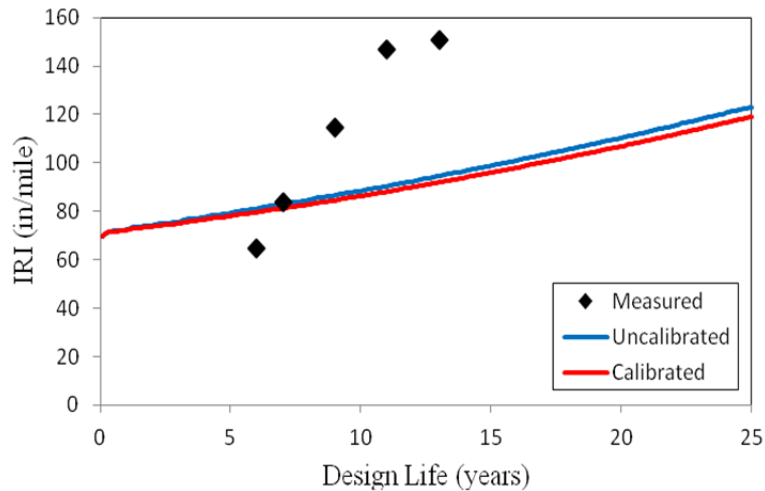


**FIGURE 10.12 Validation of the calibrated IRI model (section NMDOT 6)**

## SUMMARY OF LOCAL CALIBRATION COEFFICIENTS

- Rutting:  $\beta_{r1} = 1.1, \beta_{r2} = 1.1, \beta_{r3} = 0.8, \beta_{GB} = 0.8, \beta_{SG} = 1.2$
- Alligator Cracking:  $C_1 = 0.625, C_2 = 0.25, C_3 = 6000$
- Longitudinal Cracking:  $C_1 = 3, C_2 = 0.3, C_3 = 1000$
- IRI: Site Factor = 0.015

## CONCLUSIONS

The following conclusions are related to the local calibration of the MEPDG for flexible pavements in New Mexico:

- Initial verification runs suggest that there is significant bias in the permanent deformation prediction of default MEPDG. Only total rutting can be calibrated since there is no rut depth data for individual layers. Local calibration of the rutting calibration coefficients  $\beta_{r1}, \beta_{r2}, \beta_{r3}, \beta_{GB}$ , and  $\beta_{SG}$  is successfully achieved. The standard error of the estimate is low and bias is eliminated.
- The plot showing measured versus predicted alligator cracking before calibration indicates that the default MEPDG prediction does not match the observed values particularly well. Many field measurements have a value of zero which makes the local calibration process of this particular distress more difficult. Nonetheless, the alligator cracking calibration coefficients  $C_1, C_2$ , and  $C_3$  are optimized such that the sum of squared errors is reduced and thus many data points are brought closer to the line of equality.
- The longitudinal cracking model is even more challenging because many data points fall very close to the origin (the values are almost zero). Calibration of the longitudinal cracking coefficients  $C_1, C_2$ , and  $C_3$  does not produce as good results as those obtained for rutting and alligator cracking. However, the positive effect of calibration is noticed with many points moving closer to the line of equality and the sum of squared errors being reduced.
- In the case of the IRI model, the verification runs show that the roughness prediction by default MEPDG is relatively good. The sum of squared errors is not high and the local calibration process does not really reduce it.

## Recommendations

For most efficient and successful calibration of the MEPDG in New Mexico, the following recommendations should be implemented:

1. Local calibration requires a few more data sets. The NMDOT should establish at least 30 pavement sections for local calibration of the MEPDG. These sections should be new flexible pavements constructed with practices, techniques and materials currently

used in the state. The new pavement sections should be located in segments near to Weigh-In-Motion (WIM) sites so the traffic loading can be accurately characterized. The 30 pavement sections should be distributed among different climatic regions (from cold to warm weather) and different functional class roads (from low to high traffic).

2. Measurements of distress data (rutting, alligator cracking, longitudinal cracking, thermal cracking and IRI) must be collected every year at every section during its pavement design life following the Distress Identification Manual for the Long Term Pavement Performance Program. Eventually, these pavement sections will become damaged and rehabilitation will be carried out through an AC overlay. At that time, the monitoring effort should continue and local calibration of the MEPDG for rehabilitated pavements should be performed in the same manner.
3. Permanent deformation should be measured at every layer of the pavement section by performing trenches and/or cores. This will allow a much more precise and consistent calibration of the rutting model.
4. Creep compliance and thermal contraction coefficients of the asphalt concrete mixtures should be determined in the lab for the pavement sections. This will make local calibration of the thermal cracking model possible.

## **Chapter 11**

### **CONCLUSIONS AND IMPLEMENTATION PLAN**

#### **CONCLUSIONS**

This project has developed a MEPDG database for flexible pavements in New Mexico, and calibrated the MEPDG locally using the developed database. What has been achieved during past 4 years is not faultless; however, it constitutes a platform for what can become one of the most important sources of data for the purposes of further validating and calibrating data-intensive MEPDG models. In order to make the database popular in the state, extensive interaction and cooperation are needed from the NMDOT districts. The MEPDG database should be assigned owner(s) and updated periodically.

Based on this study, it is strongly recommended that NMDOT select a set of pavement sections (e.g. 50 sections) and monitor them on an annual basis for at least the next ten years. In addition, as new data are available, and materials (such as warm-mix asphalt, increased use of RAP) become popular in the State of New Mexico, MEPDG database and calibration should be periodically reviewed and new sections should be incorporated accordingly. The calibration methodologies that have been developed should be carried forward and applied to new data as they become available. This will increase the confidence in the results and will produce more reliable calibration factors and, in general, more robust pavement performance models.

The section below describes the related product of this research and how they can be implemented in the design of NMDOT pavements. In addition, anticipated barriers to successful implementation of MEPDG and suggestions for overcoming these predicted barriers are presented.

#### **Product 1**

The UNM research team has delivered (May 30, 2011) a comprehensive database, called MEPDG database, capable of storing all variables required for statewide implementation of MEPDG in New Mexico. Employing an in-house server at UNM, the MEPDG database was designed to run in Oracle platform (version 11g). The design of MEPDG database involved defining data that followed the MEPDG software input-output format, designing database architecture that relates foreign and primary keys and table structure, capturing geospatial features of data capable of developing GIS applications (for example, GIS maps), and designing web-interfaces for accessing the input-output data in the MEPDG database. The resulting MEPDG database was then populated with the available pavement layer, mix design and construction data including FWD, WIM, and PMS data from NMDOT databases and other sources. In addition, New Mexico pavement data available in LTPP database and climatic data (22 weather stations) from NOAA server were entered into the MEPDG database. Data have been validated using python scripts before entering into the MEPDG database. Attempts were

made to create few links for accessing NMDOT's existing databases from the MEPDG database. The integrity of MEPDG database has been ensured by validating data structure and data range, preserving primary-foreign key relations, and regular database backup.

## Product 2

Ranges of values of MEPDG inputs for New Mexico are shown in Table 11.1.

TABLE 11.1 Range of New Mexico MEPDG inputs

No	Type	Input Name	Variable	Range of Inputs	Numeric Values Assigned	Variable Type	Data Source
1	TRAFFIC	Initial two-way AADTT	$X_1$	300 to 6000		Integer	LTPP
2		Number of Lanes in Design Direction	$X_2$	1 to 3		Integer	LTPP
3		Percent of Trucks in Design Direction (%)	$X_3$	40 to 60		Non Integer	Design Guide
4		Percent of Trucks in Design Lane (%)	$X_4$	6 to 94		Non Integer	Huang, 2004
5		Operational Speed (mph)	$X_5$	35 to 75		Non Integer	NMDOT
6		AADTT Distribution by Vehicle Class 9 (%)	$X_6$	2 to 85		Non Integer	LTPP
7		AADTT Distribution by Vehicle Class 11 (%)	$X_7$	0.1 to 7		Non Integer	LTPP
8		Traffic Growth Factor	$X_8$	3 to 9		Non Integer	LTPP
9		Design Lane Width (ft)	$X_9$	10 to 12		Non Integer	LTPP
10		Tire Pressure (psi)	$X_{10}$	90 to 150		Non Integer	Design Guide
11	CLIMATE	Depth of Water Table (ft)	$X_{11}$	5 to 20		Non Integer	NMDOT
12		Climatic Zones	$X_{12}$	1 to 5	1=SouthEast	Discrete	Design Guide
					2=SouthWest		
					3=NorthWest		
					4=NorthEast		
					5=Central		

TABLE 1 Range of New Mexico MEPDG Inputs (cont.)

No	Type		Input Name	Variable	Range of Inputs	Numeric Values Assigned	Variable Type	Data Source
13	STRUCTURE	Asphalt Mix 1	Layer Thickness (in)	X <sub>13</sub>	1.5 to 3		Non Integer	NMDOT
14			Aggregate Gradation	X <sub>14</sub>	1 to 2	1=SP-III	Discrete	NMDOT
						2=SP-IV		
15			Effective Binder Content (%)	X <sub>15</sub>	9 to 12		Non Integer	NMDOT
16			Superpave Binder Grade	X <sub>16</sub>	1 to 3	1=PG 64-22	Discrete	NMDOT
						2=PG 70-28		
						3=PG 76-28		
17			Air Voids (%)	X <sub>17</sub>	4 to 7		Non Integer	LTPP
18		Asphalt Mix 2	Layer Thickness (in)	X <sub>18</sub>	2 to 8		Non Integer	NMDOT
19			Aggregate Gradation	X <sub>19</sub>	1 to 3	1=SP-II	Discrete	NMDOT
						2=SP-III		
						3=SP-IV		
20			Effective Binder Content (%)	X <sub>20</sub>	9 to 12		Non Integer	NMDOT
21			Superpave Binder Grade	X <sub>21</sub>	1 to 3	1=PG 64-22	Discrete	NMDOT
						2=PG 70-28		
						3=PG 76-28		
22			Air Voids (%)	X <sub>22</sub>	4 to 7		Non Integer	LTPP
23		Base	Layer Thickness (in)	X <sub>23</sub>	6 to 10			NMDOT
24			Material Type	X <sub>24</sub>	1 to 5	1=Crushed Gravel	Discrete	LTPP
						2=A-1-b		
						3=A-2-6		
						4=A-3		
						5=A-2-4		
25			Modulus (psi)	X <sub>25</sub>	20,000 to 40,000		Non integer	NMDOT
26		Subgrade	Material Type	X <sub>26</sub>	1 to 5	1=CL	Discrete	LTPP
						2=CL-ML		
						3=ML		
						4=SM		
						5=SP		
27			Modulus (psi)	X <sub>27</sub>	5000 to 20,000		Non integer	LTPP
28			Plastic Limit (PL)	X <sub>28</sub>	10 to 24		Non integer	NMDOT
29			Liquid Limit (LL)	X <sub>29</sub>	25 to 90		Non integer	NMDOT
30			Optimum Gravimetric Water Content (%)	X <sub>30</sub>	12 to 60		Non integer	NMDOT



### Product 3

This product is a list of methods and practices that have succeeded/failed, as relating to MEPDG calibration. An itemized description of product 3 is given below:

- The MEPDG database, at its current form, contains a wealth of data that include pavement layer information, materials, design, time series of distress or performance, traffic data, climatic data, location map, and geospatial data. This database can be used to determine average, range value of designed layer thickness, distress performance of certain pavements, traffic values at certain regions. This database should be very useful to the pavement designer, materials engineers, and pavement management and maintenance engineers. Therefore, NMDOT should encourage its pavement designers, contractors, and engineers to use the MEPDG database as soon as possible.
- Currently, the distress data required for FHWA reporting has changed from quality information to quantity based information, which is exactly MEPDG format of distress data. Therefore, the yearly PMS data should be stored directly into the MEPDG database.
- Soils and aggregate testing data as well as asphalt mix design data are currently stored either in paper copy or excel files. Much of these data are converted to MEPDG format and stored in MEPDG database. However, NMDOT should start storing these data directly into the MEPDG database as soon as possible, if not through frontend Web applications, at least through SQL scripts for Oracle backend applications.
- Currently, WIM data are used mainly for determining traffic volumetric, weight, and classifications. It is very difficult to measure the quality of the collected WIM data using the classification or volume count data. Weight data has traditionally been used to measure ESAL, which is a gross representation of traffic loading during the entire design life of the pavement. The MEPDG database has stored volume, weight, and classification data. Additionally, it stores axle load spectra data that can be used to evaluate the quality of WIM data. NMDOT can benefit from the MEPDG database by storing axle load spectra and using it for pavement design and traffic quality measure.
- The MEPDG database contains a number of (about 3000 pavement sections) incomplete data that are missing either construction information or materials data or time series of performance information. The MEPDG database contains only 32 complete datasets of which 11 datasets from LTPP sections and 21 datasets from other pavement sections in New Mexico. Of them, four sections have missing date of construction and major rehabilitations. The complete 28 data sets were used for local calibration of MEPDG software as per current status of MEPDG database.

## Product 4

Recommendations for availability of technical support to aid agencies in troubleshooting, and aid in program customization needed for adaptation to NMDOT needs.

### *Input/Upload Data*

- Most of the data used to populate the MEPDG database obtained from soft copy files, hard copy files, and other downloaded data from the NMDOT websites. Table 11.2 lists the sources of data that were populated in the MEPDG database.

TABLE 11.2 Input data source and type

Source type	Data Type
Hard Copy Files	Mix Design data
Soft Copy files	Distress data FWD data WIM data, Axle Load data Mix Design data Soils and Aggregate data
Data Downloaded from NMDOT website	County data Traffic data Shape files
NOAA Website	Climatic Data
LTPP Database	Resilient and dynamic moduli, and other data for SPS, GPS pavement sections
Database dump files of existing databases (e.g., TIMS, LIMS)	Traffic data Distress data

The soft copy files were converted into Excel files with the data required for MEPDG and then uploaded into the MEPDG database using python scripts. As per hard copy files, data were entered into excel sheets of fixed format. From the excel sheets, data were then uploaded into the MEPDG database using python scripts and other tools available in Oracle application suites. These techniques have been documented in the MEPDG database help file. Using these techniques, new data, as available or have not been entered yet, should be uploaded in the MEPDG database on a monthly basis. Ideally, uploading of data should be continued from existing hard and soft copy sources including links that enable records imported from other databases with minimal user input.

- NMDOT's materials data (soils, aggregate, asphalt) are not currently being stored in a database, rather they are stored in hard copy or non-uniform Excel files. Population of these data into MEPDG database requires that they are stored in a database or at a minimum, in Excel files that follow MEPDG data structure.

### *Scripting and Programming*

A web application has been developed for retrieving the data from MEPDG database. This web application can retrieve spatial data which can be used for developing GIS applications. To date, one frontend script has been written to enter mix design data in MEPDG database. Similar web interface or front end scripts or interface should be developed for entering other data such as soils data, aggregate data, and asphalt binder data. These scripts for data entering and viewing should be developed to enhance the MEPDG database. The following tasks are required for further development of MEPDG database:

- NMDOT should develop more web-based user-friendly interfaces to minimize user effort to obtain/re-enter required input data. These interfaces first gather selected information from users and then display the results of queries in map and table format.
- MEPDG Database should contain program that processes raw WIM data into Excel load spectra internally; currently this is done externally. Axle weight distribution tables should be automatic from a single WIM station if the station is located on a roadway. If a WIM station is not located on the same road, axle load spectra for that section should be calculated based on a statewide average of axle weight distribution tables from all the appropriate WIM sites in New Mexico.
- Distress data should be collected in MEPDG format and distress conversion should be avoided.

### *Further Develop Database Links*

For MEPDG to be an independent database it should be well connected with all other NMDOT's databases. This can be done by creating database links. A database link can be defined as a connection between the MEPDG database and the NMDOT's existing databases that allows a client to access them as one logical database (Figure 11.1). Though the UNM research team has attempted to establish database links, several problems encountered. One of the major problems with all the existing databases is lack of documentation on the databases and data. Without the documentation, it was not possible to make sense of the relations between the column names to data and the relation between the numerous tables exist in each databases. As a result, the task of developing protocols for data exchange among databases could not be accomplished fully. Further link development task should be included in the database implementation plan.

Another problem related to database link was only a very few databases contained data useful for MEPDG database. The research team has analyzed a total of 22 existing databases and found useful data only in few databases such as TIMS (old CHDB) and LIMS. The research team has established few links between the MEPDG to those few databases. Links have access models which include authenticated database connections via ODBC (Open Database Connectivity), the standard for cross-platform database access. Due to lack of knowledge of the internal structures of the existing databases and table entity or relations, the research team was not able to develop more links among these databases. Another issue related to link development was lack of validation tests due to limited database access issue. NMDOT's existing databases were not accessible outside the NMDOT (connection or VPN problem); only database dump files were made available to the UNM researchers.

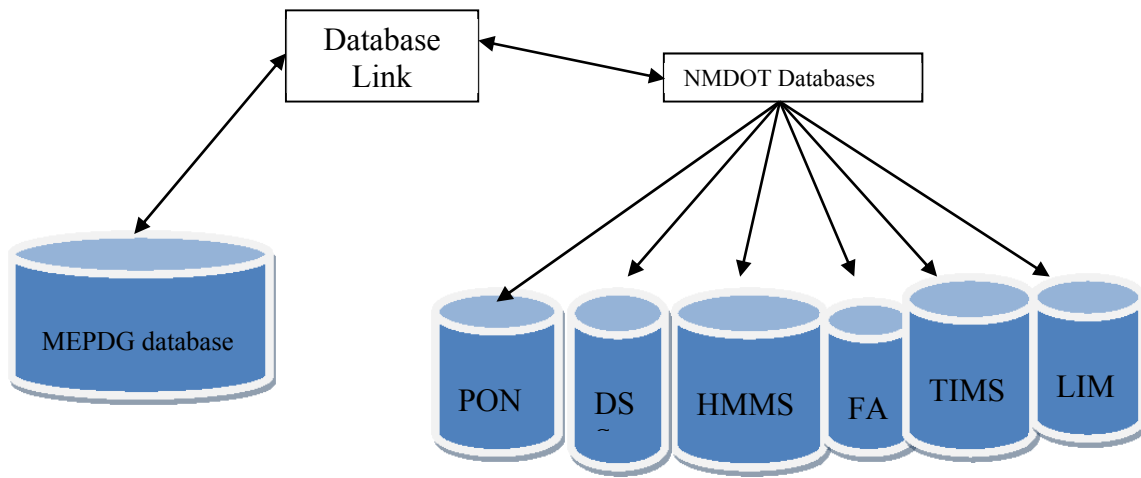


**FIGURE 11.1 Interactions of MEPDG Database with Existing NMDOT Databases**

The following tasks are required for further development of MEPDG database:

- MEPDG database should include links that enable records imported from the TIMS and other databases. MEPDG database should be updated with traffic and materials information on a monthly basis.
- To accomplish the linking task, extra compensation or personnel is need for the NMDOT IT group. As the MEPDG server was setup with the NMDOT's Oracle database group for compatibility, it is logical that such extra personnel or compensation goes to that group.

#### *Database Maintenance and Management*

The strategies for maintaining and management of the MEPDG database should follow the strategies that are common to any other database. For example, protecting data from unauthorized access (security) and database integrity tasks should follow the NMDOT's standard protocol.

- Like any other existing database of NMDOT, the MEPDG database needs to have a NMDOT database owner, who will maintain and manage the database routinely.

## Product 5

Sensitivity of the MEPDG inputs on the performance of flexible pavements is given below. Inputs are ranked on a scale of low to moderate to highly influencing the distress value as shown in Table 11.3.

TABLE 11.3 Summary of Sensitivity Outputs

Type	Terminal IRI (Y <sub>1</sub> )		Longitudinal Cracking (Y <sub>2</sub> )		Alligator Cracking (Y <sub>3</sub> )		Transverse Cracking (Y <sub>4</sub> )		AC Rutting (Y <sub>5</sub> )		Total Rutting (Y <sub>6</sub> )	
Model	MARS	GBM	MARS	GBM	MARS	GBM	MARS	GBM	MARS	GBM	MARS	GBM
High	X <sub>18</sub>	X <sub>18</sub>	X <sub>18</sub>	X <sub>18</sub>	X <sub>18</sub>	X <sub>18</sub>	X <sub>4</sub>	X <sub>28</sub>	X <sub>1</sub>	X <sub>1</sub>	X <sub>1</sub>	X <sub>1</sub>
	X <sub>1</sub>	X <sub>1</sub>	X <sub>1</sub>	X <sub>4</sub>	X <sub>1</sub>	X <sub>1</sub>	X <sub>7</sub>	X <sub>4</sub>	X <sub>4</sub>	X <sub>4</sub>	X <sub>4</sub>	X <sub>4</sub>
	X <sub>4</sub>	X <sub>4</sub>	X <sub>4</sub>	X <sub>1</sub>	X <sub>22</sub>		X <sub>28</sub>	X <sub>12</sub>	X <sub>10</sub>	X <sub>10</sub>	X <sub>8</sub>	X <sub>18</sub>
Medium	X <sub>13</sub>	X <sub>22</sub>	X <sub>17</sub>	X <sub>25</sub>	X <sub>13</sub>	X <sub>4</sub>	X <sub>15</sub>	X <sub>23</sub>	X <sub>18</sub>	X <sub>18</sub>	X <sub>10</sub>	X <sub>10</sub>
	X <sub>22</sub>	X <sub>8</sub>	X <sub>24</sub>	X <sub>24</sub>	X <sub>25</sub>	X <sub>22</sub>	X <sub>11</sub>	X <sub>11</sub>	X <sub>8</sub>	X <sub>8</sub>	X <sub>27</sub>	X <sub>27</sub>
	X <sub>8</sub>	X <sub>13</sub>	X <sub>25</sub>	X <sub>17</sub>	X <sub>3</sub>	X <sub>13</sub>	X <sub>22</sub>	X <sub>17</sub>			X <sub>30</sub>	X <sub>30</sub>
	X <sub>3</sub>	X <sub>14</sub>	X <sub>13</sub>	X <sub>13</sub>	X <sub>24</sub>	X <sub>25</sub>	X <sub>30</sub>	X <sub>21</sub>			X <sub>8</sub>	X <sub>3</sub>
	X <sub>10</sub>	X <sub>27</sub>	X <sub>27</sub>	X <sub>3</sub>		X <sub>28</sub>	X <sub>29</sub>	X <sub>7</sub>			X <sub>13</sub>	
	X <sub>27</sub>		X <sub>23</sub>			X <sub>19</sub>	X <sub>14</sub>	X <sub>18</sub>			X <sub>3</sub>	
	X <sub>26</sub>		X <sub>3</sub>			X <sub>27</sub>	X <sub>2</sub>	X <sub>2</sub>			X <sub>26</sub>	
	X <sub>16</sub>							X <sub>13</sub>				
								X <sub>15</sub>				
								X <sub>9</sub>				
Low	X <sub>24</sub>	X <sub>2</sub>	X <sub>9</sub>	X <sub>27</sub>	X <sub>7</sub>	X <sub>20</sub>	X <sub>25</sub>	X <sub>10</sub>	X <sub>30</sub>	X <sub>13</sub>	X <sub>21</sub>	X <sub>13</sub>
	X <sub>25</sub>	X <sub>3</sub>	X <sub>8</sub>	X <sub>26</sub>	X <sub>27</sub>	X <sub>21</sub>	X <sub>3</sub>		X <sub>25</sub>	X <sub>11</sub>	X <sub>5</sub>	X <sub>11</sub>
	X <sub>30</sub>	X <sub>16</sub>	X <sub>22</sub>	X <sub>11</sub>	X <sub>21</sub>	X <sub>17</sub>	X <sub>9</sub>		X <sub>5</sub>	X <sub>15</sub>	X <sub>16</sub>	X <sub>8</sub>
	X <sub>15</sub>	X <sub>26</sub>	X <sub>15</sub>	X <sub>2</sub>	X <sub>29</sub>	X <sub>26</sub>	X <sub>10</sub>		X <sub>12</sub>	X <sub>3</sub>	X <sub>9</sub>	X <sub>24</sub>
		X <sub>15</sub>	X <sub>30</sub>	X <sub>12</sub>	X <sub>5</sub>	X <sub>5</sub>			X <sub>23</sub>	X <sub>20</sub>	X <sub>15</sub>	X <sub>12</sub>
		X <sub>28</sub>		X <sub>22</sub>	X <sub>14</sub>	X <sub>9</sub>			X <sub>13</sub>	X <sub>9</sub>		X <sub>20</sub>
		X <sub>6</sub>		X <sub>23</sub>	X <sub>12</sub>				X <sub>26</sub>	X <sub>21</sub>		X <sub>28</sub>
									X <sub>24</sub>	X <sub>17</sub>		X <sub>26</sub>
									X <sub>19</sub>	X <sub>23</sub>		
									X <sub>28</sub>	X <sub>12</sub>		

Note: Variable  $x_1$  to  $x_{30}$  were defined in Table 1

## Product 6

A set of distress model coefficients for designing NMDOT pavements to allow for level 2 analysis.

Summary of Local Calibration Coefficients:

• Rutting:	$\beta_{r1} = 1.1, \beta_{r2} = 1.1, \beta_{r3} = 0.8, \beta_{GB} = 0.8, \beta_{SG} = 1.2$
• Alligator Cracking:	$C_1 = 0.625, C_2 = 0.25, C_3 = 6000$
• Longitudinal Cracking:	$C_1 = 3, C_2 = 0.3, C_3 = 1000$
• IRI:	Site Factor = 0.015

## IMPLEMENTATION PLAN

Activities necessary for successful implementation are listed below:

1. **Field Data Collection:** The MEPDG contains few complete data sets. However, for a comprehensive calibration, at least 50 pavement sections should be identified at different geographic locations in New Mexico. These sections should consider traffic, and pavement layers in the selection matrix. MEPDG distress data should be collected monthly basis and traffic data should be collected regularly using WIM. The collected data should be used to populate the MEPDG database to increase the number of complete datasets for local calibration of MEPDG software for New Mexico. Work associated with the data collection and population must be contracted.
2. **Laboratory Testing:** Laboratory testing of asphalt binder, aggregate, and soils continue to be performed to develop local materials database and models for Level 2 analysis of MEPDG. There is need for studying Freeze-thaw models (including that in EICM) that are ease of use by practitioners and calibration of models.
3. Currently, the database contains both raw and processed Falling Weight Deflectometer (FWD) data. A reliable analysis method is required to calculate subgrade modulus from FWD backcalculation analysis and to incorporate into MEPDG database.
4. Additional resource should be allocated to develop default monthly and hourly traffic distribution factors suitable for use, to developed statewide vehicle class distribution factors; and to developed statewide axle load spectra using WIM data.
5. Refine database engine and GUIs periodically. Refine database tables and add database security features. Integrate with NMDOT's PMS efforts. A very few graphical user interfaces (GUIs) were developed. However, many more GUIs can be developed to minimize user effort to obtain/re-enter required input data. Limited pavement-related data has been linked to their geographical location though GIS applications that manage, query, analyze, and visualize data graphically.
6. NMDOT needs to invest in personnel and resources to deal with the MEPDG data. Specifically, one IT person and one traffic engineer dedicated to MEPDG related database are required to assist the State Pavement Designer. A training committee for providing MEPDG training to central office and field personnel, and for explaining the benefits of MEPDG to the stakeholders: upper management, field engineers, and the industry.

## REFERENCES

- AASHTO (2010). "Guide for the Local Calibration of the Mechanistic-Empirical Pavement Design Guide." *American Assoc. of State Highway and Trans. Officials*, ISBN: 9781560514497, Washington, D.C.
- AASHTO (2008). "Mechanistic-Empirical Pavement Design Guide – A Manual of Practice", *American Assoc. of State Highway and Trans. Officials*, Washington, D.C.
- Aguiar-Moya, J. P., Banerjee, A., and Prozzi, J. A. (2009). "Sensitivity analysis of the M-E PDG using measured probability distributions of pavement layer thickness." *TRB 2009 Annual Meeting CD-ROM, Transportation Research Board*, Washington D.C.
- Ahn, S., Kandala, S., Uzan, J., and El-Basyouny, M. (2009). "Comparative analysis of input traffic data and the MEPDG output for flexible pavements in state of Arizona." *TRB 2009 Annual Meeting CD-ROM, Transportation Research Board*, Washington D.C.
- Banerjee, A., Aguiar-Moya, J. P., and Prozzi, J. A. (2009). "Calibration of Mechanistic-Empirical Pavement Design Guide Permanent Deformation Models." *Trans. Res. Rec.: J. of the TRB*, No. 2094, *TRB of the National Academies*, Washington, D.C., 12–20.
- Conover, W. J. (1980). *Practical Nonparametric Statistics*. 2nd ed. Wiley, New York, NY.
- Coree, B. (2005). "Implementing M-E Pavement Design Guide in Iowa." *Center for Transportation Research and Education. Iowa State University*, Ames, IA.
- Daniel, J. S., and Chehab, G. R. (2008). "Use of RAP mixtures in the mechanistic empirical pavement design guide." *Compendium of CD-ROM Paper, Transportation Research Board*, Washington D.C.
- De la Beaujardiere (2006). *OpenGIS Web Map Server Implementation Specification, J., Ed. Version 1.3.0*, Open Geospatial Consortium.
- FHWA (2004), DataPave Online, Release 18, July 2004, *Federal Highway Administration*, Washington, DC.
- FHWA (2007), "Long Term Pavement Performance" Standard data, DVD version, Release 21.0, VR2007.01, <http://www.fhwa.dot.gov/pavement/ltp>
- Hall, K. D., Xiao, D. X., and Wang, K. C. (2010). "Calibration of the MEPDG for Flexible Pavement Design in Arkansas." *Trans. Res. Board Annual Meeting: TRB 90th Annual Meeting Compendium of Papers CD-ROM*, Washington, D.C.
- Helton, J. C., Davis, F. J. (2002). "Illustration of sampling-based methods for uncertainty and sensitivity analysis." *Risk Analysis*, 22(3):591–622.
- Helton, J. C., Johnson, J.D., Sallaberry, C. J., Storlie, C.B. (2006) "Survey of Sampling-Based Methods for Uncertainty and Sensitivity Analysis", *Reliability Engineering and System Safety*, 91 (2006) pp. 1175-1209.
- Hoegh, K., Khazanovich, L., and Jensen, M. (2010). "Local Calibration of Mechanistic-Empirical Pavement Design Guide Rutting Model (Minnesota Road Research Project Test Sections)." *Trans. Res. Rec.: J. of the TRB*, No. 2180, *TRB of the Nat. Academies*, Washington, D.C., 130–141.



- Homma, T., and Saltelli, A. (1996). "Importance measures in global sensitivity analysis of model output." *Reliability Eng. and System Safety*, 52:1–17.
- Hong, F., Prozzi, J. A., and Leung, A. (2008). "Sampling Schemes for Weigh-in-Motion Traffic Data Collection." *Compendium of CD-ROM Paper, Transportation Research Board*, Washington D.C.
- Hora, S. C, Helton, J. C. (2003). "A distribution-free test for the relationship between model input and output when using Latin hypercube sampling." *Reliability Engineering and System Safety*, 79(3), 333–9.
- [http://download.oracle.com/docs/cd/B19306\\_01/license.102/b14199/editions.htm#CJADFHHG](http://download.oracle.com/docs/cd/B19306_01/license.102/b14199/editions.htm#CJADFHHG)
- <http://nmshtd.state.nm.us/upload/images/CHDB/US%20Routes.pdf>
- <http://www.planning.dot.gov/Documents/CaseStudy/newmexico/>.
- Huang, Y. H. (2004). Pavement Analysis and Design, 2nd edition, *Prentice Hall*, New Jersey.
- Iman, R.L. and Conover, W. J. (1979). "The use of the rank transform in regression." *Technometrics*, 21:499–509.
- Li, J., Hallenbeck, M. E., Pierce, L. M., and Uhlmeyer, J. (2009a). "Sensitivity of axle load spectra in mechanistic-empirical pavement design guide for Washington State Department of Transportation." *TRB 2009 Annual Meeting CD-ROM. Transportation Research Board*, Washington D.C.
- Li, J., Pierce, L. M., and Uhlmeyer, J. (2009). "Calibration of Flexible Pavement in Mechanistic-Empirical Pavement Design Guide for Washington State." *Trans. Res. Rec.: J. of the TRB*, No. 2095, *TRB of the National Academies*, Washington, D.C., 73–83.
- Li, S., Jiang, Y., Zhu, K., and Nantung, T. (2007). "Truck Traffic Characteristics for Mechanistic-Empirical Flexible Pavement Design: Evidences, Sensitivities, and Implications." *Compendium of CD-ROM Paper, Transportation Research Board*, Washington D.C.
- Long-Term Pavement Performance (LTPP) Database (2007). Internet Website <http://www.datapave.com>.
- Manik, A., Chatti, K and Buch, N. (2009), "A Strategy for Efficient HMA Pavement Design Using M-E PDG", *TRB 2009 Annual Meeting CD-ROM, Transportation Research Board*, Washington D.C.
- Marta Juhasz, Chuck McMillan (2010). "Influence of Dynamic Modulus on M-EPDG Outputs" *Proceedings, Canadian Technical Asphalt Association*, pp 188-216.
- Masad, S. A., and Little, D. N. (2004). "Sensitivity analysis of flexible pavement response and AASHTO 2002 design guide to properties of unbound layers." *Research Report ICAR - 504-1, Int. Center for Aggregates Research*. Austin, Texas.
- MEPDG (2010). <http://www.trb.org/mepdg/>, Accessed on March, 2010.
- MEPDG Documentation (2010). "Guide for Mechanistic-Empirical Design of New and Rehabilitated Pavement Structures." *Nat. Cooperative Highway Res. Program, TRB, Nat. Res. Council*, Washington, D.C.

- Muthadi, N. R., and Kim, Y. R. (2008). "Local Calibration of Mechanistic-Empirical Pavement Design Guide for Flexible Pavement Design." *Trans. Res. Rec.: J. of the TRB, No. 2087, TRB of the National Academies*, Washington, D.C. 131–141.
- NCDC website (2008). <http://www4.ncdc.noaa.gov/cgi-win/wwcgi.dll?WWDI~getstate~USA>
- NCHRP (2004a). "Appendix GG: Calibration of permanent deformation models for flexible pavements." *Guide for Mechanistic-Empirical Design of New and Rehabilitated Pavement Structures*. Trans Research Board, National Research Council.
- NCHRP (2004b). "Appendix HH: Field calibration of the thermal cracking model." *Guide For Mechanistic-Empirical Design of New and Rehabilitated Pavement Structures*. Transportation Research Board, National Research Council.
- NCHRP (2004c). "Appendix II: Calibration of fatigue cracking models for flexible pavements." *Guide for Mechanistic-Empirical Design of New and Rehabilitated Pavement Structures*. Transportation Research Board, National Research Council.
- NCHRP 1-37, Development of the 2002 Guide for the Design of New and Rehabilitated Pavements. <http://www.trb.org/mepdg/home.htm>.
- NCHRP 1-39, Traffic Data Collection, Analysis, and Forecasting for M-E Design.
- NCHRP 1-40A, Independent Review of the Recommended M-E PDG Software.
- NCHRP 1-40B, Local Calibration Guidance for the M-E Design of New and Rehabilitated Pavement Structures.
- NCHRP 1-40D, Changes to the MEPDG Software through Version 0.900, July 2006.
- NCHRP 1-41, Models for Predicting Reflection Cracking of HMA Overlays.
- NCHRP 1-42, Models for Predicting Top-Down Cracking Of HMA Layers.
- NCHRP 9-19, Superpave Support and Performance Models Management.
- NCHRP 9-23, Environmental Effects in Pavement Mix and Structural Design Systems.
- NCHRP 9-29, Simple Performance Tester for Superpave Mix Design.
- NCHRP 9-30a, Experimental Plan for Calibration and Validation of HMA Performance Models, etc.
- NCHRP 9-35, Aggregate Properties and Their Relationship to the Performance of Superpave HMA.
- NCHRP 9-37, Using Surface Energy Measurements to Select Materials for Asphalt Pavements.
- Personal Communication with Chuck Slocter, Oracle Database Administrator II, NMDOT.
- Rabab'ah, S., and Liang, R. Y. (2008). "Evaluation of Mechanistic Empirical Design Approach over Permeable Base Materials." *Compendium of CD-ROM Paper, Transportation Research Board*, Washington D.C.
- R-software (2010). <http://www.r-project.org/>, Accessed on May, 2010
- Scheffe, C. H. (1959). *The analysis of variance*. Wiley, New York, NY.

- Storlie, C.B., Swiler, L.P., Helton J.C., and Sallaberry, C. J. (2009). "Implementation and evaluation of nonparametric regression procedures for sensitivity analysis of computationally demanding models." *Reliability Engineering and System Safety*, 94:1735-1763.
- Sunghwan Kim, Halil Ceylan, Kasthurirangan Gopalakrishnan and Omar Smadi (2010). "Use of Pavement Management Information System for Verification of Mechanistic-Empirical Pavement Design Guide Performance Predictions", *Transportation Research Record #2153*, pp 30-39.
- Swan, D. J., Tardif, R., Hajek, J. J., and Hein, D. K. (2008). "Development of Regional Traffic Data for the M-E Pavement Design Guide." *Compendium of CD-ROM Paper*, *Transportation Research Board*, Washington D.C.
- Texas Transportation Institute, (2008). "Development of Thickness Design Tables Based on the MEPDG". *Technical Report BDH10-1*.

## Appendix 2.1

### Python Program for the Retrieval and Processing of Daily Climate Normal Data from NOAA's Servers

```
#!/usr/bin/python

from urllib import urlopen
import random
import time
from os import stat

stationListDir = "/Users/kbene/Documents/edac/Projects/Civil Engineering - NM DOT/climate
data"

baseURL = "http://cdo.ncdc.noaa.gov/climate normals/ clim84/"

#states = ["NM", "AZ", "UT", "CO", "OK", "TX"]
#stationListList =
["nm_stations.txt", "az_stations.txt", "ut_stations.txt", "co_stations.txt", "ok_stations.txt", "tx_statio
ns.txt"]

states = ["TX"]
stationListList = ["tx_stations.txt"]

outputFileName = "processedData.txt"
climateNormalFileDir = "/Users/kbene/Documents/edac/Projects/Civil Engineering - NM
DOT/climate data/climateNormalFiles"

failures = 0
stateNo = 0
for stationListFile in stationListList:
    previousStation = "xxxxxx"
    stations = []
    maxFiles = 1000
    state = states[stateNo]

    def processData(measurement):
        destinationFile.readline()
        destinationFile.readline()
        dayNum = 0
        for i in range(12):
            line = destinationFile.readline()[4:100]
            #print line
            #elements = line[0:3]
            #print elements
```

```

        for j in range(32):
            element = line[(j*3):(j*3)+3]
            #print "x"+element+"x"
            if element.strip().isdigit():
                dayNum = dayNum + 1
                record = "%s\t%s\t%s\t%s\t%s\t%s\n" %
(station,dd_lat,dd_lon,measurement,dayNum,element.strip())
                outputFile.write(record)

stationList = open(stationListDir + "/" + stationListFile, 'r')
outputFile = open(climateNormalFileDir + "/" + state + "_" + outputFileFileName, "w")

for line in stationList:
    stations.append(line.split("\t")[3])

stations.sort()

print
print "===== "

i = 0
for station in stations:
    if station == previousStation:
        continue
    elif station != ".":
        #print "%s: processing this station" % station
        requestURL = baseURL + "/" + state + "/" + state + station + ".txt"
        #print "\t" + requestURL
        destinationFilePath = climateNormalFileDir + "/" + state + station + ".txt"
        #print "\t" + destinationFilePath
        try:
            os.stat(destinationFilePath)
            continue
        except:
            if i < maxFiles:
                lat_deg = 0
                lat_min = 0
                lat_sec = 0
                lon_deg = 0
                lon_min = 0
                lon_sec = 0
                dd_lat = 0
                dd_lon = 0
                elevation = 0

```

between 0 and 2

```
#Space out requests by a random number of seconds
```

```
waitTime = random.random() * 2
print "Waiting %s seconds" % waitTime
time.sleep(waitTime)
```

```
try:
```

```
    sourceFile = urlopen(requestURL)
    destinationFile = open(destinationFilePath,"w")
    destinationFile.write(sourceFile.read())
    destinationFile.close()
    print "Finished reading/writing: %s" % requestURL
```

```
    # processing of the returned file
    destinationFile = open(destinationFilePath,"r")
```

```
    done = False
```

```
    while not done:
```

```
        line = destinationFile.readline()
        if line == " or line.startswith("<"):
            done = True
        elif line.startswith("-"):
            continue
        elif line.startswith(" Latitude"):
            #print "processing coordinates for:
```

```
%s" % line
```

```
        elements = line.split(":")[1].split()
        lat_deg = elements[0]
        lat_min = elements[1]
        lat_sec = elements[2]
        lon_deg = elements[3]
        lon_min = elements[4]
        lon_sec = elements[5]
        elevation = elements[6]
        #print lat_deg + lat_min + lat_sec +
```

```
lon_deg + lon_min + lon_sec
```

```
60.0) + (int(lat_sec) / 3600.0)
```

```
(int(lon_min) / 60.0) + (int(lon_sec) / 3600.0)
```

```
%s" % (dd_lat,dd_lon,elevation)
```

```
Temperature"):

```

```
    elif line.startswith(" Minimum
        #print "processing Minimum
```

```
temperature for: %s" % line
```

```

Temperature"):
    elif processData("tmin")
        line.startswith(" Maximum
    #print "processing Maximum
    temperature for: %s" % line

    processData("tmax")
    elif line.startswith(" Average Temperature"):
        #print "processing Average
    temperature for: %s" % line

    processData("tavg")
    elif line.startswith(" Total Precipitation"):
        #print "processing Total
    Precipitation for: %s" % line

    processData("pcp")

destinationFile.close()

print "Finished Processing: " + destinationFilePath
print
i = i+1
previousStation = station
except:
    failures = failures + 1
    print ""

*****
Failed Attempt to Retrieve and Process: %s
failure(s)

*****" %
failures

waitTime = random.random() * 30
print "Waiting %s seconds" % waitTime
time.sleep(waitTime)

stationList.close()
outputFile.close()
stateNo = stateNo + 1

print "=====
```

## Sample “Complete” Climate Normal File from New Mexico Coop Station NM290041

Provided by National Climatic Data Center/NESDIS/NOAA

Latitude, Longitude, Elevation, Elements: 36 14 00 -106 26 00 6380 XNP

DAY 1 2 3 4 5 6 7 8 9 10 11 12 13 14 15 16 17 18 19 20 21 22 23 24 25 26 27 28 29 30 31  
MONTH

DAY 1 2 3 4 5 6 7 8 9 10 11 12 13 14 15 16 17 18 19 20 21 22 23 24 25 26 27 28 29 30 31  
MONTH



JAN 43 42 42 42 42 42 42 42 42 42 42 42 42 42 42 43 43 43 43 43 43 43 44 44 44 44 44 45  
 45 45 429  
 FEB 45 45 46 46 46 46 47 47 47 48 48 48 48 49 49 49 49 50 50 50 50 51 51 51 51 52 52 52  
 487  
 MAR 53 53 53 53 54 54 54 54 55 55 55 55 56 56 56 56 57 57 57 57 58 58 58 58 59 59 59 59 60  
 60 60 564  
 APR 60 60 61 61 61 61 62 62 62 62 63 63 63 63 64 64 64 64 65 65 65 66 66 66 67 67 67 67 68  
 68 639  
 MAY 68 69 69 69 70 70 70 71 71 71 72 72 73 73 73 74 74 74 75 75 76 76 76 77 77 78 78 79 79  
 79 80 738  
 JUN 80 81 81 81 82 82 83 83 83 84 84 84 85 85 85 85 86 86 86 86 87 87 87 87 87 88 88 88 88  
 88 849  
 JUL 88 88 88 88 88 88 88 89  
 88 88 887  
 AUG 88 88 88 88 88 88 88 88 88 88 88 87 87 87 87 87 87 87 86 86 86 86 86 86 85 85 85 85 84  
 84 84 866  
 SEP 84 84 83 83 83 83 82 82 82 82 81 81 81 80 80 80 80 79 79 79 78 78 78 77 77 77 77 76 76  
 75 799  
 OCT 75 75 74 74 74 73 73 73 72 72 71 71 71 70 70 69 69 68 68 67 67 67 66 66 65 65 64 63 63  
 62 62 690  
 NOV 61 61 60 60 59 59 58 58 57 57 56 56 55 55 55 54 54 53 53 52 52 52 51 51 51 50 50 50 49  
 49 546  
 DEC 49 48 48 48 47 47 47 47 46 46 46 46 45 45 45 45 44 44 44 44 44 44 43 43 43 43 43 43 43  
 43 42 450

-----  
 Average Temperature (deg F [tenths deg F for monthly])  
 DAY 1 2 3 4 5 6 7 8 9 10 11 12 13 14 15 16 17 18 19 20 21 22 23 24 25 26 27 28 29 30 31  
 MONTH  
 -----  
 JAN 29 30 30 30 30 30 30 31 31 31  
 31 31 295  
 FEB 32 32 32 32 32 33 33 33 33 34 34 34 34 35 35 35 35 36 36 36 36 37 37 37 37 38 38 38  
 348  
 MAR 39 39 39 39 40 40 40 40 41 41 41 41 42 42 42 42 43 43 43 43 44 44 44 44 44 45 45 45 45  
 45 46 423  
 APR 46 46 46 46 46 47 47 47 47 48 48 48 48 49 49 49 49 50 50 50 50 51 51 51 52 52 52 52 53  
 53 491  
 MAY 53 54 54 55 55 55 56 56 56 57 57 57 58 58 58 59 59 59 60 60 60 61 61 61 62 62 63 63 63  
 64 64 587  
 JUN 64 65 65 65 66 66 67 67 67 67 68 68 68 69 69 69 69 70 70 70 70 71 71 71 71 71 71 72 72  
 72 687  
 JUL 72 72 72 72 73 73 73 73 73 73 73 73 73 73 73 73 74 74 74 74 74 74 74 74 74 74 74 74 74  
 73 73 733  
 AUG 73 73 73 73 73 73 73 73 73 73 72 72 72 72 72 72 72 72 71 71 71 71 71 71 70 70 70 70 69  
 69 69 716

SEP 69 68 68 68 68 67 67 67 67 66 66 66 65 65 65 64 64 64 64 63 63 63 62 62 62 61 61 60 60  
60 645  
OCT 59 59 59 58 58 57 57 57 56 56 56 55 55 54 54 54 53 53 52 52 51 51 51 50 50 49 49 48 48  
47 47 534  
NOV 47 46 46 45 45 44 44 43 43 43 42 42 41 41 41 40 40 39 39 39 38 38 38 37 37 37 36 36 36  
35 406  
DEC 35 35 34 34 34 33 33 33 33 32 32 32 32 31 31 31 31 31 31 30 30 30 30 30 30 30 29 29 29  
29 29 314

---

#### Heating Degree Days

DAY 1 2 3 4 5 6 7 8 9 10 11 12 13 14 15 16 17 18 19 20 21 22 23 24 25 26 27 28 29 30 31  
MONTH

---

JAN 36 35 35 35 35 35 35 35 34  
34 34 1103  
FEB 34 33 33 33 33 32 32 32 32 31 31 31 31 30 30 30 30 29 29 29 29 28 28 28 27 27 27 27  
846  
MAR 26 26 26 26 25 25 25 25 24 24 24 24 23 23 23 23 22 22 22 22 21 21 21 21 21 20 20 20 20  
20 19 704  
APR 19 19 19 19 19 18 18 18 18 17 17 17 17 17 16 16 16 15 15 15 15 14 14 14 13 13 13 12 12  
12 477  
MAY 11 11 11 10 10 10 9 9 9 9 8 8 8 7 7 7 7 6 6 6 5 5 5 5 5 4 4 4 4 3 3 216  
JUN 3 3 3 2 2 2 2 2 2 1 1 1 1 1 1 1 1 1 0 0 0 0 0 0 0 0 0 0 31  
JUL 0  
AUG 0-99-99-99 3  
SEP 0 0 0 1 1 1 1 1 1 1 1 1 2 2 2 2 2 3 3 3 3 3 4 4 4 5 5 5 5 6 72  
OCT 6 6 7 7 8 8 8 9 9 9 10 10 10 11 11 12 12 12 13 13 14 14 15 15 15 16 16 17 17 18 18  
366  
NOV 19 19 19 20 20 21 21 22 22 22 23 23 24 24 24 25 25 26 26 26 27 27 27 28 28 29 29 29 29  
30 734  
DEC 30 30 31 31 31 32 32 32 32 33 33 33 33 34 34 34 34 34 35 35 35 35 35 35 35 35 36 36 36  
36 36 1042

---

#### Cooling Degree Days

DAY 1 2 3 4 5 6 7 8 9 10 11 12 13 14 15 16 17 18 19 20 21 22 23 24 25 26 27 28 29 30 31  
MONTH

---

JAN 0  
FEB 0  
MAR 0  
APR 0  
MAY 0 0 0 0 0 0 0 0 0 0 0 0 0 0 0 0 0 1 1 1 1 1 1 1 1 2 2 2 2 19  
JUN 2 3 3 3 3 3 3 4 4 4 4 4 4 5 5 5 5 5 5 6 6 6 6 6 6 6 7 7 7 141  
JUL 7 7 7 7 8 8 8 8 8 8 8 8 8 8 8 8 9 9 9 9 9 9 9 9 9 9 8 8 8 8 255

AUG	8	8	8	8	8	8	8	8	8	8	7	7	7	7	7	7	7	6	6	6	6	6	6	5	5	5	5	5	5	4	206
SEP	4	4	4	3	3	3	3	3	3	2	2	2	2	2	2	2	1	1	1	1	1	1	1	1	1	1	1	1	0	0	56
OCT	-99	-99	-99	-99	0	0	0	0	0	0	0	0	0	0	0	0	0	0	0	0	0	0	0	0	0	0	0	0	0	0	4
NOV	0	0	0	0	0	0	0	0	0	0	0	0	0	0	0	0	0	0	0	0	0	0	0	0	0	0	0	0	0	0	0
DEC	0	0	0	0	0	0	0	0	0	0	0	0	0	0	0	0	0	0	0	0	0	0	0	0	0	0	0	0	0	0	0

-----

Total Precipitation (Hundreths of an Inch)

DAY	1	2	3	4	5	6	7	8	9	10	11	12	13	14	15	16	17	18	19	20	21	22	23	24	25	26	27	28	29	30	31
MONTH																															

-----

JAN	1	1	1	1	1	1	1	1	1	1	1	2	2	2	2	2	1	1	1	1	1	1	1	1	1	1	1	1	1	1	1	36
FEB	1	1	1	1	1	1	1	1	0	0	0	0	1	1	1	1	1	1	1	1	1	1	1	1	1	1	1	1	1	1	1	24
MAR	1	1	1	1	2	2	2	2	2	2	2	2	2	2	2	2	2	2	2	2	2	2	2	2	2	2	2	2	2	2	2	58
APR	2	2	2	2	2	2	2	2	2	2	2	2	2	2	2	2	2	2	2	2	2	2	2	2	2	2	2	3	3	3	3	63
MAY	3	3	3	3	3	3	3	3	3	3	3	3	3	4	4	4	4	4	3	3	3	3	3	3	3	3	3	3	3	3	3	98
JUN	3	3	3	2	2	2	2	2	2	2	2	2	2	2	2	2	2	2	3	3	3	3	3	3	3	3	3	3	3	4	4	75
JUL	4	4	4	4	4	4	4	5	5	5	5	5	5	5	5	5	5	6	6	6	6	6	6	6	6	6	6	6	6	6	6	162
AUG	6	6	6	6	7	7	7	7	7	7	7	6	6	6	6	6	6	6	6	6	6	6	6	6	6	6	6	6	6	5	5	191
SEP	5	5	5	5	5	5	5	4	4	4	4	4	4	4	4	4	4	4	4	4	4	4	4	3	3	3	3	3	3	3	3	120
OCT	3	3	3	3	3	3	3	3	3	3	3	3	3	3	3	3	3	3	3	3	3	3	3	3	3	3	3	3	2	2	2	89
NOV	2	2	2	2	2	2	2	2	2	2	2	2	2	2	2	2	2	2	2	2	2	2	2	2	2	2	2	1	1	1	1	55
DEC	1	1	1	1	1	1	1	1	1	1	1	1	1	1	1	1	1	0	1	1	1	1	1	1	1	1	1	1	1	1	1	30

## Appendix 2.3

### Sample "Partial" Climate Normal File from New Mexico Coop Station NM290022

-----  
1971-2000 Daily/Monthly Station Normals

Provided by National Climatic Data Center/NESDIS/NOAA  
-----

Station COOP ID: 290022

Station Name, State, Division, Call: ABBOTT 1 SE NM 02

Latitude, Longitude, Elevation, Elements: 36 18 00 -104 15 00 6150 P  
-----

Total Precipitation (Hundreths of an Inch)

DAY 1 2 3 4 5 6 7 8 9 10 11 12 13 14 15 16 17 18 19 20 21 22 23 24 25 26 27 28 29 30 31  
MONTH

-----  
JAN 1 0 0 29  
FEB 1 2 2 2 2 2 33  
MAR 2 2 2 2 2 2 2 2 2 2 2 2 2 2 2 3 3 3 3 3 3 3 3 3 3 3 3 3 2 77  
APR 3 3 3 2 2 2 2 2 2 2 3 3 3 3 3 3 3 3 3 3 3 3 3 3 3 3 3 4 4 85  
MAY 4 4 4 4 4 4 4 4 5 5 5 5 5 5 5 5 5 5 5 5 6 6 6 6 6 6 6 6 6 158  
JUN 6 6 7 7 7 7 7 7 7 7 7 7 7 7 7 7 7 8 8 8 8 8 8 8 8 8 8 8 8 220  
JUL 8 8 8 8 9 9 9 9 9 9 9 9 9 9 9 9 10 10 10 10 10 10 10 10 10 11 11 11 11 294  
AUG 11 11 11 11 11 11 12 12 12 12 12 12 12 11 11 11 11 11 11 11 11 11 10 10 10 10 10 9  
9 9 336  
SEP 9 8 8 8 7 7 7 7 7 6 6 6 6 6 5 5 5 5 5 5 5 4 4 4 4 4 4 4 4 169  
OCT 4 4 4 4 4 3 3 3 3 3 3 3 3 3 3 3 3 3 3 3 3 3 3 2 2 2 2 2 2 91  
NOV 2 2 2 2 2 2 2 2 2 2 2 2 2 2 1 1 1 1 1 1 1 1 1 1 1 1 1 1 1 43  
DEC 1 31  
-----

## Appendix 2.4

### Partial Sample ASCII Text File Containing Daily Climate Normal Values for Import into the Project Oracle Database

290022	36.3	-103.75	pcp	1	1
290022	36.3	-103.75	pcp	2	1
290022	36.3	-103.75	pcp	3	1
290022	36.3	-103.75	pcp	4	1
290022	36.3	-103.75	pcp	5	1
290022	36.3	-103.75	pcp	6	1
290022	36.3	-103.75	pcp	7	1
290022	36.3	-103.75	pcp	8	1
290022	36.3	-103.75	pcp	9	1
290022	36.3	-103.75	pcp	10	1

Where the first column is the coop id of the station, the second is the Latitude of the station, the third the Longitude of the station, the fourth the measurement (e.g. pcp = precipitation), the fifth the day of the year (i.e. January 1st is year-day 1, February 1st is year-day 32, etc.), and the sixth column is the measurement (in hundredths of an inch in the case of precipitation).

## Appendix 3.1

### Definition of Data Elements

#### COUNTY

The COUNTY table contains all the counties of New Mexico, and to what district to they belong.

COUNTY_ID	Unique identifier to represent every County in the State of New Mexico
COUNTY_NAME	County Name
DISTRICT_ID	Unique identifier to represent every State in New Mexico

#### DISTRICT

The DISTRICT table contains all the districts of New Mexico, and a general climatic classification per district.

CLIMATE	PMIS Climate Classification for each (Wet warm, Wet cold, dry warm, dry cold, mixed)
DISTRICT_ID	Unique identifier to represent every State in New Mexico
DISTRICT_NAME	District Name

#### ENV\_CONDITION

The ENV\_CONDITIONS table contains specific environmental information for the different pavement sections included in the database.

1_DAY_MIN_TEMP_MEAN	Minimum 1-day Annual Air temperature, °F
1_DAY_MIN_TEMP_SDV	Standard Deviation of Minimum 1-day Annual Air temperature, °F
3_DAY_MAX_TEMP_MEAN	Average 3 days maximum air temperature, °F
3_DAY_MAX_TEMP_SDV	Standard Deviation of 3-days maximum air temperature, °F
5_DAY_MAX_TEMP_MEAN	Average 5 days maximum air temperature, °F
5_DAY_MAX_TEMP_SDV	Standard Deviation of 5-days maximum air temperature, °F
7_DAY_MAX_TEMP_MEAN	Average 7 days maximum air temperature, °F
7_DAY_MAX_TEMP_SDV	Standard Deviation of 7-days maximum air temperature, °F
ADJ_LEFT_LANE_COND	Adjacent left lane condition
ADJ_LEFT_LANE_DEPTH	Adjacent left lane depth
ADJ_LEFT_LANE_TYPE	Adjacent left lane type
ADJ_LEFT_LANE_WIDTH	Adjacent left lane width
ADJ_RIGHT_LANE_COND	Adjacent right lane condition
ADJ_RIGHT_LANE_DEPTH	Adjacent right lane depth
ADJ_RIGHT_LANE_TYPE	Adjacent right lane type
ADJ_RIGHT_LANE_WIDTH	Adjacent right lane width
ALTITUDE	Altitude, ft
ANN_PRECIPITATION	Annual precipitation, in
AVG_MAX_MONTHLY_TEMP	Average maximum monthly temperature, °F
AVG_MIN_MONTHLY_TEMP	Average minimum monthly temperature, °F
CROSS_SLOPE	Cross Slope, %

DRAINAGE_CONDITION	Description of drainage conditions
DRAINAGE_TYPE	Drainage type
FROST_DEPTH	Frost Depth, in
FROST_DURATION	Frost Duration, days
FROST_INDEX	Frost Index
LATITUDE	Latitude, decimals
LOCATION_ID	Unique identifier for location of Weather station
LONGITUDE	Longitude, decimals
NO_FREEZE_THAW_CYCLE	Number of freeze/thaw cycles
SEASONS	Number of seasons that take place in specified location
SOLAR_RADIATION	Solar Radiation, kWhr/m
WEATHER_STATION	Type and number of Weather station

#### **ENV\_PRECIP\_VAR**

The ENV\_PRECIP\_VAR table contains specific information on the seasonal/monthly variation of precipitation on the different pavement sections included in the database.

LOCATION_ID	Unique identifier for location of Weather station
PERIOD	Defined as season or month
PRECIPITATION	Precipitation for the specified period, in
TYPE	Type: Seasonal/Monthly

#### **ENV\_WATER\_TABLE**

The ENV\_WATER\_TABLE table contains information on the monthly depth of the water table for the different pavement sections included in the database.

DEPTH_APR	Depth of water table in April, in
DEPTH_AUG	Depth of water table in August, in
DEPTH_DEC	Depth of water table in December, in
DEPTH_FEB	Depth of water table in February, in
DEPTH_JAN	Depth of water table in January, in
DEPTH_JUL	Depth of water table in July, in
DEPTH_JUN	Depth of water table in June, in
DEPTH_MAR	Depth of water table in March, in
DEPTH_MAY	Depth of water table in May, in
DEPTH_NOV	Depth of water table in November, in
DEPTH_OCT	Depth of water table in October, in
DEPTH_SEP	Depth of water table in September, in
LOCATION_ID	Unique identifier for location of Weather station

#### **PAV\_ADMIX**

The PAV\_ADMIX table contains information on the additives, modifiers, and admixtures included in the asphalt mixtures used on the different pavement sections included in the database.

ADDITIVE_ID	Unique Identifier for additive used in the mix
CONTENT	Additive Content, %
HMA_ID	Unique identifier for each pavement layer included in the database
TYPE	Additive Type: Additive/Modifier/Admixture

#### **PAV\_BINDER**

The PAV\_BINDER table contains specific rheological and physical information on the asphalt binders used on the different asphalt layers of the different pavement sections included in the database.

BINDER_CONTENT_VOL	Binder Content in percentage by volume, field extracted samples
BINDER_CONTENT_VOL_TST	Binder Content in percentage by volume, laboratory molded samples
BINDER_CONTENT_WT	Binder Content in percentage by Weight, field extracted samples
BINDER_CONTENT_WT_TST	Binder Content in percentage by Weight, laboratory molded samples
BINDER_ID	Unique identifier for each binder type included in the database
BINDER_MANUF	Binder manufacturer
BINDER_MOD	Is the binder modified?
BINDER_MOD_CONT	Binder Modifier Content, %
BINDER_MOD_TYPE	Binder Modification Type: SBS, SBR, latex, etc
BINDER_SOURCE	Binder Source
BINDER_TYPE	A general classification of the binder (PG Grade, AC Grade, PEN Grade, or similar)
CREEP_STIFF_64_PAV	Creep Stiffness @ 64°C on PAV binder
CREEP_STIFF_70_PAV	Creep Stiffness @ 70°C on PAV binder
CREEP_STIFF_76_PAV	Creep Stiffness @ 76°C on PAV binder
DUCTILITY	Ductility @ 5cm/min, cm
ELASTIC_RECOVERY	Elastic Recovery (100 mm elongation and cut immediately at 25°C), %
FAIL_STRAIN_64_PAV	Failure strain in direct tension @ 64°C on PAV binder
FAIL_STRAIN_70_PAV	Failure strain in direct tension @ 70°C on PAV binder
FAIL_STRAIN_76_PAV	Failure strain in direct tension @ 76°C on PAV binder
FIBER_CONT	Fiber Content, by Weight of mix
FIBER_TYPE	Fiber Type
G_64_ORG_BINDER	G*/sind@ 64°C on original binder, kPa
G_64_PAV	G*/sind@ 64°C on PAV binder, kPa
G_64_RTFO	G*/sind@ 64°C on RTFO binder, kPa
G_70_ORG_BINDER	G*/sind@ 70°C on original binder, kPa
G_70_PAV	G* sind@ 70°C on PAV binder, kPa
G_70_RTFO	G*/sind@ 70°C on RTFO binder, kPa
G_76_ORG_BINDER	G*/sind@ 76°C on original binder, kPa
G_76_PAV	G* sind@ 76°C on PAV binder, kPa
G_76_RTFO	G*/sind@ 76°C on RTFO binder, kPa
HMA_ID	Unique identifier for each HMA layer included in the database
M_VAL_64_PAV	m-value @ 64°C on PAV binder
M_VAL_70_PAV	m-value @ 70°C on PAV binder
M_VAL_76_PAV	m-value @ 76°C on PAV binder
MIN_FILLER_CONT	Mineral Filler Content
MIN_FILLER_TYPE	Mineral Filler Type
PENETRATION_25	Penetration @ 25°C, mm
SOFTENING_PT	Softening point: R&B or T800
TST_DATE	Test date for binder content
VISCOSITY_135	Viscosity @ 135°C
VISCOSITY_60	Viscosity @ 60°C



**PAV\_CONSTR**

The PAV\_CONSTR table contains information on the initial construction and maintenance and rehabilitation activities that have been performed on the pavement sections included in the database.

ANALYSIS_PERIOD	Analysis period for pavement construction
CN_CHANGE_REASON	Construction change reason, e.g., cracking seal, overlay, etc. Please refer to CODE table for description of each activity.
CONST_ID	Construction ID accounts for different construction activities involving a specific pavement section. The loWest construction ID represents the initial construction of the pavement section, and subsequent constructions represent additional activities
CSJ	Control Section Job Number
DATE_OPEN_TRAFFIC	Date pavement section was originally opened to traffic.
NO_OF_LAYERS_AC	Number of layers after current construction. If the number of layer before and after the current construction are the same, maintenance work was performed, but no layer was necessarily added.
NO_OF_LAYERS_BC	Number of existing layers before current construction.
NO_OF_LAYERS_NEW	Number of new layers added during current construction.
NO_OF_LAYERS_REMOVE	Number of removed layers that Were removed during current construction. It has to be observed that an equal number of layer before and after the current construction might indicate that some layers Were removed, but an equal number of layers Were lifted.
PER_PERIOD	Performance design period for pavement
PROJECT_TYPE	Project Type pavement section belongs to. Can be classified as: new, rehab, reconstruction
SECTION_ID	Unique identifier for each pavement section included in the database

**PAV\_FIELD\_PERF\_CRACK**

ANALYSIS_DATE	
BLK_CRACK_A_H	Area of high severity block cracking. (mean crack width greater than 19 mm or under 19 mm with moderate to high severity random cracking.)
BLK_CRACK_A_L	Area of low severity block cracking. (cracks of unknown width Well sealed or with mean width of 6 mm or less.)
BLK_CRACK_A_M	Area of moderate severity block cracking. (mean crack width from 6 to 19 mm or under 19 mm with adjacent low severity random cracking.)
CRACK_ID	Crack ID is a system assigned variable to keep track of cracking surveys performed on the different adjacent low severity random cracking.)
GATOR_CRACK_A_H	Area of alligator (fatigue) cracking of high severity. (moderately or severely spalled interconnected cracks, may be sealed, pumping may be evident.)

GATOR_CRACK_A_L	Area of alligator (fatigue) cracking of low severity. (no or few connecting cracks, not spalled or sealed, no pumping evident.)
GATOR_CRACK_A_M	Area of alligator (fatigue) cracking of high severity. (moderately or severely spalled interconnected cracks, may be sealed, pumping may be evident.)
LONG_CRACK_NWP_L_H	Length of high severity, Well sealed non-wheel path longitudinal cracking. (mean crack width greater than 19 mm or under 19 mm with adjacent moderate to high severity random cracking.)
LONG_CRACK_NWP_L_L	Length of low severity, non-wheel path longitudinal cracking. (cracks of unknown width Well sealed or with mean width of 6 mm or less.)
LONG_CRACK_NWP_L_M	Length of moderate severity, non-wheel path longitudinal cracking. (mean crack width from 6 to 19 mm or under 19 mm with adjacent low severity random cracking.)
LONG_CRACK_WP_L_H	Length of high severity, Well sealed wheel path longitudinal cracking. (mean crack width greater than 19 mm or under 19 mm with adjacent moderate to high severity random cracking.)
LONG_CRACK_WP_L_L	Length of low severity, wheel path longitudinal cracking. (cracks of unknown width Well sealed or with mean width of 6 mm or less.)
LONG_CRACK_WP_L_M	Length of moderate severity, wheel path longitudinal cracking. (mean crack width from 6 to 19 mm or under 19 mm with adjacent low severity random cracking.)
SECTION_ID	Unique identifier of each pavement section entered into the database.
SURVEY_DATE	Date survey was performed.
TRANS_CRACK_L_H	Length of high severity transverse cracking. (crack mean width greater than 19 mm or under 19 mm with adjacent moderate to high severity random cracking.)
TRANS_CRACK_L_L	Length of low severity transverse cracking. (cracks of unknown width Well sealed or with mean width of 6 mm or less.)
TRANS_CRACK_L_M	Length of moderate severity transverse cracking.
TRANS_CRACK_NO_H	Number of high severity transverse cracks. (mean crack width greater than 19 mm or under 19 mm with adjacent moderate to high severity random cracking.)
TRANS_CRACK_NO_L	Number of low severity transverse cracks. (cracks of unknown width Well sealed or with mean width of 6 mm or less.)
TRANS_CRACK_NO_M	Number of moderate severity transverse cracks. (mean crack width from 6 to 19 mm or under 19 mm with adjacent low severity random cracking.)

#### PAV\_FIELD\_PERF\_IRI

The PAV\_FIELD\_PERF\_IRI table includes IRI roughness information for the pavement sections included in the database.

AVERAGE_SPEED	Average speed of the profilometer during the test, mph
BEGINNING_DESCRIPTION	Beginning description of the run location.

DIRECTION_MEASURED	Run location direction measured.
ENDING_DESCRIPTION	Ending description of run location.
IRI_AVERAGE	Average International Roughness Index (IRI) value, in/mi.
IRI_ID	Inspection ID for IRI. It is a system assigned variable to keep track of IRI measurements performed on the different pavement sections included in the database.
IRI_LEFT_WHEEL_PATH	IRI value for left wheel path, in/mi.
IRI_RIGHT_WHEEL_PATH	IRI value for right wheel path, in/mi.
LANE_MEASURED	Identification of the lane measured.
LOAD_DATE	Date of load
OTHER_WEATHER_INFO	A description of other weather information at the time and location specified
PROFILE_DATE	Date of profile
PROFILE_TIME	Time of profile
RUN_NUMBER	Run number
SECTION_ID	Unique identifier of each pavement section entered into the database.
SLOPE_VARIANCE	Approximation of slope variance.
START_METHOD	Code designating the start method.
STOP_DISTANCE	Length of profile run as measured by profilometer.
STOP_METHOD	Code indicating the method for determining stop.
SURFACE_CONDITION	Description of the surface condition.
TEMPERATURE	Ambient air temperature.
WAVE_LENGTH_INIT	Code indicating if the wave length initialization was disabled or enabled.

#### PAV\_FIELD\_PERF\_RUT

The PAV\_FIELD\_PERF\_RUT table contains rutting information for the pavement sections included in the database.

LLH_DEPTH_1_8_MAX	Maximum left lane half straight edge 1.8 m (6 ft) depth, in.
LLH_DEPTH_1_8_MEAN	Mean left lane half straight edge 1.8 m (6 ft) depth, in.
LLH_DEPTH_1_8_MIN	Minimum left lane half straight edge 1.8 m (6 ft) depth, in.
LLH_DEPTH_1_8_STD	Left lane half straight edge 1.8 m (6 ft) depth standard deviation, in.
MAX_MEAN_DEPTH_1_8	Maximum value of left or right lane half straight edge 1.8 m (6 ft) depth mean, in.
RLH_DEPTH_1_8_MAX	Maximum right lane half straight edge 1.8 m (6 ft) depth, in.
RLH_DEPTH_1_8_MEAN	Mean right lane half straight edge 1.8 m (6 ft) depth, in.
RLH_DEPTH_1_8_MIN	Minimum right lane half straight edge 1.8 m (6 ft) depth, in.
RLH_DEPTH_1_8_STD	Right lane half straight edge 1.8 m (6 ft) depth standard

	deviation, in.
RUT_ID	Unique Identifier of Rutting Information. It is a system assigned variable to keep track of rutting measurements performed on the different pavement sections included in the database.
SECTION_ID	Unique identifier of each pavement section entered into the database.
SURVEY_DATE	Date survey was performed

#### PAV\_LAYER

The PAV\_LAYER table includes specific layer information for the different pavement sections that are included in the database. It also includes the aggregate gradation that was used on the different layers.

AGG_GRADATION	Aggregate Gradation according to NMDOT Specifications. Can be one of the following: A, B, C, D, E
AGG_SOURCE	Aggregate Source of material from current layer
AGG_TYPE	Aggregate Type for current layer. Can be classified as: Limestone, granite, gravel, blend
CONST_ID	Construction ID accounts for different construction activities involving a specific pavement section. The lowest construction ID represents the initial construction of the pavement section, and subsequent constructions represent additional activities
L_CONST_DATE	Date on which the current layer was constructed
L_OPEN_TRAFFIC_DATE	Date on which the current layer was opened to traffic
L_REMOVAL_DATE	Date on which the current layer was removed. If a layer were to be removed, no new layer is to re- use the layer number corresponding to the removed layer.
LAYER_ID	Unique identifier for each pavement layer entered into the database
LAYER_NO	Layer number. Layers are identified from 1 on, where 1 corresponds to subgrade (or bottommost layer), 2 corresponds to subbase/base (layer on top of layer 1), and so forth.
LAYER_THICKNESS_MEAN	Layer Thickness Mean, in.
LAYER_THICKNESS_SDV	Layer Thickness Standard Deviation, in.
LAYER_TYPE	Type of material that makes up current layer: Can be one of the following: HMA layer=1, Base/subbase layer=B (includes treated/untreated materials), Subgrade=G (includes treated/untreated materials), Other=O
NO_10_PASSING	Sieve analysis of aggregate from current layer. Percent passing the #10 sieve.
NO_16_PASSING	Sieve analysis of aggregate from current layer. Percent passing the #16 sieve.
NO_200_PASSING	Sieve analysis of aggregate from current layer. Percent passing the #200 sieve.
NO_4_PASSING	Sieve analysis of aggregate from current layer. Percent passing the #4 sieve.
NO_40_PASSING	Sieve analysis of aggregate from current layer. Percent passing the #40 sieve.
NO_80_PASSING	Sieve analysis of aggregate from current layer. Percent passing the #80 sieve.
NO_OF_LIFTS	Number of lifts to place current layer.
ONE_AND_HALF_PASSING	Sieve analysis of aggregate from current layer. Percent passing the 1 1/2 sieve.
ONE_AND_QUATER_PASSING	Sieve analysis of aggregate from current layer. Percent passing the 1 1/4 sieve.
FIVE_EIGHTHS_PASSING	Sieve analysis of aggregate from current layer. Percent passing the 5/8 sieve.

ONE_HALF_PASSING	Sieve analysis of aggregate from current layer. Percent passing the 1/2 sieve.
ONE_PASSING	Sieve analysis of aggregate from current layer. Percent passing the 1 sieve.
ONE_QUARTER_PASSING	Sieve analysis of aggregate from current layer. Percent passing the 1/4 sieve.
SEVEN_EIGHTHS_PASSING	Sieve analysis of aggregate from current layer. Percent passing the 7/8 sieve.
THREE_EIGHTHS_PASSING	Sieve analysis of aggregate from current layer. Percent passing the 3/8 sieve.
THREE_PASSING	Sieve analysis of aggregate from current layer. Percent passing the 3 sieve.
THREE_QUARTER_PASSING	Sieve analysis of aggregate from current layer. Percent passing the 3/4 sieve.
TWO_PASSING	Sieve analysis of aggregate from current layer. Percent passing the 2 sieve.

#### PAV\_LAYER\_BASE

The PAV\_LAYER\_BASE contains general and material subbase/base information on the different pavement sections included in the database.

AASHTO_CLASSIFICATION	AASHTO Soils Classification
COMP_STRENGTH	Compressive Strength
COMP_STRENGTH_103KPA	Compressive Strength at 103 kPa
COMP_STRENGTH_0KPA	Compressive Strength at 0 kPa
CON_DENSITY_MEAN	Construction density: Mean, %
CON_DENSITY_SDV	Construction density: Standard Deviation, %.
CON_MC_MEAN	Construction moisture content: Mean, %
CON_MC_SDV	Construction moisture content: Standard Deviation, %
CON_SEISMIC_MOD_MEAN	Construction seismic modulus: Mean, ksi.
CON_SEISMIC_MOD_SDV	Construction seismic modulus: Standard Deviation, ksi
GRANULAR_ID	Granular Layer ID (Includes Base, Subbase, treated materials, etc.)
INTERFACE_COND	Type of interface conditions present in the field
LAB_COMPACTION_EFFORT	Laboratory Compaction Effort
LAB_SEISMIC_MOD_MEAN	Laboratory seismic modulus: Mean, ksi
LAB_SEISMIC_MOD_SDV	Laboratory seismic modulus: Standard Deviation, ksi
LAYER_ID	Unique identifier for each pavement layer entered into the database
LIQUID_LIMIT	Atterberg limits: Liquid Limit
MC_SINE_APPX_A	Moisture Content Sinusoidal approximation: Constant A
MC_SINE_APPX_B	Moisture Content Sinusoidal approximation: Constant B
MC_SINE_APPX_C	Moisture Content Sinusoidal approximation: Constant C
MDD	Maximum Dry Density (MDD), pcf
OMC	Optimum Moisture Content (OMC), %
PLASTIC_INDEX	Atterberg limits: Plastic Index, 0=NP
PLASTIC_LIMIT	Atterberg limits: Plastic Limit
POISSON'S_RATIO	Poisson's Ratio
PRIME_COAT_APP_RATE	Application rate of prime coat
PRIME_COAT_TYPE	Type of prime coat
SHRINKAGE_LIMIT	Atterberg limits: Shrinkage Limit
TREATMENT_AMOUNT	Amount of treatment in percentage
TREATMENT_TYPE	Treatment Type
TX_TRIAXIAL_CLASSIFICATION	New Mexico Triaxial Classification

USC_CLASSIFICATION	Unified Soil Classification
WET_BALL_MILL	Wet Ball Mill

#### PAV\_LAYER\_HMA

The PAV\_LAYER\_HMA table is a link table between the different asphalt layers, and the additives, binder, HMA, and mix information for the layers.

ADDITIVE_ID	Unique identifier for the different additive types entered into the database
BINDER_ID	Unique identifier for each asphalt binder entered into the database
HMA_ID	Unique identifier for each HMA layer included in the database
LAYER_ID	Unique identifier for each pavement layer entered into the database
MIX_ID	Unique identifier for each individual asphalt mixture entered into the database

#### PAV\_LAYER\_HMA\_CREEP

The PAV\_LAYER\_HMA\_CREEP table contains creep results on samples from the different asphalt layers.

CREEP_COMP_1_SEC	Creep compliance value at 1 second.
CREEP_COMP_10_SEC	Creep compliance value at 10 seconds.
CREEP_COMP_100_SEC	Creep compliance value at 100 seconds.
CREEP_COMP_2_SEC	Creep compliance value at 2 seconds.
CREEP_COMP_20_SEC	Creep compliance value at 20 seconds.
CREEP_COMP_5_SEC	Creep compliance value at 5 seconds.
CREEP_COMP_50_SEC	Creep compliance value at 50 seconds.
CREEP_ID	Unique identifier for creep compliance results for each specific test specimen
CREEP_POISSON_CALC	Poisson's ratio calculated from load/deformation time histories.
CREEP_POISSON_USED	Poisson's ratio used for subsequent calculations.
HMA_ID	Unique identifier for each pavement layer entered into the database
TEST_NO	Code number indicating sample number
TEST_TEMPERATURE	Temperature at which test was performed.

#### PAV\_LAYER\_HMA\_MOD

HMA_ID	Test section identification number assigned by LTPP program. Must be combined with STATE_CODE to be unique.
INST_MR_AVG	Average instantaneous resilient modulus determined by averaging results from cycles 1, 2, and 3.
INST_MR_CYCLE_1	Instantaneous resilient modulus for load cycle 1, ksi.
INST_MR_CYCLE_2	Instantaneous resilient modulus for load cycle 2, ksi.
INST_MR_CYCLE_3	Instantaneous resilient modulus for load cycle 3, ksi.
INST_MR_POISSON_CALC_AVG	Average instantaneous calculated Poisson's ratio

	determined by averaging results from cycles 1, 2 and 3.
INST_MR_POISSON_CALC_CYCLE_1	Instantaneous Poisson's ratio for load cycle 1. Calculated from raw load/deformation time histories.
INST_MR_POISSON_CALC_CYCLE_2	Instantaneous Poisson's ratio for load cycle 2. Calculated from raw load/deformation time histories.
INST_MR_POISSON_CALC_CYCLE_3	Instantaneous Poisson's ratio for load cycle 3. Calculated from raw load/deformation time histories.
MOD_ID	Numerical code for state or province. U.S. codes are consistent with Federal Information Processing Standards.
MR_DATA_FILE_SPECIMEN_1	Name of file that contains load/deformation time histories used in calculation of resilient modulus for a given test temperature for specimen 1.
TEST_NO	Code number indicating sample number
TEST_TEMPERATURE	Temperature at which test was performed, °F
TOTAL_MR_AVG	Average total resilient modulus, ksi.
TOTAL_MR_CYCLE_1	Total resilient modulus for load cycle 1, ksi.
TOTAL_MR_CYCLE_2	Total resilient modulus for load cycle 2, ksi.
TOTAL_MR_CYCLE_3	Total resilient modulus for load cycle 3, ksi.
TOTAL_MR_POISSON_CALC_AVG	Average total calculated Poisson's ratio.
TOTAL_MR_POISSON_CALC_CYCLE_1	Total calculated Poisson's ratio for load cycle 1.
TOTAL_MR_POISSON_CALC_CYCLE_2	Total calculated Poisson's ratio for load cycle 2.
TOTAL_MR_POISSON_CALC_CYCLE_3	Total calculated Poisson's ratio for load cycle 3.

#### PAV\_LAYER\_SOIL

The PAV\_LAYER\_SOIL table contains soil properties of the sub grade of the different pavement sections included in the database.

AASHTO_CLASSIFICATION	AASHTO Soil Classification
BAR_LINEAR_SHRINKAGE	Bar Linear Shrinkage
CBR or R-VALUE	California Bearing Ratio or Resistance Value
COMP_STRENGTH_103KPA	Compressive Strength at 103 kPa
COMP_STRENGTH_OKPA	Compressive Strength at 0 kPa
CON_DENSITY_MEAN	Construction density: Mean, %
CON_DENSITY_SDV	Construction density: Standard Deviation, %
CON_MC_MEAN	Construction moisture content: Mean, %.
CON_MC_SDV	Construction moisture content: Standard Deviation, %.
CON_SEISMIC_MOD_MEAN	Construction seismic modulus: Mean, ksi.
CON_SEISMIC_MOD_SDV	Construction seismic modulus: Standard Deviation, ksi.
DCP	Dynamic Cone Penetrometer
GROUP_INDEX	Group Index
INTRFACE_COND	Type of interface conditions present in the field
LAB_COMPACTION_EFFORT	Laboratory Compaction Effort
LAB_SEISMIC_MOD_MEAN	Laboratory seismic modulus: Mean, ksi
LAB_SEISMIC_MOD_SDV	Laboratory seismic modulus: Standard Deviation, ksi
LAYER_ID	Unique identifier for each layer entered into the database

LIQUID_LIMIT	Atterberg limits: Liquid Limit
MC_SINE_APPX_A	Moisture Content Sinusoidal approximation: Constant A
MC_SINE_APPX_B	Moisture Content Sinusoidal approximation: Constant B
MC_SINE_APPX_C	Moisture Content Sinusoidal approximation: Constant C
MDD	Maximum Dry Density (MDD), pcf
MOD_SUBGRADE_REACTION	Modulus of Subgrade Reaction, ksi
OMC	Optimum Moisture Content (OMC), %.
ORG_CONTENT	Organic Content, %.
PLASTIC_INDEX	Atterberg limits: Plastic Index
PLASTIC_LIMIT	Atterberg limits: Plastic Limit
POISONS_RATIO	Poisson's Ratio
RESILIENT_MOD_CONST_K1	Resilient Modulus Function: Constant k1
RESILIENT_MOD_CONST_K2	Resilient Modulus Function: Constant k2
RESILIENT_MOD_CONST_K3	Resilient Modulus Function: Constant k3
SHRINKAGE_LIMIT	Atterberg limits: Shrinkage Limit
SOIL_ID	Unique identifier for each subgrade soil layer entered into the database
SULPHATE_POT	Sulfate potential
SWELL_POT	SWell potential
TX_TRIAXIAL_CLASSIFICATION	New Mexico Triaxial Classification
USC_CLASSIFICATION	Unified Soil Classification

#### PAV\_LAYER\_STSC

The PAV\_LAYER\_STSC table contains information on the surface treatments and surface seals used on the different pavement sections included in the database.

BINDER_RATE	Binder application rate used on surface treatment/seal coat
BINDER_TYPE	Binder type used on surface treatment/seal coat
LAYER_ID	Layer ID
STSC_ID	Surface treatment and surface curing ID

#### PAV\_MIX\_JMF

The PAV\_MIX\_JMF table contains information on the job mix formula used for the asphalt mix used on the pavement sections included in the database.

JMF_ID	Unique identifier for each Job Mix Formula
MIX_DETAIL	Mixture Design Details
MIX_ID	Unique identifier for each asphalt mixture included in the database.

#### PAV\_MIX

The PAV\_MIX table contains asphalt mixture information for the different asphalt layers of the pavement sections included in the database.

AIR_VOID_CONTENT_MEAN	Air Void Content: Mean, %.
AIR_VOID_CONTENT_SDV	Air Void Content : Standard Deviation, %.
DENSITY_MEAN	In-situ Density: Mean, %
DENSITY_SDV	In-situ Density : Standard Deviation, %.
DYNAMIC_MOD	Dynamic Modulus, ksi
DYNAMIC_STIFF	Dynamic Stiffness, ksi
FATIGUE_ID	Unique identifier for each bending beam sample entered into the database



FLOW_NUMBER	Flow Number
FLOW_TIME	Flow Time
HMA_ID	Unique identifier for each HMA layer included in the database.
HWTD_ID	Unique identifier for each Hamburg Wheel Tracking Device (HWTD) sample included in the database.
IND_TENSILE_STRENGTH	Indirect Tensile Strength, ksi.
INTERFACE_COND	Interface Condition: bounded, unbounded
JMF	Job Mix Formula
MASTER_CURVE	Master Curve or Estimate
MIX_DESIGN_PROCEDURE	Mix Design Procedure: Marshall, Hveem, SGC, TGC
MIX_ID	Unique identifier for each asphalt mixture entered into the database.
MIX_TYPE	SUPERPAVE, DENSE, UNKNOWN
MMLS3_ID	Unique identifier for each MMLS3 test result included into the database
OVERLAY_TESTER	Number of repetitions to reach failure in the overlay tester.
POISSONS_RATIO	Poisson's Ratio
RESILIENT_MOD_25	Resilient Modulus(25°C)
RESILIENT_MOD_40	Resilient Modulus(40°C)
RESILIENT_MOD_5	Resilient Modulus(5°C)
RICE_DENSITY	Rice Density: Maximum theoretical density, pcf.
TACK_COAT_RATE	Tack coat application rate
TACK_COAT_TYPE	Tack coat type
VMA	Voids in the Mineral Aggregate, %.

#### PAV\_SECTION

The PAV\_SECTION table is the main table in the database, and contains specific location, climate, and geographical information for the pavement sections included in the database.

BEG_PT_ELEV	Elevation of pavement section beginning point, as measured using GPS equipment.
BEG_PT_LAT	Latitude of pavement section beginning point, as measured using GPS equipment.
BEG_PT_LONG	Longitude of pavement section beginning point, as measured using GPS equipment.
BEG_TRM	Pavement section beginning reference marker number
BEG_TRM_DISP	Pavement section beginning reference marker displacement
COUNTY_ID	Unique identifier to represent every County in the State of New Mexico
DEPTH_BEDR	Depth to bedrock from pavement section surface
DIRECTION	Traffic travel direction. Can be classified as one of the following: East=1, West=2, North=3, South=4
END_PT_ELEV	Elevation of pavement section end point, as measured using GPS equipment.
END_PT_LAT	Latitude of pavement section end point, as measured using GPS equipment.
END_PT_LONG	Longitude of pavement section end point, as measured using GPS equipment.
END_TRM	Pavement section ending reference marker number
END_TRM_DISP	Pavement section ending reference marker displacement
FACILITY_TYPE	PMIS facility ranking. Can be ranked as: IH, US, SH, BI, BU, BS, FM, BF, PR
FOUNDATION_TYPE	Type of foundation to support roadway structure. Can be classified as one of the following: cut, fill, level
LANE_NUMBER	Lane number on pavement roadway that corresponds to pavement section
LANE_WIDTH	Lane width that corresponds to pavement section

NO_OF_LANES	Number of lanes on pavement section
ORIGINAL_DB	Database from which data was originally acquired from (LTPP, Research)
ORIGINAL_ID	ID of pavement section on the original database
ROADBED	PMIS roadbed type.
ROADWAY_NO	New Mexico Roadway number, which correspond to the NMDOT highway number or route number from PMIS
ROADWAY_TYPE	Roadway Type Classification. Can be classified as one of the following: IH=1, US=2, SH=3, Loop=4, FM=5
SECTION_ID	Section ID is a unique identifier of each pavement section entered into the database. This is a system assigned variable.
TERRAIN_GRADE	Terrain grade/slope. Can be classified as one of the following: flat=1, downhill=2, uphill=3

#### PAV\_SS\_US\_MOD

The PAV\_SS\_US\_MOD table contains modulus information for the granular materials and soils used on the different layers of the sections included in the database.

APPLIED_CONTACT_LOAD_AVG	Applied contact load average.
APPLIED_CONTACT_LOAD_STD	Applied contact load standard deviation.
APPLIED_CONTACT_STRESS_AVG	Applied contact stress average.
APPLIED_CONTACT_STRESS_STD	Applied contact stress standard deviation.
APPLIED_CYCLIC_LOAD_AVG	Actual applied cyclic load average.
APPLIED_CYCLIC_LOAD_STD	Applied cyclic load standard deviation.
APPLIED_CYCLIC_STRESS_AVG	Applied cyclic stress average.
APPLIED_CYCLIC_STRESS_STD	Applied cyclic stress standard deviation.
APPLIED_MAX_AXIAL_LOAD_AVG	Applied maximum axial load average.
APPLIED_MAX_AXIAL_LOAD_STD	Applied maximum axial load standard deviation.
APPLIED_MAX_AXIAL_STRESS_AVG	Applied maximum axial stress average.
APPLIED_MAX_AXIAL_STRESS_STD	Applied maximum axial stress standard deviation.
CON_PRESSURE	Chamber confining pressure.
DEF_LVDT_1_2_AVG	Average across cycles of the average recoverable axial deformations.
DEF_LVDT_1_2_STD	Standard deviation across cycles of the average recoverable axial deformation.
DEF_LVDT_1_AVG	Average across cycles of the recoverable axial deformation of the sample for each LVDT.
DEF_LVDT_1_STD	Standard deviation across cycles of the recoverable axial deformation.
DEF_LVDT_2_AVG	Average across cycles of the recoverable axial deformation of the sample for each LVDT.
DEF_LVDT_2_STD	Standard deviation across cycles of the recoverable axial deformation.
FIELD_SET	Sequential number indicating the field sampling event. Assigned 1 for first sample event and incremented by 1 for subsequent events.
LAYER_ID	Unique sequential number assigned to pavement layers, starting with the deepest layer (subgrade).
LOC_NO	Unique code number assigned to each sampling location indicating the sample type. The single character prefix indicates the sample type. The numeric suffix is the unique project location for the sample type.
MOD_ID	Unique identifier of modulus information for granular layers in a specific pavement section in the database.
MR_MATL_TYPE	Code designating whether the material was coarse

NOM_MAX_AXIAL_STRESS	Nominal maximum axial stress.
RES_MOD_AVG	Average resilient modulus across cycles.
RES_MOD_STD	Standard deviation of the resilient modulus across cycles.
RES_STRAIN_AVG	Average resilient strain across cycles.
RES_STRAIN_STD	Standard deviation of resilient strain across cycles.
SAMPLE_NO	Unique code number assigned to each material sample indicating the sample type and material type. The first character indicates the sample type. The second character indicates the material type. The numeric suffix is the unique sample number for the sample
TEST_DATE	Date the test was performed.
TEST_NO	Code number indicating test.

#### TEST\_FATIGUE

The TEST\_FATIGUE table contains four-point bending beam results for the asphalt mixtures included in the database.

CYCLE	Applied load cycle
FATIGUE_ID	Unique identifier for each individual fatigue test sample included in the database
MIX_ID	Unique identifier for each asphalt mixture included into the database
STIFFNESS	Stiffness at given cycle, ksi
STRAIN	Applied strain at given cycle,
TEMPERATURE	Testing temperature, °F

#### TRAFFIC

The Traffic table contains general traffic information regarding the pavement sections included in the database.

AADT_PER_LANE	Average Annual Daily Traffic (AADT) per lane for the indicated year
AVG_OVERLOADING	Average Overloading
DIR_DIST_FACTOR	Direction distribution factors
FUTURE_ESAL	Future Equivalent Single Axle Loads (ESAL)
FUTURE_ESAL_YEAR	Year of Future ESAL
GROWTH_FACTOR	Growth factor, number of trucks.
GROWTH_RATE	Growth rate in percentage
INITIAL_AADT	Initial AADT
INITIAL_ESAL	Initial ESAL
INITIAL_PER_TRUCKS	Percentage trucks, %
LANE_DIST_FACTOR	Lane distribution factor
PER_OVERLOADING	Percentage Overloading, %
SECTION_ID	Unique identifier for each pavement section included into the database.
TIRE_INFLAT_SDV	Tire inflation pressure: Standard Deviation, psi
TIRE_INFLATION_DIST	Tire Inflation Distribution type
TIRE_INFLATION_MEAN	Tire inflation pressure: Mean, psi
TRAFFIC_WANDER	Traffic wander
YEAR_INITIAL_AADT	Year initial AADT
YEAR_RECORD	Year at which traffic data is reported

#### TRAFFIC\_AXLE\_LOAD\_VAR

The TRAFFIC\_AXLE\_LOAD\_VAR table contains load variability information due to time seasonal and hourly variations.

CLASS	Vehicle and axle class type
CLASS_PER	Percentage of class type, %
DISTR_MNTH_APR	Distribution for April, %
DISTR_MNTH_AUG	Distribution for August, %
DISTR_MNTH_DEC	Distribution for December, %.
DISTR_MNTH_FEB	Distribution for February, %.
DISTR_MNTH_JAN	Distribution for January, %.
DISTR_MNTH_JUL	Distribution for July, %.
DISTR_MNTH_JUN	Distribution for June, %.
DISTR_MNTH_MAR	Distribution for March, %.
DISTR_MNTH_MAY	Distribution for May, %.
DISTR_MNTH_NOV	Distribution for November, %.
DISTR_MNTH_OCT	Distribution for October, %.
DISTR_MNTH_SEP	Distribution for September, %.
HRLY_DISTR_00	Percentage of daily traffic from 12:00 AM to 12:59 AM
HRLY_DISTR_01	Percentage of daily traffic from 01:00 AM to 01:59 AM
HRLY_DISTR_02	Percentage of daily traffic from 02:00 AM to 02:59 AM
HRLY_DISTR_03	Percentage of daily traffic from 03:00 AM to 03:59 AM
HRLY_DISTR_04	Percentage of daily traffic from 04:00 AM to 04:59 AM
HRLY_DISTR_05	Percentage of daily traffic from 05:00 AM to 05:59 AM
HRLY_DISTR_06	Percentage of daily traffic from 06:00 AM to 06:59 AM
HRLY_DISTR_07	Percentage of daily traffic from 07:00 AM to 07:59 AM
HRLY_DISTR_08	Percentage of daily traffic from 08:00 AM to 08:59 AM
HRLY_DISTR_09	Percentage of daily traffic from 09:00 AM to 09:59 AM
HRLY_DISTR_10	Percentage of daily traffic from 10:00 AM to 10:59 AM
HRLY_DISTR_11	Percentage of daily traffic from 11:00 AM to 11:59 AM
HRLY_DISTR_12	Percentage of daily traffic from 12:00 PM to 12:59 PM
HRLY_DISTR_13	Percentage of daily traffic from 01:00 PM to 01:59 PM
HRLY_DISTR_14	Percentage of daily traffic from 02:00 PM to 02:59 PM
HRLY_DISTR_15	Percentage of daily traffic from 03:00 PM to 03:59 PM
HRLY_DISTR_16	Percentage of daily traffic from 04:00 PM to 04:59 PM
HRLY_DISTR_17	Percentage of daily traffic from 05:00 PM to 05:59 PM
HRLY_DISTR_18	Percentage of daily traffic from 06:00 PM to 06:59 PM
HRLY_DISTR_19	Percentage of daily traffic from 07:00 PM to 07:59 PM
HRLY_DISTR_20	Percentage of daily traffic from 08:00 PM to 08:59 PM
HRLY_DISTR_21	Percentage of daily traffic from 09:00 PM to 09:59 PM
HRLY_DISTR_22	Percentage of daily traffic from 10:00 PM to 10:59 PM
HRLY_DISTR_23	Percentage of daily traffic from 11:00 PM to 11:59 PM
HRLY_DISTR_24	Percentage of daily traffic from 12:00 AM to 12:59 AM
QUAD_AXLE	Axial load for quad axles
SECTION_ID	Unique identifier for each pavement section included into the database.
SIN_CONST_A	Parameter A for sinusoidal model for hourly variability
SIN_CONST_B	Parameter B for sinusoidal model for hourly variability
SIN_CONST_C	Parameter C for sinusoidal model for hourly variability
SINGLE_AXLE_DUAL_WHEEL	Axial load for single axles w/double wheels
SINGLE_AXLE_SINGLE_WHEEL	Axial load for single axles w/single wheels
TANDEM_AXLE	Axial load for tandem axles
TRIDEM_AXLE	Axial load for tridem axles

### TRAFFIC\_LOAD\_SPECTRA

The TRAFFIC\_LOAD\_SPECTRA table contains information on the axle load spectra for different axle types, as well as default axle load spectra.

Axle_ID	Unique Identifier for different axle types. Axle load spectrum (or distribution) for a given type of axle (such as single axle, single axle with dual wheels, tandem, and tridem...) is composed of two elements: axle load bins and frequency for each interval.
Axle_Type	Steering=1, Single axle with wheels=2, tandem=3, tridem=4.
Bin_1	Normalized Frequency for distribution bin 1 (in %)
Bin_10	Normalized Frequency for distribution bin 10 (in %)
Bin_11	Normalized Frequency for distribution bin 11 (in %)
Bin_12	Normalized Frequency for distribution bin 12 (in %)
Bin_13	Normalized Frequency for distribution bin 13 (in %)
Bin_14	Normalized Frequency for distribution bin 14 (in %)
Bin_15	Normalized Frequency for distribution bin 15 (in %)
Bin_16	Normalized Frequency for distribution bin 16 (in %)
Bin_17	Normalized Frequency for distribution bin 17 (in %)
Bin_18	Normalized Frequency for distribution bin 18 (in %)
Bin_19	Normalized Frequency for distribution bin 19 (in %)
Bin_2	Normalized Frequency for distribution bin 2 (in %)
Bin_20	Normalized Frequency for distribution bin 20 (in %)
Bin_21	Normalized Frequency for distribution bin 21 (in %)
Bin_22	Normalized Frequency for distribution bin 22 (in %)
Bin_23	Normalized Frequency for distribution bin 23 (in %)
Bin_24	Normalized Frequency for distribution bin 24 (in %)
Bin_25	Normalized Frequency for distribution bin 25 (in %)
Bin_26	Normalized Frequency for distribution bin 26 (in %)
Bin_27	Normalized Frequency for distribution bin 27 (in %)
Bin_28	Normalized Frequency for distribution bin 28 (in %)
Bin_29	Normalized Frequency for distribution bin 29 (in %)
Bin_3	Normalized Frequency for distribution bin 3 (in %)
Bin_30	Normalized Frequency for distribution bin 30 (in %)
Bin_31	Normalized Frequency for distribution bin 31 (in %)
Bin_32	Normalized Frequency for distribution bin 32 (in %)
Bin_33	Normalized Frequency for distribution bin 33 (in %)
Bin_34	Normalized Frequency for distribution bin 34 (in %)
Bin_35	Normalized Frequency for distribution bin 35 (in %)
Bin_36	Normalized Frequency for distribution bin 36 (in %)
Bin_37	Normalized Frequency for distribution bin 37 (in %)
Bin_38	Normalized Frequency for distribution bin 38 (in %)
Bin_39	Normalized Frequency for distribution bin 39 (in %)
Bin_4	Normalized Frequency for distribution bin 4 (in %)
Bin_40	Normalized Frequency for distribution bin 40 (in %)
Bin_41	Normalized Frequency for distribution bin 41 (in %)
Bin_42	Normalized Frequency for distribution bin 42 (in %)
Bin_43	Normalized Frequency for distribution bin 43 (in %)
Bin_5	Normalized Frequency for distribution bin 5 (in %)
Bin_6	Normalized Frequency for distribution bin 6 (in %)
Bin_7	Normalized Frequency for distribution bin 7 (in %)
Bin_8	Normalized Frequency for distribution bin 8 (in %)
Bin_9	Normalized Frequency for distribution bin 9 (in %)
Bin_Width	Bins represent the intervals of axle load Weight. For steering axle and single axle with dual wheels, the bins have an interval width of 1 kip; for tandem axle, 2 kip; and for tridem axle, 3 kip.

Sta PK1 M	Peak 1 statistic, mean
Sta PK1 S	Peak 1 statistic, standard deviation
Sta PK1 W	Peak 1 statistic, Weight
Sta PK2 M	Peak 2 statistic, mean
Sta PK2 S	Peak 2 statistic, standard deviation
Sta PK2 W	Peak 2 statistic, Weight
Sta PK3 M	Peak 3 statistic, mean
Sta PK3 S	Peak 3 statistic, standard deviation

## Appendix 3.2

### SQL Script:

```
CREATE TABLE DISTRICT(DISTRICT_ID INTEGER NOT NULL ,DISTRICT_NAME VARCHAR2(100)
NOT NULL,CLIMATE VARCHAR2(30) NOT NULL);
ALTER TABLE DISTRICT ADD(CONSTRAINT DISTRICT_ID_PK PRIMARY KEY(DISTRICT_ID));
```

```
CREATE TABLE COUNTY(COUNTY_ID INTEGER NOT NULL ,COUNTY_NAME VARCHAR2(100) NOT
NULL,DISTRICT_ID INTEGER NOT NULL);
ALTER TABLE COUNTY ADD ( CONSTRAINT COUNTY_PK PRIMARY KEY (COUNTY_ID));
ALTER TABLE COUNTY ADD ( CONSTRAINT COUNTY_FK FOREIGN KEY (DISTRICT_ID)
REFERENCES DISTRICT (DISTRICT_ID));
```

```
CREATE TABLE ENV_PRECIP_VAR(
    LOCATION_ID                INTEGER NOT NULL,
    PERIOD                     VARCHAR2(100),
    PRECIPITATION              VARCHAR2(100),
    TYPE                       VARCHAR2(100)
);
ALTER TABLE ENV_PRECIP_VAR ADD ( CONSTRAINT ENV_PRECIP_VAR_PK PRIMARY KEY
(LOCATION_ID));
```

```
CREATE TABLE ENV_CONDITIONS(
    DAY_MIN_TEMP_MEAN_1        FLOAT,
    DAY_MIN_TEMP_SDV_1         FLOAT,
    DAY_MAX_TEMP_MEAN_3        FLOAT,
    DAY_MAX_TEMP_SDV_3         FLOAT,
    DAY_MAX_TEMP_MEAN_5        FLOAT,
    DAY_MAX_TEMP_SDV_5         FLOAT,
    DAY_MAX_TEMP_MEAN_7        FLOAT,
    DAY_MAX_TEMP_SDV_7         FLOAT,
    ADJ_LEFT_LANE_COND         VARCHAR2(100),
    ADJ_LEFT_LANE_DEPTH        VARCHAR2(100),
    ADJ_LEFT_LANE_TYPE         VARCHAR2(100),
    ADJ_LEFT_LANE_WIDTH        VARCHAR2(100),
    ADJ_RIGHT_LANE_COND        VARCHAR2(100),
    ADJ_RIGHT_LANE_DEPTH       VARCHAR2(100),
    ADJ_RIGHT_LANE_TYPE        VARCHAR2(100),
    ADJ_RIGHT_LANE_WIDTH       VARCHAR2(100),
    ALTITUDE                   FLOAT,
    ANN_PRECIPITATION           VARCHAR2(100),
    AVG_MAX_MONTHLY_TEMP        FLOAT,
    AVG_MIN_MONTHLY_TEMP       FLOAT,
    CROSS_SLOPE                 VARCHAR2(100),
    DRAINAGE_CONDITION          VARCHAR2(100),
    DRAINAGE_TYPE               VARCHAR2(100),
    FROST_DEPTH                 INTEGER,
    FROST_DURATION              INTEGER,
    FROST_INDEX                 INTEGER,
    LATITUDE                    FLOAT,
    LOCATION_ID                 INTEGER,
    LONGITUDE                   FLOAT,
    NO_FREEZE_THAW_CYCLE        VARCHAR2(100),
```

```

        SEASONS                                VARCHAR2(100),
        SOLAR_RADIATION                        VARCHAR2(100),
        WEATHER_STATION                        INTEGER
    );
    ALTER TABLE ENV_CONDITIONS ADD ( CONSTRAINT ENV_CONDITIONS_PK PRIMARY KEY
    (LOCATION_ID));

    CREATE TABLE ENV_WATER_TABLE(
        DEPTH_APR                                FLOAT,
        DEPTH_AUG                                FLOAT,
        DEPTH_DEC                                FLOAT,
        DEPTH_FEB                                FLOAT,
        DEPTH_JAN                                FLOAT,
        DEPTH_JUL                                FLOAT,
        DEPTH_JUN                                FLOAT,
        DEPTH_MAR                                FLOAT,
        DEPTH_MAY                                FLOAT,
        DEPTH_NOV                                FLOAT,
        DEPTH_OCT                                FLOAT,
        DEPTH_SEP                                FLOAT,
        LOCATION_ID                              INTEGER
    );
    ALTER TABLE ENV_WATER_TABLE ADD ( CONSTRAINT ENV_WATER_TABLE_PK PRIMARY KEY
    (LOCATION_ID));

    CREATE TABLE PAV_ADMIX(
        ADDITIVE_ID                              INTEGER,
        CONTENT                                  FLOAT,
        HMA_ID                                  INTEGER,
        TYPE                                      VARCHAR2(100)
    );
    ALTER TABLE PAV_ADMIX ADD ( CONSTRAINT PAV_ADMIX_PK PRIMARY KEY (ADDITIVE_ID) );

    CREATE TABLE PAV_BINDER(
        BINDER_CONTENT_VOL                        FLOAT,
        BINDER_CONTENT_VOL_TST                    FLOAT,
        BINDER_CONTENT_WT                        FLOAT,
        BINDER_CONTENT_WT_TST                    FLOAT,
        BINDER_ID                                INTEGER,
        BINDER_MANUF                            FLOAT,
        BINDER_MOD                              VARCHAR2(100),
        BINDER_MOD_CONT                          FLOAT,
        BINDER_MOD_TYPE                          VARCHAR2(100),
        BINDER_SOURCE                            VARCHAR2(100),
        BINDER_TYPE                              VARCHAR2(100),
        CREEP_STIFF_64_PAV                        VARCHAR2(100),
        CREEP_STIFF_70_PAV                        VARCHAR2(100),
        CREEP_STIFF_76_PAV                        VARCHAR2(100),
        DUCTILITY                                VARCHAR2(100),
        ELASTIC_RECOVERY                          FLOAT,
        FAIL_STRAIN_64_PAV                        VARCHAR2(100),
        FAIL_STRAIN_70_PAV                        VARCHAR2(100),
        FAIL_STRAIN_76_PAV                        VARCHAR2(100),
        FIBER_CONT                              VARCHAR2(100),
        FIBER_TYPE                              VARCHAR2(100),
        G_64_ORG_BINDER                          FLOAT,

```



```

G_64_PAV                                FLOAT,
G_64_RTFO                               FLOAT,
G_70_ORG_BINDER                         FLOAT,
G_70_PAV                                FLOAT,
G_70_RTFO                               FLOAT,
G_76_ORG_BINDER                         FLOAT,
G_76_PAV                                FLOAT,
G_76_RTFO                               FLOAT,
HMA_ID                                 INTEGER NOT NULL,
M_VAL_64_PAV                            FLOAT,
M_VAL_70_PAV                            FLOAT,
M_VAL_76_PAV                            FLOAT,
MIN_FILLER_CONT                         VARCHAR2(100),
MIN_FILLER_TYPE                        VARCHAR2(100),
PENETRATION_25                         FLOAT,
SOFTENING_PT                           VARCHAR2(100),
TST_DATE                               DATE,
VISCOSITY_135                          FLOAT,
VISCOSITY_60                          FLOAT
);
ALTER TABLE PAV_BINDER ADD ( CONSTRAINT PAV_BINDER_PK PRIMARY KEY (BINDER_ID) );

CREATE TABLE PAV_SECTION(
    BEG_PT_ELEV                          FLOAT,
    BEG_PT_LAT                           FLOAT,
    BEG_PT_LONG                          FLOAT,
    BEG_TRM                             INTEGER,
    BEG_TRM_DISP                        INTEGER,
    COUNTY_ID                           INTEGER,
    DEPTH_BEDR                          VARCHAR2(30),
    DIRECTION                           VARCHAR2(100),
    END_PT_ELEV                          FLOAT,
    END_PT_LAT                           FLOAT,
    END_PT_LONG                          FLOAT,
    END_TRM                             INTEGER,
    END_TRM_DISP                        INTEGER,
    FACILITY_TYPE                       VARCHAR2(20),
    FOUNDATION_TYPE                     VARCHAR2(20),
    LANE_NUMBER                          INTEGER,
    LANE_WIDTH                           FLOAT,
    NO_OF_LANES                         INTEGER,
    ORIGINAL_DB                          VARCHAR2(30),
    ORIGINAL_ID                         INTEGER NOT NULL,
    ROADBED                             VARCHAR2(20),
    ROADWAY_NO                          INTEGER,
    ROADWAY_TYPE                        INTEGER,
    SECTION_ID                          INTEGER,
    TERRAIN_GRADE                       VARCHAR2(20)
);
ALTER TABLE PAV_SECTION ADD(CONSTRAINT PAV_SECTION_PK PRIMARY KEY(SECTION_ID));
ALTER TABLE PAV_SECTION ADD(CONSTRAINT PAV_SECTION_FK FOREIGN KEY(COUNTY_ID)
REFERENCES COUNTY(COUNTY_ID));

CREATE TABLE PAV_CONSTR(
    ANALYSIS_PERIOD                     VARCHAR2(100),
    CN_CHANGE_REASON                    VARCHAR2(100),

```

```

CONST_ID          INTEGER,
CSJ               INTEGER,
DATE_OPEN_TRAFFIC VARCHAR2(100),
NO_OF_LAYERS_AC   INTEGER,
NO_OF_LAYERS_BC   INTEGER,
NO_OF_LAYERS_NEW  INTEGER,
NO_OF_LAYERS_REMOVE INTEGER,
PER_PERIOD        VARCHAR2(100),
PROJECT_TYPE      VARCHAR2(100),
SECTION_ID        INTEGER NOT NULL
);
ALTER TABLE PAV_CONSTR ADD(CONSTRAINT PAV_CONSTR_PK PRIMARY KEY (CONST_ID));
ALTER TABLE PAV_CONSTR ADD(CONSTRAINT PAV_CONSTR_FK FOREIGN KEY(SECTION_ID)
REFERENCES PAV_SECTION(SECTION_ID));

CREATE TABLE PAV_FIELD_PERF_CRACK(
ANALYSIS_DATE      DATE,
BLK_CRACK_A_H      VARCHAR2(100),
BLK_CRACK_A_L      VARCHAR2(100),
BLK_CRACK_A_M      VARCHAR2(100),
CRACK_ID           INTEGER,
GATOR_CRACK_A_H    VARCHAR2(100),
GATOR_CRACK_A_L    VARCHAR2(100),
GATOR_CRACK_A_M    VARCHAR2(100),
LONG_CRACK_NWP_L_H FLOAT,
LONG_CRACK_NWP_L_L FLOAT,
LONG_CRACK_NWP_L_M FLOAT,
LONG_CRACK_WP_L_H  FLOAT,
LONG_CRACK_WP_L_L  FLOAT,
LONG_CRACK_WP_L_M  FLOAT,
SECTION_ID         INTEGER NOT NULL,
SURVEY_DATE        DATE,
TRANS_CRACK_L_H    FLOAT,
TRANS_CRACK_L_L    FLOAT,
TRANS_CRACK_L_M    FLOAT,
TRANS_CRACK_NO_H   INTEGER,
TRANS_CRACK_NO_L   INTEGER,
TRANS_CRACK_NO_M   INTEGER
);
ALTER TABLE PAV_FIELD_PERF_CRACK ADD(CONSTRAINT PAV_FIELD_PERF_CRACK_PK
PRIMARY KEY (CRACK_ID));
ALTER TABLE PAV_FIELD_PERF_CRACK ADD(CONSTRAINT PAV_FIELD_PERF_CRACK_FK
FOREIGN KEY(SECTION_ID) REFERENCES PAV_SECTION(SECTION_ID));

CREATE TABLE PAV_FIELD_PERF_IRI(
AVERAGE_SPEED      FLOAT,
BEGINNING_DESCRIPTION VARCHAR2(200),
DIRECTION_MEASURED  VARCHAR2(100),
ENDING_DESCRIPTION   VARCHAR2(200),
IRI_AVERAGE         FLOAT,
IRI_ID              INTEGER,
IRI_LEFT_WHEEL_PATH  FLOAT,
IRI_RIGHT_WHEEL_PATH FLOAT,
LANE_MEASURED        VARCHAR2(100),
LOAD_DATE           DATE,
OTHER_WEATHER_INFO   VARCHAR2(100),

```

```

PROFILE_DATE          DATE,
PROFILE_TIME          DATE,
RUN_NUMBER            INTEGER,
SECTION_ID            INTEGER NOT NULL,
SLOPE_VARIANCE        FLOAT,
START_METHOD          VARCHAR2(100),
STOP_DISTANCE         INTEGER,
STOP_METHOD           VARCHAR2(100),
SURFACE_CONDITION     VARCHAR2(100),
TEMPERATURE           FLOAT,
WAVE_LENGTH_INIT      VARCHAR2(50)
);
ALTER TABLE PAV_FIELD_PERF_IRI ADD(CONSTRAINT PAV_FIELD_PERF_IRI_PK PRIMARY
KEY(IRI_ID));
ALTER TABLE PAV_FIELD_PERF_IRI ADD(CONSTRAINT PAV_FIELD_PERF_IRI_FK FOREIGN
KEY(SECTION_ID) REFERENCES PAV_SECTION(SECTION_ID));

CREATE TABLE PAV_FIELD_PERF_RUT(
    LLH_DEPTH_1_8_MAX    FLOAT,
    LLH_DEPTH_1_8_MEAN   FLOAT,
    LLH_DEPTH_1_8_MIN    FLOAT,
    LLH_DEPTH_1_8_STD    FLOAT,
    MAX_MEAN_DEPTH_1_8   FLOAT,
    RLH_DEPTH_1_8_MAX    FLOAT,
    RLH_DEPTH_1_8_MEAN   FLOAT,
    RLH_DEPTH_1_8_MIN    FLOAT,
    RLH_DEPTH_1_8_STD    FLOAT,
    RUT_ID                INTEGER NOT NULL,
    SECTION_ID            INTEGER NOT NULL,
    SURVEY_DATE           DATE
);
ALTER TABLE PAV_FIELD_PERF_RUT ADD(CONSTRAINT PAV_FIELD_PERF_RUT_PK PRIMARY
KEY(RUT_ID));
ALTER TABLE PAV_FIELD_PERF_RUT ADD(CONSTRAINT PAV_FIELD_PERF_RUT_FK FOREIGN
KEY(SECTION_ID) REFERENCES PAV_SECTION(SECTION_ID));

CREATE TABLE PAV_LAYER(
    AGG_GRADATION         VARCHAR2(10),
    AGG_SOURCE            VARCHAR2(100),
    AGG_TYPE              VARCHAR2(30),
    CONST_ID              INTEGER,
    L_CONST_DATE          DATE,
    L_OPEN_TRAFFIC_DATE   DATE,
    L_REMOVAL_DATE        DATE,
    LAYER_ID              INTEGER,
    LAYER_NO              INTEGER,
    LAYER_THICKNESS_MEAN  FLOAT,
    LAYER_THICKNESS_SDV   FLOAT,
    LAYER_TYPE            VARCHAR2(100),
    NO_10_PASSING         VARCHAR2(100),
    NO_16_PASSING         VARCHAR2(100),
    NO_200_PASSING        VARCHAR2(100),
    NO_4_PASSING          VARCHAR2(100),
    NO_40_PASSING         VARCHAR2(100),
    NO_80_PASSING         VARCHAR2(100),
    NO_OF_LIFTS           VARCHAR2(100),

```

```

ONE_AND_HALF_PASSING    FLOAT,
ONE_AND_QUATER_PASSING  FLOAT,
FIVE_EIGHTHS_PASSING    FLOAT,
ONE_HALF_PASSING         FLOAT,
ONE_PASSING              FLOAT,
ONE_QUATER_PASSING       FLOAT,
SEVEN_EIGHTHS_PASSING   FLOAT,
THREE_EIGHTHS_PASSING   FLOAT,
THREE_PASSING            FLOAT,
THREE_QUATER_PASSING     FLOAT,
TWO_PASSING              FLOAT
);
ALTER TABLE PAV_LAYER ADD(CONSTRAINT PAV_LAYER_PK PRIMARY KEY(LAYER_ID));
ALTER TABLE PAV_LAYER ADD(CONSTRAINT PAV_LAYER_FK FOREIGN KEY (CONST_ID)
REFERENCES PAV_CONSTR(CONST_ID));

CREATE TABLE PAV_LAYER_BASE(
    AASHTO_CLASSIFICATION    VARCHAR2(100),
    COMP_STRENGTH             VARCHAR2(100),
    COMP_STRENGTH_103KPA      FLOAT,
    COMP_STRENGTH_OKPA        FLOAT,
    CON_DENSITY_MEAN          FLOAT,
    CON_DENSITY_SDV           FLOAT,
    CON_MC_MEAN               FLOAT,
    CON_MC_SDV                FLOAT,
    CON_SEISMIC_MOD_MEAN      FLOAT,
    CON_SEISMIC_MOD_SDV       FLOAT,
    GRANULAR_ID               INTEGER,
    INTRFACE_COND             VARCHAR2(100),
    LAB_COMPACTION_EFFORT     VARCHAR2(100),
    LAB_SEISMIC_MOD_MEAN      FLOAT,
    LAB_SEISMIC_MOD_SDV       FLOAT,
    LAYER_ID                  INTEGER,
    LIQUID_LIMIT              VARCHAR2(100),
    MC_SINE_APPX_A            VARCHAR2(100),
    MC_SINE_APPX_B            VARCHAR2(100),
    MC_SINE_APPX_C            VARCHAR2(100),
    MDD                       FLOAT,
    OMC                       FLOAT,
    PLASTIC_INDEX             FLOAT,
    PLASTIC_LIMIT             FLOAT,
    POISONS_RATIO             FLOAT,
    PRIME_COAT_APP_RATE       FLOAT,
    PRIME_COAT_TYPE           FLOAT,
    SHRINKAGE_LIMIT           FLOAT,
    TREATMENT_AMOUNT          FLOAT,
    TREATMENT_TYPE            VARCHAR2(100),
    TX_TRIAXIAL_CLASSIFICATION VARCHAR2(100),
    USC_CLASSIFICATION         VARCHAR2(100),
    WET_BALL_MILL             VARCHAR2(100)
);
ALTER TABLE PAV_LAYER_BASE ADD(CONSTRAINT PAV_LAYER_BASE_PK PRIMARY
KEY(GRANULAR_ID));
ALTER TABLE PAV_LAYER_BASE ADD(CONSTRAINT PAV_LAYER_BASE_FK FOREIGN
KEY(LAYER_ID) REFERENCES PAV_LAYER(LAYER_ID));

```

```

CREATE TABLE PAV_LAYER_HMA(
    ADDITIVE_ID          INTEGER,
    BINDER_ID            INTEGER,
    HMA_ID               INTEGER,
    LAYER_ID             INTEGER,
    MIX_ID               INTEGER
);
ALTER TABLE PAV_LAYER_HMA ADD(CONSTRAINT PAV_LAYER_HMA_PK PRIMARY
KEY(HMA_ID));
ALTER TABLE PAV_LAYER_HMA ADD(CONSTRAINT PAV_LAYER_HMA_FK1
FOREIGN KEY(ADDITIVE_ID) REFERENCES PAV_ADMIX(ADDITIVE_ID));
ALTER TABLE PAV_LAYER_HMA ADD(CONSTRAINT PAV_LAYER_HMA_FK2
FOREIGN KEY(BINDER_ID) REFERENCES PAV_BINDER(BINDER_ID));
ALTER TABLE PAV_LAYER_HMA ADD(CONSTRAINT PAV_LAYER_HMA_FK3
FOREIGN KEY(LAYER_ID) REFERENCES PAV_LAYER(LAYER_ID));

CREATE TABLE PAV_LAYER_HMA_CREEP(
    CREEP_COMP_1_SEC      FLOAT,
    CREEP_COMP_10_SEC     FLOAT,
    CREEP_COMP_100_SEC    FLOAT,
    CREEP_COMP_2_SEC      FLOAT,
    CREEP_COMP_20_SEC     FLOAT,
    CREEP_COMP_5_SEC      FLOAT,
    CREEP_COMP_50_SEC     FLOAT,
    CREEP_ID              INTEGER,
    CREEP_POISSON_CALC     FLOAT,
    CREEP_POISSON_USED     FLOAT,
    HMA_ID                INTEGER,
    TEST_NO               INTEGER,
    TEST_TEMPERATURE       FLOAT
);
ALTER TABLE PAV_LAYER_HMA_CREEP ADD(CONSTRAINT PAV_LAYER_HMA_CREEP_PK
PRIMARY KEY(CREEP_ID));
ALTER TABLE PAV_LAYER_HMA_CREEP ADD(CONSTRAINT PAV_LAYER_HMA_CREEP_FK
FOREIGN KEY(HMA_ID) REFERENCES PAV_LAYER_HMA(HMA_ID));

CREATE TABLE PAV_LAYER_HMA_MOD(
    HMA_ID               INTEGER,
    STATE_CODE           INTEGER,
    INST_MR_AVG          FLOAT,
    INST_MR_CYCLE_1      VARCHAR2(100),
    INST_MR_CYCLE_2      VARCHAR2(100),
    INST_MR_CYCLE_3      VARCHAR2(100),
    INST_MR_POISSON_CALC_AVG  FLOAT,
    INST_MR_POISSON_CALC_CYCLE_1  FLOAT,
    INST_MR_POISSON_CALC_CYCLE_2  FLOAT,
    INST_MR_POISSON_CALC_CYCLE_3  FLOAT,
    MOD_ID              INTEGER,
    MR_DATA_FILE_SPECIMEN_1  VARCHAR2(100),
    TEST_NO             INTEGER,
    TEST_TEMPERATURE     FLOAT,
    TOTAL_MR_AVG         FLOAT,
    TOTAL_MR_CYCLE_1     FLOAT,
    TOTAL_MR_CYCLE_2     FLOAT,
    TOTAL_MR_CYCLE_3     FLOAT,
    TOTAL_MR_POISSON_CALC_AVG  FLOAT,

```

```

TOTAL_MR_POISSON_CALC_CYCLE_1FLOAT,
TOTAL_MR_POISSON_CALC_CYCLE_2FLOAT,
TOTAL_MR_POISSON_CALC_CYCLE_3FLOAT
);
ALTER TABLE PAV_LAYER_HMA_MOD ADD(CONSTRAINT PAV_LAYER_HMA_MOD_PK PRIMARY
KEY(MOD_ID));

```

```

ALTER TABLE PAV_LAYER_HMA_MOD ADD(CONSTRAINT PAV_LAYER_HMA_MOD_FK
FOREIGN KEY(HMA_ID) REFERENCES PAV_LAYER_HMA(HMA_ID));

```

```

CREATE TABLE PAV_LAYER_SOIL(
    AASHTO_CLASSIFICATION          VARCHAR2(100),
    BAR_LINEAR_SHRINKAGE           VARCHAR2(100),
    CBR                           FLOAT,
    COMP_STRENGTH_103KPA           FLOAT,
    COMP_STRENGTH_OKPA            FLOAT,
    CON_DENSITY_MEAN              FLOAT,
    CON_DENSITY_SDV               FLOAT,
    CON_MC_MEAN                   FLOAT,
    CON_MC_SDV                    FLOAT,
    CON_SEISMIC_MOD_MEAN          FLOAT,
    CON_SEISMIC_MOD_SDV           FLOAT,
    DCP                           VARCHAR2(100),
    GROUP_INDEX                   VARCHAR2(100),
    INTRFACE_COND                 VARCHAR2(100),
    LAB_COMPACTION_EFFORT          VARCHAR2(100),
    LAB_SEISMIC_MOD_MEAN          FLOAT,
    LAB_SEISMIC_MOD_SDV           FLOAT,
    LAYER_ID                      INTEGER,
    LIQUID_LIMIT                  VARCHAR2(100),
    MC_SINE_APPX_A                VARCHAR2(20),
    MC_SINE_APPX_B                VARCHAR2(20),
    MC_SINE_APPX_C                VARCHAR2(20),
    MDD                           FLOAT,
    MOD_SUBGRADE_REACTION         VARCHAR2(100),
    OMC                           FLOAT,
    ORG_CONTENT                   FLOAT,
    PLASTIC_INDEX                 INTEGER,
    PLASTIC_LIMIT                 INTEGER,
    POISONS_RATIO                 FLOAT,
    RESILIENT_MOD_CONST_K1        VARCHAR2(50),
    RESILIENT_MOD_CONST_K2        VARCHAR2(50),
    RESILIENT_MOD_CONST_K3        VARCHAR2(50),
    SHRINKAGE_LIMIT               INTEGER,
    SOIL_ID                      INTEGER,
    SULPHATE_POT                  VARCHAR2(50),
    SWELL_POT                     VARCHAR2(50),
    TX_TRIAXIAL_CLASSIFICATION    VARCHAR2(50),
    USC_CLASSIFICATION            VARCHAR2(50)

```

```

);
ALTER TABLE PAV_LAYER_SOIL ADD(CONSTRAINT PAV_LAYER_SOIL_PK PRIMARY
KEY(SOIL_ID));
ALTER TABLE PAV_LAYER_SOIL ADD(CONSTRAINT PAV_LAYER_SOIL_FK FOREIGN
KEY(LAYER_ID) REFERENCES PAV_LAYER(LAYER_ID));

```

```

CREATE TABLE PAV_LAYER_STSC(

```

```

        BINDER_RATE                FLOAT,
        BINDER_TYPE                VARCHAR2(30),
        LAYER_ID                  INTEGER,
        STSC_ID                   INTEGER
    );
    ALTER TABLE PAV_LAYER_STSC ADD(CONSTRAINT PAV_LAYER_STSC_PK PRIMARY
    KEY(STSC_ID));
    ALTER TABLE PAV_LAYER_STSC ADD(CONSTRAINT PAV_LAYER_STSC_FK FOREIGN
    KEY(LAYER_ID) REFERENCES PAV_LAYER(LAYER_ID));

    CREATE TABLE PAV_MIX(
        AIR_VOID_CONTENT_MEAN      FLOAT,
        AIR_VOID_CONTENT_SDV       FLOAT,
        DENSITY_MEAN               FLOAT,
        DENSITY_SDV                FLOAT,
        DYNAMIC_MOD                 FLOAT,
        DYNAMIC_STIFF              VARCHAR2(30),
        FATIGUE_ID                 INTEGER,
        FLOW_NUMBER                 INTEGER,
        FLOW_TIME                   DATE,
        HMA_ID                     INTEGER,
        HWTID_ID                   INTEGER,
        IND_TENSILE_STRENGTH        FLOAT,
        INTERFACE_COND              VARCHAR2(30),
        JMF                        VARCHAR2(30),
        MASTER_CURVE               FLOAT,
        MIX_DESIGN_PROCEDURE        VARCHAR2(50),
        MIX_ID                      INTEGER,
        MIX_TYPE                    VARCHAR2(50),
        MMLS3_ID                   INTEGER,
        OVERLAY_TESTER              INTEGER,
        POISSONS_RATIO             FLOAT,
        RESILIENT_MOD_25            VARCHAR2(30),
        RESILIENT_MOD_40            VARCHAR2(30),
        RESILIENT_MOD_5             VARCHAR2(30),
        RICE_DENSITY                FLOAT,
        TACK_COAT_RATE              FLOAT,
        TACK_COAT_TYPE              FLOAT,
        VMA                        FLOAT
    );
    ALTER TABLE PAV_MIX ADD(CONSTRAINT PAV_MIX_PK PRIMARY KEY(MIX_ID));
    ALTER TABLE PAV_MIX ADD(CONSTRAINT PAV_MIX_FK FOREIGN KEY(HMA_ID) REFERENCES
    PAV_LAYER_HMA(HMA_ID));

    CREATE TABLE PAV_MIX_JMF(
        JMF_ID                     INTEGER,
        MIX_DETAIL                  VARCHAR2(100),
        MIX_ID                      INTEGER
    );
    ALTER TABLE PAV_MIX_JMF ADD(CONSTRAINT PAV_MIX_JMF_PK PRIMARY KEY(JMF_ID));
    ALTER TABLE PAV_MIX_JMF ADD(CONSTRAINT PAV_MIX_JMF_FK FOREIGN KEY(MIX_ID)
    REFERENCES PAV_MIX(MIX_ID));

    CREATE TABLE PAV_SS_US_MOD(
        APPLIED_CONTACT_LOAD_AVG   FLOAT,
        APPLIED_CONTACT_LOAD_STD   FLOAT,

```

```

APPLIED_CONTACT_STRESS_AVG      FLOAT,
APPLIED_CONTACT_STRESS_STD      FLOAT,
APPLIED_CYCLIC_LOAD_AVG         FLOAT,
APPLIED_CYCLIC_LOAD_STD         FLOAT,
APPLIED_CYCLIC_STRESS_AVG       FLOAT,
APPLIED_CYCLIC_STRESS_STD       FLOAT,
APPLIED_MAX_AXIAL_LOAD_AVG      FLOAT,
APPLIED_MAX_AXIAL_LOAD_STD      FLOAT,
APPLIED_MAX_AXIAL_STRESS_AVG    FLOAT,
APPLIED_MAX_AXIAL_STRESS_STD    FLOAT,
CON_PRESSURE                     VARCHAR2(20),
DEF_LVDT_1_2_AVG                FLOAT,
DEF_LVDT_1_2_STD                FLOAT,
DEF_LVDT_1_AVG                  FLOAT,
DEF_LVDT_1_STD                  FLOAT,
DEF_LVDT_2_AVG                  FLOAT,
DEF_LVDT_2_STD                  FLOAT,
FIELD_SET                       VARCHAR2(30),
LAYER_ID                        INTEGER,
LOC_NO                          INTEGER,
MOD_ID                          INTEGER,
MR_MATL_TYPE                    VARCHAR2(30),
NOM_MAX_AXIAL_STRESS            VARCHAR2(30),
RES_MOD_AVG                     FLOAT,
RES_MOD_STD                     FLOAT,
RES_STRAIN_AVG                  FLOAT,
RES_STRAIN_STD                  FLOAT,
SAMPLE_NO                       INTEGER,
TEST_DATE                       DATE,
TEST_NO                         INTEGER
);
ALTER TABLE PAV_SS_US_MOD ADD(CONSTRAINT PAV_SS_US_MOD_PK PRIMARY KEY(MOD_ID));
ALTER TABLE PAV_SS_US_MOD ADD(CONSTRAINT PAV_SS_US_MOD_FK FOREIGN
KEY(LAYER_ID) REFERENCES PAV_LAYER(LAYER_ID));

CREATE TABLE TEST_FATIGUE(
    FATIGUE_ID                    INTEGER,
    MIX_ID                       INTEGER,
    STIFFNESS                     VARCHAR2(30),
    STRAIN                       VARCHAR2(30),
    TEMPERATURE                   FLOAT
);
ALTER TABLE TEST_FATIGUE ADD(CONSTRAINT TEST_FATIGUE_PK PRIMARY KEY(FATIGUE_ID));
ALTER TABLE TEST_FATIGUE ADD(CONSTRAINT TEST_FATIGUE_FK FOREIGN KEY(MIX_ID)
REFERENCES PAV_MIX(MIX_ID));

CREATE TABLE TEST_HWTD(
    CYCLE                        VARCHAR2(30),
    DEFORMATION                   VARCHAR2(30),
    HWTD_ID                      INTEGER,
    MIX_ID                       INTEGER,
    TEMPERATURE                   FLOAT
);
ALTER TABLE TEST_HWTD ADD(CONSTRAINT TEST_HWTD_PK PRIMARY KEY(HWTD_ID));

```



```
ALTER TABLE TEST_HWTD ADD(CONSTRAINT TEST_HWTD_FK FOREIGN KEY(MIX_ID)
REFERENCES PAV_MIX(MIX_ID));
```

```
CREATE TABLE TEST_MMLS3(
    CYCLE                                VARCHAR2(30),
    DEFORMATION                          VARCHAR2(30),
    MIX_ID                              INTEGER,
    MMLS3_ID                            INTEGER,
    TEMPERATURE                          FLOAT
);
ALTER TABLE TEST_MMLS3 ADD(CONSTRAINT TEST_MMLS3_PK PRIMARY KEY(MMLS3_ID));
ALTER TABLE TEST_MMLS3 ADD(CONSTRAINT TEST_MMLS3_FK FOREIGN KEY(MIX_ID)
REFERENCES PAV_MIX(MIX_ID));
```

```
CREATE TABLE TRAFFIC(
    AADT_PER_LANE                        VARCHAR2(30),
    AVG_OVERLOADING                      FLOAT,
    DIR_DIST_FACTOR                      VARCHAR2(30),
    FUTURE_ESAL                         VARCHAR2(30),
    FUTURE_ESAL_YEAR                    VARCHAR2(30),
    GROWTH_FACTOR                       INTEGER,
    GROWTH_RATE                         FLOAT,
    INITIAL_AADT                        VARCHAR2(30),
    INITIAL_ESAL                        VARCHAR2(30),
    INITIAL_PER_TRUCKS                  FLOAT,
    LANE_DIST_FACTOR                    VARCHAR2(30),
    PER_OVERLOADING                     FLOAT,
    SECTION_ID                          INTEGER,
    TIRE_INFLAT_SDV                     FLOAT,
    TIRE_INFLATION_DIST                 VARCHAR2(30),
    TIRE_INFLATION_MEAN                 FLOAT,
    TRAFFIC_WANDER                      VARCHAR2(30),
    YEAR_INITIAL_AADT                   VARCHAR2(20),
    YEAR_RECORD                         VARCHAR2(20)
);
```

```
ALTER TABLE TRAFFIC ADD(CONSTRAINT TRAFFIC_PK PRIMARY KEY(SECTION_ID));
```

```
CREATE TABLE TRAFFIC_AXLE_LOAD_VAR(
    CLASS                                VARCHAR2(30),
    CLASS_PER                            FLOAT,
    DISTR_MNTH_APR                       FLOAT,
    DISTR_MNTH_AUG                       FLOAT,
    DISTR_MNTH_DEC                       FLOAT,
    DISTR_MNTH_FEB                       FLOAT,
    DISTR_MNTH_JAN                       FLOAT,
    DISTR_MNTH_JUL                       FLOAT,
    DISTR_MNTH_JUN                       FLOAT,
    DISTR_MNTH_MAR                       FLOAT,
    DISTR_MNTH_MAY                       FLOAT,
    DISTR_MNTH_NOV                       FLOAT,
    DISTR_MNTH_OCT                       FLOAT,
    DISTR_MNTH_SEP                       FLOAT,
    HRLY_DISTR_00                        FLOAT,
    HRLY_DISTR_01                        FLOAT,
    HRLY_DISTR_02                        FLOAT,
```

HRLY_DISTR_03	FLOAT,
HRLY_DISTR_04	FLOAT,
HRLY_DISTR_05	FLOAT,
HRLY_DISTR_06	FLOAT,
HRLY_DISTR_07	FLOAT,
HRLY_DISTR_08	FLOAT,
HRLY_DISTR_09	FLOAT,
HRLY_DISTR_10	FLOAT,
HRLY_DISTR_11	FLOAT,
HRLY_DISTR_12	FLOAT,
HRLY_DISTR_13	FLOAT,
HRLY_DISTR_14	FLOAT,
HRLY_DISTR_15	FLOAT,
HRLY_DISTR_16	FLOAT,
HRLY_DISTR_17	FLOAT,
HRLY_DISTR_18	FLOAT,
HRLY_DISTR_19	FLOAT,
HRLY_DISTR_20	FLOAT,
HRLY_DISTR_21	FLOAT,
HRLY_DISTR_22	FLOAT,
HRLY_DISTR_23	FLOAT,
HRLY_DISTR_24	FLOAT,
QUAD_AXLE	VARCHAR2(30),
SECTION_ID	INTEGER,
SIN_CONST_A	VARCHAR2(30),
SIN_CONST_B	VARCHAR2(30),
SIN_CONST_C	VARCHAR2(30),
SINGLE_AXLE_DUAL_WHEEL	VARCHAR2(30),
SINGLE_AXLE_SINGLE_WHEEL	VARCHAR2(30),
TANDEM_AXLE	VARCHAR2(30),
TRIDEM_AXLE	VARCHAR2(30)

);

ALTER TABLE TRAFFIC\_AXLE\_LOAD\_VAR ADD(CONSTRAINT TRAFFIC\_AXLE\_LOAD\_VAR\_PK  
PRIMARY KEY(SECTION\_ID));

CREATE TABLE TRAFFIC\_LOAD\_SPECTRA(  
    Axle\_ID                    INTEGER,  
    Bin\_1                      FLOAT,  
    Bin\_10                     FLOAT,  
    Bin\_11                     FLOAT,  
    Bin\_12                     FLOAT,  
    Bin\_13                     FLOAT,  
    Bin\_14                     FLOAT,  
    Bin\_15                     FLOAT,  
    Bin\_16                     FLOAT,  
    Bin\_17                     FLOAT,  
    Bin\_18                     FLOAT,  
    Bin\_19                     FLOAT,  
    Bin\_2                      FLOAT,  
    Bin\_20                     FLOAT,  
    Bin\_21                     FLOAT,  
    Bin\_22                     FLOAT,  
    Bin\_23                     FLOAT,  
    Bin\_24                     FLOAT,  
    Bin\_25                     FLOAT,  
    Bin\_26                     FLOAT,

Bin_27	Float,
Bin_28	Float,
Bin_29	Float,
Bin_3	Float,
Bin_31	Float,
Bin_32	Float,
Bin_33	Float,
Bin_34	Float,
Bin_35	Float,
Bin_36	Float,
Bin_37	Float,
Bin_38	Float,
Bin_39	Float,
Bin_4	Float,
Bin_41	Float,
Bin_42	Float,
Bin_43	Float,
Bin_5	Float,
Bin_6	Float,
Bin_7	Float,
Bin_8	Float,
Bin_9	Float,
Bin_Width	VarChar2(40),
Sta_PK1_M	Float,
Sta_PK1_S	Float,
Sta_PK1_W	Float,
Sta_PK2_M	Float,
Sta_PK2_S	Float,
Sta_PK2_W	Float,
Sta_PK3_M	Float,
Sta_PK3_S	Float

```

);
ALTER TABLE TRAFFIC_LOAD_SPECTRA ADD (CONSTRAINT TRAFFIC_LOAD_SPECTRA_PK
PRIMARY KEY(Axle_ID));

COMMIT;

```

## Appendix 4.1

### Python Script to Populate All Distress Data

```
Python Script
#!/usr/local/bin/python
import os
import cx_Oracle
import re
user = 'dbuser'
passwd = 'Rafi1234'
sid = 'gismepdg'
port = '1521'
host = 'mepdg.unm.edu'

DSN = cx_Oracle.makedsn(host, port, sid)
orcl = cx_Oracle.connect(user, passwd, DSN)
curs = orcl.cursor()
fname='2008 Flexible Distress Data_temp.txt'
f = open(fname, 'r')
text = str(f.read())
a=re.split("\t\n",text)
i = 0
while i < len(a):
    sql='select max(id) from distress_data_dump'
    curs.execute(sql)
    j=curs.fetchall()
    for row in j:
        distress_id=row[0]

        distress_id = distress_id + 1
        print distress_id
        sql=""" insert into
distress_data_dump(id,route,lane_direction,mile_point,district,year_data_taken,PATCHING,EDGE_CRACKS,
ALLIGATOR_CRACKS,TRANSVERSE_CRACKS,LONGITUDINAL_CRACKS,RUTTING_AND_SHOVING,
BLEEDING,RAVELING_AND_WEATHERING)
        values('%s','%s','%s','%s','%s','%s','%s','%s','%s','%s','%s','%s','%s','%s','%s')"""
        %(distress_id,a[i],a[i+1],a[i+2],a[i+3],a[i+4],0,0,0,0,0,0,0,0,0)
        print sql
        curs.execute(sql)
        curs.execute("commit")

    if int(a[i+6]) == 1:
        sql=""" update distress_data_dump set RAVELING_AND_WEATHERING_HIGH = 0 ,
        RAVELING_AND_WEATHERING_MEDIUM = 0 , RAVELING_AND_WEATHERING_LOW = %s
where id = %s """%(a[i+7],distress_id)
        print sql
        curs.execute(sql)
        curs.execute("commit")
    if int(a[i+6]) == 2:
        sql=""" update distress_data_dump set RAVELING_AND_WEATHERING_HIGH = 0 ,
        RAVELING_AND_WEATHERING_MEDIUM = %s , RAVELING_AND_WEATHERING_LOW = 0
where id = %s """%(a[i+7],distress_id)
        print sql
```

```

        curs.execute(sql)
        curs.execute("commit")
    if int(a[i+6]) == 3:
        sql=" update distress_data_dump set RAVELING_AND_WEATHERING_HIGH = %s ,
            RAVELING_AND_WEATHERING_MEDIUM = 0 , RAVELING_AND_WEATHERING_LOW = 0
where id = %s"%(a[i+7],distress_id)
        print sql
        curs.execute(sql)
        curs.execute("commit")
    if int(a[i+6]) == 0:
        sql=" update distress_data_dump set RAVELING_AND_WEATHERING_HIGH = 0 ,
            RAVELING_AND_WEATHERING_MEDIUM = 0 , RAVELING_AND_WEATHERING_LOW = 0
where id = %s"%(distress_id)
        print sql
        curs.execute(sql)
        curs.execute("commit")

    if int(a[i+9]) == 1:
        sql=" update distress_data_dump set BLEEDING_HIGH = 0 ,
            BLEEDING_MEDIUM = 0 , BLEEDING_LOW = %s where id = %s"%(a[i+10],distress_id)
        print sql
        curs.execute(sql)
        curs.execute("commit")
    if int(a[i+9]) == 2:
        sql=" update distress_data_dump set BLEEDING_HIGH = 0 ,
            BLEEDING_MEDIUM = %s , BLEEDING_LOW = 0 where id = %s"%(a[i+10],distress_id)
        print sql
        curs.execute(sql)
        curs.execute("commit")
    if int(a[i+9]) == 3:
        sql=" update distress_data_dump set BLEEDING_HIGH = %s ,
            BLEEDING_MEDIUM = 0 , BLEEDING_LOW = 0 where id = %s"%(a[i+10],distress_id)
        print sql
        curs.execute(sql)
        curs.execute("commit")
    if int(a[i+9]) == 0:
        sql=" update distress_data_dump set BLEEDING_HIGH = 0 ,
            BLEEDING_MEDIUM = 0 , BLEEDING_LOW = 0 where id = %s"%(distress_id)
        print sql
        curs.execute(sql)
        curs.execute("commit")

    if int(a[i+12]) == 1:
        sql=" update distress_data_dump set RUTTING_AND_SHOVING_HIGH = 0 ,
            RUTTING_AND_SHOVING_MEDIUM = 0 , RUTTING_AND_SHOVING_LOW = %s where id = %s
"%(a[i+13],distress_id)
        print sql
        curs.execute(sql)
        curs.execute("commit")
    if int(a[i+12]) == 2:
        sql=" update distress_data_dump set RUTTING_AND_SHOVING_HIGH = 0 ,
            RUTTING_AND_SHOVING_MEDIUM = %s , RUTTING_AND_SHOVING_LOW = 0 where id = %s
"%(a[i+13],distress_id)
        print sql
        curs.execute(sql)

```

```

        curs.execute("commit")
    if int(a[i+12]) == 3:
        sql=" update distress_data_dump set RUTTING_AND_SHOVING_HIGH = %s ,
            RUTTING_AND_SHOVING_MEDIUM = 0 , RUTTING_AND_SHOVING_LOW = 0 where id = %s
        """%(a[i+13],distress_id)
        print sql
        curs.execute(sql)
        curs.execute("commit")
    if int(a[i+12]) == 0:
        sql=" update distress_data_dump set RUTTING_AND_SHOVING_HIGH = 0 ,
            RUTTING_AND_SHOVING_MEDIUM = 0 , RUTTING_AND_SHOVING_LOW = 0 where id = %s
        """(distress_id)
        print sql
        curs.execute(sql)
        curs.execute("commit")

    if int(a[i+15]) == 1:
        sql=" update distress_data_dump set LONGITUDINAL_CRACKS_HIGH = 0 ,
            LONGITUDINAL_CRACKS_MEDIUM = 0 , LONGITUDINAL_CRACKS_LOW = %s where id = %s
        """%(a[i+16],distress_id)
        print sql
        curs.execute(sql)
        curs.execute("commit")
    if int(a[i+15]) == 2:
        sql=" update distress_data_dump set LONGITUDINAL_CRACKS_HIGH = 0 ,
            LONGITUDINAL_CRACKS_MEDIUM = %s , LONGITUDINAL_CRACKS_LOW = 0 where id = %s
        """%(a[i+16],distress_id)
        print sql
        curs.execute(sql)
        curs.execute("commit")
    if int(a[i+15]) == 3:
        sql=" update distress_data_dump set LONGITUDINAL_CRACKS_HIGH = %s ,
            LONGITUDINAL_CRACKS_MEDIUM = 0 , LONGITUDINAL_CRACKS_LOW = 0 where id = %s
        """%(a[i+16],distress_id)
        print sql
        curs.execute(sql)
        curs.execute("commit")
    if int(a[i+15]) == 0:
        sql=" update distress_data_dump set LONGITUDINAL_CRACKS_HIGH = 0 ,
            LONGITUDINAL_CRACKS_MEDIUM = 0 , LONGITUDINAL_CRACKS_LOW = 0 where id = %s
        """(distress_id)
        print sql
        curs.execute(sql)
        curs.execute("commit")
    if int(a[i+18]) == 1:
        sql=" update distress_data_dump set TRANSVERSE_CRACKS_HIGH = 0 ,
            TRANSVERSE_CRACKS_MEDIUM = 0 , TRANSVERSE_CRACKS_LOW = %s where id = %s
        """%(a[i+19],distress_id)
        print sql
        curs.execute(sql)
        curs.execute("commit")
    if int(a[i+18]) == 2:
        sql=" update distress_data_dump set TRANSVERSE_CRACKS_HIGH = 0 ,
            TRANSVERSE_CRACKS_MEDIUM = %s , TRANSVERSE_CRACKS_LOW = 0 where id = %s
        """%(a[i+19],distress_id)

```

```

print sql
curs.execute(sql)
curs.execute("commit")
if int(a[i+18]) == 3:
    sql=" update distress_data_dump set TRANSVERSE_CRACKS_HIGH = %s ,
        TRANSVERSE_CRACKS_MEDIUM = 0 , TRANSVERSE_CRACKS_LOW = 0 where id = %s
"%(a[i+19],distress_id)
    print sql
    curs.execute(sql)
    curs.execute("commit")
if int(a[i+18]) == 0:
    sql=" update distress_data_dump set TRANSVERSE_CRACKS_HIGH = 0 ,
        TRANSVERSE_CRACKS_MEDIUM = 0 , TRANSVERSE_CRACKS_LOW = 0 where id = %s
"%(distress_id)
    print sql
    curs.execute(sql)
    curs.execute("commit")
if int(a[i+21]) == 1:
    sql=" update distress_data_dump set ALLIGATOR_CRACKS_HIGH = 0 ,
        ALLIGATOR_CRACKS_MEDIUM = 0 , ALLIGATOR_CRACKS_LOW = %s where id = %s
"%(a[i+22],distress_id)
    print sql
    curs.execute(sql)
    curs.execute("commit")
if int(a[i+21]) == 2:
    sql=" update distress_data_dump set ALLIGATOR_CRACKS_HIGH = 0 ,
        ALLIGATOR_CRACKS_MEDIUM = %s , ALLIGATOR_CRACKS_LOW = 0 where id = %s
"%(a[i+22],distress_id)
    print sql
    curs.execute(sql)
    curs.execute("commit")
if int(a[i+21]) == 3:
    sql=" update distress_data_dump set ALLIGATOR_CRACKS_HIGH = %s ,
        ALLIGATOR_CRACKS_MEDIUM = 0 , ALLIGATOR_CRACKS_LOW = 0 where id = %s
"%(a[i+22],distress_id)
    print sql
    curs.execute(sql)
    curs.execute("commit")
if int(a[i+21]) == 0:
    sql=" update distress_data_dump set ALLIGATOR_CRACKS_HIGH = 0 ,
        ALLIGATOR_CRACKS_MEDIUM = 0 , ALLIGATOR_CRACKS_LOW = 0 where id = %s
"%(distress_id)
    print sql
    curs.execute(sql)
    curs.execute("commit")
if int(a[i+24]) == 1:
    sql=" update distress_data_dump set EDGE_CRACKS_HIGH = 0 ,
        EDGE_CRACKS_MEDIUM = 0 , EDGE_CRACKS_LOW = %s where id = %s "%(a[i+25],distress_id)
    print sql
    curs.execute(sql)
    curs.execute("commit")
if int(a[i+24]) == 2:
    sql=" update distress_data_dump set EDGE_CRACKS_HIGH = 0 ,
        EDGE_CRACKS_MEDIUM = %s , EDGE_CRACKS_LOW = 0 where id = %s "%(a[i+25],distress_id)
    print sql
    curs.execute(sql)

```

```

    curs.execute("commit")
if int(a[i+24]) == 3:
    sql=" update distress_data_dump set EDGE_CRACKS_HIGH = %s ,
        EDGE_CRACKS_MEDIUM = 0 , EDGE_CRACKS_LOW = 0 where id = %s"%(a[i+25],distress_id)
    print sql
    curs.execute(sql)
    curs.execute("commit")
if int(a[i+24]) == 0:
    sql=" update distress_data_dump set EDGE_CRACKS_HIGH = 0 ,
        EDGE_CRACKS_MEDIUM = 0 , EDGE_CRACKS_LOW = 0 where id = %s"%(distress_id)
    print sql
    curs.execute(sql)
    curs.execute("commit")
if int(a[i+27]) == 1:
    sql=" update distress_data_dump set PATCHING_HIGH = 0 ,
        PATCHING_MEDIUM = 0 , PATCHING_LOW = %s where id = %s"%(a[i+28],distress_id)
    print sql
    curs.execute(sql)
    curs.execute("commit")
if int(a[i+27]) == 2:
    sql=" update distress_data_dump set PATCHING_HIGH = 0 ,
        PATCHING_MEDIUM = %s , PATCHING_LOW = 0 where id = %s"%(a[i+28],distress_id)
    print sql
    curs.execute(sql)
    curs.execute("commit")
if int(a[i+27]) == 3:
    sql=" update distress_data_dump set PATCHING_HIGH = %s ,
        PATCHING_MEDIUM = 0 , PATCHING_LOW = 0 where id = %s"%(a[i+28],distress_id)
    print sql
    curs.execute(sql)
    curs.execute("commit")
if int(a[i+27]) == 0:
    sql=" update distress_data_dump set PATCHING_HIGH = 0 ,
        PATCHING_MEDIUM = 0 , PATCHING_LOW = 0 where id = %s"%(distress_id)
    print sql
    curs.execute(sql)
    curs.execute("commit")
i = i + 29
End of Distress Python Script

```



## Appendix 4.2

### Test.Map File Code

```
MAP
NAME test
STATUS ON
SIZE 600 400
EXTENT -109.050173 31.332172 -103.001964 37.000293
UNITS DD
SHAPEPATH ./mapfiles/shapes
IMAGECOLOR 255 255 255

WEB
  IMAGEPATH "/ms4w/tmp/ms_tmp/"
  IMAGEURL "/ms_tmp/"
METADATA
  "ows_title"      "mepdg test server"
  "ows_onlineresource" "http://mepdg.unm.edu/cgi-bin/mapserv.exe?map=mapfiles/test.map&"
  "ows_srs"        "EPSG:4326"
  "wfs_title"      "MEPDG TEST SERVER" ## REQUIRED
  "wfs_onlineresource" "http://mepdg.unm.edu/cgi-bin/mapserv.exe?map=mapfiles/test.map&" ##
Recommended
  "wfs_srs"        "EPSG:4326" ## Recommended
END
END
PROJECTION
  "init=epsg:4326"
END
LAYER
  NAME COUNTY
  TYPE POLYGON
  CONNECTION
  "dbuser/Rafi1234@((DESCRIPTION=(ADDRESS_LIST=(ADDRESS=(PROTOCOL=TCP)(HOST=localhost)(PORT=1521)))
(CONNECT_DATA=(SID=gismepdg)))"
  CONNECTIONTYPE oraclespatial
  DATA "GEOM FROM COUNTY2008 USING SRID 4326"
  DUMP TRUE
  METADATA
    "ows_title"      "NMCOUNTY"
    "LatLonBoundingBox" "-109.5 31.3322 -103.002 37.0003"
    "wfs_title"      "NMCOUNTY"
    "gml_featureid"  "CNTY_FIPS"
  END
CLASS
  STYLE
    OUTLINECOLOR 0 0 0
    COLOR 0 128 128
  END
END
PROJECTION
  "init=epsg:4326"
END
END
END
```